Technische Universität München
TUM School of Natural Sciences

# Structural and cellular mechanisms of interleukin 12 family cytokine biogenesis

**Isabel Sarah Aschenbrenner**

Vollständiger Abdruck der von der TUM School of Natural Sciences der Technischen Universität München zur Erlangung des akademischen Grades einer

**Doktorin der Naturwissenschaften (Dr. rer. nat.)**

genehmigten Dissertation.

Vorsitz: Prof. Dr. Martin Zacharias

Prüfer*innen der Dissertation:

1. Prof. Dr. Matthias J. Feige
2. Prof. Dr. Johannes Buchner
3. Priv.-Doz. Dr. Julia Esser-von Bieren

Die Dissertation wurde am 08.03.2023 bei der Technischen Universität München eingereicht und durch die TUM School of Natural Sciences am 13.04.2023 angenommen.

*Die Weltenseele wird von dem Glück der Menschen gespeist. Unsere einzige Verpflichtung besteht darin, den persönlichen Lebensplan zu erfüllen. Alles ist ein Ganzes. Und wenn du etwas ganz fest willst, dann wird das ganze Universum dazu beitragen, dass du es auch erreichst.*

Aus *Der Alchimis*t von Paulo Coelho

## Parts of this thesis have been published in peer-reviewed journals:

An interspecies analysis reveals molecular construction principles of interleukin 27.
Müller, S.I.[1], **Aschenbrenner, I.**[1], Zacharias, M., Feige, M.J.
*J. Mol. Biol.* (2019) 431(12): 2383-2393.

Influence of glycosylation on IL-12 family cytokine biogenesis and function.
Bohnacker, S.[1], Hildenbrand, K.[1], **Aschenbrenner, I.**[1], Müller, S.I., Esser-von Bieren, J., Feige, M.J.
*Mol. Immunol.* (2020) 126: 120-128.

Biogenesis and engineering of interleukin 12 family cytokines.
Hildenbrand, K.[1], **Aschenbrenner, I.**[1], Franke, F.C., Devergne, O., Feige, M.J.
*Trends Biochem Sci.* (2022) 47(11): 936-949.

A comprehensive set of ER protein disulfide isomerase family members supports the biogenesis of pro-inflammatory interleukin 12 family cytokines.
Mideksa, Y.G.[1], **Aschenbrenner, I.**[1], Fux, A., Kaylani, D., Weiß, C.A.M., Nguyen, T., Bach, N.C., Lang, K., Sieber, S.A., Feige, M.J.
*J. Biol. Chem.* (2022) 298(12): 102677.

Assembly-dependent structure formation determines the human interleukin-12/interleukin-23 secretion ratio.
**Aschenbrenner, I.**, Lopez, A., Siebenmorgen, T., Parr, M., Ruckgaber, P., Miesl, A., Rührnößl, F., Catici, D., Haslbeck, M., Sattler, M., Frishman, D., Zacharias, M., Feige, M.J.
Manuscript in preparation.

[1] These authors contributed equally.

**Parts of this thesis have been presented at scientific conferences:**

14th ER & Redox Club meeting (International Conference)
08.05. - 10.05.2019, Herrsching am Ammersee, Germany
Flashtalk and poster presentation:
*An interspecies analysis reveals molecular construction principles of interleukin 27.*

SFB1035 – PhD and Postdoc Retreat 2019 (Annual SFB Meeting)
13.05. - 15.05.2019, Roggenburg, Germany
Poster presentation:
*A species comparison reveals molecular construction principles of interleukin 27.*

Susan Lindquist School on Proteostasis (EMBO FEBS Lecture Course)
29.11. - 02.12.2021, virtual meeting
Flashtalk:
*Structural and cellular mechanisms of interleukin 12 family cytokine biogenesis.*

Cytokines 2022 – 10th Annual Meeting of the International Cytokine & Interferon Society (International Conference)
20.09. - 23.09.2022, Hawaii, States
Poster presentation:
*Rational engineering of a folding pathway changes mechanism and chaperone dependency of interleukin secretion*.

**Research topics that are not covered in this thesis, but have been presented at scientific conferences:**

CRC TRR 338 LETSimmun Retreat (Annual TRR Meeting)
19.07. - 20.07.2022, München, Germany
Flashtalk and poster presentation:
*More effects, less side effects: Rationally engineering interleukin 12 for cancer treatment.*

# Abstract

Interleukins (ILs) are immunoregulatory proteins that are secreted by immune cells and mediate cell-cell communication by circulating in the tissue environment. Connecting innate and adaptive immunity, the IL-12 family is of particular interest due to its unique structural properties and important biological functions. Each IL-12 family member is a heterodimer composed of a four-helix bundle α-subunit and an all-β structure β-subunit. The four key members, IL-12, IL-23, IL-27, and IL-35, are made up of only five shared building blocks, with each β-chain participating in two ILs and one α-subunit occurring in two different cytokines. In humans, α-subunits are incompletely structured in isolation and thus retained by molecular chaperones in the endoplasmic reticulum (ER). They rely on their β-subunit to become structured, pass the ER quality control (ERQC) and become secreted as assembled, mature cytokines. Despite the chain sharing promiscuity, IL-12 family members' functionalities are distinct and range from mostly pro- to anti-inflammatory. As key players of our immune system they are intimately involved in multiple pathologies from autoimmunity to cancer.

In recent years we have gained a broader understanding of how IL-12 family biogenesis and assembly are regulated on the cellular level and what the underlying molecular principles are. Structural insights into their receptor engagement closed the gap to downstream immunological signaling. Nevertheless, only a comprehensive picture of folding and assembly of the IL-12 family cytokines, with all the molecular details, renders it possible to move forward by translating these insights for targeted interventions in immune signaling and immunotherapies.

With this dissertation, I could complete this picture a bit further. We investigated the role of an intramolecular disulfide bond for IL-27α secretion-competency and concomitantly for a common, evolutionary conserved design principle in IL-27. By elucidating the impact of glycosylation on the biogenesis and functionality of all IL-12 family members, we could further dissect principles behind ERQC. Important mechanistic insights into IL folding and assembly were provided by a thorough analysis of the ER chaperone repertoire acting on incompletely folded α-subunits of pro-inflammatory IL-12 and IL-23. Furthermore, we rationally engineered a folding-competent IL-23α subunit that allowed us to assess regulatory principles in IL heterodimerization. These studies cover not only the structural and cellular mechanisms underlying IL-12 family cytokine biogenesis and assembly control but are also the first steps towards applying this knowledge for future biomedical therapeutics by rational IL-12 family protein engineering.

# Zusammenfassung

Interleukine sind immunregulatorische Proteine, die von Immunzellen sezerniert werden und Zell-Zell-Kommunikation vermitteln, indem sie im Gewebe zirkulieren. Als Bindeglied zwischen angeborener und adaptiver Immunität ist die Interleukin (IL)-12 Familie aufgrund ihrer einzigartigen strukturellen Eigenschaften und wichtigen biologischen Funktionen von besonderem Interesse. Jedes Mitglied der IL-12 Familie ist ein Heterodimer, welches aus einer aus vier Helices gebündelten α-Untereinheit und einer β-Untereinheit mit vollständiger β-Faltblatt Struktur besteht. Die vier Hauptmitglieder, IL-12, IL-23, IL-27 und IL-35, bestehen aus nur fünf gemeinsamen Bausteinen, wobei jede β-Kette in zwei Interleukinen und eine α-Untereinheit in zwei verschiedenen Zytokinen vorkommt. Beim Menschen sind die α-Untereinheiten unvollständig strukturiert, wenn allein vorkommend, und werden daher von molekularen Chaperonen im endoplasmatischen Retikulum (ER) zurückgehalten. Sie sind auf ihre β-Untereinheit angewiesen, um gefalten zu werden, die ER-Qualitätskontrolle (ERQC) zu passieren und als assembliertes, reifes Zytokin sekretiert zu werden. Trotz der Promiskuität bei der Kettennutzung sind die Funktionen der IL-12 Familienmitglieder unterschiedlich und reichen von hauptsächlich pro- bis anti-inflammatorisch. Als Schlüsselzytokine unseres Immunsystems sind sie an zahlreichen Pathologien, von Autoimmunität bis Krebs, eng beteiligt.

In den letzten Jahren haben wir ein umfassenderes Verständnis dafür gewonnen, wie die Biogenese und Assemblierung der IL-12 Familie auf zellulärer Ebene reguliert werden und welche molekularen Prinzipien ihnen zugrunde liegen. Strukturelle Einblicke in die Rezeptorbindung haben die Lücke zu den nachgeschalteten immunologischen Signalwegen geschlossen. Doch erst ein umfassendes Bild von Faltung und Assemblierung der Zytokine der IL-12 Familie, mit allen molekularen Details, macht es möglich, voranzuschreiten und diese Erkenntnisse für gezielte Eingriffe in die Immunsignalgebung und Immuntherapien zu nutzen.

Mit dieser Dissertation konnte ich dieses Bild ein wenig weiter vervollständigen. Wir untersuchten die molekulare Rolle einer intramolekularen Disulfidbindung für die Sekretionsfähigkeit von IL-27α und gleichzeitig für ein generelles, evolutionär konserviertes Konstruktionsprinzip von IL-27. Durch die Aufklärung der Auswirkungen von Glykosylierung auf die Biogenese und Funktionalität aller IL-12 Familienmitglieder konnten wir die Prinzipien hinter der ERQC weiter aufschlüsseln. Eine gründliche Analyse des ER Chaperon-Repertoires, das auf unvollständig gefaltete α-Untereinheiten von pro-inflammatorischem IL-12 und IL-23 wirkt, lieferte wichtige mechanistische Einblicke in die IL-Faltung und -Assemblierung. Darüber hinaus konnten wir eine faltungskompetente

IL-23α Untereinheit rational konstruieren, welche es uns ermöglichte regulatorische Prinzipien bei der IL-Heterodimerisierung zu untersuchen. Diese Studien decken nicht nur die strukturellen und zellulären Mechanismen ab, die der Biogenese und Kontrolle der Assemblierung von Zytokinen der IL-12 Familie zugrunde liegen, sondern sind auch die ersten Schritte Richtung Anwendung dieses Wissens für zukünftige biomedizinische Therapeutika durch rationales Proteinengineering der IL-12 Familie.

# Abbreviations

| | |
|---|---|
| APC | antigen-presenting cell |
| BiP | immunoglobulin heavy-chain binding protein |
| BL | Burkitt lymphoma |
| Breg | regulatory B cell |
| BRET | bioluminescence resonance energy transfer |
| CAR | chimeric antigen receptor |
| CD | circular dichroism |
| CHR | cytokine-binding homology region |
| CHX | cycloheximide |
| CLC | cardiotrophin-like cytokine |
| CNTF | ciliary neurotrophic factor |
| CNX | calnexin |
| CRT | calreticulin |
| cryo-EM | cryo-electron microscopy |
| DAMP | damage-associated molecular pattern |
| DC | dendritic cell |
| DiazK | $N^6$-((2-(3-methyl-3H-diazirin-3-yl)ethoxy)carbonyl)-L-lysine |
| DSP | dithiobis(succinimidyl propionate) |
| DTT | dithiothreitol |
| EAE | experimental autoimmune encephalitis |
| EBI3 | Epstein-Barr virus-induced gene 3 |
| EBV | Epstein-Barr virus |
| EDEM | ER degradation enhancing $\alpha$-mannosidase-like protein |
| ER | endoplasmic reticulum |
| ER Man | ER Mannosidase |
| ERAD | ER-associated degradation |
| ERdj | ER DnaJ like protein |
| ERGIC | ER-Golgi intermediate compartment |
| Ero | ER oxidoreductin |
| Fab | antigen-binding fragment |
| FnIII | fibronectin type III |
| Foxp3 | forkhead box protein P3 transcription factor |
| Glc | glucosidase |
| GM-CSF | granulocyte-macrophage colony-stimulating factor |
| gp130 | glycoprotein 130 |
| GRP | glucose-regulated protein |
| GSH | glutathione |
| GSSG | glutathione disulfide |
| HDX | hydrogen/deuterium exchange |
| HEK | human embryonic kidney |
| HMW | high molecular weight |
| HPLC | high performance liquid chromatography |
| HSP | heat shock protein |
| IBD | inflammatory bowel disease |
| IFN | interferon |
| Ig | immunoglobulin |

| | |
|---|---|
| IL | interleukin |
| IP | immunoprecipitation |
| ITC | isothermal titration calorimetry |
| Jak | Janus kinase |
| MHC | major histocompatibility complex |
| MS | mass spectrometry |
| NBD | adenosine nucleotide-binding domain |
| NEF | nucleotide exchange factor |
| NFAT | nuclear factor of activated T cells |
| NK | natural killer |
| NMR | nuclear magnetic resonance |
| NP | neuropoietin |
| PAMP | pathogen-associated molecular pattern |
| PBMC | peripheral blood mononuclear cell |
| PDI | protein disulfide isomerase |
| PD-L1 | program death-ligand 1 |
| PPIase | peptidyl-prolyl isomerase |
| QC | quality control |
| SBD | substrate binding domain |
| SERCA | sarco/endoplasmic reticulum $Ca^{2+}$-ATPase |
| SPR | surface plasmon resonance |
| SRP | signal recognition particle |
| STAT | signal transducer and activator of transcription |
| TCR | T cell receptor |
| Th | T helper cell |
| TNF | tumor necrosis factor |
| Treg | regulatory T cell |
| UGGT | UDP-glucose:glycoprotein glucosyltransferase |
| UPR | unfolded protein response |

# Table of contents

# 1 Introduction

## 1.1 Protein folding

In 1962, Anfinsen postulated that proteins contain all the information for their biologically active structure encoded in their amino acid sequence [1]. He claimed that this should be possible as the native protein conformation is the thermodynamically most stable one in the cell [2]. This idea and its validation were awarded by the Nobel Prize in Chemistry in 1972. As unfolded polypeptide chains have many degrees of freedom, correct protein folding into the native structure seemed like searching for a needle, illustrating the native protein conformation, in the haystack, representing the huge conformational space [3]. This led to the apparent paradox and question, how proteins can fold so quickly, sometimes even within microseconds, when there are so many possible conformations a protein could adopt [4]. By now, we better understand driving forces in rapid protein folding: Thermal motions cause conformational changes, which drive proteins to bury hydrophobic side chains in the aqueous milieu, the so-called hydrophobic collapse, and result in hydrogen bonds, van der Waals interactions, and electrostatic interactions within the polypeptide chain [5]. Illustrated in an energetic landscape, protein folding to its native state can be schematically represented in a folding funnel diagram. The funnel-like shape arises because the horizontally plotted configurational entropy, thus the number of accessible configurations, decreases as the effective potential energy, plotted vertically, decreases [6]. Unfolded proteins of high energy can adopt several non-native structures and take random steps to incrementally descend the funnel-shaped protein folding landscape to finally reach their native-like, low-energy conformation [4]. Even when a protein is kinetically trapped in a local energy minimum as an intermediate state, folding helpers like chaperones can assist by lowering free-energy barriers and navigate the protein to another route towards its native state [7]. In computer simulations a physical forcefield can be applied on a protein and combined with the knowledge on a vast number of solved structures available in the Protein Data Bank, we are proceeding to accurately predict protein folding and structure with the help of artificial intelligence *in silico* [5, 8, 9].

## 1.2 The endoplasmic reticulum as hub for protein folding and quality control

The endoplasmic reticulum (ER) is the gateway for proteins of the secretory pathway, like cytokines, hormones, chemokines, or antibodies, that are destined for secretion from cells into the extracellular space. In contrast to protein secretion directly across the plasma membrane, as described for prokaryotes, eukaryotic cells utilize the ER as entry point for secretory proteins which are first delivered to and then translocated across the plasma

membrane [10]. Evolutionarily evolved by invagination of the plasma membrane, this organelle is physically segregated from the cytosol and chemically resembles already the final destination of secretory proteins, the extracellular milieu [11]. This spatial segregation allows protein modifications that would not occur in the cytosol, like glycosylation, disulfide bond formation, or proline hydroxylation, to take place in the ER. Many of these modifications either change the physical properties or functionality of the protein, facilitate protein interaction, or result in targeting the polypeptide to particular ER-resident folding factors [12]. The ER functions as a global protein folding factory in which proteins assemble and mature into their correctly folded and biologically active form. There are multiple modifications and folding pathways, which are assisted by enzymes and molecular chaperone complexes in the ER (Figure 1). The ER also serves as checkpoint in protein quality control, termed ER quality control (ERQC), to secure onward vesicular transport and secretion of proteins only in their thermodynamically stable, native state [13]. If a protein does not pass ERQC, this organelle furthermore facilitates elimination of such misfolded proteins by the ER-associated degradation (ERAD) pathway [14]. Since approximately one third of the human proteome are secretory proteins and need to traverse the ER, its importance becomes even more apparent [12].

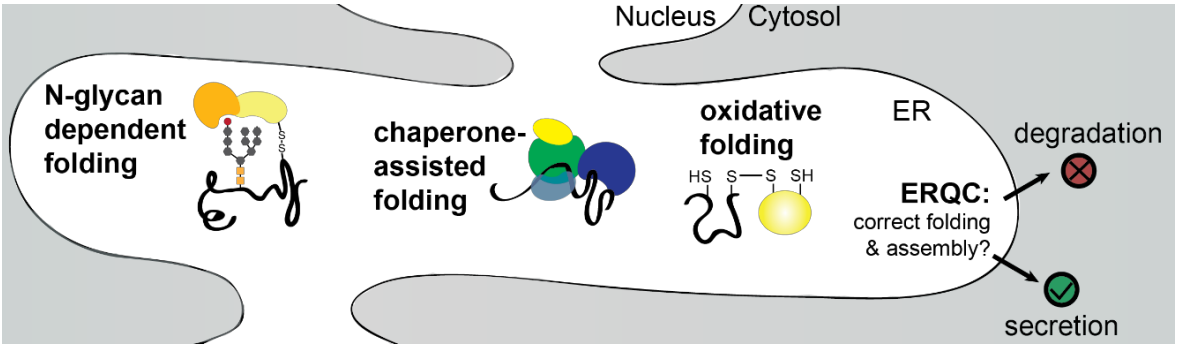


**Figure 1. The endoplasmic reticulum (ER) as hub for protein folding and quality control (QC).** Protein folding in the ER is supported by *N*-glycosylation and the lectin chaperone system, by a diverse chaperone repertoire preventing protein aggregation, promoting native interactions, and protein assembly, and by disulfide bond formation catalyzed by thiol-disulfide oxidoreductases. If a protein folds into its native structure, it can pass ERQC and subsequently traverse the Golgi to finally become secreted. In contrast, misfolded or aggregated proteins are recognized by the ERQC system and are degraded in the ER-associated degradation (ERAD) pathway.

To facilitate proper protein folding, modifications, and assembly in the ER, the extracellular-like milieu in this organelle needs to provide an appropriate environment for this [15]. Most importantly, the ER enables disulfide bond formation by its more oxidizing state in contrast to the reducing cytosol [16]. Still, a hyperoxidizing redox milieu would lead to cysteine mispairings and thereby impair productive folding. Thus, maintaining the redox balance is a condition *sine qua non*. The ER comprises oxidizing equivalents in form of the atypic tripeptide glutathione disulfide (GSSG) and the reduced species, glutathione (GSH), as counterpart [17]. The relevance of the GSSG:GSH potential as driving force for biological

reactions is nowadays critically discussed [18]. The concentration ratio might rather reflect a steady state redox potential and the functional importance of GSH in reductive processes is challenged, as alternative electron donors might exist [18, 19]. What is certain is that derived from GSSG:GSH ratios the redox potential in the ER is shifted towards a more oxidizing potential than it is in the cytosol [17]. Besides the redox balance, the ER depends on ATP supply, as it has no energy generating system itself to maintain ATP-hydrolyzing chaperones functional [12]. Furthermore, as many folding factors bind to and rely on $Ca^{2+}$ ions as cofactors, luminal calcium concentrations are stably high [20]. This is preserved by sarco/endoplasmic reticulum $Ca^{2+}$-ATPases (SERCAs), which actively pump $Ca^{2+}$ ions into the ER [21].

### 1.2.1 Protein transport into the mammalian endoplasmic reticulum

The secretory pathway starts by translocation of nascent proteins across the ER membrane into the ER lumen. In eukaryotic cells, most secretory proteins are delivered to the ER by the signal recognition particle (SRP) pathway. In this pathway, an N-terminal hydrophobic signal peptide in the unfolded protein emerges from the ribosomal exit tunnel and is recognized by the conserved SRP [22]. The ribosome-nascent chain-SRP complex then binds to the ER membrane via the SRP receptor [23]. This interaction directs the complex to the ER membrane-pore Sec61 in a GTP-dependent manner. This pore functions as translocon and enables co-translational translocation of the polypeptide chain across the ER membrane [10, 24]. Nevertheless, this Sec61-mediated transport also occurs post-translationally with molecular chaperones of the heat shock protein (HSP)70 family maintaining the synthesized protein in a partially unfolded, translocation-competent state under ATP consumption. There is evidence that further Sec61-associated components are also involved [25]. After protein translocation into the ER lumen, the signal peptide gets cleaved by the signal peptidase complex located in the ER membrane [26].

### 1.2.2 *N*-linked glycans help proteins fold

For efficient protein folding in the ER, *N*-glycosylation is often of importance. Prior to protein glycosylation, the oligosaccharide is assembled on a lipid carrier for transfer. A membrane-bound, dolichyl-pyrophosphate-linked glycan precursor is enzymatically built up, first on the cytoplasmic side and after flipping, on the ER luminal side. The core oligosaccharide $Glc_3Man_9GlcNAc_2$ is added co-translationally to the growing nascent polypeptide containing the N-X-S/T consensus motif [27]. The undefined amino acid X in this sequence must not be an aspartic acid or proline residue and, depending on its identity and resulting conformation, efficiency of glycan transfer is modulated [28, 29]. The core glycan is transferred to the peptide chain in the ER lumen by the oligosaccharyl-transferase complex

and is linked through an *N*-glycosidic bond to the asparagine side chain of the common sequon. Subsequently, terminal glucose and mannose residues are trimmed by ER glucosidases and mannosidases as the glycoprotein matures. This glycan trimming plays a pivotal role in protein biogenesis and ERQC (Figure 2) and takes place in concert with chaperones and carbohydrate-binding proteins, so-called lectins. Prominent lectins are the membrane-bound calnexin (CNX) and soluble calreticulin (CRT) [13]. CNX/CRT come into action when two of the three glucoses of the *N*-linked sugar moiety on the nascent or newly synthesized polypeptide are trimmed away by Glucosidase (Glc) I and II [30]. Then, CNX/CRT can bind and additional folding factors like the glycoprotein-specific oxidoreductase ERp57 are recruited by CNX/CRT to interact with the glycosylated, incompletely folded protein [31]. This cochaperone aids in the formation of correct disulfide bonds and oxidative folding of the glycoprotein [32]. Subsequent trimming of the third glucose releases the protein from the CNX/CRT cycle, allowing it to exit the ER and traverse further along the secretory pathway. However, if folding is incomplete, the UDP-glucose:glycoprotein glucosyltransferase (UGGT) acts as folding sensor. It reverses glucose trimming by glucosylation of the partially, but incompletely folded protein and thereby reshuffles it to the CNX/CRT cycle, allowing for another round of folding assistance [33, 34]. In contrast, for misfolded or mutant proteins with a prolonged residence time in the ER, sequential mannosidase trimming is performed by ER Mannosidase (ER Man) I and ER degradation enhancing α-mannosidase-like proteins, termed EDEM1-3 [35, 36].

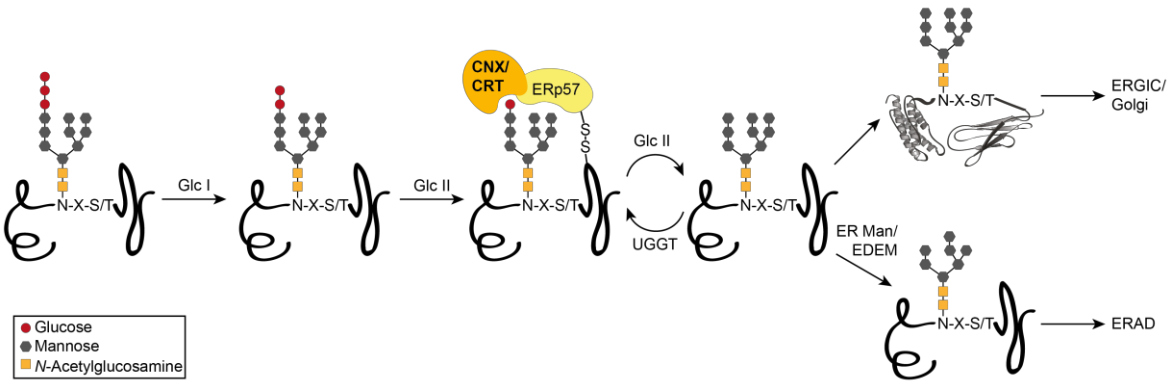


**Figure 2. The calnexin (CNX)/calreticulin (CRT) cycle.** The core oligosaccharide $Glc_3Man_9GlcNAc_2$ is transferred co-translationally to the asparagine (N) residue of the consensus sequence N-X-S/T of the newly synthesized polypeptide by the oligosaccharyl-transferase complex. Glucose trimming is sequentially performed by Glucosidase (Glc) I and II. When only one glucose residue is left, the lectin chaperones CNX (membrane-bound) or CRT (soluble) can bind the *N*-glycosylated polypeptide. Other chaperones like the protein disulfide isomerase (PDI) family member ERp57 are recruited and aid in protein folding. The final glucose is trimmed by Glc II, releasing the correctly folded protein from the ER to be further transported to the ER-Golgi intermediate compartment (ERGIC) and Golgi. If the polypeptide is still not natively structured, the folding sensor UDP-glucose:glycoprotein glucosyltransferase (UGGT) adds a glucose residue to the folding intermediate, making it a substrate for the CNX/CRT cycle. Ultimately misfolded proteins are recognized by the ER Mannosidase (ER Man) I or by ER degradation enhancing α-mannosidase-like proteins (EDEMs). Mannose trimming targets the protein to the ER-associated degradation (ERAD) pathway.

Given that the mannosidase acts quite slowly, this enzymatic trimming is thought to have some kind of timer function [37]. As mannose-trimmed proteins are excluded from reentering the CNX/CRT cycle, the protein is targeted for degradation via ERAD [38]. This elaborate ERQC mechanism is of outmost importance since CNX/CRT was found to interact with practically all glycoproteins investigated to date [31].

After successful protein folding and release from the ER, the *N*-linked glycan is further modified, acquiring a more diverse and complex structure while the glycoprotein traverses the ER-Golgi intermediate compartment (ERGIC) and Golgi to its final intracellular or extracellular destination. The Golgi apparatus provides another layer of glycosylation QC and secures reliable sugar chain processing as the glycan patterns are functionally linked to protein trafficking and sorting [39]. Hydrophilic carbohydrate modifications of proteins facilitate not only QC mechanisms, but also have beneficial effects in the final extracellular milieu by increasing protein solubility, enhancing thermodynamic stability, diminishing the aggregation propensity, and protecting from proteolysis [40]. Moreover, dependent on the primary, secondary, and tertiary structure, *O*-glycosylation of a serine or threonine residue can be initiated in the Golgi [41]. This modification expands glycan functions by its role in recognition processes, modulation of enzyme activity, and regulation of physiological or pathological signaling [41]. Taken together, differential terminal glycosylation allows a fine-tuning of protein properties without an underlying change in amino acid sequence of the protein [37].

### 1.2.3 The endoplasmic reticulum as a home for chaperones

Folding within the ER is assisted by chaperones, which interact transiently with unfolded or partially folded proteins to stabilize them, prevent protein aggregation, and aid in native structure formation. Furthermore, they act as folding sensors during ERQC. The main ER chaperone families are the HSP70 family, the HSP90 family, the HSP40 family, peptidyl-prolyl isomerases (PPIases), lectin chaperones as described in 1.2.2, and thiol-disulfide oxidoreductases described in more detail in 1.2.4 [13]. In general, there is a large variety but also functional redundancy of ER folding factors [12].

For the classical HSP70 family, the glucose-regulated protein (GRP)78, also known as immunoglobulin heavy-chain binding protein (BiP), is the only ER-localized member and often referred to as master regulator of ER function [13]. By binding to various nascent or newly synthesized proteins, it assists in their folding (Figure 3). Like other HSP70 chaperones, it contains an ATPase catalytic site in the N-terminal adenosine nucleotide-binding domain (NBD) and a C-terminal substrate binding domain (SBD). Both domains are linked to provide allosteric coupling [42, 43]. This structural setup allows BiP to regulate

client binding and release by conformational changes and ATP hydrolysis. In an ATP-bound state, the SBD first recognizes and binds to exposing hydrophobic regions of the client protein, which is often recruited to BiP by a HSP40 cochaperone (Figure 3, step 1) [44]. The low-affinity client:BiP interactions with high on-off rates are stabilized upon ATP hydrolysis in the NBD. This triggers a conformational change to loose contacts between NBD and SBD and lid closing of the SBD (Figure 3, step 2) [45]. This ATP hydrolysis in BiP's nucleotide cycle is accelerated by the J domain of HSP40 cochaperones [46]. Release of ADP and rebinding of ATP is induced by nucleotide exchange factors (NEFs) like Sil1 or the HSP110 family member GRP170, and subsequently, the SBD lid reopens allowing the client protein to dissociate (Figure 3, step 3) [47].

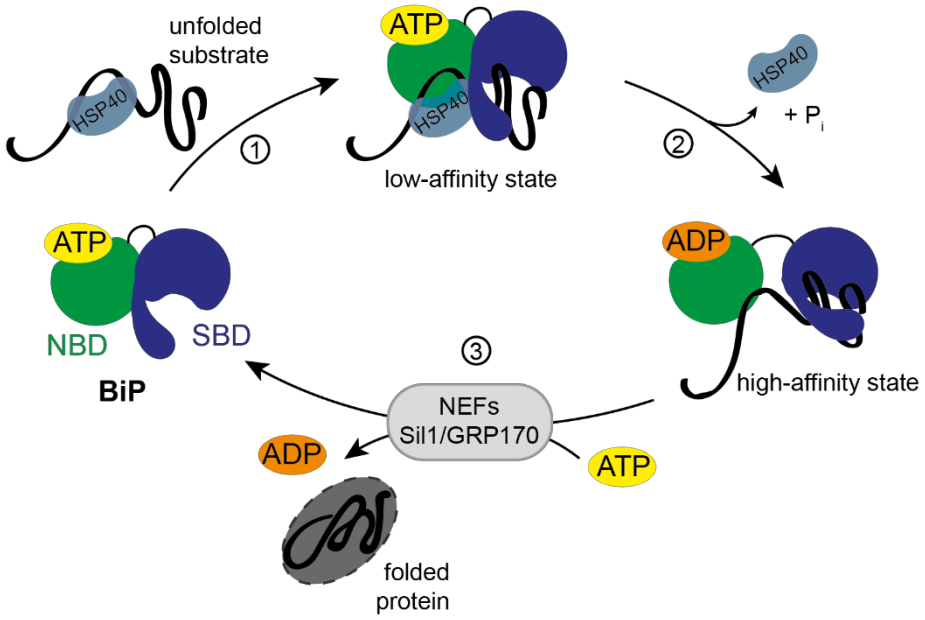


**Figure 3. ATPase cycle of immunoglobulin heavy-chain binding protein (BiP).** BiP consists of a nucleotide binding domain (NBD, green) with the ATPase catalytic site and a substrate binding domain (SBD, dark violet). The unfolded client protein often gets recruited by a HSP40 cochaperone to the SBD of BiP (1) which binds its substrate with low affinity and high on-off rates in the ATP-bound state. The HSP40 cochaperone stimulates ATP hydrolysis in the NBD upon which the cochaperone dissociates, NBD and SBD are in loose contact and BiP closes its lid (2). To induce substrate release from BiP, nucleotide exchange factors (NEFs) like Sil1 or GRP170 facilitate ADP-ATP exchange in the NBD resulting in lid opening of BiP.

This chaperoning cycle with BiP protects the unfolded protein with its surface-exposed hydrophobic regions from aggregation and helps in efficient folding to the native structure in which the hydrophobic residues should be buried [12]. The binding preference to short hydrophobic sequences explains BiP's vast client spectrum and how this chaperone discriminates between unfolded and folded proteins [43]. BiP is not only regulated by HSP40 proteins and NEFs but also interacts with protein disulfide isomerases (PDI) and PPIases [48]. Its role in assembly of protein complexes is well-studied for immunoglobulin (Ig)G antibodies [49]. IgG consists of two heavy and two light chains with four or two β-sheet structured Ig domains, respectively. As one can deduct from its name immunoglobulin heavy chain binding protein, BiP binds to one domain within the heavy chain: the

unassembled, unstructured $C_H1$ domain. In the absence of the light chain, association with BiP retains the incompletely assembled Ig intermediate in the cell, preventing it from immature secretion [50, 51]. Upon assembly with the light chain, the $C_H1$ domain is released from stable interaction with BiP and can form its intramolecular disulfide bridge as well as the covalent bond to the light chain [50]. This regulation mechanism is highly important as unassembled heavy chains have an incomplete antigen-binding domain which would lead to unspecific immune responses. Besides its role in productive protein folding, assembly control, and calcium homeostasis [12], BiP is also involved in ERAD and in regulating ER stress responses [52, 53].

For the HSP90 family, the only known ER member in humans is GRP94. Despite being one of the most abundant proteins in the ER, constituting around 5-10% of the ER luminal content with an approximate concentration of 10 mg/ml [54], it is not essential for viability and interacts with only a restricted set of protein substrates. It mainly recognizes incompletely assembled proteins, like for the major histocompatibility complex (MHC) class II [55], or already fully disulfide-bonded intermediates, like for the Ig light chain [56], but not early folding intermediates. Besides its role as ATP-hydrolyzing molecular chaperone [57], it was reported to function as peptide carrier for T cell immunization [58]. This remains highly controversial, as it does not seem to be a major *in vivo* function of GRP94 [59], and further functions of this abundant protein need to be defined.

Cochaperones of BiP belong to the HSP40/DnaJ family. In mammalians, there are eight members with a conserved J domain, thus termed ER DnaJ like proteins (ERdjs). Some of them bind directly to unfolded protein substrates of the secretory pathway and transfer them to BiP while at the same time stimulating BiP's ATPase activity (Figure 3). As they have a lower affinity to BiP in its ADP state, they dissociate from BiP after client transfer [60]. Other properties of ERdjs include association with the translocon (ERdj1-3) or with the retrotranslocon (ERdj4), reductase activity as PDI family member (ERdj5), aiding in protein maturation (ERdj6), protein sorting to lysosomal degradation (ERdj8), and ER stress or ERAD functions (ERdj3-6) [12, 43]. For ERdj7, functional insights are still missing. All these functionalities, supporting folding or assisting in degradation, are connected to BiP functions. Interestingly, ERdj3 and ERdj6 can exit the ER and localize to the extracellular space or cytosol during ER stress [61, 62].

Another ER-resident chaperone family, that is involved in protein folding, are the PPIases. In accelerating the *cis/trans* isomerization of the peptide bond preceding prolines, which is a rate limiting step in structure formation, they assist in rapid folding but also ERAD [63]. Prominent members are the BiP-associated FKBP7 [64] and cyclophilin b, that promotes folding of the $C_H1$ domain of IgG proteins [65].

### 1.2.4 Oxidative folding in the endoplasmic reticulum

Disulfide bond formation is largely restricted to secreted proteins and proteins that are resident in organelles of the secretory pathway. Folding, stability, and oligomerization of such proteins often depend on disulfide bridges within their structure. This finding is supported by the fact that inhibition of disulfide bond formation by the reducing agent dithiothreitol (DTT) induces ER stress [66]. An explanation for this stress induction, besides misfolding, is that unpaired cysteines are often handles in the ERQC system. Disulfide bond formation is an error-prone modification as wrongly connected cysteines occur [67] and bond formation is rather slow, thus limiting protein folding and secretion [68]. The chaperone family responsible for catalyzing the reduction, formation, and isomerization of disulfide bonds in proteins is the PDI family [69]. In general, intra- or intermolecular disulfide bonds in proteins are formed by oxidation of two free thiols. To act as thiol-disulfide oxidoreductases, PDI family members contain the catalytic active-site CXXC motif within thioredoxin-like domains [70]. The two cysteines of the motif allow these chaperones to exchange disulfide bonds and allow disulfide bonding in clients (Figure 4). By being structurally diverse and consisting of different numbers of thioredoxin domains, PDIs have evolved a large functional spectrum with distinct substrate specificities, redox propensities, or additional chaperone functions [71, 72]. Moreover, the affiliation to this family is rather founded on ER localization and similarity in sequence and structure, with the thioredoxin-like domain as common unit, than based on the same functionality. This becomes clear as some of the approximate 20 members have just one cysteine residue or a non-catalytic thioredoxin-like domain, like ERp27 that lacks the active site cysteines [73].

The founding member of this family is PDI [74]. PDI interacts with a broad range of substrates and can introduce disulfides by oxidase activity, break disulfides as reductase or rearrange incorporated disulfide by its isomerase functionality. By binding to polypeptides, it prevents protein aggregation as molecular chaperone [68]. In contrast, ERp57 interacts very specifically with *N*-glycosylated proteins to catalyze disulfide bond formation of bound glycoproteins in association with CNX/CRT (Figure 2) [75]. Furthermore, it has been shown that ERp57 reduces disulfides of partially folded proteins and thereby assists in ERAD-associated retrotranslocation of these proteins [76]. In general, ER retention of PDIs is secured by a C-terminal ER retention signal sequence, KDEL, making them ER-resident proteins. Different from that, ERp44 localizes mainly to the ERGIC and cis-Golgi, corresponding with its role as patrolling PDI. It not only controls the secretion of assembled, disulfide-linked oligomers as second checkpoint in the post-ER pathway but also keeps key ER enzymes, devoid of localization motifs, in the ER [77]. For pro-inflammatory and cysteine-rich cytokines, like heterodimeric interleukin (IL)-12 and the

α-subunit IL-23α, ERp44 controls the complete and correct assembly [77-79]. A different function apart from oxidoreductase functionality is reported for ERdj5, which comprises five thioredoxin-like domains and one N-terminal J-domain, which mediates binding and stimulation of ATP-hydrolysis of BiP [80]. Another PDI member which associates non-covalently with BiP is ERp5. It exhibits substrate specificity towards BiP clients [81]. In ER stress, ERp5 also associates with proteins of the unfolded protein response (UPR) pathway, maintaining this cellular reaction in a physiological range [82].

As PDIs help reduced nascent proteins to form disulfides, PDIs in turn are reduced (Figure 4, step 1). To maintain the PDIs' function in oxidative folding, the ER must provide oxidizing equivalents. The ER oxidoreductin-1α (Ero1α) and Ero1β are enzymes required to re-oxidize PDIs by electron transfer to their cofactor FAD (Figure 4, step 2) and finally to oxygen, leading to hydrogen peroxide formation as by-product (Figure 4, step 3). Ero1α has four cysteines which are used as electron shuttles and furthermore provide the possibility for a feedback mechanism in which its oxidase function is controlled by the redox state as well as PDI substrate availability [83]. To regulate the production of potentially harmful reactive oxygen species, peroxide-consuming processes involve mammalian ER peroxidases that reduce $H_2O_2$ to water [84-86].

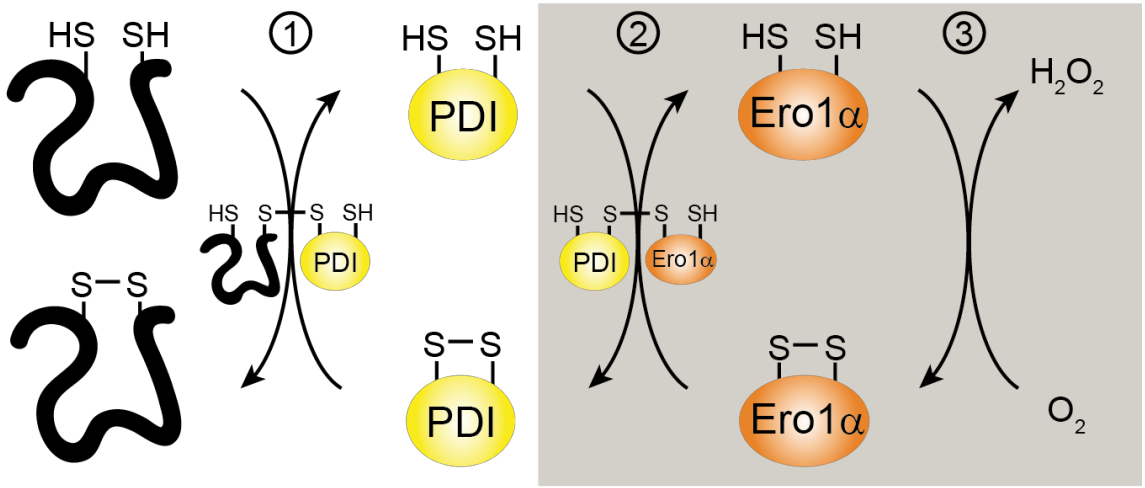


**Figure 4. Protein disulfide isomerase (PDI) activity cycle.** The thiol-disulfide oxidoreductase PDI catalyzes disulfide bond formation of reduced client proteins by disulfide interchange activity (1). A mixed disulfide between the client protein and PDI occurs as intermediate of this redox reaction. To maintain oxidase activity of PDI, regeneration of PDI is required (shaded in orange). PDI is re-oxidized by ER oxidoreductin-1α (Ero1α) (2) utilizing oxygen as final electron acceptor, resulting in hydrogen peroxide generation as by-product (3) that is detoxified to water by ER peroxidases.

### 1.2.5 Maintaining cellular proteostasis by ER-associated degradation

Even though proteins are stabilized by a vast repertoire of molecular chaperones [7] and undergo diverse posttranslational modifications like glycosylation, disulfide bond formation, proline isomerization, or lipidation that support their folding process [87], misfolding can

occur. Non-native, incompletely folded proteins are retained within the ER and are selectively degraded if folding and maturation eventually fail [13]. Degradation of accumulated misfolded or misassembled proteins in the ER by ERAD helps to maintain protein homeostasis. Degradation is physically separated from ER folding by utilizing the cytosolic ubiquitin-proteasome system [38, 88]. For that, the ERAD substrate is identified by ERQC-associated chaperones or lectins, which keep their substrates in a degradation-competent state. Retrotranslocation from the ER to the cytosol takes place in an energy-dependent manner and the substrate is polyubiquitinated by E3 ubiquitin ligases to finally get degraded by the proteasome [89, 90]. Besides ERAD, ER-phagy allows to engulf whole parts of the ER network by autophagosomes, which results in degradation by fusion with the lysosome [91]. Other cellular degradation pathways are linked to the Golgi QC and plasma membrane QC, which might either act substrate-specific or in some cases cooperate with the other pathways to prevent fatal cellular imbalance [89]. Under stress conditions, unfolded proteins might severely accumulate in the ER lumen and activate the UPR pathway. It is mediated by ER stress transducers IRE1, PERK, and ATF6, whose activation proceeds independently from each other in ER-stressed cells. The UPR helps to reduce the protein load in the ER by attenuation of general protein synthesis and translocation, and increases levels of chaperones and ERAD proteins by transcriptional activation. For example, UPR induces EDEM1 overexpression and thereby accelerates protein degradation, in this case even independent of both glycosylation and mannose trimming of *N*-glycans [92]. Thus, UPR enhances the cellular capacity to cope with an overwhelming mass of misfolded proteins. Nevertheless, if severe ER stress persists, UPR can lead to cell death [93].

## 1.3 Overview of our immune system

In our daily life, our immune system is nothing we perceive actively. Nonetheless, whenever it is out of balance or when we are sick, we are reminded of how important this overarching system is for our everyday wellbeing. The mechanisms by which our immune system functions are complex. To break it down, there are two main branches of immunity: the innate and adaptive immunity (Figure 5) [94].

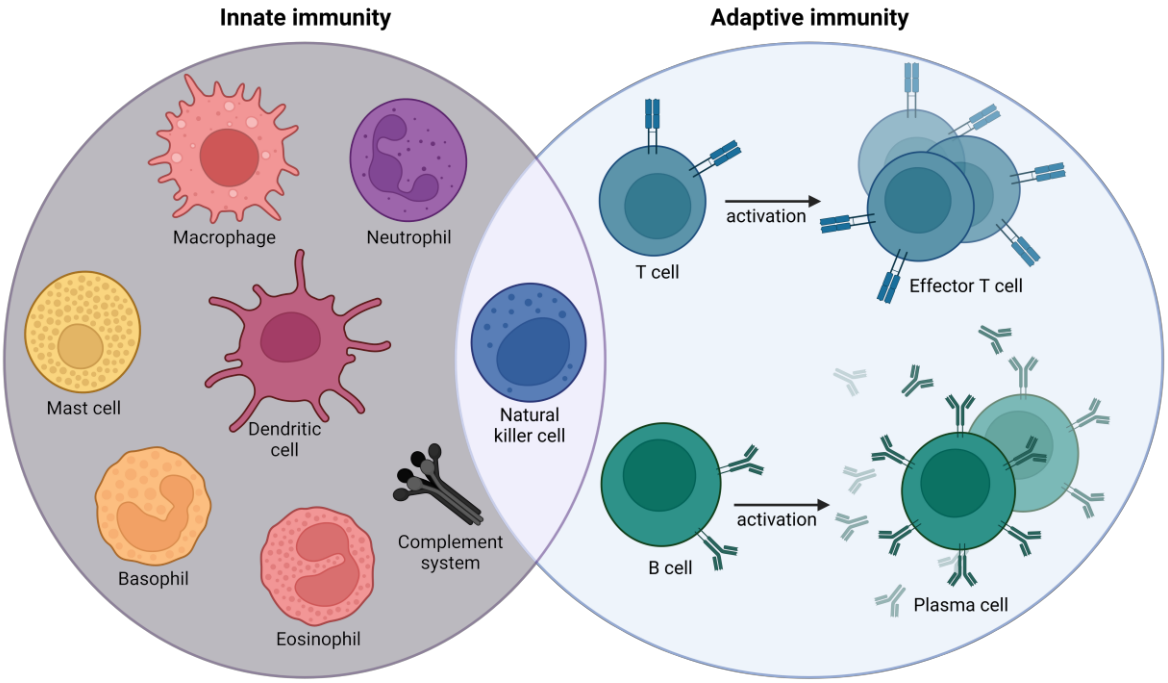


**Figure 5. Cellular composition of the innate and adaptive immunity.** The innate immune system allows a rapid first line of defense against pathogens utilizing physical barriers, cytokine production, complement activation, and innate immune cells. A slow, but highly specific immune response is mediated by cells of the adaptive immunity resulting in the production of antigen-specific antibodies by plasma cells or in effector T cells.

The innate immunity utilizes germline-encoded receptors to distinguish self from non-self and recognize molecular patterns of infectious non-self. These pattern recognition receptors bind to conserved pathogen-associated molecular patterns (PAMPs) of pathogens trying to enter via skin, respiratory, or gastrointestinal routes [95, 96]. The innate immune system also discriminates safe from dangerous molecules. If the host cell is damaged or dying, molecules from within cells are released and recognized as damage-associated molecular patterns (DAMPs) [97]. Mannose-binding lectin is a soluble pattern recognition molecule, whereas Toll-like receptors are pattern recognition receptors on the cell surface. Cell types bearing such innate receptors are natural killer (NK) cells, dendritic cells (DCs), mast cells, basophils, eosinophils, and phagocytes (Figure 5, Innate immunity) [95, 98]. After receptor binding, downstream signaling leads to rapid cell differentiation into short-lived effector cells by differential gene expression. Common functions to get rid of infections are antigen presentation, apoptosis, inflammatory chemokine and cytokine expression, and phagocytosis [99]. Another innate effector function is mediated by the complement system. It is composed of inert serum or membrane-associated proteins that can identify pathogens or damaged cells and lead to enhanced clearance of these by patrolling phagocytic cells as well as by cell lysis [100]. For example, macrophages and neutrophils are both phagocytes that engulf pathogens to mediate clearance. This innate activation allows immediate induction of pro-inflammatory, antimicrobial immune responses [101].

Adaptive immunity, on the other hand, is more a somatic memory with antigen-specific effector cells, where specificity results from receptor gene arrangement. These cells recognize rather details of the pathogen's molecular structure and form an acquired immune response [94]. Especially if pathogens escape the early, innate immune responses, this system comes into action. Due to being highly antigen-specific, effector activation is not immediate but delayed [102]. Cells of the adaptive immune system include T lymphocytes, which mature in the thymus, and B lymphocytes as antibody-producing cells originating from the bone marrow (Figure 5, Adaptive immunity). Both express antigen-specific receptors and are activated by antigen-presenting cells (APCs), such as macrophages, B cells, or DCs. For example, upon innate immune stimuli, DCs degrade foreign proteins into peptides by macropinocytosis and load them onto MHC class II molecules. Naïve CD4+ T cells can recognize the presented peptides and get activated and differentiate. Here, cytokines come into play: Different DCs secrete different cytokines upon distinct innate signals. These cytokines are means of immune cell communication and generate specific adaptive immune responses by receptor binding and signaling, thus bridging innate and adaptive immunity. Likewise, B cell development is dependent on antigen contact and cytokine stimuli by activated cells [102]. B cells differentiate either in short-lived antibody-secreting plasma cells or memory B cells, which facilitate more rapid immune responses upon repeated antigen exposure. A special B cell subset are regulatory B cells (Bregs), which limit ongoing immune responses to counterbalance immune overreactions and reestablish immune homeostasis [103]. T lymphocytes can be classified into two, functionally distinct T cell subtypes based on their cluster of differentiation surface markers. The first subtype are T helper cells (Th, CD4+) comprising Th1, Th2, Th17, Th9, and regulatory T cells (Tregs). Differentiation, starting from an antigen-specific, naïve Th0 cell, is dependent on the type of interacting APC and the prevailing cytokine milieu. Th subsets are distinct in the cytokines they secrete and thereby shape the cellular immune reaction differently. Similar to Bregs, Tregs are essential for maintaining tolerance and limiting chronic inflammations by their suppressive functions. However, they can thereby also limit antitumor immunity [104]. In contrast, the main function of the second subtype, cytotoxic T cells (CD8+), is the direct elimination of infected cells or tumor cells which they recognize during circulation via antigen-T cell receptor (TCR) interactions [102].

NK cells exert biological functions that can be attributed to both innate and adaptive immunity and thereby blur the borders between the two arms of immunity (Figure 5). Due to their constitutive cytotoxic functions, they act like effector lymphocytes of the innate immunity. But they also show attributes of the adaptive immunity: They can dynamically adapt their functions to the environment, possess activating and inhibitory receptors, and there is evidence for an NK cell antigen-specific memory [105].

## 1.4 Introduction to the interleukin 12 cytokine family

As our immune system is an immensely complex, multi-layered system in which immune reaction homeostasis and regulation are vital, immune cell communication has to be efficient and reliable. This is, among others, ensured by regulatory cytokines, the ILs. As soluble peptide hormones, they get secreted by immune cells, regulate cell proliferation, inflammation, and immunity by binding to their respective receptors, and perform multifaceted functions [106]. To date, more than 60 cytokines have been designated as ILs [107], which are classified according to their structural features. Among those, only four belong to the IL-12 family, which stand out due to their unique structural properties. In contrast to other human ILs, it is the only cytokine family with a strictly heterodimeric setup. Each heterodimer consists of one four-helix bundle α-subunit with α-helices arranged in an up-up-down-down fashion, and one all-β structured β-subunit with fibronectin type III (FnIII) and, in case of IL-12β, Ig-like domains (Figure 6A). The four members of the IL-12 cytokine family are made up of only five subunits, three α- and two β-chains, thus extensive subunit sharing is a key feature (Figure 6B) [108]. The family includes IL-12 comprising IL-12α (also called IL-12p35) and IL-12β (IL-12p40), IL-23 composed of IL-23α (IL-23p19) and IL-12β, IL-27 comprising IL-27α (IL-27p28) and Epstein-Barr virus-induced gene 3 (EBI3 or IL-27β), and IL-35 composed of IL-12α and EBI3. IL-12 and IL-23 are disulfide-linked heterodimers, whereas the subunit interactions within IL-27 and IL-35 are non-covalent [108].

The chain-sharing theme also applies to the IL-12 family receptors, which are heterodimers as well and partially composed of shared receptor chains, but with completely distinct downstream signaling for each IL (Figure 6C). Signaling is transduced by the receptor chain heterodimers, activating the Janus kinase (Jak)-signal transducer and activator of transcription (STAT) signaling pathway to direct intracellular transcription [109]. An exception here are IL-35 signaling receptors, which can be also homodimeric (Figure 6D, right) [110, 111]. IL-12 family cytokines bridge the innate and adaptive immune system, as they are produced by APCs and regulate T cell functions, except IL-35, which is mainly secreted by Treg and Breg cells [108, 112]. The functional spectrum of the IL-12 family ranges from mostly pro-inflammatory to immunomodulatory to mostly inhibitory [108]. That these multifaceted functions are required for a balanced immune reaction becomes clear in host defense and pathologies like autoimmunity and cancer.

Even if the existence of further IL-12 family members remains debated, new subunit pairings were reported (Figure 6D, left). IL-27α and IL-12β were synthetically fused to obtain so-called IL-Y [113], and a cytokine termed IL-39 of IL-23α pairing with EBI3 has been reported in mice, but not in humans [114, 115]. Further expanding IL-12 family cytokine functions,

some isolated IL-12 family subunits are secreted and have immunological roles on their own (Figure 6D, middle). These functions can be mediated by pairing with other secreted cytokines or soluble receptor chains [116-120].

In this heterodimeric IL-12 family, chain sharing promiscuity is a common feature. Because of its immunological potency in connecting the innate and adaptive immunity, there needs to be tight regulation and control for cytokine biogenesis and secretion. For human IL-12 cytokines, a clear principle underlying their biogenesis could be identified: In isolation, α-subunits are incompletely folded and are dependent on their β-subunits for efficient secretion [78, 79, 121]. If remaining unpaired, α-subunits are targeted for ERAD [122]. In contrast, the β-subunits are secreted on their own and induce secretion of their respective α-subunits by assembly-induced folding of these, representing a regulatory layer in cytokine biogenesis which can be also found for other proteins of our immune system like antibodies and the TCR [49, 123]. Intriguingly, for murine IL-27, this behavior in secretion-competency is reversed for its α-subunit IL-27α and its β-subunit EBI3 [121, 124]. As human β-subunits are secretion-competent, an additional layer of complexity but also regulation in cytokine signaling arises from reported autonomous immunological functions of these single subunits [116, 125-131]. Another control mechanism in IL-12 family cytokine biogenesis is the engagement of the cellular chaperone machinery in which hydrophobic regions or cysteine residues in α-subunits are often involved as stabilizing anchors [78, 79]. Glycosylation of the IL-12 family cytokines would not only allow recruitment of lectin-based chaperones, but might also have general stabilizing effects on the heterodimers [12].

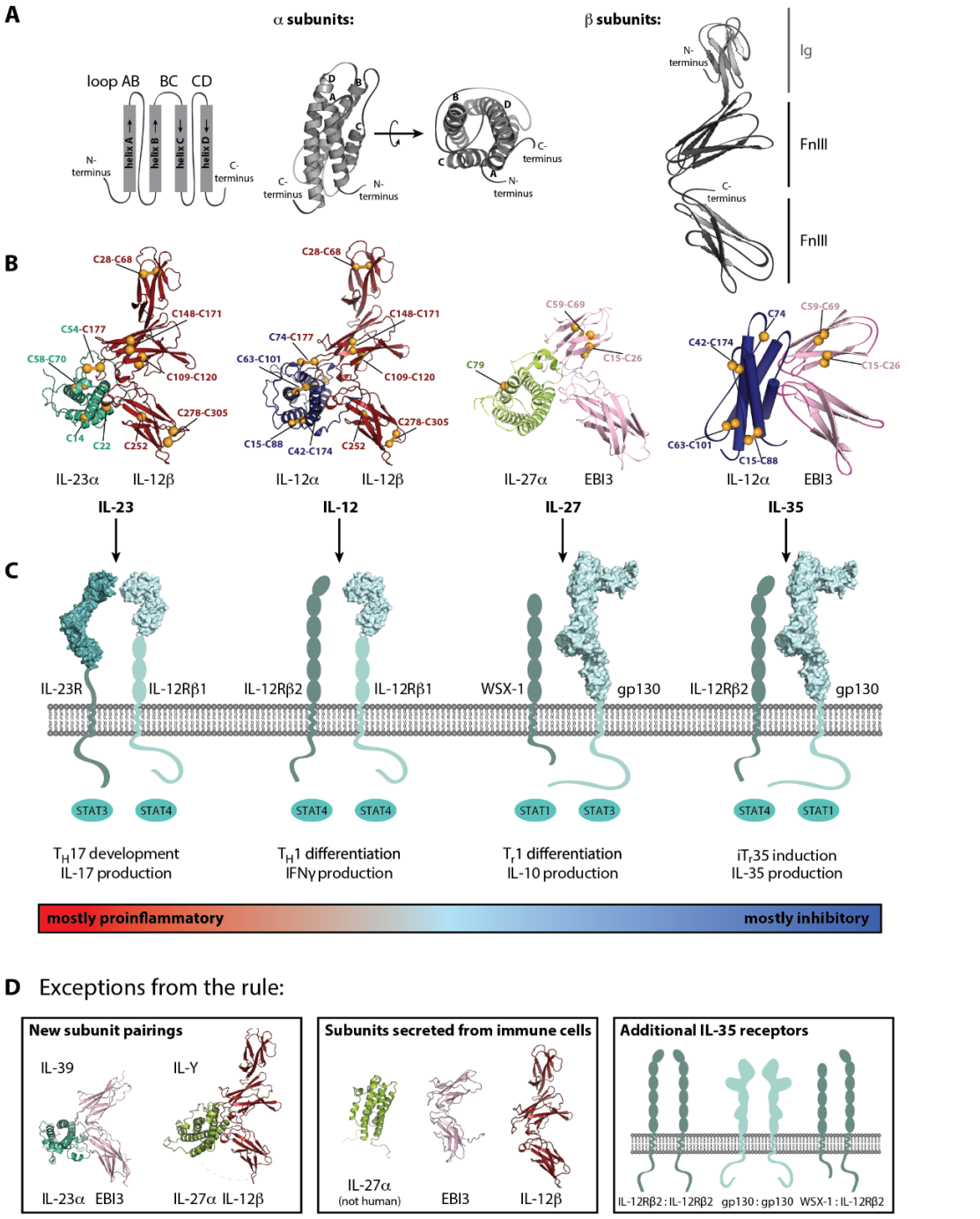


**Figure 6. Structure, functions, and exceptions from general principles behind interleukin (IL-12) cytokines and receptors. A.** Structural features of IL-12 family subunits. The α-subunits are four-helix bundle proteins with an up-up-down-down topology of helices connected via loops. The β-subunits comprise two fibronectin type III (FnIII) domains and, in the case of IL-12β, one N-terminal immunoglobulin (Ig)-like domain. **B.** The heterodimeric IL-12 family members share their chains, at which one α-subunit (IL-23α, IL-12α, IL-27α) pairs with one β-subunit (IL-12β, EBI3) to form IL-12, IL-23, IL-27, or IL-35, respectively. For IL-23 (PDB: 3D87), IL-12 (PDB: 3HMX), and IL-27 (PDB: 7ZXK), crystal structures are depicted, whereas for IL-35 a hypothetical model is shown. Free cysteines and disulfide bonds are highlighted as orange spheres, residue numbering begins after the signal sequence. **C.** Chain sharing further extends to IL-12 family receptors, which form heterodimers to transmit IL signaling via the Janus kinase (Jak1, Jak2, Tyk2)-signal transducer and activator of transcription (STAT1, STAT3, STAT4) pathway. High-resolution structures are shown for IL-23R (PDB: 5MZV), gp130 (PDB: 3L5H), and IL-12βR1 (PDB: 6WDP). The functional spectrum ranges from mostly pro- to mostly anti-inflammatory. **D.** Left: New, but still rather hypothetical IL-12 family members IL-39 and IL-Y. Middle: Single subunits expanding the IL-12 cytokine repertoire. Right: Additional receptor chain pairings for IL-35, reported for murine T and B cells [110, 111]. This figure was taken from [132] and was edited according to recent structural work [133].

## 1.5 Structural insights and cellular regulation of IL-12 cytokine biogenesis

In general, IL-12 family members are heterodimers consisting of an α-subunit and a β-subunit. To form the functional α:β heterodimer and eventually be secreted, subunits first need to assemble in the ER to follow the eukaryotic secretory pathway. Along this path, IL-12 cytokine biogenesis is not only supported by cellular machineries but also regulated to control immune system functions. With the focus on human IL-12 cytokines, the structural prerequisites and layers of cellular regulation in successful cytokine biogenesis in the ER will be described in the following.

### 1.5.1 Structural features of the IL-12 family

Evolutionary evolved from 'classical' cytokines and their receptors, the IL-12 family heterodimers resemble a helical cytokine and its receptor [134]. Like for other type I cytokines, the α-subunits (IL-12α, IL-23α, and IL-27α) belong to the class of the long chain four-helix bundles with the arrangement of helices A-D in an up-up-down-down topology [135]. Long AB- and CD-loops permit this kind of helix arrangement [136]. The β-subunits (IL-12β and EBI3) structurally resemble the extracellular, cytokine-binding homology region (CHR) of class I α-chain receptors containing tandem FnIII domains (Figure 6A) [137]. These receptors interact with cytokines through loops at the boundary of the two FnIII domains (Figure 6B) [138]. A hallmark pattern of two inter-strand disulfide bridges in the N-terminal FnIII domain and the highly conserved WSXWS motif in the second FnIII domain characterize these subunits [136, 139-141]. For the IL-12/IL-23 β-subunit, aromatic residues of its WSEWA motif are involved in intramolecular π-cation stacking [142]. Moreover, IL-12β contains an additional N-terminal Ig-like domain (D1), which fold was structurally first described by Yoon et al. [136]. The relative orientation of D1 to the FnIII domains (D2, D3) is unusual because of its nearly orthogonal engagement, but is structurally supported by an N-linked sugar modification, which extends across the D1-D2 interface [136, 142]. The β-subunit EBI3 lacks the Ig-like domain [143, 144].

According to an IL-6 structure-based "site 1-2-3" architectural paradigm, these heterodimeric cytokines have three distinct sites of interaction in which the α-helical cytokine represents the center of the complex [141, 145]: Site 1 is the interaction site between the four-helix bundle α-subunit to its soluble receptor, thus β-subunit. For IL-12 family members, this site corresponds to the heterodimer interface, which will be described in more detail in the following. The numbering of amino acids is adapted to central structural publications, for IL-12 [136] and IL-23 [142] excluding the ER signal sequence, and for IL-27 [121, 133, 146-148] counting residues including the ER signal sequence. Site 2 and 3 both

mediate interactions between the cytokine and receptor chains. Structural characteristics of IL-12 cytokines binding to their respective receptors are summarized in 1.6.

### 1.5.2 Biogenesis of IL-12

Human IL-12 was first described in 1989 as natural killer cell stimulatory factor [149]. This heterodimer comprises the α-subunit IL-12α,p35 which is disulfide-linked to the β-subunit IL-12β,p40 [136]. Based on the crystal structure and comprehensive analyses, the unique structural nature and, particularly, its heterodimerization interface could be revealed (Figure 7A, box). Distinct from other class I cytokine-receptor complexes, the α:β binding interface is characterized by an interlocking topography with the central arginine residue Arg189 in IL-12α helix D projecting into a deep arginine-binding pocket of IL-12β. This pocket has a negatively charged Asp290 at its base to form an Arg-Asp salt bridge and is surrounded by several other charged residues as well as hydrophobic interactions extending the interface [136]. Subunit interactions are mediated by helices A and D as well as the AB-loop of IL-12α, which pack against the connecting loops of FnIII domains, thus D2 and D3 of IL-12β. The interchain disulfide bond is formed by Cys74, located in the AB loop of IL-12α, and Cys177 of IL-12β. This bond is stabilizing, but not required for heterodimerization [78, 136].

In contrast to the well-defined and specific α:β interface, IL-12α misfolds in isolation, forming incorrect disulfide bonds and various molecular redox species, including homodimers and oligomers [78]. This misfolding results in recognition of IL-12α by ER chaperones, including PDI family members, and cellular retention [78, 150, 151]. Based on the investigation that two of the three intramolecular disulfide bonds of the α-subunit are dispensable for assembly-induced folding by the β-subunit and subsequent IL-12 secretion [78], IL-12α cysteine:PDI interactions might rather have a regulatory function. In contrast to IL-12α in isolation, co-expression of its β-subunit inhibits or corrects α-subunit misfolding by efficient assembly into its native structure and allows secretion of the covalently linked IL-12 heterodimer [78, 152] (Figure 7A). Nevertheless, it is intriguing that intracellular IL-12α forms well-defined homodimeric species, thus arguing for partial structuring if unpaired. Additionally, even when seemingly misfolded, at least parts of the above-described dimerization interface may be present to allow rapid rescue by IL-12β and ensure secretion of mostly pro-inflammatory acting IL-12. Besides the importance of oxidative folding in IL-12α biogenesis, IL-12 subunits undergo glycosylation as posttranslational modification [153-155]. Apart from typical intracellular assembly, a two-cell version of IL-12 in pathogen dissemination i*n vivo* is discussed [118]. If IL-12β is absent, IL-12α is degraded via ERAD [122], in which the PDI ERdj5 might act as ER reductase to promote efficient degradation

of misfolded protein [78]. Unlike IL-12α, the human IL-12β is secreted alone, acting as independent cytokine in its monomeric and homodimeric forms [126, 128, 131, 156].

### 1.5.3 Biogenesis of IL-23

IL-23 is a disulfide-bonded heterodimer, comprising IL-23α,p19 and IL-12β,p40 [157]. Even though sharing the subunit IL-12β with IL-12, an altered docking mode of the four-helix bundle α-subunit to the common β-subunit could be revealed within the IL-23 crystal structure [142]. A somewhat tilted and rotated arrangement of the α:β heterodimer results in a different footprint of IL-12β binding to helices A and D of IL-23α or IL-12α, respectively. Therefore, a charged Arg159 of IL-23α projects into the IL-12β arginine-binding pocket with Asp290 at its base, surrounded by a network of hydrophobic contacts as well as hydrogen bonds in the surrounding shell (Figure 7B, box). Like in IL-12, IL-23α is disulfide linked to IL-12β via its Cys54 located in the AB loop. Compared to the largely disordered AB loop in IL-12α, this covalent linkage leads to numerous more, surrounding AB loop residues that contribute to the IL-23 interface. Even though the critical hotspot of IL-12 is mimicked by interaction of IL-23α with IL-12β, and the β-subunit utilizes the same binding surface to contact its α-subunit, most residues involved in the interface are unique pairwise contacts, which make them promising targets in therapeutics. These structural differences might also be explained by only 15% sequence identity between IL-12α and IL-23α [142].

Similar to the α-subunit of IL-12, IL-23α forms multiple, non-native redox species if unpaired [78, 79] and depends on the shared β-subunit for assembly-induced secretion [157]. The only cysteine residues required for IL-23 biogenesis form a single internal disulfide bond within correctly folded IL-23α, whereas the two free cysteines and the interchain cysteine are dispensable for α:β heterodimerization and IL-23 secretion [79]. Nevertheless, those cysteines induce IL-23α dimer formation in isolation. Unpaired IL-23α seems to be highly flexible and helix A is largely unstructured [79] (Figure 7B). As this first helix also contains the free cysteine residues, it is not surprising that these residues act as chaperone binding sites of IL-23α, stabilizing the protein while unassembled and preventing premature degradation. Like for IL-12α, cellular retention is mediated by interaction of IL-23α with PDIs, e.g., the ER recruitment chaperone ERp44, acting synergistically with HSP70 chaperone BiP [79]. Upon assembly with IL-12β, folding of IL-23α, especially of its helix A, is induced and chaperone recognition sites become buried within the native structure [79]. This allows passing the ERQC and release from the ER after productive oxidative folding of IL-23α and α:β assembly.

### 1.5.4 Biogenesis of IL-27

The non-covalent heterodimer IL-27 consists of the α-subunit IL-27α,p28 and the β-subunit EBI3 [124]. EBI3 is rather unique among the IL-6/IL-12 family members as it lacks the N-terminal Ig-like domain [143]. Based on structural similarities of IL-27α to other IL-6 family cytokines, i.e., ciliary neurotrophic factor (CNTF), cardiotrophin-like cytokine (CLC), and neuropoietin (NP), conserved key residues of interface interaction were identified (Figure 7C, box): The aromatic, solvent-exposed residue Trp97 of IL-27α binds to Phe97 of EBI3, dominating a rather hydrophobic area. This interaction is surrounded by the positively charged arginine residue Arg216 of IL-27α and negatively charged residues of EBI3 [146, 158]. This type of “knobs and holes” shape for interface residues could be verified via mutation and can be also found for other cytokines [144]. Available IL-27 models are in accordance with the recently solved crystal structure for IL-27 [133] and high-resolution cryo-electron microscopy (cryo-EM) analyses of the quaternary IL-27 receptor complex [133, 147, 148], which confirm that helices A and D, the AB loop, and the C-terminus of IL-27α are involved in α:β heterodimer interface interactions.

This IL-27α:EBI3 heterodimerization is a prerequisite for human IL-27α secretion, as it is retained in the cell in isolation [121]. Like for the other IL-12 family α-subunits, ER retention and subsequent ERAD of unassembled IL-27α is mediated by chaperone binding. The unique glutamic acid stretch (poly-Glu loop) in its CD loop reveals to be structurally dynamic and exposed hydrophobic residues of IL-27α, which become buried upon EBI3 interaction, cause BiP binding [121] (Figure 7C). Assembly-induced stabilization of the four-helical subunit and heterodimer secretion is mediated by co-expression of the β-subunit EBI3 [124], allowing further posttranslational modification of IL-27 by *O*-glycosylation in the Golgi [121, 124]. In contrast to IL-12α and IL-23α, oxidative folding is not involved in human IL-27α biogenesis, as it has only one cysteine that remains free due to the non-covalent nature of IL-27 [121, 124].

### 1.5.5 Biogenesis of IL-35

The α-subunit IL-12α of IL-35 is shared with IL-12 and its β-subunit EBI3 is also a component of IL-27 [159]. Even though efficient subunit pairing of IL-12α with EBI3 was reported [160], the heterodimerization interface of IL-35 remains completely undefined. Mutation of critical and even peripheral residues for IL-12 and IL-27 heterodimerization [136, 142, 146] did not affect IL-12α/EBI3 pairing [160], indicating distinct structural criteria for subunit pairing compared to the other IL-12 family members. Also the observation that bacterially produced IL-12α can be reconstituted to form IL-12, and EBI3-conditioned

supernatant is sufficient to reconstitute IL-27, but both failed to rebuild IL-35 [161], suggests a rather transient, weak interaction between IL-35 subunits.

Even if this interaction is rather labile, pairing with EBI3 is required for IL-12α secretion as heterodimeric IL-35 [159]. Compared to efficient secretion of IL-12β, even in excess to IL-12 [162], EBI3 is secreted quite inefficiently in isolation [159]. This might be an explanation for also weak IL-35 secretion. Nevertheless, IL-35 subunits seem to mutually enhance their secretion by reciprocal stabilization (Figure 7D). Interestingly, EBI3, as rather instable subunit, was found to be associated with the lectin chaperone CNX [163]. Though CNX normally interacts with membrane-associated, newly synthesized glycoproteins [164], it was reported that EBI3 bound to CNX augments IL-23R expression by also binding IL-23R in a peptide-dependent manner, forming a tripartite complex [165]. Thus, EBI3 might exhibit chaperone-like, intracellular functions independent of its role as β-subunit in IL-27 or IL-35.

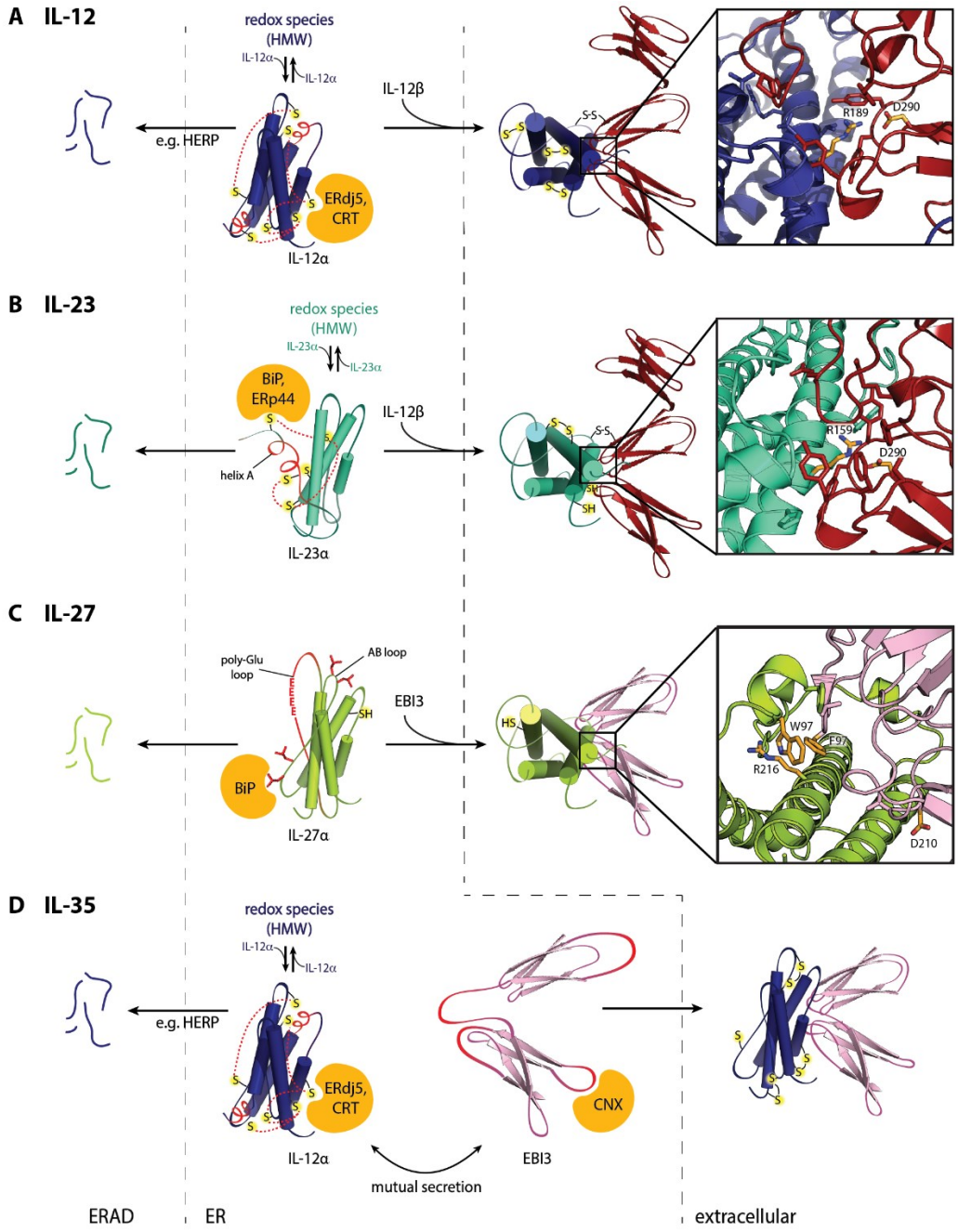


**Figure 7. Molecular mechanisms of IL-12 family cytokine biogenesis.** Overview of structural prerequisites in cytokine biogenesis. For each family member, molecular elements crucial for endoplasmic reticulum (ER) quality control are highlighted in red, and cellular chaperones involved in assembly control are depicted in orange. Successful biogenesis of heterodimeric cytokines in the ER allows proceeding along the secretory pathway until secretion into the extracellular space. If biogenesis fails, subunits get degraded via ER-associated degradation (ERAD). Subunit pairing represents a regulatory layer with precisely defined interactions in heterodimerization interfaces, which are shown as magnified images (boxes). Critical interface residues are labeled and marked in orange, with surrounding residues involved in stabilizing salt-bridges or hydrophobic interactions shown as sticks in the structures (IL-12, PDB: 3HMX; IL-23, PDB: 3D87; IL-27, PDB: 7ZXK). Residues are numbered without, for IL-12 and IL-23, or with, for IL-27, ER signal sequence **A.** IL-12α forms non-native redox species of high molecular weight (HMW) by disulfide bonds (red broken lines) in isolation and gets rescued by assembly-induced folding with IL-12β. Thus, disulfide-linked IL-12 forms by charged interaction involving the arginine-binding pocket and gets secreted. **B.** In absence of IL-12β, IL-23α also forms erroneous disulfide-linked redox species and is highly flexible in structure. Helix A is unstructured and acts, together with its two free cysteines, as chaperone recognition site. Covalent IL-23 heterodimers contain a charged interface. **C.** For IL-27α, exposed hydrophobic residues result in cellular retention if unpaired. The interface of non-covalently linked IL-27 comprises aromatic and charged interactions. **D.** Subunits of IL-35 mutually enhance their secretion by co-expression. By now, there is no structural data available for IL-35. This figure was taken from [132] and modified based on recent structural insights [133].

## 1.6 Structural characteristics of IL-12 family cytokine receptor complexes

Based on the similarity of IL-12 family cytokines to IL-6 family cytokines, structural principles of receptor complex formation were often derived from the four α-helix bundle IL-6 binding to its unique α-chain receptor IL-6Rα and the common glycoprotein (gp)130 chain (Figure 8) [145, 166]. Thereby, IL-6 interacts on opposing helical faces with IL-6Rα (site 1) and gp130 (site 2) before it engages a second gp130 molecule (site 3) to form the hexameric complex consisting of two molecules each of IL-6, IL-6Rα, and gp130 [145, 167]. For site 2, the CHR domain of the receptor chain is involved in binding, whereas for site 3 an N-terminal Ig-like domain of the second receptor is required. For IL-12 family member receptor chains, this Ig-like domain mediating site 3 interactions can be found only in gp130, for IL-27 and IL-35, IL-12Rβ2 for IL-12, and IL-23R for IL-23.The hexameric IL-6 receptor complex mediates signaling through the Jak/STAT pathway [168], which is also utilized by IL-12 family members.

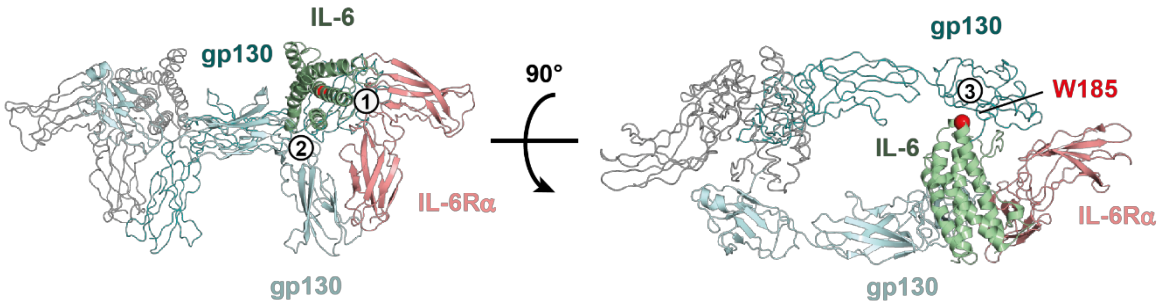


**Figure 8. Structure of the IL-6 signaling complex.** The hexameric receptor complex contains the α-helical IL-6 (green) binding to IL-6Rα (salmon) and gp130 chains (pale cyan and teal) (PDB: 1P9M). Secondary copies of IL-6:IL-6Rα are depicted in gray. Interaction sites 1-3 are marked with circled numbers. The critical tryptophan residue (W185) for site 3 interaction is highlighted as red sphere.

Due to recent analyses of IL-12 family cytokine receptor complexes [133, 147, 148, 169-171], we have access to detailed insights into the structural biology of the signaling complexes and their so-called site 2 and site 3 interactions. They are described in the following, with critical residues numbered including the signal sequence for all IL-12 family members. These findings help to better understand the diversity of immunological downstream functions, described in 1.7, even though mediated by shared receptor chains.

### 1.6.1 The IL-12 receptor complex

For IL-12, both signaling receptor chains IL-12Rβ1 and IL-12Rβ2 are similar to gp130 in sequence and structure [172]. Due to this similarity, a hexameric complex like for IL-6, composed of two IL-12 molecules and each receptor chain was proposed [136]. In contrast, a cryo-EM map of the complete IL-12 receptor complex revealed the quaternary assembly of (IL-12α/IL-12β)/IL-12Rβ2/IL-12Rβ1 (Figure 9) [170]. Unlike the IL-6 paradigm, which

states IL-6/gp130 site 2 being located opposite of IL-6/IL-6Rα site 1 on the four-helix bundle cytokine, IL-12Rβ1 binds directly to IL-12β and not to IL-12α [173]. This highly specific interaction of IL-12Rβ1 CHR with the intersection of Ig-like D1 and FnIII D2 of IL-12β comprises charge complementarity, hydrogen bonding, and also hydrophobic interactions [170]. This binding mode seems to be universal irrespective of IL-12β in IL-12, IL-23, or even monomeric IL-12β [169]. For site 3 interactions between IL-12 and the private IL-12Rβ2, residue Tyr189 in human IL-12α might be of relevance, though this remains more a speculation [174]. For biological functionality, this highly cytokine-specific interaction with IL-12Rβ2 at site 3 mediates intracellular STAT4 activation via phosphorylation by receptor-associated cytoplasmic Jak2 and Tyk2 tyrosine kinases [175, 176].

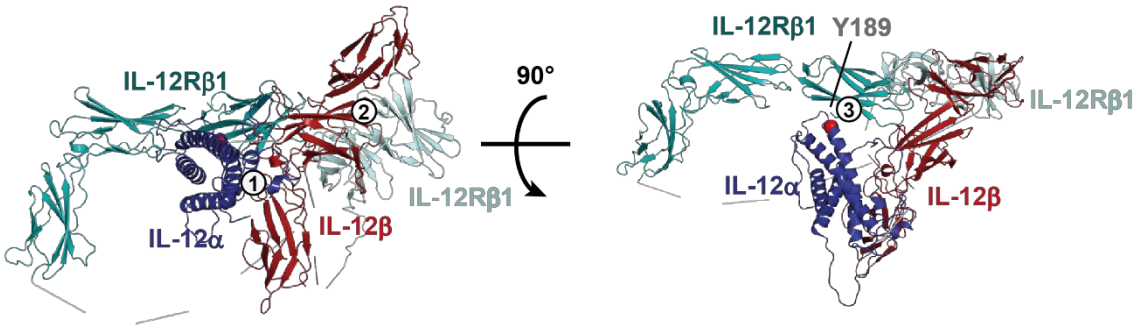


**Figure 9. Structure of the IL-12 signaling complex.** IL-12α (blue) binds to the β-subunit IL-12β (dark red) via site 1. Interaction site with receptor chains IL-12Rβ1 (pale cyan) or IL-12Rβ2 (teal) is labeled with site 2 and 3, respectively (PDB: 3HMX for IL-12, AlphaFold [8] for receptor chains with superposition on IL-23 receptor complex, PDB: 6WDQ). Interaction sites 1-3 are marked with circled numbers. Tyrosine residue (Y189) of IL-12α located at site 3 is highlighted as red sphere, even though functional relevance has not been shown until now.

Antagonization of IL-12 signaling was reported to be performed by IL-12β,p40 which has functional roles, e.g., as homodimer or in its monomeric form as anti-autoimmune cytokine requiring only IL-12βR1, and not IL-12Rβ2 receptor chain [128, 130, 177, 178]. These structural insights now allow fine-tuning of cytokine signaling by molecular engineering. A T cell-biased IL-12 partial agonist, which preserves interferon (IFN)γ induction by CD8+ T cells but impairs cytokine production from NK cells, could be engineered. This cytokine design allows reduction of IL-12 functional pleiotropy and supports anti-tumor effects without NK cell-mediated toxicity. The reason for this effect is that T cells react more sensitive to IL-12 compared to NK cells, as IL-12 receptor chains are upregulated on T cells by TCR antigen stimulation [170].

### 1.6.2 The IL-23 receptor complex

For IL-23, site 2 is identical to IL-12, as receptor chain IL-12Rβ1 is shared and the β-subunit IL-12β mediates receptor complex assembly in a convergent manner (Figure 10) [170]. Similar to the specific IL-12Rβ2 receptor of IL-12, the private receptor chain IL-23R

possesses an N-terminal Ig-like domain which engages with IL-23 according to available crystal structures [170, 171, 173] comparable to site 3 interactions between IL-6 and gp130 [145]. This interaction is anchored by the aromatic Trp156 residue in helix D of IL-23α which stacks against a peptide plane of a Gly residue in the IL-23R N-terminal Ig domain. This tryptophan turns out to be a crucial amino acid for IL-23 receptor complex structure and the pro-inflammatory functionality mediated by IL-23 binding [170, 171]. The IL-12β subunit helps in correctly positioning site 3 with its domains D2 and D3 [173]. The two FnIII domains of IL-23R, forming the CHR, are not involved in IL-23 binding [171]. Thus, IL-23R binding activates IL-23 for cooperative, high-affinity IL-12Rβ1 recruitment and formation of the cytokine-receptor complex [171], even though IL-23 subunits bind to individual IL-23 receptor chains [173]. Recently, a ligand-induced conformational change after high-affinity binding of IL-23 to the preformed IL-23R:IL-12Rβ1 heterodimer was proposed based on proximity-based Nano-bioluminescence resonance energy transfer (BRET) experiments [179, 180]. This requires complex formation of inactive receptor chains prior to IL-23 engagement to enable signal transduction [181]. Whereas IL-12β is a shared gateway for STAT signaling-induction by IL-12Rβ1/Tyk2 for cytokines IL-12 and IL-23, IL-23 leads to STAT3 phosphorylation by binding to the IL-23 signaling complex [170].

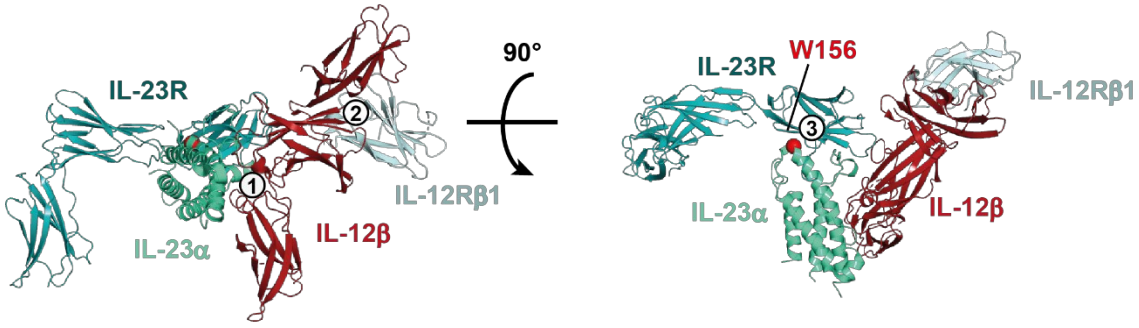


**Figure 10. Structure of the IL-23 signaling complex.** The α-subunit IL-23α (green) binds to the β-subunit IL-12β (dark red) via site 1. Interaction sites with receptor chains IL-12Rβ1 (pale cyan) and IL-23R (teal) are labeled with site 2 and 3, respectively (PDB: 6WDQ). Interaction sites 1-3 are marked with circled numbers. The critical tryptophan residue (W156) of IL-23α for site 3 interaction is highlighted as red sphere.

Like for IL-12, it was proposed that IL-12β,p40 can antagonize IL-23 signaling [131]. Antibody-based IL-23 signaling inhibitors are Briakinumab, which targets the D1-D2 junction of IL-12β but in a tilted manner which also results in inhibition of IL-23R binding [171, 182], and Ustekinumab, which prevents interaction of IL-12Rβ1 with D1 of IL-12β, accounting for its dual role in IL-12 and IL-23 neutralization [183]. Antibodies Tildrakizumab, Risankizumab, and Guselkumab all likely target IL-23 binding to IL-23R, but no antibody-bound IL-23 structures are available yet [184].

### 1.6.3 The IL-27 receptor complex

As IL-12β engages with the receptor chain IL-12βR1 by its Ig-like D1, it is likely that IL-12 family members IL-27 and IL-35 use a different mechanism to assemble their receptor complexes as their β-subunit EBI3 contains only two FnIII domains and no Ig-like domain. Very recently, cryo-EM structures of the IL-27 quaternary receptor signaling complex were solved, which provide structural insights into the assembly of IL-27 with IL-27Rα (also known as WSX-1/TCCR) and the shared receptor gp130 (Figure 11) [148, 185]. In contrast to IL-12/IL-23 receptor complex structures, IL-27α weakly interacts with both receptor chains, reminiscent to the classical IL-6 paradigm. Site 2 is located opposing to the IL-27α:EBI3 interface (site 1). It comprises interactions between the CHR of IL-27Rα and exposed IL-27α surfaces. These contacts are further stabilized by electrostatic interactions between EBI3 and IL-27Rα D2 [133, 147, 148, 166, 186]. Even though not resolved in the available crystal structure [133], a cryo-EM structure shows interaction of the characteristic IL-27α polyGlu loop with IL-27Rα [148]. In general, this structural setup explains the inability of IL-27α to mediate IL-27 signaling in absence of EBI3 [187]. Site 3 interactions, corresponding to the recruitment of gp130 to IL-27, are independent of IL-27Rα binding. Similar to site 3 interactions of other IL-12 family members [170] and IL-6 [145], a tryptophan residue (Trp197) in IL-27α anchors the interaction with Ig-like domain D1 of gp130 and is essential for receptor chain binding [146, 148, 188]. Though EBI3 is also associated with gp130 interactions, the canonical cytokine recognition sites at gp130 D2 and D3 remain unoccupied. The arrangement of the IL-27 receptor complex directs an intracellular cascade driven by phosphorylation of STAT1 and STAT3 by Jak1 and Jak2 [147, 189, 190]. Antagonistic behavior of IL-27α for gp130-mediated signaling was reported [187], even though binding of IL-27α to gp130 seems negligible [147].

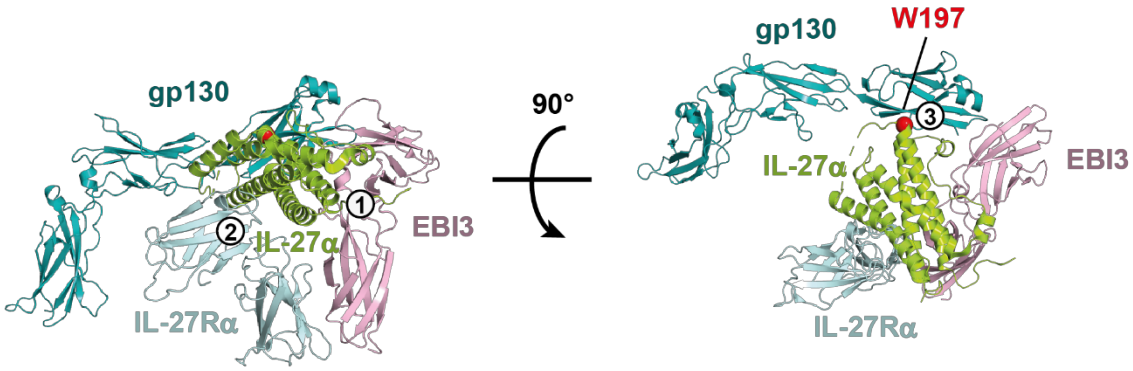


**Figure 11. Structure of the IL-27 signaling complex.** The α-subunit IL-27α (lime) binds to its β-subunit EBI3 (light pink) via site 1. Interaction sites with receptor chains IL-27Rα (pale cyan) and gp130 (teal) are labeled with site 2 and 3, respectively (PDB: 7U7N). Interaction sites 1-3 are marked with circled numbers. The critical tryptophan residue (W197) of IL-27α for site 3 interaction is highlighted as red sphere.

### 1.6.4 The IL-35 receptor complex

For IL-35, signaling is mediated via heterodimeric assembly of IL-12Rβ2 and gp130 on T cells, but also homodimers of each receptor chain seem to bind IL-35 (Figure 6D, right) [110]. For B cells, a novel heterodimeric IL-35 receptor comprising IL-12Rβ2 together with IL-27Rα was identified [111]. By receptor shuffling by Floss et al., canonical IL-35 signaling via STAT1 and STAT3 could be detected [191], which was consistent with IL-35 signaling in B cells [111] but seemed opposing to downstream signaling in T cells via STAT1:STAT4 heterodimers [110]. Taken together, these findings indicate that the IL-12 family member IL-35 signals via different receptors and signal transducers depending, for example, on the cell type. This unusual receptor repertoire needs to be investigated in more detail to better understand IL-35 and its biology.

## 1.7 The immunobiology of IL-12 family members

Despite chain-sharing promiscuity of IL-12 family members and receptor chains, IL-12 family cytokines span a broad functional spectrum from mostly pro-inflammatory to mostly inhibitory. How this divergent immunology is performed by different immune cells and how IL-12 cytokines contribute to immune-mediated diseases will be described in the following.

### 1.7.1 Immune-activating IL-12 promotes cell-mediated immunity

The founding member of the IL-12 family was first described as natural killer cell stimulatory factor produced by a human B lymphoblastoid cell line which was transformed with Epstein-Barr virus (EBV) [149]. IL-12 was also named as cytotoxic lymphocyte maturation factor, as it was found to synergize with IL-2 to activate cytotoxic lymphocytes [192]. As it can be concluded from the names, IL-12 functions in the proliferation of CD8+ T cells and NK cells, enhances their cytotoxic effects, and contributes to the production of IFNγ [149, 192-194]. Associated with the innate ability to recognize microbial pathogens, IL-12 is produced by peripheral blood mononuclear cells (PBMCs), predominantly by monocytes, DCs, macrophages, and B cells [194]. This cytokine is required for cell-mediated resistance against intracellular pathogens and microbial challenges, like it was shown for *Leishmania major* [195], *Listeria monocytogenes* [196], and *Toxoplasma gondii* [197]. Triggered by IL-12, polarization of naïve CD4+ T cells towards the Th1 phenotype is induced during infection and inflammation and results in IFNγ induction [198]. IL-12-mediated IFNγ production directly correlates with STAT4 expression and subsequent production of the transcription factor T-bet [199]. These downstream signaling processes are required for optimal IL-12Rβ2 receptor chain expression [200] and help to increase and sustain IL-12 responsiveness in Th1 cells [201]. IL-12-mediated immune response by the specific Th1

subset [202] goes along with IL-12-inhibited IL-4 production and suppression of Th2 cell responses [203]. In summary, IL-12 is key for inflammatory reactions in fighting infections but also tumors.

### 1.7.2 Pro-inflammatory IL-23 induces Th17 responses

Based on the observations that mice deficient in each of the IL-12 subunits, thus IL-12α,p35-/- and IL-12β,p40-/-, were not precise phenocopies in pathogen challenge implied that IL-12β might pair with another cytokine subunit. Pathogen burden in IL-12β,p40-/- mice was higher [204] and in T cell-mediated neuroinflammation models, like experimental autoimmune encephalitis (EAE), IL-12p40-/- showed resistance [205]. Reason for this is the most pro-inflammatory cytokine of the IL-12 family, IL-23, for which IL-12β assembles with IL-23α [206]. Like IL-12, IL-23 is secreted by activated APCs, i.e., DCs and macrophages [157, 200]. Its immunological role differs from IL-12, as it is not required for Th1-IFNγ responses but is essential in the development of pro-inflammatory cytokine IL-17-producing CD4+ T cells, also named Th17 cells [206, 207]. In contrast to IL-12, naïve T cells do not respond to IL-23 whereas memory T cells proliferate when stimulated with IL-23 [157, 208]. For a stabilized Th17 phenotype, IL-23-induced and STAT3- and RORγt-mediated expression of IL-23R creates a positive feedback loop, further enhancing IL-23 expression [108]. This novel IL-23-IL-17 immune axis allows rapid recruitment of neutrophils to sites of acute infection with extracellular bacteria and fungi, allowing time for the induction of potent Th1 responses [200], and also promotes the natural epithelial barrier [112]. Due to IL-23-induced expression of IL-17A, IL-17F, IL-6, tumor necrosis factor α (TNFα) which synergizes with IL-17, and granulocyte-macrophage colony-stimulating factor (GM-CSF), IL-23 has an important role in pathogenic Th17 responses and autoimmune pathogenesis [207-209]. Several chronic inflammatory diseases were found to be associated with IL-17, which was IL-23-induced and T cell-derived: inflammatory bowel disease (IBD) [210], rheumatoid arthritis [209, 211], the chronic cutaneous inflammation psoriasis [212, 213], and multiple sclerosis [214]. In psoriasis, the most common chronic, immune-mediated skin disorder which affects around 2% of the world's population [215], IL-23 causes both stabilization of IL-17 expression and IL-22 production by skin-infiltrating Th17 cells [216]. Neuroinflammation is investigated with the rodent disease model of EAE, resembling the human disease multiple sclerosis in which IL-23-induced GM-CSF might promote the recruitment of myeloid cells to the central nervous system [217]. However, this relation should be taken with caution since there are also contradicting findings in which IL-23 appear to limit GM-CSF production [218]. There is also evidence that IL-23 mediates cancer progression by promotion of angiogenesis, induction of tumor-promoting inflammation in the surrounding tumor microenvironment [219], and failure of the adaptive

immune surveillance to infiltrate those tumors [220]. How important immunobalance between IL-12 and IL-23 cytokine signaling is, becomes clear for Treg cells of the adaptive immunity. Tregs are required for limiting autoimmune reactions and resolving inflammation but might also prevent effective cancer immunity by dampening antitumor immune responses. As many tumors produce IL-23 in high levels, T cells upregulate IL-23R. This expression of IL-23R by Tregs is linked to poor prognosis. Ablation of IL-23 receptor expression by Tregs concurrently increases IL-12 receptor expression, thus IFNγ production and subsequent recruitment of activated CD8+ T cells, promoting the antitumor response [221]. Taken together, IL-23 has its major role in Th17 induction and sustainment, resulting in pro-inflammatory IL-17 secretion.

With the knowledge that IL-12 and IL-23 contribute differently to diseases, not only anti-IL-12β antibodies, like Ustekinumab [183, 222], but also IL-23α targeting antibodies, like Guselkumab and Tildrakizumab [223], were developed and approved against psoriasis. These more recent IL-17/IL-23 specific antibodies show beneficial effects in therapeutic treatment of organ-specific autoimmune pathologies, without disrupting the IL-12-IFNγ pathway [200, 223], and research continues on anti-IL-23 therapies [224]. Even today, distinction between immunological roles of IL-12 and IL-23 is still being reevaluated, e.g., with IL-12 heterodimer-specific antibodies [225].

### 1.7.3 The multifaceted IL-27 acts as immunomodulatory cytokine

IL-27 is secreted by activated APCs in the early phase after antigen-mediated activation or during resolution of autoimmune responses [108]. Moreover, it is also produced in non-immune cells including placental cells [226] and bone cells [227]. One of its multifaceted immune functions is the promotion of clonal expansion of naïve but not memory CD4+ T cells, acting in synergy with IL-12 to trigger IFNγ production [124]. IL-27 plays an important role in the early stages of Th1 commitment, as it regulates IL-12 responsiveness by expression of T-bet and IL-12Rβ2 [228]. Resulting IFNγ production helps in clearance of *Listeria monocytogenes* or *Leishmania major* infections, whereby IL-27 is dispensable for sustained Th1 responses [229, 230]. In constrast, to down-modulate excessive IL-27-driven Th1-mediated immune responses in pathologies like T cell-mediated hepatitis, IL-27 antagonism by an IL-27 point mutant with an abrogated binding site 3 was investigated [146]. IL-27 enhances also CD8+ T cell- and NK cell-mediated IFNγ production, when in co-culture with IL-12 and IL-2, but does not support Th2 cytokine production of activated T cells [124, 231]. In contrast to the pro-inflammatory functions, IL-27 acts also in an inhibitory manner. It was shown that this IL-12 family member limits pathological T cell responses in microbial challenges like infections with *Toxoplasma gondii* [232] and *Trypanosoma cruzi*

[233] but also in Th17-associated immunopathology in autoimmune diseases like EAE, colitis, or rheumatoid arthritis [234-236]. Though suppression of Th17-biased EAE seems to be independent of IL-10, for regulation of Th1-biased EAE, IL-10 is required. Therefore, IL-27 promotes IL-10 production by T regulatory 1 (Tr1) cells, most prominently under Th1 and Th2 conditions [235, 237]. Additionally, IL-27 suppresses GM-CSF expression in CD4+ T cells and induces expression of program death-ligand 1 (PD-L1) in myeloid cells, inhibiting neuroinflammation [238]. To temper T cell-mediated immune reactions, IL-27 blocks production of IL-2, a potent T cell growth and survival factor, and Th2 responses in concert with IL-12 [146, 239]. As surface expression of IL-27R$\alpha$ is not only found on naïve T cells, effector and memory CD4+ and CD8+ T cells, and resting NK cells, but also on Tregs, IL-27-mediated inhibition of IL-2 production might limit Treg proliferation and result in systemic inflammation [108, 112]. In colitis, for example, the role of IL-27 still remains unclear as there is evidence for and against the promotion of colitis [112, 240]. Not only involved in chronic inflammations, IL-27 engages also in cancer and antitumor responses [241, 242]. Taken together, IL-27 is an immunoregulatory cytokine, which has multiple pro-inflammatory, i.e., Th1 differentiation, and anti-inflammatory, i.e., suppression of Th17 and induction of Tr1 cells, roles dependent on its environment and presence of further immune system modulators.

### 1.7.4 Immune-suppressive IL-35 completes the IL-12 family functional range

While IL-12, IL-23, and IL-27 are found to be secreted by APCs, the inhibitory cytokine IL-35 was reported to be expressed by forkhead box protein P3 (Foxp3)+ Tregs [243]. It can elicit the conversion of conventional, naïve T cells into a peripheral, induced Treg cell population, termed iTr35, that does not express the transcription factor Foxp3 but produces IL-35 [244]. With that, IL-35 mediates suppression of T cell proliferation and blocks the development of Th1 and Th17 cells. Thereby, IL-35 positively affects autoimmune disease severity and results in infectious tolerance [243, 244]. Apart from IL-35 secretion by Tregs, this cytokine induces development of IL-35-producing Breg cells, which suppress NK cell-mediated anti-tumor responses [245]. Thus, IL-35 is also associated with immune escape in cancer, being a main barrier for effective anti-tumor therapies [246]. Additionally, IL-35 was also detected to be secreted by non-immune cells, like placental trophoblasts [159], suggesting an even more complex role in immunobiology. Taken together, IL-35 is the only strict immune-suppressive family member and acts by suppression of conventional T cells and induction of iTr35 conversion.

### 1.7.5 Expanding the immunoregulatory complexity by single subunit cytokines

In contradiction to the observation that the α-subunit of IL-23 shows no biological activity by itself [157] and seems to form non-native redox species in isolation [79], the constitutive overexpression of IL-23α in many murine cell types was associated with spontaneous multi-organ inflammation [247]. Moreover, intracellular IL-23α acts as endothelial pro-inflammatory peptide by promoting leukocyte migration and attachment. Association of IL-23α with the cytokine subunit gp130 stimulates STAT3 signaling, which exacerbates giant-cell arteritis [248].

For IL-12β, a building block of IL-12 and IL-23, immunocompetency is suggested in isolation, as this cytokine subunit is secreted in excess to the heterodimeric cytokines [162]. It is reported to antagonize IL-12 and IL-23 signaling in its monomeric or homodimeric form [130, 131, 177]. Binding only to IL-12Rβ1 [178], it acts as chemoattractant for myeloid cells, seems to be associated with respiratory viral infections, and regulates nitric oxide synthase expression [127, 129]. The monomeric IL-12β can attenuate autoimmune signaling, e.g., in EAE, by suppression of IL-12Rβ1 internalization, which is mediated by IL-12, IL-23, or homodimeric IL-12β [119, 128]. Since structural insights into IL-12β homodimer assembly are lacking, there are still fundamental open questions about the physiological relevance of monomeric *versus* homodimeric IL-12β, whose answers would make therapeutic targeting of IL-12β functions possible.

For secretion-competent murine IL-27α (IL-30) [124, 187], *in vivo* antagonization of IL-27 signaling was shown [187, 249], making it especially interesting as immunosuppressant for autoimmune diseases or systemic inflammations [249]. Not only antagonistic, but also agonistic properties of murine IL-27α and activation of gp130, and not WSX-1, were reported. This signaling can be conducted via trans-signaling with soluble IL-6Rα or by classical signaling with IL-6Rα or, at higher IL-30 concentrations, completely alone in absence of EBI3 or IL-6Rα [117]. In contrast to mice, human IL-27α is dependent on its β-subunit EBI3 for secretion while a single amino acid exchange confers this dependence. By cytokine engineering, a secretion-competent and functional human IL-27α was designed, which provides the possibility of treating inflammatory diseases [121].

Also for EBI3, which is secreted in isolation [124], an independent role in maternal tolerance during pregnancy was reported [226]. Moreover, IL-6 trans-signaling is proposed together with IL-6 and gp130, which would promote pro-inflammatory IL-6 functions [116]. Interestingly, intracellular EBI3 seems to be involved in proper IL-23R folding together with CNX. With this, it enhances not only the intracellular expression but also cell-surface

presentation of IL-23R. This augmentation of IL-23R protein expression by EBI3 might affect susceptibility to IBD [165].

To sum this overview of IL-12 cytokine immunobiology up, the diversity of IL-12 family cytokine functions is still expanding. How IL-12 cytokines respond in various physiological and pathological contexts is very distinct and functional roles remain to be clarified even further. In the future, biological relationships need to be confirmed, and new biologically active cytokines might be identified and characterized. This will allow targeted approaches and novel therapeutic strategies to guarantee balanced immune reactions by pro- and anti-inflammatory signaling molecules.

## 1.8 Aim and scope of this dissertation

The IL-12 family is a suitable, immunologically important model to study general mechanisms of the multi-layered ERQC. The ER is the hub for protein folding: Protein modification by *N*-glycosylation is not only a handle for the CNX/CRT cycle but also stabilizes the proteins folding. A huge, interconnected chaperone network prevents protein aggregation and assists in productive folding. And lastly, oxidative folding aided by PDIs results in correct protein disulfide formation.

The role of (free) cysteine residues in ER retention, misfolding, and degradation has already been thoroughly assessed for IL-12$\alpha$ and IL-23$\alpha$. For IL-27$\alpha$, differences in secretion-competency between human and mouse could also be explained by chaperone-controlled heterodimer assembly and disulfide bond formation. Nevertheless, crucial questions and details about interleukin biogenesis in the ER, equipped with various folding enzymes and chaperones, and related ERQC mechanisms remain unanswered.

In terms of oxidative folding in the ER: Is intramolecular disulfide bond formation a general, cross-species conserved principle for IL-27$\alpha$? Can we therefore expand our observations on human *versus* murine IL-27$\alpha$ ability to secrete to a universal trait for passing ERQC?

Like disulfide bond formation, *N*-glycosylation is one of the most prevalent ER-acquired modifications, therefore raising the questions: How are IL-12 family members glycosylated? Does glycosylation affect interleukin biogenesis and assembly? And is the biological activity of cytokines dependent on this protein modification, thereby having a great impact on immune homeostasis and possible therapeutic interventions in cytokine-associated pathologies?

Lastly, as ER-resident chaperones have already been reported to influence IL-12 family cytokine folding and ERQC, how can we obtain detailed insights into the cellular chaperone repertoire acting on IL-12 family members? What can we learn from diverse chaperones

acting on different subunits? Is cytokine heterodimer assembly affected by chaperones when IL subunits are shared and does this thereby also affect relative cytokine secretion, thus shifting immune reactions?

I have been addressing all these questions in this dissertation to provide a more comprehensive picture of the complex regulation and maturation of ILs in the ER.

## 1.9 Overview of methods

**Cloning, DNA constructs, and siRNA.** Interleukin cDNAs were cloned into different vectors depending on the subsequent experimental usage. Where indicated, constructs were equipped with N- or C-terminal tags separated by GS- or GA-linker repeats. Mutants were generated by site-directed mutagenesis. For restriction-based cloning, appropriate restriction enzymes were utilized. All constructs were verified by sequencing. Silencer® Select siRNAs were purchased (Thermo Fisher Scientific).

**Cell culture and transient transfections.** Human embryonic kidney (HEK) 293T, COS-7, and Burkitt lymphoma (BL)-2 cells were cultured according to the provider's recommendation. Transient transfections were carried out in p35 or p60 cell culture dishes using GeneCellin (Eurobio), Lipofectamine™ 3000 (Thermo Fisher Scientific), or METAFECTENE® PRO (Biontex) according to the manufacturer's instructions. For siRNA-mediated knockdowns, siRNA was added to cells using Lipofectamine™ RNAiMAX (Thermo Fisher Scientific).

**Immunoblotting experiments.** For secretion experiments, secreted proteins were analyzed separately from cell lysates. In de-glycosylation experiments, cell medium was treated with de-glycosylation enzymes according to the manufacturer's protocol to investigate the *N*- and *O*-glycosylation state of proteins. Redox-status experiments were conducted to assess disulfide bond formation. To induce translational arrest and determine protein removal rates, cycloheximide (CHX) chases were performed. Co-immunoprecipitation (co-IP) was used to study protein-protein interactions in the cell lysate, especially for chaperone-client complexes, and in the medium. Immunoblots were used to detect proteins of interest by specific antibodies and chemiluminescence detection.

**Site-specific introduction of unnatural amino acids for photocrosslinking.** Incorporation of the unnatural amino acid $N^6$-((2-(3-methyl-3H-diazirin-3-yl)ethoxy)carbonyl)-L-lysine (DiazK) by genetic code expansion and subsequent photocrosslinking was utilized to enable pulldown also of transient IL subunit-chaperone complexes for co-IP and mass spectrometry (MS) analyses.

**Recombinant protein production and purification.** Interleukin subunits or heterodimers were recombinantly expressed in *E. coli* or ExpiCHO cells and purified by affinity and size exclusion chromatography thereafter. For nuclear magnetic resonance (NMR) experiments, protein was purified from *E. coli* cultured in media supplemented with $^{15}$N-ammonium chloride and $^{13}$C-glucose.

**Biophysical protein characterization.** Hydrogen/deuterium exchange (HDX) and NMR experiments were used to assess structural dynamics and conformational changes of proteins. Secondary protein structure was analyzed by circular dichroism (CD) spectroscopy. Protein integrity was confirmed by high performance liquid chromatography (HPLC). Protein binding affinity and binding thermodynamics were investigated by isothermal titration calorimetry (ITC) and surface plasmon resonance (SPR) experiments.

**Cytokine functionality assays.** Receptor chain binding of cytokines was studied by NanoBRET™ Assay. Signaling activation measured by STAT phosphorylation was assessed after BL-2 cell stimulation with IL-27 cytokine.

**Sequence analysis, homology modeling, and structural analyses.** Sequence alignments were performed for evolutionary and conservation analyses between species and proteins. Appropriate servers were used to evaluate protein glycosylation. Homology modeling was used when there was no existing protein structure and analyzed in PyMOL.

**Quantification and statistical analyses.** Where indicated, signals were quantified and statistically analyzed with the stated statistical test.

Details of the applied methods and further methods performed by collaboration partners can be found in the respective “Material and methods” or “Experimental procedures” section of the publications.

# 2 Publications

## 2.1 An interspecies analysis reveals molecular construction principles of interleukin 27

Published by Stephanie I. Müller[1], **Isabel Aschenbrenner**[1], Martin Zacharias, and Matthias J. Feige in *Journal of Molecular Biology* (2019) 431(12): 2383-2393. DOI: 10.1016/j.jmb.2019.04.032

([1] equal contribution)

**Contribution:** All experiments were performed by Stephanie I. Müller and **Isabel Aschenbrenner**. Stephanie I. Müller, **Isabel Aschenbrenner**, Martin Zacharias, and Matthias J. Feige analyzed data and wrote the paper.

### 2.1.1 Summary

The immunoregulatory cytokine IL-27 is a heterodimer composed of the α-subunit IL-27α and the β-subunit EBI3. In mice, IL-27α is naturally secreted into the extracellular space as it is structurally stabilized by a single, intramolecular disulfide bond. In contrast, human IL-27α does not contain any disulfide bridges, is incompletely folded in isolation, and depends on assembly with its partner subunit EBI3 to fold and pass the ERQC. The β-subunits for both species behave reciprocally to their respective α-subunits in terms of secretion behavior: murine EBI3 is retained in the cell when unassembled, whereas human EBI3 is secreted alone. Here, we assessed whether retention *versus* secretion of IL-27α generally depends on intramolecular disulfide bond formation and whether the composite nature of IL-27, one secretion-competent subunit pairing with a secretion-incompetent, is an evolutionary conserved construction principle among species. We combined evolutionary analyses with *in silico* and cell biological approaches to better understand the underlying molecular mechanisms. In addition, since there was no experimentally determined structure available, we investigated human IL-27 subunit interactions by mutagenesis-guided molecular docking and molecular dynamics simulations.

Considering that autonomous folding and secretion of murine *versus* human IL-27α relies on one disulfide bond-forming cysteine pair, we aligned IL-27α sequences of 15 different species and clustered them into five different classes, dependent on the number and location of cysteine residues. Structurally, by homology model generation, as well as experimentally we could show that proximity of cysteines resulted in internal disulfide bond formation and correlated with autonomous secretion of IL-27α. This structural trait proves

to be a cross-species conserved determinant for secretion-competent IL-27α, potentially being of immunoregulatory relevance.

As human EBI3 is capable to enable or increase secretion of IL-27α of other species, we pursued a comprehensive mutational approach to reveal structural details of the human IL-27 interface and to assess evolutionary conservation throughout species. Experimental data on single point mutants in the context of EBI3-induced secretion of IL-27α were used to guide molecular simulations. The refined model for the human IL-27 heterodimer was experimentally verified and revealed that predicted IL-27α interface residues are highly conserved among species. Comparing the IL-27 model with IL-12/IL-23 crystal structures, a slightly rotated and translated arrangement of α- and β-subunits in respective complexes stands out.

By testing the secretion-competency of EBI3 from species with secretion-competent or secretion-incompetent IL-27α, we showed that a reciprocal secretion behavior of the constituent subunits is a general construction principle for IL-27: always one secretion-competent subunit pairs with an assembly-dependent one. Nonetheless, as we show that two secretion-incompetent subunits can also pair and be secreted together, this IL-27 setup might have evolved due to functional rather than structural reasons.

In summary, the evolutionary conserved, molecular basis for IL-27α secretion is an intramolecular disulfide bond stabilizing its fold. The pairing of one secretion-competent with one secretion-incompetent subunit is a common design principle in IL-27 biogenesis. Thereby, the secreted single subunit, as IL-27α for mice or EBI3 for humans, expands the cytokine repertoire of species, thus possibly being of outmost biological relevance. The detailed structural insight into the IL-27 subunit interface and its cross-species conservation opens possibilities for future cytokine engineering.

### 2.1.2 Manuscript

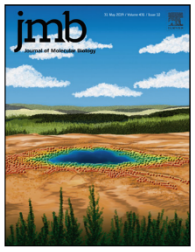

# An Interspecies Analysis Reveals Molecular Construction Principles of Interleukin 27

**Stephanie I. Müller[1,†], Isabel Aschenbrenner[1,†], Martin Zacharias[2] and Matthias J. Feige[1,]**

*1 - **Center for Integrated Protein Science at the Department of Chemistry and Institute for Advanced Study,** Technical University of Munich, 85748 Garching, Germany*
*2 - **Center for Integrated Protein Science at the Physics Department,** Technical University of Munich, 85748 Garching, Germany*

***Correspondence to Martin Zacharias and Matthias J. Feige:** Technical University of Munich, Department of Physics, James-Franck-Str. 1, 85748 Garching, Germany. Technical University of Munich, Department of Chemistry, Lichtenbergstr. 4, 85748 Garching, Germany. martin.zacharias@mytum.de, matthias.feige@tum.de*
https://doi.org/10.1016/j.jmb.2019.04.032
***Edited by Amy Keating***

## Abstract

Interleukin 27 (IL-27) is a cytokine that regulates inflammatory responses. It is composed of an α subunit (IL-27α) and a β subunit (EBI3), which together form heterodimeric IL-27. Despite this general principle, IL-27 from different species shows distinct characteristics: Human IL-27α is not secreted autonomously while EBI3 is. In mice, the subunits show a reciprocal behavior. The molecular basis and the evolutionary conservation of these differences have remained unclear. They are biologically important, however, since secreted IL-27 subunits can act as cytokines on their own.

Here, we show that formation of a single disulfide bond is an evolutionary conserved trait, which determines secretion-competency of IL-27α. Furthermore, combining cell-biological with computational approaches, we provide detailed structural insights into IL-27 heterodimerization and find that it relies on a conserved interface. Lastly, our study reveals a hitherto unknown construction principle of IL-27: one secretion-competent subunit generally pairs with one that depends on the other to induce its secretion.

Taken together, these findings significantly extend our understanding of IL-27 biogenesis as a key cytokine and highlight how protein assembly can influence immunoregulation.



## Introduction

Secreted proteins like cytokines, extracellular enzymes or antibodies are produced in the endoplasmic reticulum (ER) and released by cells to interact with their environment. In multicellular organisms, most physiological functions essentially depend on secreted proteins. Interleukins (ILs), as a prime example, mediate immune cell communication. They maintain organism homeostasis by activating or suppressing defense mechanisms. It is thus of utmost importance that secreted ILs possess their correct structure, which defines their biological activity. A dedicated quality control (QC) system in the ER, composed of chaperones and folding enzymes [1,2], ensures that ILs and other secretory proteins fold and assemble correctly before being released into the extracellular space.

For interleukin 27 (IL-27), a member of the heterodimeric IL-12 cytokine family [3,4], cellular QC is not only a means to prevent secretion of aberrant proteins, but also a way to modulate immune reactions: IL-27 consists of the α subunit IL-27α and the β subunit Epstein–Barr virus induced gene 3 (EBI3) [5]. IL-27 is secreted by antigen-presenting cells and signals *via* a heterodimeric receptor composed of IL-27Rα and gp130 to regulate immune functions, mainly by controlling T cell differentiation [4–9]. In mice, IL-27α is stabilized by a single disulfide bond and therefore can pass ERQC and be secreted from cells without its partner subunit EBI3 to act within the murine cytokine repertoire [5,10–13]. In humans, however, IL-27α is incompletely folded in isolation and depends on EBI3 to leave the cell [5,13]. Interestingly, EBI3 behaves reciprocally to IL-27α in these two species: human

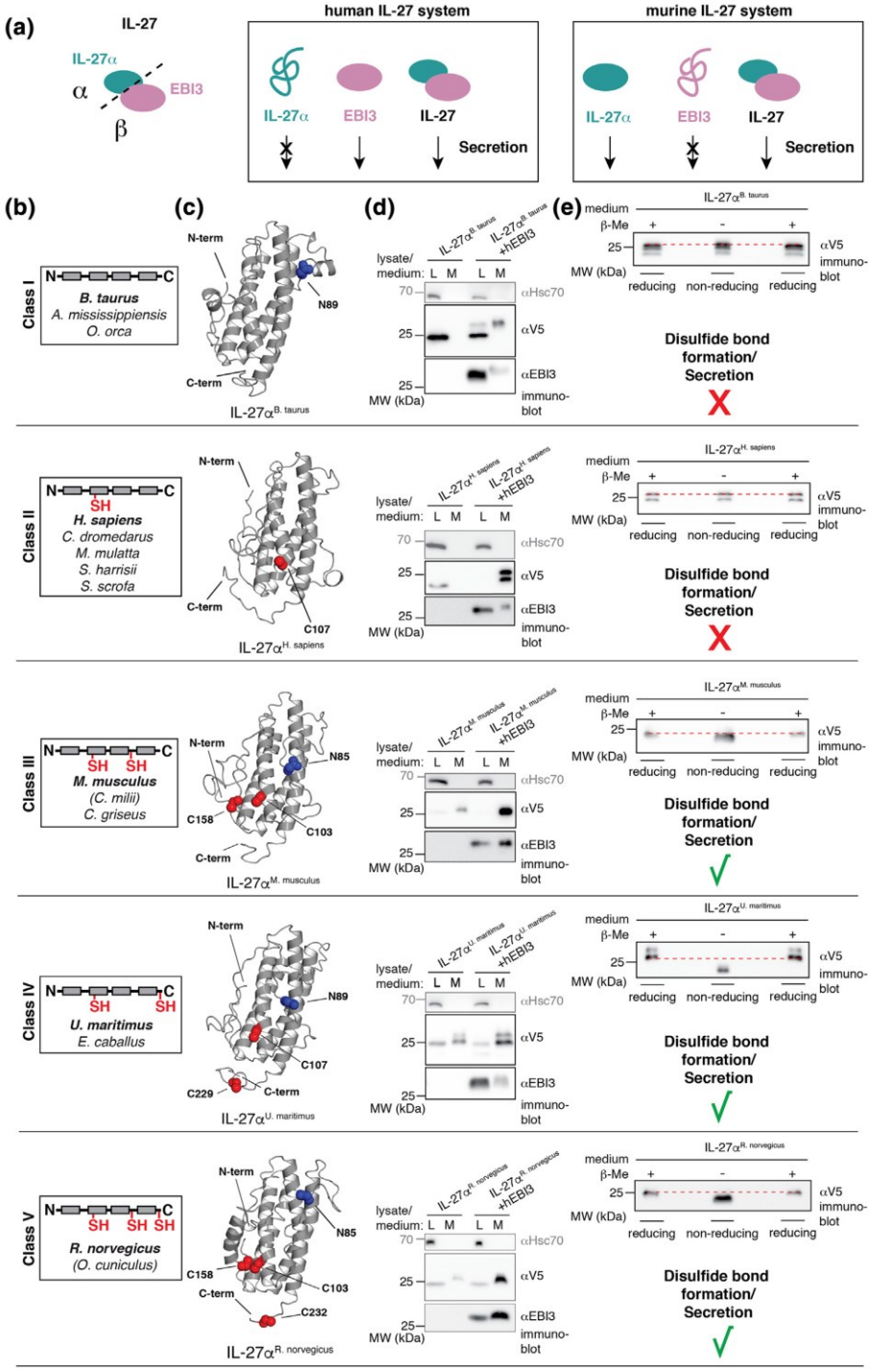


**Fig. 1** (*legend on next page*)

EBI3 can be secreted in absence of human IL-27α [5] and has been proposed to be an immunomodulator of maternal tolerance during pregnancy [14]. Murine EBI3, in contrast, is retained in cells and cannot be secreted without its α subunit [5,15]. The molecular mechanisms underlying EBI3 retention *versus* secretion remain unclear. Furthermore, although immunological functions of IL-27 have been well characterized [8,9], its structure remains unresolved. While IL-27α is predicted to have the typical 4-helix bundle structure of type I cytokines [16], EBI3 is homologous to soluble members of the class I cytokine receptor family like IL-6Rα, consisting of two Fibronectin III domains connected by a hinge region [17].

To provide insights into general construction principles of the key cytokine IL-27, further define its structural setup and immunoregulatory capabilities, we pursued an approach combining evolutionary analyses with structural investigations. We define basic criteria of IL-27α and EBI3 secretion and show how the IL-27 system has evolved to maintain immune balance in various organisms.

## Results

### Disulfide bond formation is an evolutionary conserved determinant for IL-27α secretion

In all species examined, IL-27 is a heterodimeric cytokine composed of IL-27α and EBI3 (Fig. 1a). Its assembly control, however, varies in different organisms: Human IL-27α (hIL-27α) is retained in the cell and can only be secreted upon co-expression of its β subunit EBI3 [5]. Murine IL-27α (mIL-27α), in contrast, is secretion-competent on its own and acts as a cytokine [5,10–12] (Fig. 1a). Very recently, it has been shown that the folding- and secretion-competency of human and murine IL-27α can be changed by introducing or eliminating a single disulfide-bond forming Cys residue, respectively [13]. In order to reveal if disulfide bond formation is a more general, evolutionary conserved trait that defines autonomous IL-27α secretion, we performed a multiple sequence alignment of IL-27α from 15 different species, laying emphasis on the number and location of Cys in the sequences (Supplementary Fig. S1a). This alignment allowed us to group IL-27α into five different classes. These either contain no Cys (class I), a single Cys (class II), two Cys with the second Cys being located centrally (class III) or towards the C-terminus of the protein (class IV), or three Cys (class V) (Fig. 1b and Supplementary Fig. S1a). To structurally understand how the Cys residues are arranged within the proteins, we generated homology models for the various α subunits (Fig. 1c and Supplementary Fig. S1b). The modeled structures illustrate that, whenever present, the first Cys is always located in the second α-helix of IL-27α. The second Cys is located either in a characteristic poly-Glu loop of IL-27α [18] (class III and V) or towards the C-terminus of the protein (class IV), where also the third Cys in class V is located (Fig. 1b and c).

Based on this *in silico* analysis, we proceeded to test two hypotheses concerning IL-27α experimentally. First, that predicted proximity of two Cys in the modeled structure is sufficient for disulfide bond formation to occur. And second, that disulfide bond formation correlates with autonomous secretion of IL-27α. Towards this end, we analyzed the secretion behavior and disulfide bond formation of representatives from each class. In complete agreement with our hypotheses, we found that whenever none or a single Cys was present, IL-27α was dependent on assembly with EBI3 for secretion (classes I and II, Fig. 1b and d and Supplementary Fig. S1b and c). In agreement with this data, IL-27α of classes I and II did not form a disulfide bond (Fig. 1e and Supplementary Fig. S1d). The presence of two or more Cys, however, always

**Fig. 1.** Folding- and secretion-competency of IL-27α depend on disulfide bond formation. (a) Schematic of the heterodimeric IL-27, consisting of the non-covalently linked subunits IL-27α and EBI3. In humans (left box), IL-27α is retained in cells in isolation and depends on co-expression of EBI3, whereas in mice (right box), IL-27α is secretion-competent and is needed to induce EBI3 secretion. (b) Classification of IL-27α was performed according to the number and location of Cys residues. Species belonging to each class are listed – with the representative species selected for experiments in bold. The location of Cys (red) in helix 2 (box, gray), loop 3 (line, black) and/or the C-terminus (C) are depicted within a schematic structure of IL-27α. Parenthesized species share the same number of Cys but slightly differ in Cys location compared to the class consensus. (c) Homology models of IL-27α subunits from representative species of classes I-V. Within the 4-helix bundle structure, Cys residues (red) and predicted *N*-glycosylation sites (blue) are shown in a CPK representation. (d) Secretion-competency of IL-27α varies between classes. IL-27α of class I (no Cys) or class II (single Cys) is retained in cells in isolation (L), whereas co-expression with human EBI3 (hEBI3) induces its secretion (M). With two or three Cys (classes III, IV and V), IL-27α is secretion-competent even in absence of the β subunit. 2% L/M were applied to the gel and blotted with the indicated antibodies. Hsc70 served as a loading control. (e) Disulfide bond formation as a prerequisite for folding- and secretion-competency of IL-27α. Secretion-competent IL-27α (classes III-V) forms a disulfide bond. Secreted α subunits were analyzed by non-reducing SDS-PAGE and blotted with anti-V5 antibody. 1–2% medium (M) were applied to the gel and blotted with the indicated antibodies. Where indicated (+), samples were treated with β-mercaptoethanol (β-Me) to reduce disulfide bonds. To highlight mobility differences, dashed lines are shown. *N*-glycosylated IL-27α from *B. taurus*, *M. musculus* and *R. norvegicus* were deglycosylated with PNGase F prior to SDS-PAGE analysis. (d, e) L, lysate. M, medium. MW, molecular weight.

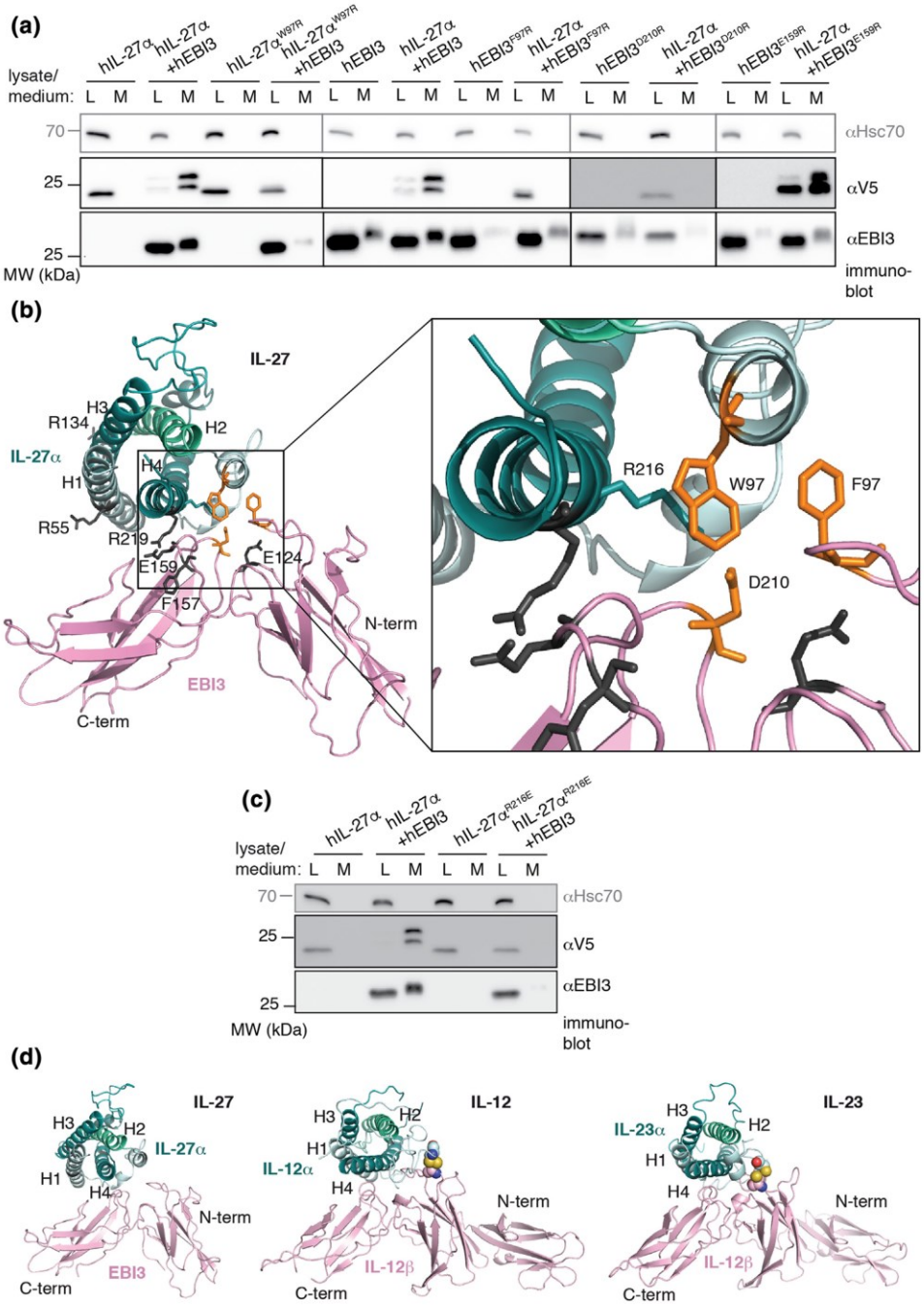


**Fig. 2.** A structural analysis of IL-27 heterodimerization. (a) hIL-27α$^{W97R}$, hEBI3$^{F97R}$ and hEBI3$^{D210R}$ but not hEBI3$^{E159R}$ disrupt subunit interactions in IL-27. EBI3$^{D210R}$ contained a C-terminal FLAG-tag. (b) Molecular docking of human IL-27 shows hIL-27α$^{W97}$, hEBI3$^{F97}$ and hEBI3$^{D210}$ to be located within the interface of the human α and β subunit. Helices 1–4 (H1–4) in IL-27α are indicated. (c) The hIL-27α$^{R216E}$ mutation disrupts IL-27 formation. (d) Comparison of docked IL-27 with IL-12 and IL-23 crystal structures. Disulfide bonds in IL-12 and IL-23 are shown in a CPK representation. Helices 1–4 (H1–4) in the α subunits are indicated. (a, c) L, lysate. M, medium. MW, molecular weight. 2% L/M were applied to the gel and blotted with the indicated antibodies. Hsc70 served as a loading control.

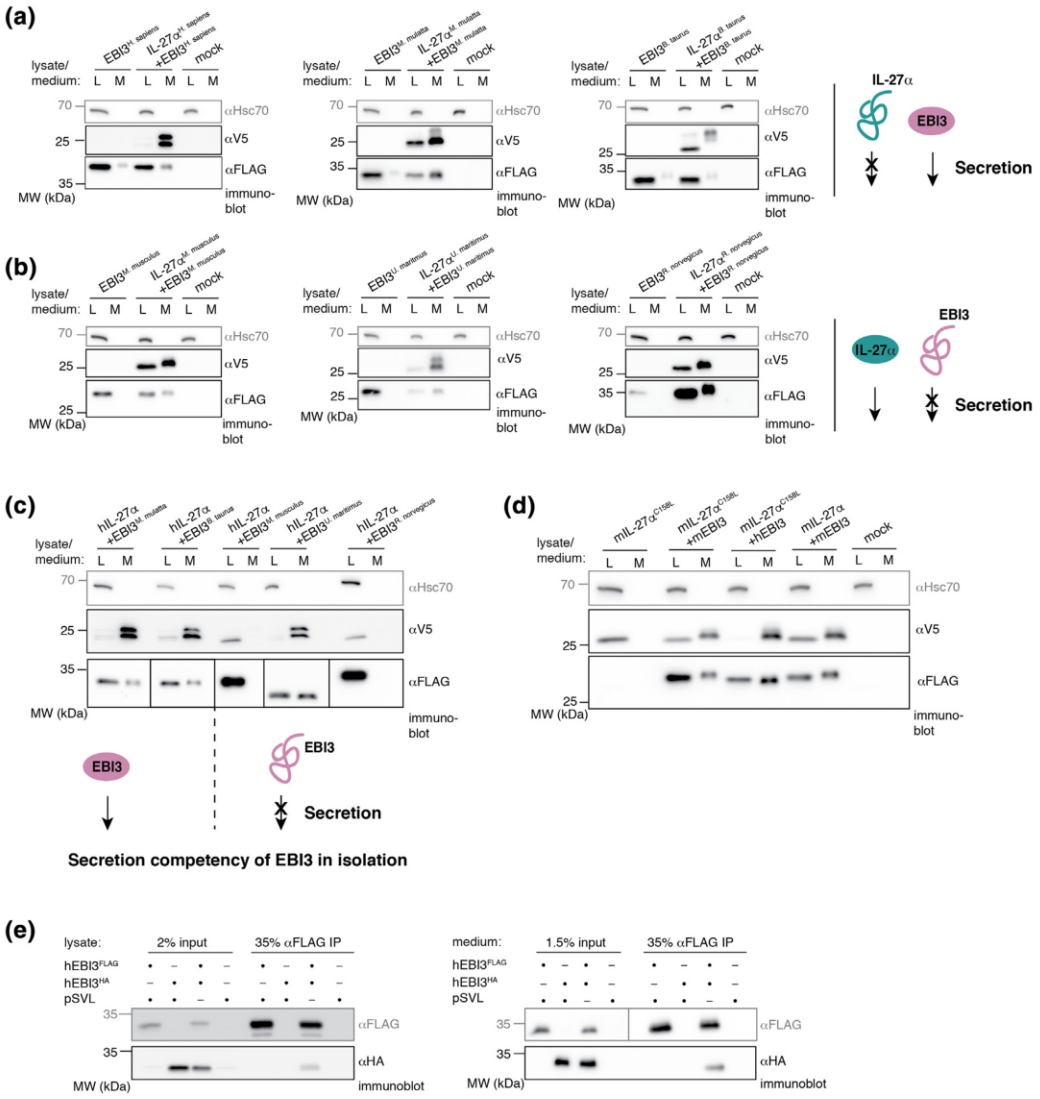


**Fig. 3.** An evolutionary conserved molecular construction principle of IL-27. (a,b) In all species tested, secretion-competent EBI3 subunits pair with secretion-incompetent IL-27α subunits to form IL-27 and *vice versa*. (a) EBI3 is secretion-competent (M) in isolation whenever its corresponding IL-27α is secretion-incompetent alone. (b) EBI3 from species with secretion-competent IL-27α is secretion-incompetent and thus retained in cells in isolation (L). Darker exposures are shown for EBI3 in Supplementary Fig. S3. (c) Secretion-incompetent hIL-27α was co-expressed with EBI3 from different species, being itself either secretion-competent or -incompetent as indicated. Secretion-incompetent EBI3 proteins were not able to induce hIL-27α secretion except for polar bear EBI3. (d) The secretion-incompetent mIL-27α$^{C158L}$ mutant and mEBI3 mutually induce their secretion. (e) EBI3 forms homodimers. 35% lysate or medium of cells transfected with FLAG-tagged EBI3/mock and/or HA-tagged EBI3 was immunoprecipitated with anti-FLAG antibody, applied together with input samples to the gel and immunoblotted with the indicated antibodies (MW, molecular weight). (a-d) L, lysate. M, medium. MW, molecular weight. 2% L/M were applied to the gel and blotted with the indicated antibodies. Hsc70 served as a loading control.

rendered IL-27α secretion-competent in isolation (classes III, IV and V in Fig. 1b and d). Autonomous secretion of IL-27α was always concurrent with disulfide bond formation (Fig. 1e). In agreement with the structural models, a larger number of residues between Cys connected by an intramolecular disulfide bond resulted in a larger shift of IL-27α under non-reducing conditions on SDS-PAGE gels (*e.g.* mouse *versus* polar bear IL-27α in Fig. 1e). Furthermore, whenever *N*-linked glycosylation sites were predicted

(Fig. 1c and Supplementary Fig. S1a and b), modification of these sites upon secretion could be detected (Fig. 1d and Supplementary Fig. S1c and e). Remarkably, human EBI3 (hEBI3) was able to induce or increase secretion of IL-27α from all species tested (Fig. 1d and Supplementary Fig. S1c). Taken together, our data show that disulfide bond formation is an evolutionary conserved determinant for autonomous secretion and thus potential biological functions of IL-27α. Furthermore, our findings point towards a conserved mode of IL-27 heterodimerization that we next investigated further.

**A structural analysis of the IL-27 interface reveals evolutionary conservation**

Despite its important immunological functions, no experimentally determined structure is available for IL-27 yet. Thus, to provide further structural insights into IL-27 heterodimerization, we decided to use a mutational approach combined with docking and molecular dynamics (MD) simulations. A broad set of mutations was selected based on i) a previous structural analysis of IL-27 heterodimerization [16], and ii) the homology of IL-27 to CNTF, IL-12 and IL-23 [16,19–22]. This approach led to nine possible interface residues (Fig. 2a and b and Supplementary Fig. S2a), which we tested experimentally by single point mutations. To investigate the effect of the different mutations, we analyzed hEBI3-induced secretion of hIL-27α. Secretion of hIL-27α can be assessed *via O*-glycosylation, which occurs during Golgi passage: while hIL-27α populates a single species only detectable in the lysate (L, Fig. 2a), co-expression of hEBI3 induces secretion into the medium concomitant with the formation of different *O*-glycosylated species (M, Fig. 2a) [13]. Using this assay, we found that in agreement with previous data [16], hIL27a$^{W97R}$, hEBI3$^{F97R}$ and hEBI3$^{D210R}$ disrupted hIL-27α secretion (Fig. 2a). The hEBI3$^{E159R}$ mutant, in contrast to what has been reported previously [16], did not inhibit hIL-27α secretion in our experiments (Fig. 2a). This is in agreement with studies on mouse EBI3 [23] and may be due to the different assays used: induction of hIL-27α secretion by EBI3 would also report on weak interactions, as opposed to co-immunoprecipitations [16]. All other five residues tested did not inhibit EBI3-induced secretion of hIL-27α (Supplementary Fig. S2b-d). Together, this provided us with a comprehensive set of disruptive and non-disruptive single point mutants, which we used to guide a docking approach combined with MD refinement simulations (Fig. 2b). In the obtained model, Trp97 of hIL-27α is located at the center of the interface and binds at the hinge region between the two domains of hEBI3. It contacts Phe97 and, in addition, several other residues in hEBI3 such as Leu96, Thr209 and Asp210. The model predicts a salt bridge contact between Arg216 in hIL-27α and Asp210 in hEBI3 as well as a stacking contact between Phe94 (hIL-27α) and Phe97 (hEBI3) that further stabilizes binding. In order to test our model experimentally, we substituted Arg216 in hIL-27α with a negatively charged Glu residue, which would interrupt the predicted interaction between hIL-27α Arg216 and hEBI3 Asp210 (Fig. 2b). In complete agreement with our docking, the mutant hIL-27α$^{R216E}$ disrupted IL-27 formation (Fig. 2c). The model was also compatible with all residues found to be of lesser or no importance for binding on both partners (Supplementary Fig. S2a-d) since these residues are not at the interface, with the exception of Arg219 in hIL-27α. However, the guanidinium group of Arg219 does not form any specific contact, *e.g.* a salt bridge with the hEBI3 partner, compatible with the finding that substitution of this residue did not interfere with complex formation (Supplementary Fig. S2c, right panel). Importantly, all the IL-27α residues that form the predicted interface (defined as residues in contact with residues of the hEBI3 partner, *i.e.* a side chain atom-atom distance of $<5$ Å) are highly conserved among the IL-27α molecules from different species (Supplementary Fig. S2e). This is consistent with our finding that human EBI3 could induce secretion of IL-27α from all tested species (Fig. 1d). Interestingly, despite this fact, some differences appeared to exist in the molecular details of interactions: co-expression of hEBI3$^{F97R}$ could not induce secretion of IL-27α from Tasmanian devil and monkey, like observed for human IL-27α (Fig. 2a and Supplementary Fig. S2f). IL-27α from cow and pig, however, were able to leave the cell in the presence of this mutant (Supplementary Fig. S2f). A comparison of IL-27α residues from these species, predicted to be located at the interface with hEBI3, did not indicate any difference (Supplementary Fig. S2e). Hence, the structural model suggests that the origin of the different behavior of IL-27α from Tasmanian devil and monkey *versus* cow and pig is not associated with residue differences at the subunit interface. It might thus be possible that hEBI3$^{F97R}$ has generally lower affinity to (any) IL-27α and this weak subunit association is sufficient for IL-27α from pig and cow to fold correctly and assemble, whereas it is insufficient in case of IL-27α from Tasmanian devil and monkey.

Similar to the known structures of IL-12 [19] and IL-23 [20], helix 4 (H4) of hIL-27α contributed most to the interface with hEBI3 (Fig. 2d). Interestingly, despite this overall similarity, the arrangement of the hIL-27α subunit relative to the β subunit was slightly rotated and translated in the IL-27 model – which positions the residues found critical for IL-27 formation at the interface – compared to the corresponding placement in the IL-12 and IL-23 complexes (Fig. 2d). A global arrangement like in IL-12 and IL-23 would shift the critical Trp97 in IL-27α away from the interface. Note, that both in the IL-12 and IL-23 complex the arrangement of α and

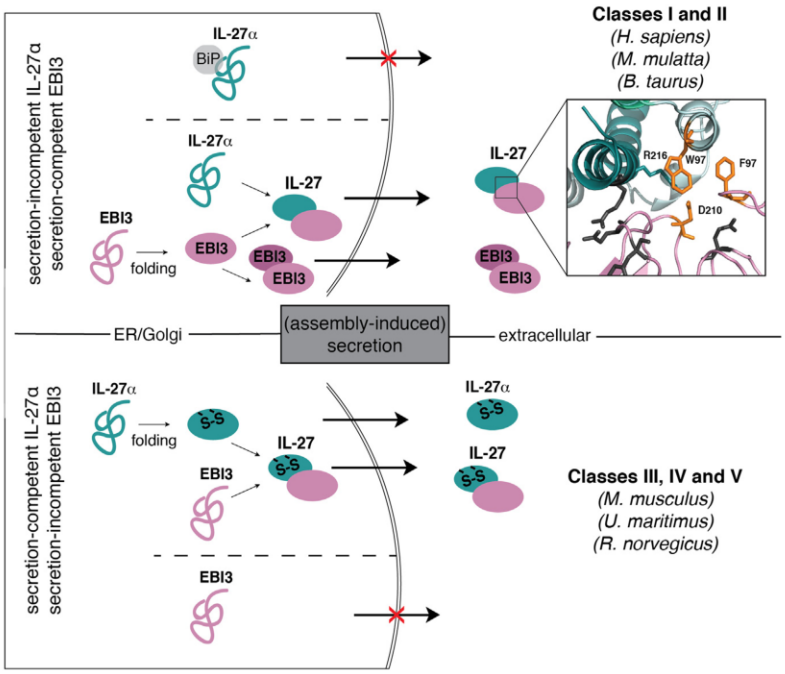


**Fig. 4.** A model for IL-27 biogenesis. Secretion-incompetent IL-27α (classes I and II) pairs with secretion-competent EBI3 and *vice versa* (classes III, IV and V). Species from which IL-27 was investigated in this study are shown in brackets. Disulfide bond formation (S-S) determines folding and secretion-competency of IL-27α subunits. IL-27α is retained in the cell by BiP binding if no disulfide bond is present [13]. EBI3 can form homodimers (shown for human EBI3 in this study). The inset highlights the heterodimerization interface of human IL-27 as defined in this study.

β partners is stabilized by an intermolecular disulfide bond (Fig. 2d) that is absent in IL-27 and may contribute to the slightly shifted arrangement. Taken together, our approach provides an improved structural model for IL-27 that is compatible with our comprehensive mutational analysis and reveals molecular details of αβ heterodimerization modes within the IL-12 family.

### Reciprocally induced secretion of its constituent subunits is an evolutionary conserved trait of IL-27

Reminiscent of the IL-27α subunit, the IL-27β subunit EBI3 shows a different secretion behavior depending on the species. In humans, EBI3 can be secreted without co-expressing its corresponding IL-27α subunit, albeit weakly ([24] and Fig. 3a). In contrast, in mice, IL-27α is needed to induce EBI3 secretion ([5,15] and Fig. 3b). Interestingly, in both species, one secretion-competent subunit thus pairs with one secretion-incompetent subunit to form IL-27, only differing in the allocation of these traits to α or β subunit (depicted by the scheme in Fig. 3a and b on the right). Intrigued by this observation, we investigated if this construction principle was evolutionary conserved by testing the secretion-competency of the β subunit from species, where the α subunit is either secretion-incompetent (monkey and cow) or secretion-competent (polar bear and rat). Strikingly, EBI3 from monkey and cow were secreted into the medium without co-expression of IL-27α (Fig. 3a and Supplementary Fig. S3). Moreover, EBI3 from polar bear and rat were retained in cells in isolation and only secreted into the medium upon co-expression of their secretion-competent α subunits (Fig. 3b and Supplementary Fig. S3). Our data thus suggest that combination of a secretion-competent with a secretion-incompetent subunit is a common construction principle of IL-27. In the light of this finding, we wondered if only IL-27 subunits that co-evolved with assembly-dependent partner subunits were able to induce their secretion. To test this idea, we co-expressed human IL-27α with EBI3 from five different species and analyzed if the subunits were retained in or secreted by the cells (Fig. 3c). In complete agreement with this idea, hIL-27α was well-secreted upon co-expression of secretion-competent monkey and cow EBI3, but was retained in the cell when co-expressed with secretion-incompetent EBI3 from mouse and rat (Fig. 3c). The only exception from this rule was EBI3 from polar bear, which induced hIL-27α secretion comparable to secretion-competent EBI3 species. This pointed towards the interesting possibility that two secretion-incompetent subunits could in principle pair to become secreted together. To further test this, we examined if mEBI3 could induce secretion of the previously described mutant mIL-27α$^{C158L}$. This mutant is rendered secretion-incompetent in isolation by replacing Cys158 by Leu, removing its disulfide bond [13]. Indeed, co-expression with mEBI3 led to secretion of both subunits, mEBI3 and mIL-27α$^{C158L}$ (Fig. 3d), constituting another

example of two secretion-incompetent subunits that can become secreted together. This finding furthermore underscores that mIL-27α$^{C158L}$ together with mEBI3 recapitulates the behavior of the human system in regard to IL-27α, which qualifies it as a tool to further analyze the IL-27α and IL-27 biology in mouse models.

Lastly, we were wondering in which assembly state EBI3 would be secreted. This is of relevance, since generally two receptor chains are needed to initiate signaling by IL-12 family members [3]. Co-immunoprecipitation experiments of differentially tagged human EBI3 revealed the formation of homodimers in cells as well as in the medium (Fig. 3e), showing that EBI3 can be secreted as a homodimer. In this context it is noteworthy, that the shared IL-12/IL-23 β subunit (IL-12β) can also be secreted autonomously, including formation of a homodimer, and performs immunoregulatory functions [25,26].

## Summary

In conclusion, our study reveals that disulfide bond formation is an evolutionary conserved determinant of IL-27α secretion and its potential role as a cytokine (Fig. 4). Furthermore, by an in-depth mutational and computational analysis, we were able to provide detailed insights into the molecular architecture of the IL-27 interface, which will also help in future engineering approaches. And lastly, our study reveals a hitherto unappreciated but intriguing setup of the IL-27 system, where one secretion-competent subunit pairs with one, that needs to assemble in order to be secreted. Our data show that this is not rooted in the biophysics of IL-27 subunit assembly, since we also could generate pairs of two assembly-incompetent subunits that mutually promoted their secretion. This suggests that the combinatorial principle realized for IL-27 has evolved for a functional benefit rather than due to structural requirements, *e.g.* to maintain a functional and balanced immune system. Using different protein assembly states with distinct functionalities appears to be a common design principle in immune systems to extend the signaling repertoire of cytokines and maintain immune homeostasis [12,13,25,27–29].

## Materials and methods

### Constructs for mammalian expression

For mammalian expression, all interleukin cDNAs were cloned into the pSVL vector (Amersham BioSciences). Human interleukin cDNAs (hIL-27α and hEBI3) were obtained from OriGene and amino acid sequences correspond to the UniProt accession numbers Q8NEV9 and Q14213, respectively. For a species comparison of IL-27α, sequences corresponding to GenBank identifiers NP_001158125.1 (*Bos taurus*), EHH31550.1 (*Macaca mulatta*), NP_663611.1 (*Mus musculus*), XP_344963.5 (*Rattus norvegicus*), XP_012398754.1 (*Sarcophilus harrisii*) and XP_008683452.1 (*Ursus maritimus*) were synthesized by GeneArt (Thermo Fisher Scientific) with optimized codon-usage for human expression. A $(GS)_4$-linker followed by a V5-tag was introduced at the C-terminus of the different IL-27α constructs. For a species comparison of EBI3, sequences corresponding to GenBank identifiers AAI49503.1 (*Bos taurus*), XP_014977995.1 (*Macaca mulatta*), NP_001102891.1 (*Rattus norvegicus*) and XP_008709480.1 (*Ursus maritimus*) were synthesized by GeneArt with optimized codon-usage for human expression (Thermo Fisher Scientific). Mouse EBI3 cDNA, according to GenBank identifier NM_015766.2 (*Mus musculus*), was obtained from OriGene. Where indicated, EBI3 genes were C-terminally tagged with a $(GS)_4$-linker followed by a FLAG- or an HA-tag. Mutants were generated by site-directed mutagenesis. All constructs were sequenced.

### Cell culture and transient transfections

Human embryonic kidney (HEK) 293 T cells were cultured in Dulbecco's modified Eagle's medium (DMEM) containing L-Ala-L-Gln (AQmedia, Sigma-Aldrich) supplemented with 10% (v/v) fetal bovine serum (FBS; Biochrom or Gibco, Thermo Fisher Scientific) at 37 °C and 5% $CO_2$. The medium was complemented with a 1% (v/v) antibiotic-antimycotic solution (25 µg/ml amphotericin B, 10 mg/ml streptomycin and 10,000 units of penicillin; Sigma-Aldrich) (complete DMEM). Transient transfections were carried out in in either poly D-lysine coated p35 or p60 dishes (BioCoat, Corning) or p60 dishes (Corning BioCoat) using GeneCellin (BioCellChallenge) according to the manufacturer's instructions. Equal amounts of constructs or empty vector were transfected with a total DNA amount of 2 µg (p35) or 4 µg (p60).

### Secretion and redox experiments

For secretion and redox-status experiments by immunoblotting, cells were transfected for 8 h, washed twice with phosphate buffered saline (PBS; Sigma-Aldrich) and then supplemented with fresh medium for another 16 h. To analyze secreted proteins, the medium was centrifuged for 5 min, 300 *g*, 4 °C. Subsequently, the supernatant was transferred into a new reaction tube and supplemented with 0.1 volumes of 500 mM Tris/HCl, pH 7.5, 1.5 M NaCl, complemented with 10x Roche complete Protease Inhibitor w/o EDTA (Roche Diagnostics). Prior to lysis, cells were

washed twice in ice-cold PBS. Cell lysis was carried out in RIPA buffer (50 mM Tris/HCl, pH 7.5, 150 mM NaCl, 1.0% Nonidet P40 substitute, 0.5% sodium deoxycholate, 0.1% SDS, 1x Roche complete Protease Inhibitor w/o EDTA; Roche Diagnostics) on ice. Both lysate and medium samples were centrifuged for 15 min, 20,000 g, 4 °C. *N*-glycosylated IL-27α from *B. taurus*, *S. harrissii, M. musculus* and *R. norvegicus* were deglycosylated with PNGase F (SERVA) under non-reducing conditions according to the manufacturer's instructions prior to running redox gels to improve visibility of disulfide-induced down-shifts of proteins on SDS-polyacrylamide gel electrophoresis (PAGE) gels. Endo H (New England Biolabs) deglycosylation experiments were carried out according to the protocol of the manufacturer. Samples were supplemented with 0.2 volumes of 5x Laemmli buffer (0.3125 M Tris/HCl pH 6.8, 10% SDS, 50% glycerol, bromphenol blue) containing either 10% (v/v) β-mercaptoethanol (β-Me) for reducing SDS-PAGE or 100 mM *N*-Ethylmaleimide (NEM) for non-reducing SDS-PAGE.

### Immunoprecipitation experiments

For co-immunoprecipitation (co-IP) experiments of FLAG-tagged proteins, cells were washed twice with ice-cold PBS. Cell lysis was carried out in Triton buffer (50 mM Tris/HCl, pH 7.5, 150 mM NaCl, 1 mM EDTA, 1% Triton X-100, 1x Roche complete Protease Inhibitor w/o EDTA; Roche Diagnostics) on ice. Lysates were cleared by centrifugation at 20,000 *g*, 15 min, 4 °C. ANTI-FLAG M2 Affinity Gel (Sigma-Aldrich, A2220) was used for immunoprecipitation according to the manufacturer's protocol using Triton buffer for washes. Proteins were eluted by adding 2x Laemmli buffer (supplemented with 4% (v/v) β-Me) and boiling at 95 °C for 5 min. For immunoprecipitations of secreted proteins, the medium was treated as described for the analysis of secreted protein and subsequently treated like the lysate, using ANTI-FLAG M2 Affinity Gel.

### Immunoblotting

For immunoblots, samples were run on 12% SDS-PAGE gels or 8–16% gradient gels (Bio-Rad, for redox experiments of IL-27α *M. musculus* and *R. norvegicus*) and transferred to polyvinylidene difluoride (PVDF) membranes by blotting overnight (o/n) at 30 V and 4 °C. Thereafter, membranes were blocked for at least 3 h with Tris-buffered saline (TBS) containing skim milk powder and Tween-20 (M-TBST; 25 mM Tris/HCl, pH 7.5, 150 mM NaCl, 5% *w/v* skim milk powder, 0.05% v/v Tween-20) or gelatin buffer (0.1% gelatin, 15 mM Tris/HCl, pH 7.5, 130 mM NaCl, 1 mM EDTA, 0.1% Triton X-100, 0.002% $NaN_3$) for Hsc70 immunoblots. Binding of the primary antibody was carried out o/n at 4 °C with anti-Hsc70 (Santa Cruz, sc-7298, 1:1000) in gelatin buffer, anti-V5 (Abcam, ab27671, 1:1000), anti-FLAG (Sigma-Aldrich, F7425, 1:1000) and anti-HA (BioLegend, 902,302, 1:1000) antibodies in M-TBST. Anti-EBI3 (1:20 in PBS) antiserum has been described previously [14]. Species-specific HRP-conjugated secondary antibodies (Santa Cruz Biotechnology; 1:10,000 in M-TBST) were used. Immunoblots were detected using Amersham ECL prime (GE Healthcare) and a Fusion Pulse 6 imager (Vilber Lourmat).

### Sequence analysis, homology modeling and structural analyses

Multiple DNA sequence alignments were performed using Clustal Omega [30] and depicted with BoxShade server (EMBnet). Homology models of isolated IL-27α subunits were generated using iTasser [38]. For generating starting structures for protein–protein docking we followed the homology modeling procedure of Rousseau *et al.* [16]. It is based on a structure-based alignment of IL-27α and hEBI3 sequences to the IL-6 family of cytokines. Structural models of hIL-27α and hEBI3 were generated using the program Modeller [31] and are based on the alignment with known ciliary neurotrophic factor (CNTF) cytokine (pdb: 1cnt) and IL-6 (pdb: 1p9m) structures. For structure modeling the alignments as published by Rousseau *et al.* [16] were used. Generated models were energy minimized (5000 steps) using the Amber18 package [32]) to remove any residual sterical overlap. Docking searches were performed using the protein–protein docking program ATTRACT [33,34]. In ATTRACT, partner proteins are represented by a reduced protein model with four centers per residue [35] to allow rapid energy minimization of docked complexes. The initial search was restricted to starting placements in the vicinity of ~ 20 Å from the Trp97 residue on the hIL-27α side and to ~20 Å from Phe97, Asp210 on the hEBI3 partner protein. Substitution of any of these three residues was found experimentally to disrupt hIL-27α secretion induced by hEBI3. Hence, it is reasonable to assume that these residues are located at the protein–protein interface. Initial docking geometries were energy minimized and favorable docking solutions were screened for geometries with residues hIL-27α Trp97 and hEBI3 Phe97, Asp210 located at the interface and residues substitutions not affecting binding outside of the interface. The most favorable binding geometry was refined at atomic resolution after superimposing the atomistic model structures onto the docked model complex. Refinement was performed by energy minimization (5000 steps) followed by atomistic MD simulation (5 ns using the Amber18 package [32]) and first using an implicit (generalized Born) solvation model [36] for 5 ns at 300 K. A center of mass distance restraint between protein partners was included to avoid dissociation during the refinement step because of possible sterical overlap in the starting structure. For further relaxation of sterical strain the structure was

solvated in explicit TIP3P water [37] and equilibrated for another 10 ns at 300 K at constant pressure (1 bar) after heating up the system over a time frame of 1 ns. The resulting structure fulfilled the experimental restraints such that all residues critical for binding are at the interface and those substitution positions that were found experimentally not to affect binding are all located >6 Å (mostly >10 Å) from the binding interface. An exception is Arg219 in hIL-27α that is located at the rim of the protein–protein interface (Fig. 2b). However, the side chain of Arg219 is not forming specific (*e.g.* salt bridge) contacts to the hEBI3 partner. In the final model hIL-27α Trp97 is in contact with several aromatic and non-polar interface residues of hEBI3 (including hEBI3 Phe97). The Asp210 in hEBI3 forms a salt bridge with Arg216 of hIL-27α. Visualization and structural alignments and further structural analyses were performed using Yasara Structure (www.yasara.org) and PyMOL (PyMOL Molecular Graphics System, Version 2.0 Schrödinger, LLC).

## Acknowledgements

We are grateful to Odile Devergne, INSERM/France, for the kind gift of anti-EBI3 antiserum. SIM gratefully acknowledges a PhD scholarship by the German Academic Scholarship Foundation. MJF is a Rudolf Mößbauer Tenure Track Professor and as such gratefully acknowledges funding through the Marie Curie COFUND program and the Technical University of Munich Institute for Advanced Study, funded by the German Excellence Initiative and the European Union Seventh Framework Program under Grant Agreement 291763. MJF gratefully acknowledges funding of our work on interleukins by the Daimler and Benz Stiftung. This work was performed in the framework of the German Research Foundation (DFG) Sonderforschungsbereich 1035, projects B02 and B11.

## Author contributions

MJF and SIM conceived the experimental part of the study, MZ conceived the docking part. All experiments were performed by SIM and IA. MZ performed docking simulations. All authors analyzed data and wrote the paper.

## Conflict of interest

The authors declare no conflict of interest.

## Appendix A. Supplementary data

Supplementary data to this article can be found online at https://doi.org/10.1016/j.jmb.2019.04.032.

*Received 25 March 2019;*
*Received in revised form 18 April 2019;*
*Accepted 19 April 2019*
Available online 26 April 2019

***Keywords:***
Interleukins;
Protein assembly;
Protein docking;
Protein evolution

†These authors contributed equally to this work.

## References

[1] I. Braakman, N.J. Bulleid, Protein folding and modification in the mammalian endoplasmic reticulum, Annu. Rev. Biochem. 80 (2011) 71–99.
[2] M.H. Smith, H.L. Ploegh, J.S. Weissman, Road to ruin: targeting proteins for degradation in the endoplasmic reticulum, Science. 334 (2011) 1086–1090.
[3] D.A. Vignali, V.K. Kuchroo, IL-12 family cytokines: immunological playmakers, Nat. Immunol. 13 (2012) 722–728.
[4] C.A. Hunter, R. Kastelein, Interleukin-27: balancing protective and pathological immunity, Immunity. 37 (2012) 960–969.
[5] S. Pflanz, J.C. Timans, J. Cheung, R. Rosales, H. Kanzler, J. Gilbert, et al., IL-27, a heterodimeric cytokine composed of EBI3 and p28 protein, induces proliferation of naive CD4(+) T cells, Immunity. 16 (2002) 779–790.
[6] S. Pflanz, L. Hibbert, J. Mattson, R. Rosales, E. Vaisberg, J. F. Bazan, et al., WSX-1 and glycoprotein 130 constitute a signal-transducing receptor for IL-27, J. Immunol. 172 (2004) 2225–2231.
[7] G. Trinchieri, S. Pflanz, R.A. Kastelein, The IL-12 family of heterodimeric cytokines: new players in the regulation of T cell responses, Immunity. 19 (2003) 641–644.
[8] S. Aparicio-Siegmund, C. Garbers, The biology of interleukin-27 reveals unique pro- and anti-inflammatory functions in immunity, Cytokine Growth Factor Rev. 26 (2015) 579–586.
[9] H. Yoshida, C.A. Hunter, The immunobiology of interleukin-27, Annu. Rev. Immunol. 33 (2015) 417–443.
[10] S. Crabe, A. Guay-Giroux, A.J. Tormo, D. Duluc, R. Lissilaa, F. Guilhot, et al., The IL-27 p28 subunit binds cytokine-like factor 1 to form a cytokine regulating NK and T cell activities requiring IL-6R for signaling, J. Immunol. 183 (2009) 7692–7702.
[11] J.S. Stumhofer, E.D. Tait, W.J. Quinn III, N. Hosken, B. Spudy, R. Goenka, et al., A role for IL-27p28 as an antagonist of gp130-mediated signaling, Nat. Immunol. 11 (2010) 1119–1126.
[12] C. Garbers, B. Spudy, S. Aparicio-Siegmund, G.H. Waetzig, J. Sommer, C. Holscher, et al., An interleukin-6 receptor-dependent molecular switch mediates signal transduction of the IL-27 cytokine subunit p28 (IL-30) via a gp130 protein receptor homodimer, J. Biol. Chem. 288 (2013) 4346–4354.
[13] S.I. Muller, A. Friedl, I. Aschenbrenner, J. Esser-von Bieren, M. Zacharias, O. Devergne, et al., A folding switch regulates interleukin 27 biogenesis and secretion of its alpha-subunit as a cytokine, Proc. Natl. Acad. Sci. U. S. A. 116 (2019) 1585–1590.
[14] O. Devergne, A. Coulomb-L'Hermine, F. Capel, M. Moussa, F. Capron, Expression of Epstein-Barr virus-induced gene 3, an interleukin-12 p40-related molecule, throughout human

pregnancy: involvement of syncytiotrophoblasts and extravillous trophoblasts, Am. J. Pathol. 159 (2001) 1763–1776.
[15] O. Shimozato, A. Sato, K. Kawamura, M. Chiyo, G. Ma, Q. Li, et al., The secreted form of p28 subunit of interleukin (IL)-27 inhibits biological functions of IL-27 and suppresses anti-allogeneic immune responses, Immunology. 128 (2009) 816–825.
[16] F. Rousseau, L. Basset, J. Froger, N. Dinguirard, S. Chevalier, H. Gascan, IL-27 structural analysis demonstrates similarities with ciliary neurotrophic factor (CNTF) and leads to the identification of antagonistic variants, Proc. Natl. Acad. Sci. U. S. A. 107 (2010) 19420–19425.
[17] M.J. Boulanger, D.C. Chow, E.E. Brevnova, K.C. Garcia, Hexameric structure and assembly of the interleukin-6/IL-6 alpha-receptor/gp130 complex, Science. 300 (2003) 2101–2104.
[18] A.J. Tormo, L.A. Beaupre, G. Elson, S. Crabe, J.F. Gauchat, A polyglutamic acid motif confers IL-27 hydroxyapatite and bone-binding properties, J. Immunol. 190 (2013) 2931–2937.
[19] C. Yoon, S.C. Johnston, J. Tang, M. Stahl, J.F. Tobin, W.S. Somers, Charged residues dominate a unique interlocking topography in the heterodimeric cytokine interleukin-12, EMBO J. 19 (2000) 3530–3541.
[20] P.J. Lupardus, K.C. Garcia, The structure of interleukin-23 reveals the molecular basis of p40 subunit sharing with interleukin-12, J. Mol. Biol. 382 (2008) 931–941.
[21] N.Q. McDonald, N. Panayotatos, W.A. Hendrickson, Crystal structure of dimeric human ciliary neurotrophic factor determined by MAD phasing, EMBO J. 14 (1995) 2689–2699.
[22] F. Rousseau, S. Chevalier, C. Guillet, E. Ravon, C. Diveu, J. Froger, et al., Ciliary neurotrophic factor, cardiotrophin-like cytokine, and neuropoietin share a conserved binding site on the ciliary neurotrophic factor receptor alpha chain, J. Biol. Chem. 283 (2008) 30341–30350.
[23] L.L. Jones, V. Chaturvedi, C. Uyttenhove, J. Van Snick, D.A. Vignali, Distinct subunit pairing criteria within the heterodimeric IL-12 cytokine family, Mol. Immunol. 51 (2012) 234–244.
[24] O. Devergne, M. Birkenbach, E. Kieff, Epstein-Barr virus-induced gene 3 and the p35 subunit of interleukin 12 form a novel heterodimeric hematopoietin, Proc. Natl. Acad. Sci. U. S. A. 94 (1997) 12041–12046.
[25] F.P. Heinzel, A.M. Hujer, F.N. Ahmed, R.M. Rerko, In vivo production and function of IL-12 p40 homodimers, J. Immunol. 158 (1997) 4381–4388.
[26] S.Y. Lee, Y.O. Jung, D.J. Kim, C.M. Kang, Y.M. Moon, Y.J. Heo, et al., IL-12p40 homodimer ameliorates experimental autoimmune arthritis, J. Immunol. 195 (2015) 3001–3010.
[27] D. Chow, X. He, A.L. Snow, S. Rose-John, K.C. Garcia, Structure of an extracellular gp130 cytokine receptor signaling complex, Science. 291 (2001) 2150–2155.
[28] E.H. Duitman, Z. Orinska, E. Bulanova, R. Paus, S. Bulfone-Paus, How a cytokine is chaperoned through the secretory pathway by complexing with its own receptor: lessons from interleukin-15 (IL-15)/IL-15 receptor alpha, Mol. Cell. Biol. 28 (2008) 4851–4861.
[29] G. Espigol-Frigole, E. Planas-Rigol, H. Ohnuki, O. Salvucci, H. Kwak, S. Ravichandran, et al., Identification of IL-23p19 as an endothelial proinflammatory peptide that promotes gp130-STAT3 signaling, Sci. Signal. 9 (2016) ra28.
[30] F. Sievers, A. Wilm, D. Dineen, T.J. Gibson, K. Karplus, W. Li, et al., Fast, scalable generation of high-quality protein multiple sequence alignments using Clustal omega, Mol. Syst. Biol. 7 (2011) 539.
[31] A. Sali, T.L. Blundell, Comparative protein modelling by satisfaction of spatial restraints, J. Mol. Biol. 234 (1993) 779–815.
[32] T.S. Lee, D.S. Cerutti, D. Mermelstein, C. Lin, S. LeGrand, T. J. Giese, et al., GPU-accelerated molecular dynamics and free energy methods in Amber18: performance enhancements and new features, J. Chem. Inf. Model. 58 (2018) 2043–2050.
[33] M. Zacharias, Protein-Protein Docking with a Reduced Protein Model Accounting for Side-Chain Flexibility, Protein Sci. vol. 12 (2003) 1271–1282.
[34] S.J. de Vries, C.E. Schindler, I. Chauvot de Beauchene, M. Zacharias, A web interface for easy flexible protein-protein docking with ATTRACT, Biophys. J. 108 (2015) 462–465.
[35] S. Fiorucci, M. Zacharias, Binding site prediction and improved scoring during flexible protein-protein docking with ATTRACT, Proteins. 78 (2010) 3131–3139.
[36] J. Mongan, C. Simmerling, J.A. McCammon, D.A. Case, A. Onufriev, Generalized born model with a simple, robust molecular volume correction, J. Chem. Theory Comput. 3 (2007) 156–169.
[37] W.L. Jorgensen, C. Jenson, Temperature dependence of TIP3P, SPC, and TIP4P water from NPT Monte Carlo simulations: seeking temperatures of maximum density, J. Comput. Chem. 19 (1998) 1179–1186.
[38] J. Yang, R. Yan, A. Roy, D. Xu, J. Poisson, Y. Zhang, The I-TASSER Suite: Protein structure and function prediction, Nat. Methods 12 (2015) 7–8.

### 2.1.3 Supplementary material to the manuscript

# An Interspecies Analysis Reveals Molecular Construction Principles of Interleukin 27

Stephanie I. Müller[1,*], Isabel Aschenbrenner[1,*], Martin Zacharias[2] and Matthias J. Feige[1]

[1] Center for Integrated Protein Science at the Department of Chemistry and Institute for Advanced Study, Technical University of Munich, 85748 Garching, Germany

[2] Center for Integrated Protein Science at the Physics Department, Technical University of Munich, 85748 Garching, Germany

* These authors contributed equally to this work.

Corresponding authors:
Martin Zacharias
Technical University of Munich
Department of Physics
James-Franck-Str. 1
85748 Garching, Germany
Tel: +49-89289-12335
Fax: +49-89289-12444
E-mail: martin.zacharias@mytum.de

Matthias J. Feige
Technical University of Munich
Department of Chemistry
Lichtenbergstr. 4
85748 Garching, Germany
Tel: +49-89289-13667
Fax: +49-89289-10698
E-mail: matthias.feige@tum.de

## Supplementary Material

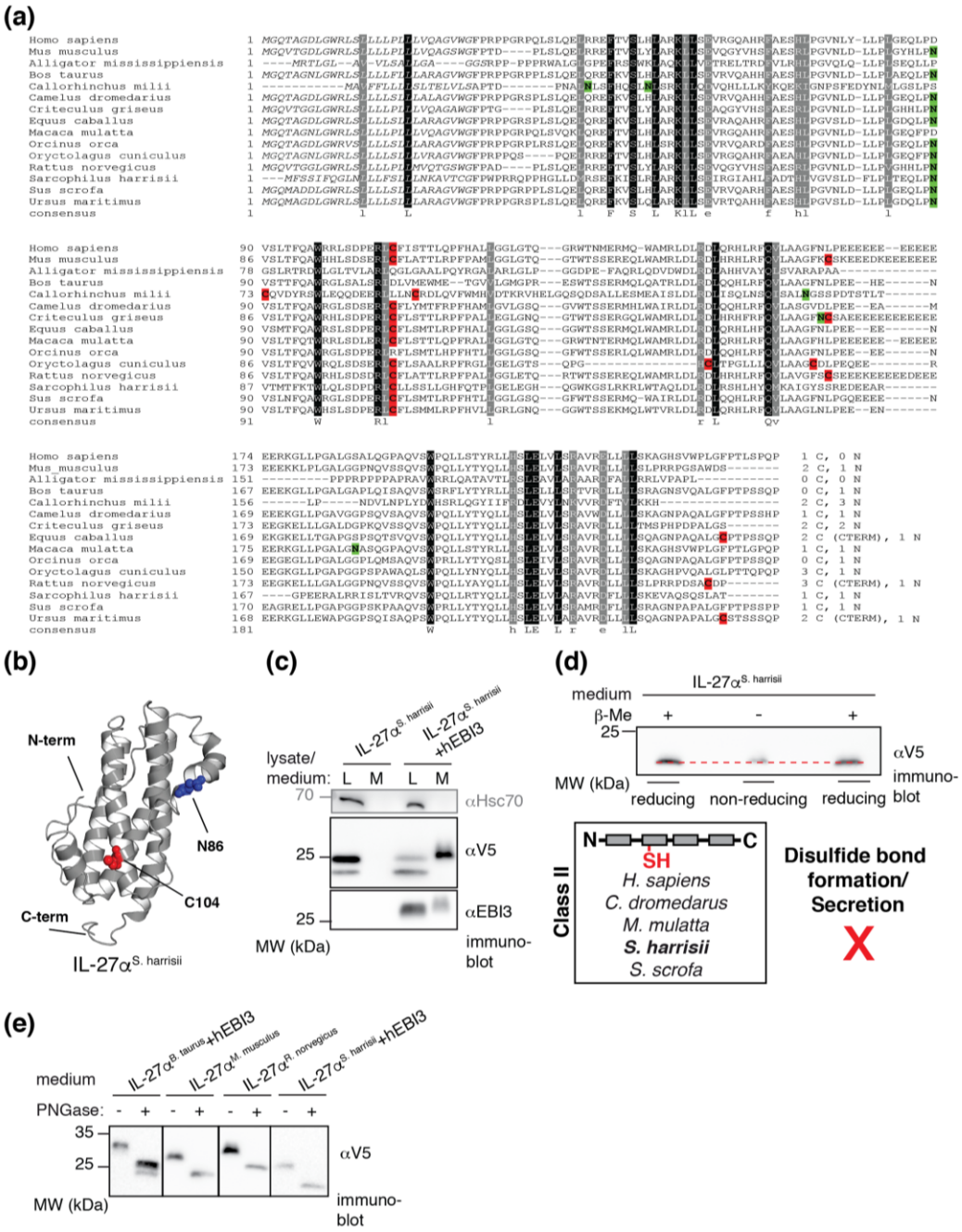


**Supplementary Fig. S1** Species comparison as a basis for an IL-27α classification based on number and location of Cys residues. (a) An IL-27α sequence alignment shows potentially folding-relevant differences in the amino acid sequences from 15 different species as cause of distinct secretion behavior. Identical residues are shaded in black, homologous amino acids in gray, *N*-glycosylation sites in green and Cys

residues in red. ER import sequences are shown in italic. Numbers of Cys residues and predicted *N*-glycosylation sites (N) are listed at the end of each sequence. (b) Homology model of *Sarcophilus harrisii* IL-27α as a further representative of class II. (c) *S. harrisii* IL-27α is not secretion-competent in isolation (L, lysate) but becomes secreted upon co-expression of hEBI3 (M, medium). 2% L/M was applied to the gel and blotted with the indicated antibodies. Hsc70 served as a loading control. (d) Absence of disulfide bond formation due to a single Cys residue within *S. harrissii* IL-27α. 2% deglycosylated medium was analyzed by non-reducing SDS-PAGE like in Fig. 1c. No mobility shift was visible, indicating absence of a disulfide bond (class II). (e) Deglycosylation control of PNGase F-treated IL-27α species. For improved mobility shift visualization on redox blots (classes III-V), *N*-glycosylated IL-27α medium samples of the depicted species were previously deglycosylated with PNGase F (indicated with (+)). 2% medium was applied to the gel and blotted with anti-V5-antibody. (c-e), MW, molecular weight.

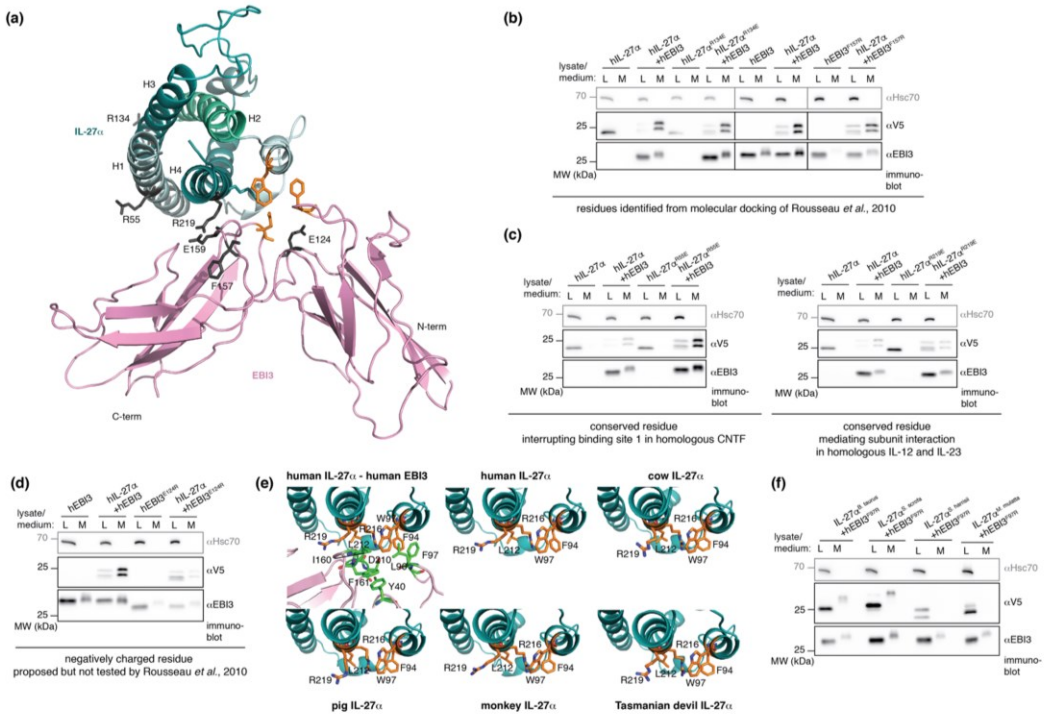


**Supplementary Fig. S2** Test of possible interface residues for disruption of human IL-27 subunit interaction. (a) Molecular docking of IL-27 showing residues identified as non-essential for subunit interactions in gray. (b) Secretion behavior of IL-27 subunit mutants identified by a molecular docking from Rousseau *et al.* [16]. All mutants shown did not disrupt IL-27 formation, as hIL-27α mutants became secreted upon co-expression of hEBI3. Likewise, shown hEBI3 mutants did not prevent hIL-27α secretion. (c) hIL-27α$^{R55E}$ (Arg25 in CNTF, which disrupts formation of CNTF/CNTFRα heterodimers [22]) is secreted into the medium upon co-expression of hEBI3. The same applies to hIL-27α$^{R219E}$ (Arg189 in IL-12α and Arg159 in IL-23α, which disrupt formation of IL-12 and IL-23 heterodimers, respectively [16]). (d) Mutation of hEBI3 Glu124, a residue proposed but not tested by Rousseau *et al.* [16], did not prevent secretion of hIL-27α into the medium. (e) Interface residues of hIL-27α-hEBI3, hIL-27α and IL-27α from cow, pig, monkey and Tasmanian devil. (f) hEBI3$^{F97R}$ shows differences in promoting secretion of IL-27α subunits from the species shown. (b-d, f)

L, lysate. M, medium. MW, molecular weight. 2% L/M were applied to the gel and blotted with the indicated antibodies. Hsc70 served as a loading control.

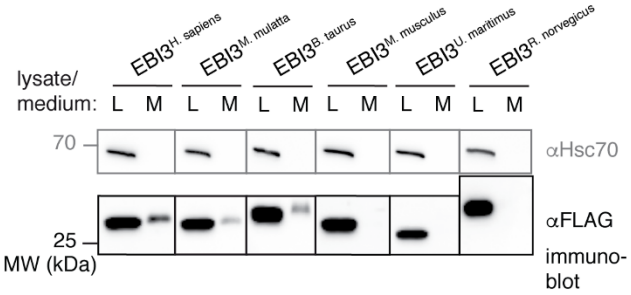


**Supplementary Fig. S3** Overexposure of immunoblots for EBI3 secretion. Depending on the species, EBI3 was secreted (M, medium) or retained in cells in isolation (L, lysate). 2% L/M were applied to the gel and blotted with anti-FLAG antibody. Hsc70 served as a loading control. MW, molecular weight.

### 2.1.4 Permission to reprint the manuscript

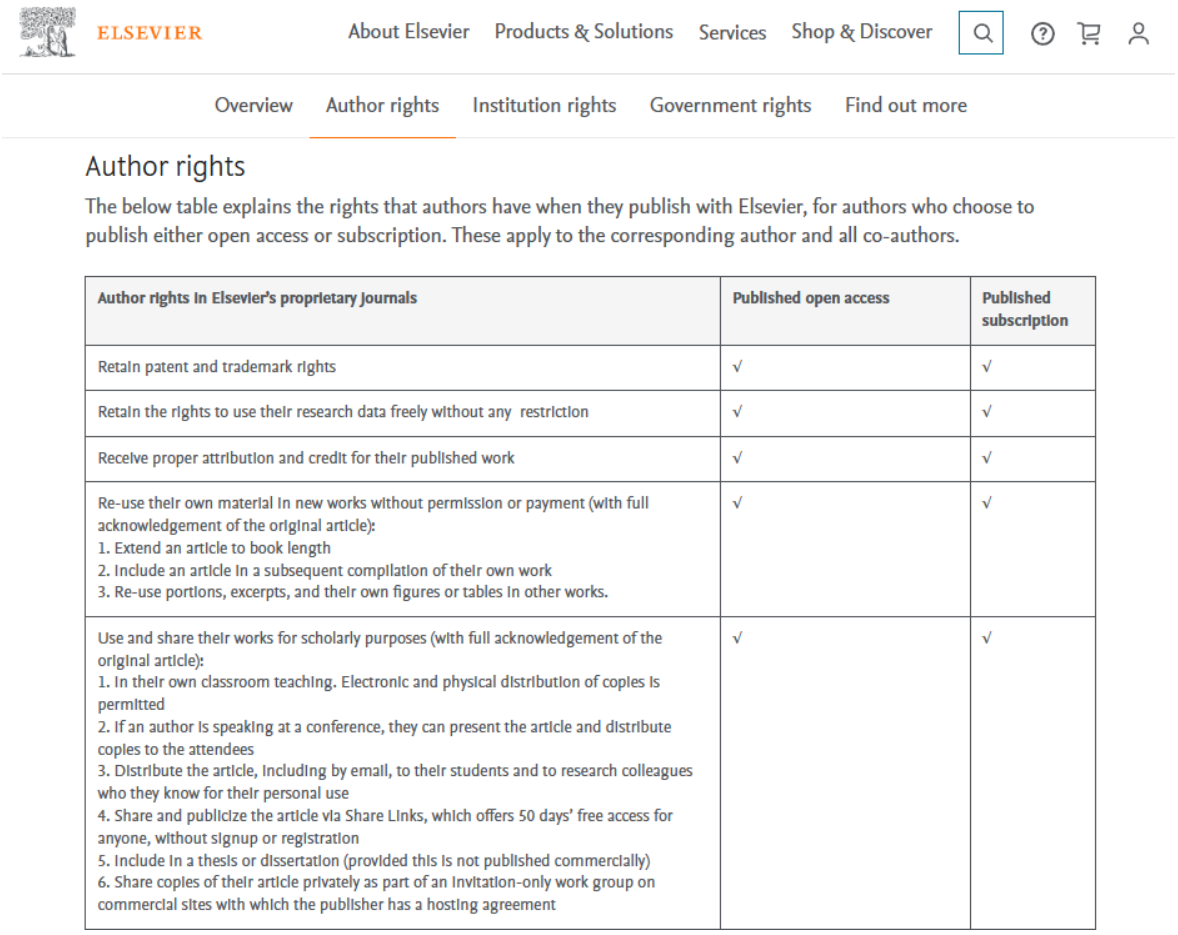

ELSEVIER About Elsevier Products & Solutions Services Shop & Discover

Overview Author rights Institution rights Government rights Find out more

## Author rights

The below table explains the rights that authors have when they publish with Elsevier, for authors who choose to publish either open access or subscription. These apply to the corresponding author and all co-authors.

| Author rights in Elsevier's proprietary journals | Published open access | Published subscription |
|---|---|---|
| Retain patent and trademark rights | √ | √ |
| Retain the rights to use their research data freely without any restriction | √ | √ |
| Receive proper attribution and credit for their published work | √ | √ |
| Re-use their own material in new works without permission or payment (with full acknowledgement of the original article):<br>1. Extend an article to book length<br>2. Include an article in a subsequent compilation of their own work<br>3. Re-use portions, excerpts, and their own figures or tables in other works. | √ | √ |
| Use and share their works for scholarly purposes (with full acknowledgement of the original article):<br>1. In their own classroom teaching. Electronic and physical distribution of copies is permitted<br>2. If an author is speaking at a conference, they can present the article and distribute copies to the attendees<br>3. Distribute the article, including by email, to their students and to research colleagues who they know for their personal use<br>4. Share and publicize the article via Share Links, which offers 50 days' free access for anyone, without signup or registration<br>5. Include in a thesis or dissertation (provided this is not published commercially)<br>6. Share copies of their article privately as part of an invitation-only work group on commercial sites with which the publisher has a hosting agreement | √ | √ |

## 2.2 Influence of glycosylation on IL-12 family cytokine biogenesis and function

Published by Sina Bohnacker[1], Karen Hildenbrand[1], **Isabel Aschenbrenner**[1], Stephanie I. Müller, Julia Esser-von Bieren, and Matthias J. Feige in *Molecular Immunology* (2020) 126: 120-128.
DOI: 10.1016/j.molimm.2020.07.015

([1] equal contribution)

**Contribution:** Experiments were performed by Sina Bohnacker, Karen Hildenbrand, **Isabel Aschenbrenner**, and Stephanie I. Müller. Sina Bohnacker, Karen Hildenbrand, **Isabel Aschenbrenner**, Stephanie I. Müller, Julia Esser-von Bieren, and Matthias J. Feige analyzed data. Sina Bohnacker, Karen Hildenbrand, **Isabel Aschenbrenner**, Julia Esser-von Bieren, and Matthias J. Feige wrote the paper.

### 2.2.1 Summary

IL-12 family members are heterodimeric cytokines which are structurally complex as they extensively share their subunits within the family. Each β-subunit is shared by two distinct α-subunits resulting in four cytokines made up of only five subunits (IL-12α:IL-12β, IL-23α:IL-12β, IL-27α:EBI3, IL-12α:EBI3). Despite of subunit sharing, a broad functional spectrum is covered by this family. Like other secretory proteins, IL-12 cytokines acquire posttranslational modifications along the secretory pathway. Besides oxidative folding by intra- or intermolecular disulfide bond formation, each member is glycosylated. In this study, we comprehensively investigated *N*- and *O*-glycosylation of human IL-12 family cytokines and the impact of glycosylation on their biogenesis and biologic functionality.

Based on glycosylation predictions by sequence analyses for each of the human IL-12 family member subunits, we assessed the overall glycosylation status by enzymatic assays. We performed an enzymatic digest by PNGase F to detect *N*-glycosylation or used *O*-Glycosidase to assess *O*-glycosylation. Subsequently, we used a mutational approach to identify and confirm the individual glycosylation sites by electrophoretic mobility shifts. *N*-glycosylation sites were defined for IL-12α, IL-12β, and EBI3. Thus, every IL-12 family heterodimer is *N*-glycosylated in at least one subunit. *N*-glycosylation sites of β-subunits are located within the two FnIII domains but not in the Ig-like domain of IL-12β. Two *O*-glycosylated residues were detected C-terminally in IL-27α by sequence comparison of the human IL-27α with the non-glycosylated murine subunit. Hence, human IL-23α is the only non-glycosylated subunit.

As glycosylation is often critical for efficient protein folding and QC in the ER, we assessed the impact of this modification on cytokine biogenesis. For humans, β-subunits are secreted in isolation, whereas for assembly-induced secretion of the α-subunits heterodimerization is required. Both IL-12 and IL-23 showed secretion independent of their glycosylation status as could be also confirmed for their shared β-subunit IL-12β. In contrast, EBI3 lacking glycosylation is completely retained in the cell, but interaction with IL-27α, either with or without *O*-glycosylation, enabled its secretion. In case of IL-27, both non-glycosylated subunits mutually enhanced their secretion. A different behavior was revealed for IL-35, as the non-glycosylated subunits IL-12α and EBI3 were not co-secreted at all. Interaction of the glycosylation mutant of one of the IL-35 subunits with the other wild-type subunit caused at least severe reduction in the wild-type subunit's secretion. For EBI3, the glycosylation site Asn105 was revealed as crucial for efficient secretion.

As the glycosylation state did not affect IL-12, IL-23, and IL-27 biogenesis, we examined its role for cytokine signaling. Induction of IFNγ gene expression in PBMCs by IL-12 was not impaired when stimulated with IL-12 glycosylation variants compared to the wildtype. For IL-23, IL-17 production by PBMCs seemed not significantly dependent on IL-23 glycosylation. Only for IL-27, STAT1 phosphorylation in BL-2 cells was reduced when *N*-glycosylation of EBI3 was absent.

Taken together, for each of the human IL-12 family member subunits we defined the glycosylation sites and could prove that glycosylation is dispensable for heterodimer biogenesis except for IL-35. Lack of glycosylation strongly impacts cytokine functionality only for IL-27. Giving that glycosylation affects secretion, heterodimerization, and activity of the IL-12 family members to different extents, this provides the basis for selective cytokine modulation via targeting their glycosylation in future immunotherapies.

## 2.2.2 Manuscript

Molecular Immunology 126 (2020) 120–128

Contents lists available at ScienceDirect

Molecular Immunology

journal homepage: www.elsevier.com/locate/molimm

Short communication

# Influence of glycosylation on IL-12 family cytokine biogenesis and function

Sina Bohnacker[a,b,1], Karen Hildenbrand[a,1], Isabel Aschenbrenner[a,1], Stephanie I. Müller[a], Julia Esser-von Bieren[b,**], Matthias J. Feige[a,*]

[a] Department of Chemistry and Institute for Advanced Study, Technical University of Munich, 85748, Garching, Germany
[b] Center of Allergy & Environment (ZAUM), Technical University of Munich and Helmholtz Zentrum München, 80802, Munich, Germany

ARTICLE INFO

*Keywords:*
interleukins
protein glycosylation
protein assembly
protein secretion
immune signaling

ABSTRACT

The interleukin 12 (IL-12) family of cytokines regulates T cell functions and is key for the orchestration of immune responses. Each heterodimeric IL-12 family member is a glycoprotein. However, the impact of glycosylation on biogenesis and function of the different family members has remained incompletely defined.

Here, we identify glycosylation sites within human IL-12 family subunits that become modified upon secretion. Building on these insights, we show that glycosylation is dispensable for secretion of human IL-12 family cytokines except for IL-35. Furthermore, our data show that glycosylation differentially influences IL-12 family cytokine functionality, with IL-27 being most strongly affected.

Taken together, our study provides a comprehensive analysis of how glycosylation affects biogenesis and function of a key human cytokine family and provides the basis for selectively modulating their secretion *via* targeting glycosylation.

## 1. Introduction

Interleukins (ILs) are secreted proteins that regulate immune cell function. Among the more than 60 ILs known to date (Akdis et al., 2016), the interleukin 12 (IL-12) family is functionally and structurally particularly complex (Tait Wojno et al., 2019; Vignali and Kuchroo, 2012). Each of its family members is a heterodimer composed of an α- and a β-subunit with extensive subunit sharing occurring in the family: IL-12 consists of IL-12α and IL-12β (Gubler et al., 1991; Kobayashi et al., 1989; Stern et al., 1990; Wolf et al., 1991), the latter is shared with IL-23 where IL-12β pairs with IL-23α (Oppmann et al., 2000). Likewise, EBI3 is the β-subunit for IL-27, where it pairs with IL-27α (Pflanz et al., 2002), but also for IL-35, where it assembles with IL-12α (Collison et al., 2007; Devergne et al., 1997). This structural complexity goes hand in hand with the broad functional spectrum of the IL-12 family. All family members are produced by antigen presenting cells and regulate T cell functions, thus connecting innate and adaptive immunity, except for IL-35, which is mainly produced by regulatory T and B cells (Tait Wojno et al., 2019; Vignali and Kuchroo, 2012). IL-12 family cytokines span a broad range of pro-inflammatory, immuno-regulatory and anti-inflammatory functions and are involved in diseases from infection *via* autoimmunity to cancer (Croxford et al., 2012; Sawant et al., 2015; Teng et al., 2015; Trinchieri et al., 2003; Yoshida and Hunter, 2015). The structural complexity and functional repertoire of the family are extended even further by the fact that also isolated IL-12 family subunits can be secreted and act as regulatory molecules in the immune system (Dambuza et al., 2017; Espigol-Frigole et al., 2016; Garbers et al., 2013; Gately et al., 1996; Lee et al., 2015; Ling et al., 1995; Muller et al., 2019b; Stumhofer et al., 2010).

Like other secreted mammalian proteins, IL-12 family cytokines are produced in the endoplasmic reticulum (ER). There, they also obtain their native structure and assemble into heterodimeric complexes before being transported further along the secretory pathway towards the cell surface for secretion. Most secreted proteins acquire post-translational modifications in the ER, with disulfide bond formation between cysteines and glycosylation of Asn residues being the most prevalent ones (Braakman and Bulleid, 2011). IL-12 family cytokines are no exception to this rule: human IL-12α, IL-12β, and EBI3 are *N*-glycosylated and each subunit except IL-27α contains at least one intramolecular disulfide bond. Additionally, IL-12 and IL-23 are disulfide-linked heterodimers (Carra et al., 2000; Devergne et al., 1996; Lupardus and Garcia, 2008; Oppmann et al., 2000; Pflanz et al., 2002; Podlaski et al.,

* Corresponding author at: Technical University of Munich, Department of Chemistry, Lichtenbergstr. 4, 85748 Garching, Germany.
** Corresponding author at: Center of Allergy & Environment (ZAUM), Technical University of Munich and Helmholtz Zentrum München, Biedersteiner Str. 29, 80802, Munich, Germany.
*E-mail addresses:* julia.esser@tum.de (J.E.-v. Bieren), matthias.feige@tum.de (M.J. Feige).
[1] These authors contributed equally to this work.

https://doi.org/10.1016/j.molimm.2020.07.015
Received 24 April 2020; Accepted 20 July 2020
Available online 18 August 2020

1992; Yoon et al., 2000). For all human IL-12 family α-subunits it was shown that oxidative folding is a key step in their biogenesis and functional roles have been delineated for intra- and intermolecular IL-12 family cytokine disulfide bonds (Jones et al., 2012; Meier et al., 2019; Muller et al., 2019a; Muller et al., 2019b; Reitberger et al., 2017; Yoon et al., 2000). In contrast, the role of glycosylation in IL-12 family biogenesis and function remains incompletely defined. Several studies indicate that glycosylation of IL-12, on its α- and on its β-subunit, is dispensable for IL-12 secretion and function *per se* – but modulates IL-12 activity (Aparicio-Siegmund et al., 2014; Carra et al., 2000; Ha et al., 2002; Podlaski et al., 1992). No comprehensive analyses are available for IL-23, IL-27 or IL-35 yet in this regard. In this study, we thus systematically investigated the effect of *N*- and *O*-glycosylation, the latter occurring in the Golgi, on IL-12 family cytokine biogenesis and function.

## 2. Materials and Methods

### 2.1. Constructs

Human interleukin cDNAs (Origene) were cloned into the pSVL vector (Amersham BioSciences) for mammalian expression. Mutants were generated by site-directed mutagenesis. All constructs were sequenced.

### 2.2. Sequence analysis, structural modeling and structural analyses

*N*-glycosylation sites were predicted by the NetNGlyc 1.0 Server (http://www.cbs.dtu.dk/services/NetNGlyc/) and *O*-glycosylation sites were assessed by the NetOGlyc 4.0 Server (http://www.cbs.dtu.dk/services/NetOGlyc/) (Steentoft et al., 2013). Both servers evaluate the potential of glycosylation by using a threshold. Sequence alignments were performed with Clustal Omega (Sievers et al., 2011). Structures were taken from the PDB database (3D87, 3HMX) and missing loops were modeled using Yasara Structure (www.yasara.org) with a subsequent steepest descent energy minimization. The homology-modeled structure of IL-27 was used (Muller et al., 2019a). Structures were depicted with PyMOL (PyMOL Molecular Graphics System, Version 2.0 Schrödinger, LLC).

### 2.3. Cell culture and transient transfections

Human embryonic kidney (HEK) 293T cells were cultured in Dulbecco's modified Eagle's medium (DMEM) containing L-Ala-L-Gln (AQmedia, Sigma Aldrich), supplemented with 10% (v/v) fetal bovine serum (FBS; Gibco, ThermoFisher) and 1% (v/v) antibiotic-antimycotic solution (25 µg/ml amphotericin B, 10 mg/ml streptomycin, and 10,000 units of penicillin; Sigma-Aldrich) at 37 °C and 5% $CO_2$. Transient transfections were carried out in poly D-lysine coated p35 dishes (VWR), or uncoated p60 dishes (VWR) for the functionality assays, using GeneCellin (Eurobio) according to the manufacturer's protocol. A total DNA amount of 2 µg (p35) or 4 µg (p60) was used. The α-subunit DNA was co-transfected with the β-subunit DNA or empty pSVL vector in equal amounts (IL-27), in a ratio of 1:2 (IL-23) or 2:1 (IL-12, IL-35) for secretion and de-glycosylation experiments. BL-2 cells were cultured in RPMI-1640 medium with L-Gln and sodium bicarbonate (Sigma-Aldrich), supplemented with 20% (v/v) heat-inactivated FBS (Gibco, ThermoFisher) and 1% (v/v) antibiotic-antimycotic solution (25 µg/ml amphotericin B, 10 mg/ml streptomycin, and 10,000 units of penicillin; Sigma-Aldrich) at 37 °C and 5% $CO_2$.

### 2.4. Immunoblotting experiments

For secretion and de-glycosylation experiments, cells were transfected for 8 h and then supplemented with fresh medium for another 16 h. To analyze secreted proteins, the medium was centrifuged (5 min, 300xg, 4 °C), transferred to a new reaction tube and supplemented with 0.1 volumes 500 mM Tris/HCl, pH 7.5, 1.5 M NaCl, complemented with 10x Roche complete Protease Inhibitor w/o EDTA (Roche Diagnostics). Cells were lysed after washing twice with ice-cold PBS. Cell lysis was carried out in RIPA buffer (50 mM Tris/HCl, pH 7.5, 150 mM NaCl, 1% Nonidet P40 substitute, 0.5% DOC, 0.1% SDS, 1x Roche complete Protease Inhibitor w/o EDTA; Roche Diagnostics) on ice. Both lysate and medium samples were centrifuged (15 min, 15,000xg, 4 °C). Samples were de-glycosylated with PNGase F (SERVA) or a mix of *O*-Glycosidase and α2-2,6,8 Neuraminidase (New England Biolabs) according to the manufacturer's protocol. For SDS-PAGE, samples were supplemented with 0.2 volumes of 5x Laemmli buffer (0.3125 M Tris/HCl, pH 6.8, 10% SDS, 50% glycerol, bromphenol blue) containing 10% (v/v) β-mercaptoethanol (β-Me). For immunoblots, samples were run on 12% SDS-PAGE gels and transferred to polyvinylidene difluoride (PVDF) membranes by blotting overnight (o/n) at 30 V (4 °C). After blocking the membrane with Tris-buffered saline (25 mM Tris/HCl, pH 7.5, 150 mM NaCl; TBS) containing 5% (w/v) skim milk powder and 0.05% (v/v) Tween-20 (M-TBST), binding of the primary antibody was carried out o/n at 4 °C with anti-Hsc70 (Santa Cruz, sc-7298, 1:1,000), anti-IL-12β (abcam ab133752, 1:500), anti-IL-12α (abcam ab133751, 1:500), anti-IL-23α (BioLegend 511202, 1:500), anti-IL-27α (R&D Systems, Bio-Techne, 1:200) in M-TBST containing 0.002% $NaN_3$ or anti-EBI3 antiserum (Devergne et al., 2001) (1:20) in PBS. Species-specific HRP-conjugated secondary antibodies (Santa Cruz Biotechnology; 1:10,000 in M-TBST or 1:5,000 for IL-23α in M-TBST) were used to detect the proteins. Amersham ECL prime (GE Healthcare) and a Fusion Pulse 6 imager (Vilber Lourmat) were used for detection.

### 2.5. Functionality assays

The **IL-12 activity assay** was performed following a previously published protocol (Reitberger et al., 2017). CD14-negative PMBCs were thawed and resuspended in RPMI-1640 (Thermo Fisher Scientific) supplemented with 10% heat-inactivated FBS (GE Healthcare) and 100 µg/ml streptomycin, 1 µg/ml gentamicin, 100 units/ml penicillin, and 2 mM L-glutamine (Thermo Fisher Scientific). Cells were seeded at a density of $5 \times 10^5$ cells/ml and stimulated with the supernatants of transfected HEK293T cells expressing the IL-12 constructs for 24 h at 37 °C and 5% $CO_2$. After harvesting (2 min, 1,000xg, 4 °C), cells were washed once with PBS prior to lysis in RLT buffer (Qiagen) supplemented with 1% β-Me. Total RNA was isolated (QuickRNA™ MicroPrep, Zymo Research) and cDNA (High-Capacity cDNA Reverse Transcription Kit, Thermo Fisher Scientific) was synthesized following the instructions of the manufacturer's protocol. Real-time PCR was performed using a ViiA 7 Real-Time PCR System (Applied Biosystems, Thermo Fisher Scientific) and the FastStart Universal SYBR Green Master Mix (Roche). Transcript levels were normalized to actin (ACTB forward, 5'-GGATGCAGAAGGAGATCACT-3'; ACTB reverse, 5'-CGATC CACACGGAGTACTTG-3'; IFNγ forward, 5'-TCAGCCATCACTTGGAT GAG-3'; IFNγ reverse, 5'-CGAGATGACTTCGAAAAGCTG-3').

For the **IL-23 activity test**, CD14-negative PBMCs were thawed in RPMI-1640 (Thermo Fisher Scientific) and 300,000 cells were resuspended in 100 µl RPMI-1640 supplemented with 5% human serum (Sigma Aldrich), 1% non-essential amino acids, 100 µg/ml streptomycin, 100 units/ml penicillin, 1 mM sodium pyruvate, and 2 mM L-glutamine (Thermo Fisher Scientific). The cells were stimulated with HEK293T supernatants containing 100 ng/ml secreted IL-23 constructs, previously quantified *via* immunoblotting with the help of recombinant IL-23 (R&D), and 10 µg/ml Phytohemagglutinin-L (Sigma Aldrich) for 72 h at 37 °C and 5% $CO_2$. After harvesting (2 min, 1,000xg, 4 °C), supernatants were analyzed for IL-17 secretion using human IL-17 DuoSet ELISA (R&D Systems), according to the manufacturer's protocol.

For IL-12 and IL-23, a **receptor activation assay** was performed using IL-12 or IL-23 iLite® reporter cells (Svar Life Science AB), respectively, according to the supplier's instructions. The cells were

stimulated with HEK293T supernatants containing 10 ng/ml secreted IL-12 or IL-23 constructs, previously quantified *via* immunoblotting by comparing immunoblot signals to those of recombinant IL-12 or IL-23 with known concentrations (R&D Systems). The firefly and renilla luminescence signals were detected *via* the Dual-Glo Luciferase Assay System (Promega) in a multimode microplate reader (CLARIOstar Plus, BMG LABTECH).

To determine **IL-27 activity** dependent on its glycosylation pattern, BL-2 cells were stimulated with IL-27 protein, derived from transiently transfected HEK293T, secreted into the medium. Protein amounts of the IL-27 variants used in this functionality assay were determined by quantification *via* immunoblotting with anti-IL-27α antibody (R&D Systems, Bio-Techne, 1:200) relative to the wild-type protein signal prior to stimulation. BL-2 cells were starved o/n in serum-free RPMI-1640 and seeded into uncoated 48-well plates (Sigma-Aldrich) resuspended in RPMI-1640 supplemented with 0.5% (w/v) bovine serum albumin (BSA; Sigma A3294) at a cell number of $1 \times 10^6$ cells/well. Subsequently, cells were stimulated for one hour with IL-27 protein or control supernatant (mock) and the reaction was stopped by adding ice-cold PBS. Cells were transferred to reaction tubes, centrifuged (5 min, 300xg, 4 °C) and lysed with NP-40 lysis buffer (50 mM Tris/HCl, pH 7.5, 150 mM NaCl, 0.5% NP40, 0.5% DOC) supplemented with 1x Roche complete Protease Inhibitor w/o EDTA (Roche Diagnostics) and 1x Phosphatase Inhibitor (SERVA). The supernatant (5 min, 20,000xg, 4 °C centrifugation) was complemented with 0.2 volumes 5x Laemmli buffer containing 10% (v/v) β-Me and loaded on 12% SDS-PAGE gels. After blotting o/n, membranes were washed with TBS, blocked with TBS containing 5% (w/v) skim milk powder and 0.1% (v/v) Tween-20 for one hour, washed again with TBS with 0.1% Tween-20 and incubated in the primary antibody (α-STAT1 or α-STAT1-P, Cell Signaling Technology, 1:1,000 in TBS with 5% (w/v) BSA, 0.1% Tween-20) o/n. Anti-rabbit HRP-conjugated antibody (Santa Cruz Biotechnology; 1:10,000 in 5% (w/v) skim milk powder and 0.1% (v/v) Tween-20 in TBS) was used for subsequent detection.

### 2.6. Quantification and statistics

Immunoblots were quantified using the Bio-1D software (Vilber Lourmat). Statistical analyses were performed using Prism (GraphPad Software). Differences were considered statistically significant when $p < 0.05$. Where no statistical data are shown, all experiments were performed at least two times, with one representative experiment selected.

## 3. Results

### 3.1. Defining IL-12 family subunit glycosylation sites

Glycosylation often is a major determinant of protein biogenesis and function. To develop a comprehensive understanding of the role of glycosylation within the IL-12 family, we first aimed at defining glycosylation sites within each constituent subunit. In this study, all analyses and experiments were performed on the human proteins. Based on a sequence analysis (Fig. S1a), multiple *N*-glycosylation sites are expected to be present within both IL-12 subunits (IL-12α, IL-12β) as well as in EBI3, the β-subunit of IL-27 and IL-35 (Fig. 1a). For both β-subunits, the Asn residues predicted to be *N*-glycosylated are located within the two Fibronectin type-III (FnIII) domains, whereas the immunoglobulin (Ig) domain of IL-12β lacks glycosylation sites. The remaining subunits of the heterodimeric IL-12 family, IL-23α and IL-27α, are not predicted to be *N*-glycosylated (Figs. 1a and S1a).

Hence, at least one subunit of every IL-12 family cytokine is predicted to be *N*-glycosylated (Fig. 1a). To assess these predictions, we first investigated the overall glycosylation status of each IL-12 family subunit by enzymatic assays. Subsequently, if glycosylation was detectable, we identified modified residues by mutational analyses (Fig. 1b). In these experiments, αβ pairs were always co-expressed and secreted cytokines were analyzed. Using PNGase F, which removes *N*-linked glycans, electrophoretic mobility shifts were observed for IL-12α, IL-12β, and EBI3 but not for IL-23α and IL-27α (Fig. 1b), verifying overall predictions of *N*-glycosylation (Figs. 1a and S1a). Likewise, *O*-Glycosidase was used to detect *O*-glycosylation of each IL-12 family subunit. Of note, secreted wild-type IL-12α migrates differently when enzymatically digested with the *O*-Glycosidase mix. However, this mix also contains α2-2,6,8 Neuraminidase, which cleaves terminal sialic acid residues from glycosylation moieties. IL-12α has previously been shown to be modified with sialic acid (Carra et al., 2000), which is consistent with this observation. In agreement with this notion, the mutant IL-12α$^{N93,107Q}$ lacking *N*-glycosylation sites did not show any different migration upon this enzymatic de-glycosylation treatment any more (Fig. 1b). The shift in molecular weight for wild-type IL-12α can thus most likely be attributed to the enzymatic removal of terminal sialic acid residues from the complex *N*-linked sugar moiety, which arises from glycoprotein processing along the secretory pathway (Bohm et al., 2015; Zhang et al., 2019). In contrast, IL-27α was found to be *O*-glycosylated (Fig. 1a and b), in agreement with previous studies (Muller et al., 2019a; Muller et al., 2019b; Pflanz et al., 2002).

Using mutational analyses, we next proceeded to identify individual glycosylation sites within each modified subunit. For IL-12α, mutation of two Asn residues (N93, N107), both predicted to be *N*-glycosylation sites (Fig. S1a), to Gln resulted in a protein with the same electrophoretic migration behavior as the wild-type counterpart after PNGase F treatment (Fig. 1b). Furthermore, treating this mutant with PNGase F did not lead to any further changes in electrophoretic mobility, verifying that mutation of N93 and N107 was sufficient to abolish IL-12α *N*-glycosylation (Fig. 1b).

Using mutated variants of IL-12β (IL-12β$^{N125,135,222,303Q}$) and EBI3 (EBI3$^{N55,105Q}$) that lacked all possible glycosylation sites, we could verify *N*-glycosylation of these two proteins (Fig. 1a and b). In EBI3$^{N55,105Q}$, only the two predicted sites were mutated (Fig. S1a), and confirmed by electrophoretic mobility shift assays (Fig. 1b). In case of IL-12β, two Asn residues were predicted to be *N*-glycosylated (N135 and N222, Fig. S1a) but only N222 could be experimentally validated (Fig. S1b). Since secreted IL-12β$^{N222Q}$ still showed glycosylation, we analyzed further possible *N*-glycosylation sites that were below the threshold for glycosylation-prediction (Fig. S1b). This approach revealed that also N125 and N303 were glycosylated to a certain extent in IL-12β.

To identify *O*-glycosylated Ser/Thr residues within human IL-27α, we made use of the fact that murine IL-27α is not *O*-glycosylated (Muller et al., 2019a; Muller et al., 2019b; Pflanz et al., 2002) despite approximately 75% sequence conservation. A sequence alignment of the murine and human IL-27 α-subunits showed only few Ser and Thr residues that were present in the human but not the murine protein (Fig. S2a). Focusing on surface-exposed residues among those (Fig. S2b), mutational analyses of respective residues in a secretion-competent human IL-27α variant (Muller et al., 2019b) identified two C-terminal *O*-glycosylated residues, T238 and S240 (Fig. S2c). Mutation of these residues to Ala completely abolished *O*-glycosylation in human IL-27α (Figs. 1b and S2c).

Taken together, we could confirm predicted and identify new glycosylation sites of human IL-12 family cytokine subunits. Although modifications of subunits vary within the IL-12 family, each heterodimer was modified (Fig. 1a and b). Next, we thus aimed at defining how glycosylation affected heterodimerization and secretion of each IL-12 family cytokine.

### 3.2. Glycosylation is essential for IL-35 secretion, but not for secretion of other IL-12 family members

When expressed in isolation, all human IL-12 family α-subunits are retained in the cell. Only the presence of a corresponding β-subunit

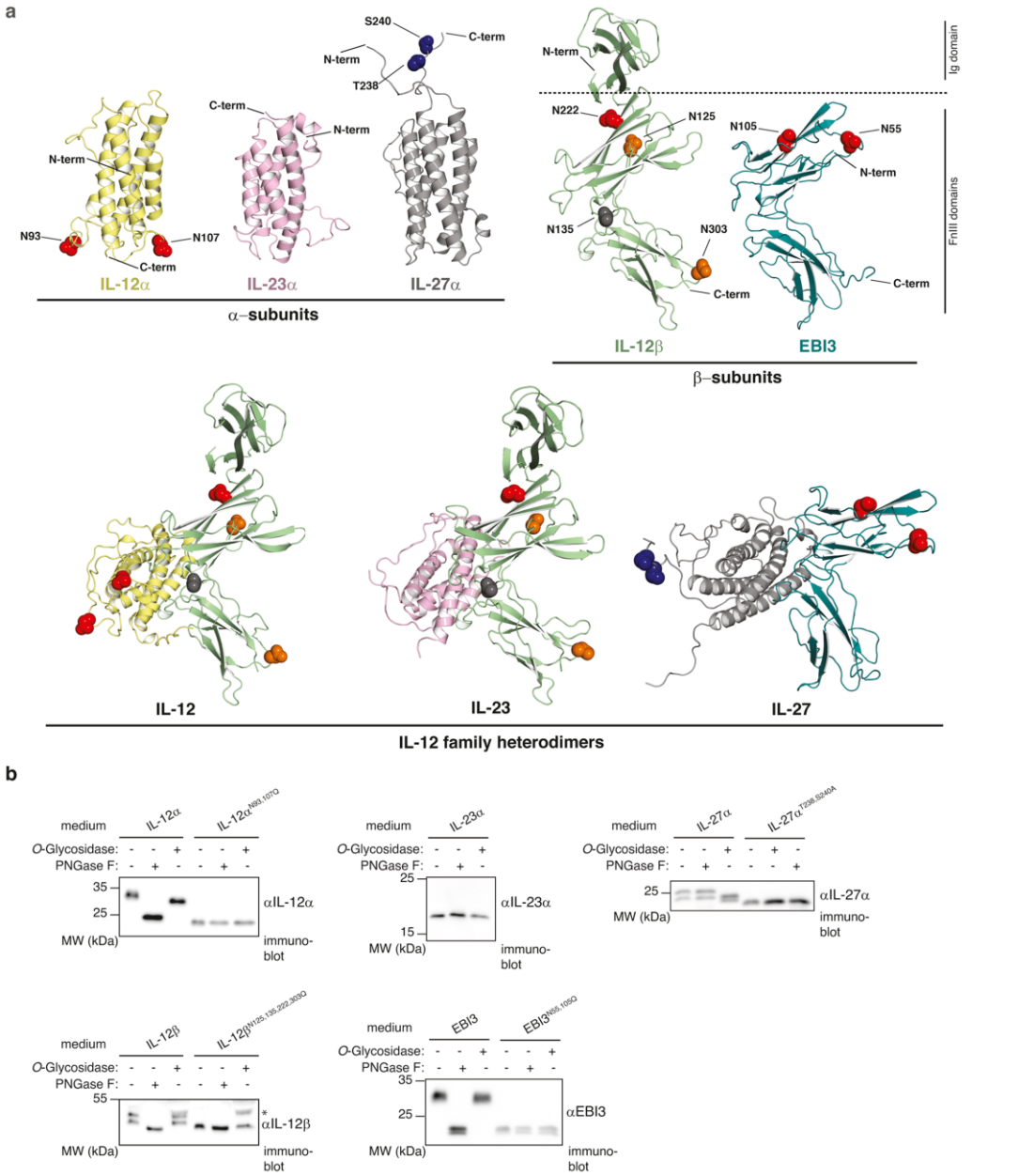


**Fig. 1.** Interleukin 12 family cytokines differ in their glycosylation patterns. (a) Top: Structural overview and glycosylation sites of the five shared subunits of the heterodimeric IL-12 family. Within the structures of the 4-helix bundle α-subunits IL-12α (PDB: 3HMX), IL-23α (PDB: 3D87), and the homology model of IL-27α (Muller et al., 2019a), glycosylation sites are labeled and shown in a CPK representation. The β-subunits IL-12β (PDB: 3HMX) and EBI3 (homology model, (Muller et al., 2019a)) possess predicted *N*-glycosylation sites in the Fibronectin III (FnIII) domains, but not in the immunoglobulin (Ig) domain of IL-12β. Experimentally verified *N*-glycosylation sites are shown in red, *O*-glycosylation sites in blue. For IL-12β, the residue N135 (gray) was predicted as *N*-glycosylation site but could not be experimentally verified. Instead, two other *N*-glycosylation sites (N125, N303) that were below the threshold for prediction, were experimentally identified as glycosylation-modified and are shown in orange. Bottom: The heterodimers IL-12 (PDB: 3HMX) and IL-23 (PDB: 3D87) share IL-12β (green), whereas the β-subunit EBI3 (cyan) is part of IL-27 (homology model, (Muller et al., 2019a)) and IL-35 (no structural model available). (b) Verification of the predicted glycosylation sites of IL-12 family subunits by enzymatic treatment (PNGase F or *O*-Glycosidase) and mutagenesis of the respective sites. IL-12α is *N*-glycosylated at N93 and N107, whereas IL-23α is not glycosylated. IL-27α is *O*-glycosylated at two residues (T238, S240). Both β-chains, IL-12β and EBI3, are *N*-glycosylated at multiple sites (IL-12β: N125, N222, N303; EBI3: N55, N105). For EBI3, a double band pattern arose only after enzymatic digest and thus seems to be an artefact related to the enzymatic treatment. α- and β-subunits were co-expressed and treated with PNGase F or *O*-Glycosidase/Neuraminidase. 1.8% medium, or 3.6% medium in case of IL-12β, was applied to the gel and blotted with antibodies against the respective subunits. Electrophoretic mobility shifts indicate de-glycosylation. The asterisk indicates non-specific detection of the Neuraminidase. MW, molecular weight.

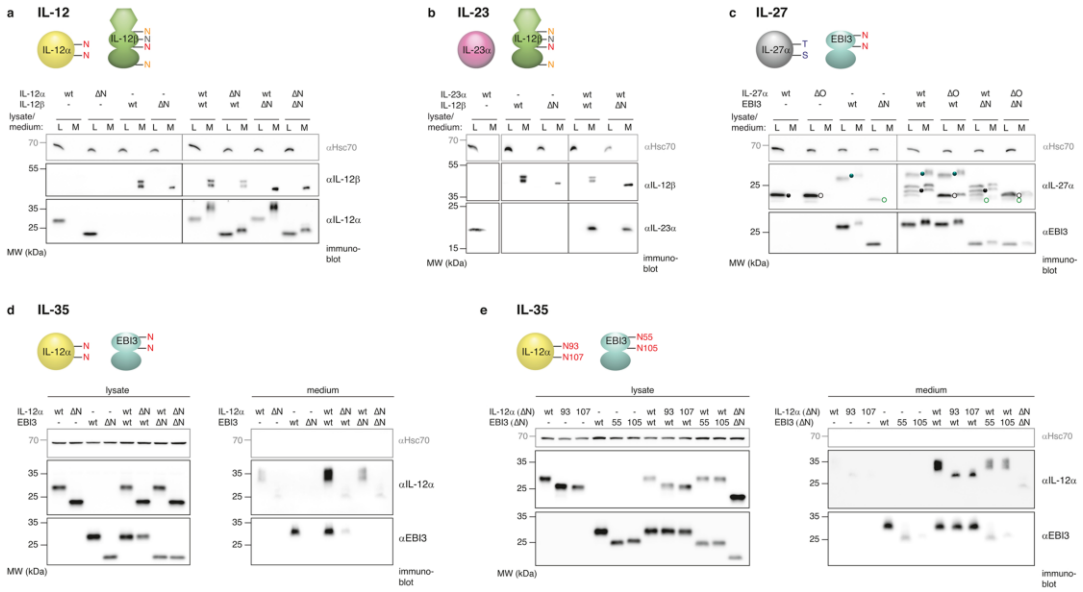


**Fig. 2.** Impact of glycosylation on IL-12 family cytokine secretion. (a-d) All human wild-type α-subunits are secretion-incompetent in isolation (IL-12α, IL-23α, IL-27α) and retained in cells (L). Their pairing with secretion-competent wild-type β-subunits (IL-12β, EBI3) to form the heterodimeric ILs induces secretion into cell media (M). (a) For IL-12, glycosylation mutants do neither affect the formation of the heterodimer nor its secretion behavior. (b) IL-23 heterodimer formation is not affected by lacking glycosylation of IL-12β and is secreted similarly to the wild type. (c) For IL-27, the α-subunit lacking *O*-glycosylation (open gray circle) behaves analogous to the wild type (filled gray circle), whereas the mutant EBI3 without *N*-glycosylation (open cyan circle) is retained in cells in isolation in contrast to wild-type EBI3 (filled cyan circle). Co-transfection of both subunits results in heterodimer formation as both non-glycosylated cytokine subunits become secreted. The used αIL-27α antibody detects also the EBI3 subunit. (d) For IL-35, both IL-12α$^{\Delta N}$ and EBI3$^{\Delta N}$ are not secreted in isolation and heterodimer formation is severely impaired. (e) Secretion behavior and heterodimer formation of IL-35 are affected by the individual *N*-glycosylation sites of IL-12α and EBI3. IL-12α$^{N93Q}$ and IL-12α$^{N107Q}$ are only secreted to a much lower extent upon co-expression with EBI3, compared to the wild type. Similarly, the individual EBI3 glycosylation mutants are mostly retained in isolation and only induce reduced secretion levels of IL-12α. (d-e) To facilitate an analysis regarding low IL-35 secretion levels, lysate and medium samples were analyzed on separate blots. (a-e) ΔN and ΔO indicate subunits where *N*-glycosylation sites are mutated to Gln or *O*-glycosylation sites are mutated to Ala, respectively. In the schematic models, circles represent the 4-helix bundle α-subunits, hexamers stand for the Ig domains and ellipses for the FnIII domains of the β-subunits. L, lysate. M, medium. MW, molecular weight. 2% L/M (in (b): 4% L/M, for IL-23α transfected alone 6.4% L/M, in (d-e): 6% M) were applied to the gel and blotted with antibodies against the respective subunits. Hsc70 served as a loading control.

leads to assembly-induced secretion of the heterodimeric cytokine (Devergne et al., 1997; Gubler et al., 1991; Oppmann et al., 2000; Pflanz et al., 2002). Conversely, IL-12β is readily secreted in isolation, whereas EBI3 shows only inefficient secretion (Devergne et al., 1996; Ling et al., 1995). Thus, heterodimerization is a prerequisite for secretion of most of the IL-12 subunits to occur or increase. This suggests that glycosylation, which is often coupled to ER folding and quality control processes, may impact IL-12 family cytokine secretion. To assess the effect of subunit glycosylation on the secretion of single subunits as well as heterodimer formation, we investigated the secretion behavior of each IL-12 family member.

For IL-12 and IL-23, even the complete absence of glycosylation did not result in pronounced effects on secretion and thus heterodimerization (Fig. 2a and b). IL-12β$^{N125,135,222,303Q}$ (IL-12β$^{\Delta N}$) behaved comparable to the wild-type protein with regard to its secretion levels and was still able to induce secretion of IL-12α, its non-glycosylated variant IL-12α$^{N93,107Q}$ (IL-12α$^{\Delta N}$) (Fig. 2a) and the naturally non-glycosylated IL-23α (Fig. 2b).

In contrast to IL-12β, glycosylation of EBI3 turned out to be essential for its secretion as EBI3$^{N55,105Q}$ (EBI3$^{\Delta N}$) was not secreted in isolation anymore (Fig. 2c and d). Wild-type EBI3 induced the secretion of both IL-27α and IL-27α$^{T238,S240A}$ (IL-27α$^{\Delta O}$), lacking *O*-glycosylation. Interestingly, although retained itself, EBI3$^{\Delta N}$ also induced secretion of both these IL-27α variants and was co-secreted (Fig. 2c). Thus, IL-27 subunit mutants lacking glycosylation are still able to interact and enhance their mutual secretion despite being secretion-incompetent in isolation.

Although sharing the same β-subunit as IL-27, secretion of IL-35 was strongly affected by missing glycosylation (Fig. 2d). Mutation of either of its subunits, IL-12α or EBI3, was sufficient to block or severely reduce secretion of the other subunit in this heterodimeric cytokine. Furthermore, co-expression of non-glycosylated IL-12α$^{\Delta N}$ and EBI3$^{\Delta N}$ showed no co-secretion into the medium (Fig. 2d). The fact that IL-12α$^{\Delta N}$ reduced secretion of wild-type EBI3, which is secretion-competent on its own, implies that heterodimerization still occurred for this pair leading to retention of the heterodimeric cytokine by ER quality control. Based on these findings, we examined the effect of the individual glycosylation sites of each IL-35 subunit. IL-12α single mutants N93Q and N107Q were secreted upon co-expression of EBI3, but to a lesser extent than wild-type IL-12α (Fig. 2e). The two individual EBI3 mutants N55Q and N105Q were secreted in isolation, but to decreased levels, which was not further enhanced upon IL-12α co-expression. Especially glycosylation at N105 seemed to be critical for efficient secretion of EBI3 (Fig. 2e).

In summary, the absence of glycosylation affects the secretion of IL-12 family cytokines in a surprisingly different manner. IL-12 and IL-23 seem to be secreted independently of their glycosylation status, whereas deleting glycosylation in IL-27 subunits led to a decreased secretion. Most pronounced effects were observed for IL-35, where absence of glycosylation caused an almost complete and dominant retention in the cell.

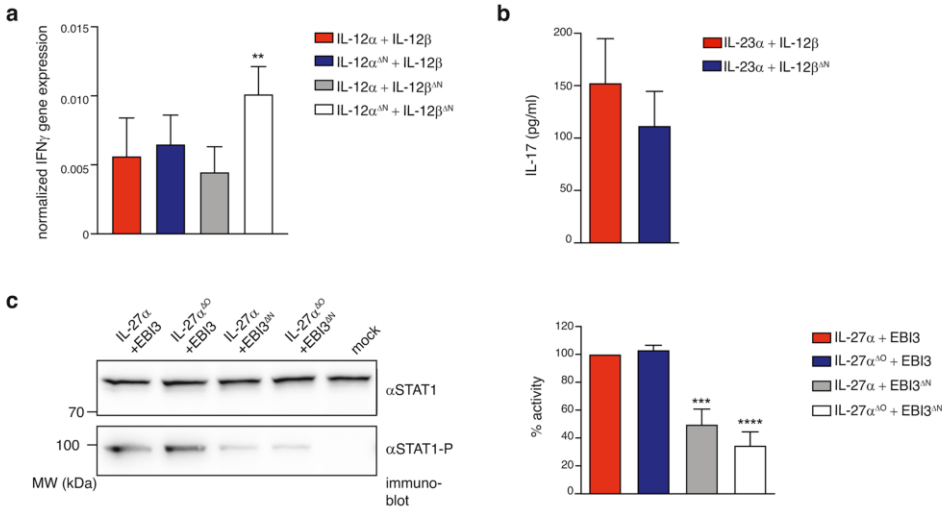


**Fig. 3.** Glycosylation influences the functionality of IL-12 family cytokines differently. (a) Glycosylation states of IL-12α and IL-12β influence biological functionality of heterodimeric IL-12. Stimulation of human peripheral blood mononuclear cells (PBMCs) with the indicated IL-12 glycosylation-variants show IFNγ induction by all analyzed heterodimers measured by qPCR. Data were normalized to secretion levels (Fig. S3a) and transcription levels were normalized to actin. The IL-12 heterodimer lacking glycosylation in both subunits shows significantly enhanced gene expression levels compared to the wild-type proteins. Data are presented as mean ± SEM, PBMCs were from n = 9 donors. Statistical significance was determined by the Friedman test (more than 2 groups). (b) IL-23 function is not significantly affected by lacking glycosylation. PBMCs were stimulated with previously quantified supernatants of HEK293T cells co-transfected with IL-23α and IL-12β variants (Fig. S3b). IL-17 production measured in the supernatant *via* ELISA, was not significantly changed for the glycosylation mutant. Data are shown as mean ± SEM, PBMCs were from n = 6 donors. Statistical significance was calculated using a two-tailed paired t-test. (c) Functionality of IL-27 depends on the glycosylation states of EBI3. Stimulation of human BL-2 cells with differently glycosylated IL-27, using previously quantified HEK293T supernatants co-transfected with IL-27α and EBI3 (Fig. S3c), shows significantly reduced cytokine signaling for EBI3$^{\Delta N}$ in complex with IL-27α or IL-27α$^{\Delta O}$. Levels of STAT1 phosphorylation (α-STAT1-P) were quantified and indicate receptor activation by heterodimeric IL-27. αSTAT1-immunoblot signals serve as loading control. Activity levels were determined from at least four independent experiments (shown ± SEM). Signals were normalized to the wild-type signal which was set to 100% activity. Statistical significance was calculated using a two-way ANOVA. (a-c) **p < 0.01, ***p < 0.001, and ****p < 0.0001 indicate statistical significance. Mock, empty vector transfection. MW, molecular weight.

### *3.3. Lack of glycosylation does not compromise IL-12- or IL-23-mediated responses, but reduces IL-27 signaling*

Our data indicate that for the IL-12 family members IL-12, IL-23, and IL-27 glycosylation was dispensable for heterodimer formation and secretion (Fig. 2). For these three cytokines, we thus investigated the impact of glycosylation on their biological functions by comparison of the different glycosylation mutants with their wild-type counterparts.

A major physiological activity of IL-12 is the induction of IFNγ expression (Chan et al., 1991). We therefore assessed the IL-12-induced IFNγ production in human peripheral blood mononuclear cells (PBMCs) by qPCR, using wild-type IL-12 and its glycosylation mutants (Figs. 3a and S3a). All IL-12 glycosylation variants induced IFNγ gene expression (Fig. 3a). Mutation of *N*-glycosylation sites in either the α- or β-subunit (IL12α$^{\Delta N}$ + IL-12β, IL12α + IL-12β$^{\Delta N}$) did not significantly change the level in gene expression compared to wild-type IL-12. Surprisingly, non-glycosylated IL-12 (IL12α$^{\Delta N}$ + IL-12β$^{\Delta N}$) showed a particularly strong increase of IFNγ-induction in PBMCs (Fig. 3a), whereas a slight decrease in receptor activation of IL-12 iLite® reporter cells compared to wild-type heterodimer was observed (Fig. S4a).

Next, we examined the dependency of IL-23 signaling on cytokine glycosylation by measuring IL-23-induced IL-17 production in PBMCs (Langrish et al., 2005). Since IL-23α has no glycosylation sites (Fig. 1), only IL-17 production after stimulation with wild-type IL-23 and the mutant heterodimer consisting of IL-23α and IL-12β$^{\Delta N}$ were assessed using ELISA (Figs. 3b and S3b). In these experiments, no significant change in IL-17 secretion was observed for wild-type IL-23α in comparison to the non-glycosylated variant (Fig. 3b). Stimulation of IL-23 iLite® reporter cells with the IL-23 glycosylation mutant (IL-23α + IL-12β$^{\Delta N}$) showed a slightly reduced receptor activation (Fig. S4b).

Lastly, we assessed the impact of glycosylation on IL-27 activity. Toward this end, we used the lymphoma BL-2 cell line which, in response to IL-27 stimulation, shows induction of STAT1 phosphorylation (Dietrich et al., 2014). Quantification of the phospho-STAT1 signals *via* immunoblotting confirmed signaling-competency for all IL-27 glycosylation variants in BL-2 cells (Figs. 3c and S3c). The heterodimer composed of IL-27α$^{\Delta O}$ and wild-type EBI3 showed no significant change in activity compared to IL-27. In contrast, the activity of the complex of wild-type IL-27α with EBI3$^{\Delta N}$ as well as of the non-glycosylated IL-27 heterodimer (IL-27α$^{\Delta O}$ + EBI3$^{\Delta N}$) was significantly decreased in comparison to IL-27 wild type (Fig. 3c).

Taken together, glycosylation in the interleukin-12 family does not seem to be essential for cytokine signaling. However, not only the secretion but also the biological functions of IL-12 family cytokines seem to be affected by the absence of glycosylation to a different extent: IL-27 signaling was reduced when EBI3 lacked glycosylation, whereas IL-12 and IL-23 function was less dependent of their glycosylation status, which may however modulate responses induced by these cytokines (Ha et al., 2002).

## 4. Discussion

In this study we provide a comprehensive analysis of how glycosylation influences human IL-12 family cytokine biogenesis and function. This extends previous studies on the impact of disulfide bond formation within IL-12 family cytokines (Jalah et al., 2013; Meier et al., 2019; Muller et al., 2019a; Muller et al., 2019b; Reitberger et al., 2017; Yoon et al., 2000) by insights into the second major post-translational

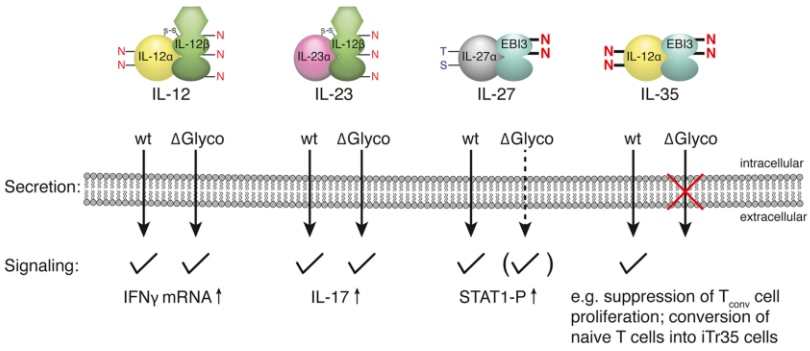


**Fig. 4.** The impact of glycosylation on human IL-12 family biogenesis and function. All heterodimeric wild-type (wt) IL-12 family cytokines are secreted and show biological function. IL-35 wild-type signaling was previously described (Collison et al., 2012; Collison et al., 2007). Both, IL-12 and IL-23 were secreted irrespective of their glycosylation status and also their biological functions (IFNγ gene expression and IL-17 production, respectively) were not compromised by lacking glycosylation. In contrast, lacking glycosylation of IL-27 led to a decreased secretion and signaling (phosphorylation of STAT1). Non-glycosylated IL-35 was almost completely retained in the cell. Red letters indicate *N*-glycosylated sites, blue letters *O*-glycosylated sites. Bold letters indicate glycosylation sites critical for secretion and functionality.

modification occurring in the ER. We could verify that all IL-12 family subunits except IL-23α are glycosylated and identified new glycosylation sites. Moreover, our study reveals that loss of glycosylation affects secretion, heterodimer formation and biological activity of the IL-12 family members to different extents (Fig. 4).

A general principle for the human IL-12 family is assembly-induced folding of the α-subunit by a suitable β-subunit and subsequent secretion of the heterodimeric cytokine (Devergne et al., 1997; Gubler et al., 1991; Jalah et al., 2013; Meier et al., 2019; Muller et al., 2019b; Oppmann et al., 2000; Pflanz et al., 2002; Reitberger et al., 2017). It can thus be expected that whenever glycosylation is a prerequisite for proper β-subunit folding and assembly with its cognate α-subunit, effects on cytokine secretion should be dominant. In complete agreement with this idea, non-glycosylated and consequently cell-retained EBI3 abrogated secretion of IL-35 and significantly reduced IL-27 secretion. Interestingly, although diminished, mutant IL-27 subunits (IL-27α and EBI3) lacking glycosylation were still able to interact and induce their mutual secretion despite being secretion-incompetent in isolation. This possibility of pairing of two secretion-incompetent subunits to become secreted together has previously been observed in the context of oxidative subunit folding for IL-27 (Muller et al., 2019a). It suggests that IL-27 subunits are (partially) folded even when lacking glycosylation but still expose features that do not allow them to pass ER quality control. Among the four human IL-12 family cytokines investigated, our study reveals IL-35 formation to be most strongly dependent on glycosylation. This may explain failed attempts of IL-35 reconstitution using a recombinant non-glycosylated IL-12α subunit purified from bacteria (Aparicio-Siegmund et al., 2014).

In contrast to EBI3, IL-12β without glycosylation behaved comparable to its wild-type counterpart and still formed IL-12 and IL-23. Thus, heterodimers containing IL-12β are in general less affected by their extent of glycosylation than those containing EBI3. Of note, IL-12 and IL-23 contain intermolecular disulfide bridges (Lupardus and Garcia, 2008; Yoon et al., 2000), which may facilitate heterodimer secretion even without other stabilizing factors like sugar moieties. In agreement with this notion, IL-12 and IL-23 were still functional with regard to IFNγ or IL-17 induction in human lymphocytes, respectively, and exhibited receptor activation capabilities in reporter cell lines. In contrast, we observed impaired functionality for IL-27, when its β-subunit lacked *N*-glycosylation.

IL-12 family cytokines are attractive therapeutic targets and potential biopharmaceuticals (Muller et al., 2019b; Tait Wojno et al., 2019; Teng et al., 2015; Vignali and Kuchroo, 2012; Yan et al., 2016; Yeku and Brentjens, 2016). Our study assesses the impact of glycosylation on IL-12 family cytokine secretion and functionality by a limited number of tests and therefore builds the basis for further pharmaceutical investigations. Although we observed functionality for non-glycosylated IL-12 family cytokines, it should be considered that the biological activity of the tested cytokines may vary dependent on their glycosylation patterns. Furthermore, glycosylation serves not only as a checkpoint for trafficking along the secretory pathway but also influences protein characteristics such as solubility, stability, and biodistribution within the human body, as already investigated for an antibody-p40 fusion protein (Bootz et al., 2016). On the other hand, since our study reveals IL-12, IL-23, and IL-27 to be secreted and functional even when completely lacking glycosylation, modifying glycosylation patterns may also open new doors towards rationally modifying IL-12 family cytokine functionality, as exemplified by G-CSF (Chamorey et al., 2002).

Finally, it is noteworthy that deleting glycosylation sites abolished IL-35 formation yet was compatible with formation of functional IL-12 and IL-27, which each share one subunit with IL-35. In the light of the chain sharing promiscuity within the IL-12 family this is relevant, since a simple knockout of single IL-12 family subunits generally affects more than one of the heterodimeric family members. Mutating glycosylation sites may thus be a viable way to selectively delete individual IL-12 family members from an organism's cytokine repertoire. Our findings concerning glycosylation-dependent secretion of IL-35 could be of particular interest with regard to the immunosuppressive role of this cytokine (Vignali and Kuchroo, 2012; Xue et al., 2019), e.g. in cancer forms that are difficult to treat (Mirlekar et al., 2018; Pylayeva-Gupta et al., 2016). As our study identifies a pivotal role for IL-35 subunit glycosylation in IL-35 formation, its targeting could represent a promising strategy for future immunotherapies.

## 5. Conclusions

In this study, we characterized the human IL-12 family in regard of their glycosylation profile. We were able to verify that at least one subunit of all IL-12 family members is glycosylated and furthermore identified new glycosylation sites. Our data indicate that loss of glycosylation does not severely affect IL-12 and IL-23 secretion, heterodimer formation, and biological activity. In contrast, non-glycosylated IL-27 shows partially impaired biogenesis and reduced signaling, whereas missing glycosylation of IL-35 led to complete retention in the cell. These findings extend our insights into this key cytokine family and provide a possibility to selectively remove individual IL-12 cytokines from an organism's cytokine repertoire.

## Author contributions

MJF conceived the study. Experiments were performed by SB, KH, IA, and SIM. SB, KH, IA, SIM, JEvB, and MJF analyzed data. SB, KH, IA, JEvB, and MJF wrote the paper.

## Declaration of Competing Interest

A patent on IL-27 glycosylation mutants has been submitted.

## Acknowledgements

We are grateful to Odile Devergne, INSERM/France, for the kind gift of anti-EBI3 antiserum. Furthermore, we thank the group of Dr. Stefanie Eyrich for the kind gift of PHA and T-cell medium. IA gratefully acknowledges a PhD scholarship by the Studienstiftung des Deutschen Volkes and KH by the Cusanuswerk.

This study was supported by a Helmholtz Young Investigator grant (VH-NG-1331) by the Helmholtz Initiative and Networking fund of the Helmholtz Association to JEvB. MJF is a Rudolf Mößbauer Tenure Track Professor and as such gratefully acknowledges funding through the Marie Curie COFUND program and the Technical University of Munich Institute for Advanced Study, funded by the German Excellence Initiative and the European Union Seventh Framework Program under Grant Agreement291763. This work was performed within the framework of SFB 1035 (German Research Foundation DFG, Sonderforschungsbereich 1035, Projektnummer 201302640, project B11).

## Appendix A. Supplementary data

Supplementary material related to this article can be found, in the online version, at doi:https://doi.org/10.1016/j.molimm.2020.07.015.

## References

Akdis, M., Aab, A., Altunbulakli, C., Azkur, K., Costa, R.A., Crameri, R., Duan, S., Eiwegger, T., Eljaszewicz, A., Ferstl, R., Frei, R., Garbani, M., Globinska, A., Hess, L., Huitema, C., Kubo, T., Komlosi, Z., Konieczna, P., Kovacs, N., Kucuksezer, U.C., Meyer, N., Morita, H., Olzhausen, J., O'Mahony, L., Pezer, M., Prati, M., Rebane, A., Rhyner, C., Rinaldi, A., Sokolowska, M., Stanic, B., Sugita, K., Treis, A., van de Veen, W., Wanke, K., Wawrzyniak, M., Wawrzyniak, P., Wirz, O.F., Zakzuk, J.S., Akdis, C.A., 2016. Interleukins (from IL-1 to IL-38), interferons, transforming growth factor beta, and TNF-alpha: Receptors, functions, and roles in diseases. J Allergy Clin Immunol 138, 984–1010.

Aparicio-Siegmund, S., Moll, J.M., Lokau, J., Grusdat, M., Schroder, J., Plohn, S., Rose-John, S., Grotzinger, J., Lang, P.A., Scheller, J., Garbers, C., 2014. Recombinant p35 from bacteria can form Interleukin (IL-)12, but Not IL-35. PLoS One 9, e107990.

Bohm, E., Seyfried, B.K., Dockal, M., Graninger, M., Hasslacher, M., Neurath, M., Konetschny, C., Matthiessen, P., Mitterer, A., Scheiflinger, F., 2015. Differences in N-glycosylation of recombinant human coagulation factor VII derived from BHK, CHO, and HEK293 cells. BMC Biotechnol 15, 87.

Bootz, F., Venetz, D., Ziffels, B., Neri, D., 2016. Different tissue distribution properties for glycosylation variants of fusion proteins containing the p40 subunit of murine interleukin-12. Protein Eng Des Sel 29, 445–455.

Braakman, I., Bulleid, N.J., 2011. Protein folding and modification in the mammalian endoplasmic reticulum. Annu Rev Biochem 80, 71–99.

Carra, G., Gerosa, F., Trinchieri, G., 2000. Biosynthesis and posttranslational regulation of human IL-12. Journal of immunology 164, 4752–4761.

Chamorey, A.L., Magne, N., Pivot, X., Milano, G., 2002. Impact of glycosylation on the effect of cytokines. A special focus on oncology. Eur Cytokine Netw 13, 154–160.

Chan, S.H., Perussia, B., Gupta, J.W., Kobayashi, M., Pospisil, M., Young, H.A., Wolf, S.F., Young, D., Clark, S.C., Trinchieri, G., 1991. Induction of interferon gamma production by natural killer cell stimulatory factor: characterization of the responder cells and synergy with other inducers. J Exp Med 173, 869–879.

Collison, L.W., Delgoffe, G.M., Guy, C.S., Vignali, K.M., Chaturvedi, V., Fairweather, D., Satoskar, A.R., Garcia, K.C., Hunter, C.A., Drake, C.G., Murray, P.J., Vignali, D.A., 2012. The composition and signaling of the IL-35 receptor are unconventional. Nature immunology 13, 290–299.

Collison, L.W., Workman, C.J., Kuo, T.T., Boyd, K., Wang, Y., Vignali, K.M., Cross, R., Sehy, D., Blumberg, R.S., Vignali, D.A., 2007. The inhibitory cytokine IL-35 contributes to regulatory T-cell function. Nature 450, 566–569.

Croxford, A.L., Mair, F., Becher, B., 2012. IL-23: one cytokine in control of autoimmunity. European journal of immunology 42, 2263–2273.

Dambuza, I.M., He, C., Choi, J.K., Yu, C.R., Wang, R., Mattapallil, M.J., Wingfield, P.T., Caspi, R.R., Egwuagu, C.E., 2017. IL-12p35 induces expansion of IL-10 and IL-35-expressing regulatory B cells and ameliorates autoimmune disease. Nat Commun 8, 719.

Devergne, O., Birkenbach, M., Kieff, E., 1997. Epstein-Barr virus-induced gene 3 and the p35 subunit of interleukin 12 form a novel heterodimeric hematopoietin. Proceedings of the National Academy of Sciences of the United States of America 94, 12041–12046.

Devergne, O., Coulomb-L'Hermine, A., Capel, F., Moussa, M., Capron, F., 2001. Expression of Epstein-Barr virus-induced gene 3, an interleukin-12 p40-related molecule, throughout human pregnancy: involvement of syncytiotrophoblasts and extravillous trophoblasts. Am J Pathol 159, 1763–1776.

Devergne, O., Hummel, M., Koeppen, H., Le Beau, M.M., Nathanson, E.C., Kieff, E., Birkenbach, M., 1996. A novel interleukin-12 p40-related protein induced by latent Epstein-Barr virus infection in B lymphocytes. J Virol 70, 1143–1153.

Dietrich, C., Candon, S., Ruemmele, F.M., Devergne, O., 2014. A soluble form of IL-27Ralpha is a natural IL-27 antagonist. Journal of immunology 192, 5382–5389.

Espigol-Frigole, G., Planas-Rigol, E., Ohnuki, H., Salvucci, O., Kwak, H., Ravichandran, S., Luke, B., Cid, M.C., Tosato, G., 2016. Identification of IL-23p19 as an endothelial proinflammatory peptide that promotes gp130-STAT3 signaling. Sci Signal 9 ra28.

Garbers, C., Spudy, B., Aparicio-Siegmund, S., Waetzig, G.H., Sommer, J., Holscher, C., Rose-John, S., Grotzinger, J., Lorenzen, I., Scheller, J., 2013. An interleukin-6 receptor-dependent molecular switch mediates signal transduction of the IL-27 cytokine subunit p28 (IL-30) via a gp130 protein receptor homodimer. J Biol Chem 288, 4346–4354.

Gately, M.K., Carvajal, D.M., Connaughton, S.E., Gillessen, S., Warrier, R.R., Kolinsky, K.D., Wilkinson, V.L., Dwyer, C.M., Higgins Jr., G.F., Podlaski, F.J., Faherty, D.A., Familletti, P.C., Stern, A.S., Presky, D.H., 1996. Interleukin-12 antagonist activity of mouse interleukin-12 p40 homodimer in vitro and in vivo. Ann N Y Acad Sci 795, 1–12.

Gubler, U., Chua, A.O., Schoenhaut, D.S., Dwyer, C.M., McComas, W., Motyka, R., Nabavi, N., Wolitzky, A.G., Quinn, P.M., Familletti, P.C., et al., 1991. Coexpression of two distinct genes is required to generate secreted bioactive cytotoxic lymphocyte maturation factor. Proceedings of the National Academy of Sciences of the United States of America 88, 4143–4147.

Ha, S.J., Chang, J., Song, M.K., Suh, Y.S., Jin, H.T., Lee, C.H., Nam, G.H., Choi, G., Choi, K.Y., Lee, S.H., Kim, W.B., Sung, Y.C., 2002. Engineering N-glycosylation mutations in IL-12 enhances sustained cytotoxic T lymphocyte responses for DNA immunization. Nature biotechnology 20, 381–386.

Jalah, R., Rosati, M., Ganneru, B., Pilkington, G.R., Valentin, A., Kulkarni, V., Bergamaschi, C., Chowdhury, B., Zhang, G.M., Beach, R.K., Alicea, C., Broderick, K.E., Sardesai, N.Y., Pavlakis, G.N., Felber, B.K., 2013. The p40 Subunit of Interleukin (IL)-12 Promotes Stabilization and Export of the p35 Subunit: implications for improved IL-12 cytokine production. J Biol Chem 288, 6763–6776.

Jones, L.L., Chaturvedi, V., Uyttenhove, C., Van Snick, J., Vignali, D.A., 2012. Distinct subunit pairing criteria within the heterodimeric IL-12 cytokine family. Mol Immunol 51, 234–244.

Kobayashi, M., Fitz, L., Ryan, M., Hewick, R.M., Clark, S.C., Chan, S., Loudon, R., Sherman, F., Perussia, B., Trinchieri, G., 1989. Identification and purification of natural killer cell stimulatory factor (NKSF), a cytokine with multiple biologic effects on human lymphocytes. J Exp Med 170, 827–845.

Langrish, C.L., Chen, Y., Blumenschein, W.M., Mattson, J., Basham, B., Sedgwick, J.D., McClanahan, T., Kastelein, R.A., Cua, D.J., 2005. IL-23 drives a pathogenic T cell population that induces autoimmune inflammation. J Exp Med 201, 233–240.

Lee, S.Y., Jung, Y.O., Kim, D.J., Kang, C.M., Moon, Y.M., Heo, Y.J., Oh, H.J., Park, S.J., Yang, S.H., Kwok, S.K., Ju, J.H., Park, S.H., Sung, Y.C., Kim, H.Y., Cho, M.L., 2015. IL-12p40 Homodimer Ameliorates Experimental Autoimmune Arthritis. Journal of immunology 195, 3001–3010.

Ling, P., Gately, M.K., Gubler, U., Stern, A.S., Lin, P., Hollfelder, K., Su, C., Pan, Y.C., Hakimi, J., 1995. Human IL-12 p40 homodimer binds to the IL-12 receptor but does not mediate biologic activity. Journal of immunology 154, 116–127.

Lupardus, P.J., Garcia, K.C., 2008. The structure of interleukin-23 reveals the molecular basis of p40 subunit sharing with interleukin-12. J Mol Biol 382, 931–941.

Meier, S., Bohnacker, S., Klose, C.J., Lopez, A., Choe, C.A., Schmid, P.W.N., Bloemeke, N., Ruhrnossl, F., Haslbeck, M., Bieren, J.E., Sattler, M., Huang, P.S., Feige, M.J., 2019. The molecular basis of chaperone-mediated interleukin 23 assembly control. Nat Commun 10, 4121.

Mirlekar, B., Michaud, D., Searcy, R., Greene, K., Pylayeva-Gupta, Y., 2018. IL35 Hinders Endogenous Antitumor T-cell Immunity and Responsiveness to Immunotherapy in Pancreatic Cancer. Cancer immunology research 6, 1014–1024.

Muller, S.I., Aschenbrenner, I., Zacharias, M., Feige, M.J., 2019a. An Interspecies Analysis Reveals Molecular Construction Principles of Interleukin 27. J Mol Biol 431, 2383–2393.

Muller, S.I., Friedl, A., Aschenbrenner, I., Esser-von Bieren, J., Zacharias, M., Devergne, O., Feige, M.J., 2019b. A folding switch regulates interleukin 27 biogenesis and secretion of its alpha-subunit as a cytokine. Proceedings of the National Academy of Sciences of the United States of America 116, 1585–1590.

Oppmann, B., Lesley, R., Blom, B., Timans, J.C., Xu, Y., Hunte, B., Vega, F., Yu, N., Wang, J., Singh, K., Zonin, F., Vaisberg, E., Churakova, T., Liu, M., Gorman, D., Wagner, J., Zurawski, S., Liu, Y., Abrams, J.S., Moore, K.W., Rennick, D., de Waal-Malefyt, R., Hannum, C., Bazan, J.F., Kastelein, R.A., 2000. Novel p19 protein engages IL-12p40 to form a cytokine, IL-23, with biological activities similar as well as distinct from IL-12. Immunity 13, 715–725.

Pflanz, S., Timans, J.C., Cheung, J., Rosales, R., Kanzler, H., Gilbert, J., Hibbert, L., Churakova, T., Travis, M., Vaisberg, E., Blumenschein, W.M., Mattson, J.D., Wagner, J.L., To, W., Zurawski, S., McClanahan, T.K., Gorman, D.M., Bazan, J.F., de Waal Malefyt, R., Rennick, D., Kastelein, R.A., 2002. IL-27, a heterodimeric cytokine composed of EBI3 and p28 protein, induces proliferation of naive CD4(+) T cells. Immunity 16, 779–790.

Podlaski, F.J., Nanduri, V.B., Hulmes, J.D., Pan, Y.C., Levin, W., Danho, W., Chizzonite, R., Gately, M.K., Stern, A.S., 1992. Molecular characterization of interleukin 12. Arch Biochem Biophys 294, 230–237.

Pylayeva-Gupta, Y., Das, S., Handler, J.S., Hajdu, C.H., Coffre, M., Koralov, S.B., Bar-Sagi, D., 2016. IL35-Producing B Cells Promote the Development of Pancreatic Neoplasia.

Cancer Discov 6, 247–255.
Reitberger, S., Haimerl, P., Aschenbrenner, I., Esser-von Bieren, J., Feige, M.J., 2017. Assembly-induced folding regulates interleukin 12 biogenesis and secretion. J Biol Chem 292, 8073–8081.
Sawant, D.V., Hamilton, K., Vignali, D.A., 2015. Interleukin-35: Expanding Its Job Profile. J Interferon Cytokine Res.
Sievers, F., Wilm, A., Dineen, D., Gibson, T.J., Karplus, K., Li, W., Lopez, R., McWilliam, H., Remmert, M., Soding, J., Thompson, J.D., Higgins, D.G., 2011. Fast, scalable generation of high-quality protein multiple sequence alignments using Clustal Omega. Mol Syst Biol 7, 539.
Steentoft, C., Vakhrushev, S.Y., Joshi, H.J., Kong, Y., Vester-Christensen, M.B., Schjoldager, K.T., Lavrsen, K., Dabelsteen, S., Pedersen, N.B., Marcos-Silva, L., Gupta, R., Bennett, E.P., Mandel, U., Brunak, S., Wandall, H.H., Levery, S.B., Clausen, H., 2013. Precision mapping of the human O-GalNAc glycoproteome through SimpleCell technology. Embo j 32, 1478–1488.
Stern, A.S., Podlaski, F.J., Hulmes, J.D., Pan, Y.C., Quinn, P.M., Wolitzky, A.G., Familletti, P.C., Stremlo, D.L., Truitt, T., Chizzonite, R., et al., 1990. Purification to homogeneity and partial characterization of cytotoxic lymphocyte maturation factor from human B-lymphoblastoid cells. Proceedings of the National Academy of Sciences of the United States of America 87, 6808–6812.
Stumhofer, J.S., Tait, E.D., Quinn 3rd, W.J., Hosken, N., Spudy, B., Goenka, R., Fielding, C.A., O'Hara, A.C., Chen, Y., Jones, M.L., Saris, C.J., Rose-John, S., Cua, D.J., Jones, S.A., Elloso, M.M., Grotzinger, J., Cancro, M.P., Levin, S.D., Hunter, C.A., 2010. A role for IL-27p28 as an antagonist of gp130-mediated signaling. Nature immunology 11, 1119–1126.
Tait Wojno, E.D., Hunter, C.A., Stumhofer, J.S., 2019. The Immunobiology of the Interleukin-12 Family: Room for Discovery. Immunity 50, 851–870.
Teng, M.W., Bowman, E.P., McElwee, J.J., Smyth, M.J., Casanova, J.L., Cooper, A.M., Cua, D.J., 2015. IL-12 and IL-23 cytokines: from discovery to targeted therapies for immune-mediated inflammatory diseases. Nat Med 21, 719–729.
Trinchieri, G., Pflanz, S., Kastelein, R.A., 2003. The IL-12 family of heterodimeric cytokines: new players in the regulation of T cell responses. Immunity 19, 641–644.
Vignali, D.A., Kuchroo, V.K., 2012. IL-12 family cytokines: immunological playmakers. Nature immunology 13, 722–728.
Wolf, S.F., Temple, P.A., Kobayashi, M., Young, D., Dicig, M., Lowe, L., Dzialo, R., Fitz, L., Ferenz, C., Hewick, R.M., et al., 1991. Cloning of cDNA for natural killer cell stimulatory factor, a heterodimeric cytokine with multiple biologic effects on T and natural killer cells. Journal of immunology 146, 3074–3081.
Xue, W., Yan, D., Kan, Q., 2019. Interleukin-35 as an Emerging Player in Tumor Microenvironment. Journal of Cancer 10, 2074–2082.
Yan, J., Mitra, A., Hu, J., Cutrera, J.J., Xia, X., Doetschman, T., Gagea, M., Mishra, L., Li, S., 2016. Interleukin-30 (IL27p28) alleviates experimental sepsis by modulating cytokine profile in NKT cells. J Hepatol 64, 1128–1136.
Yeku, O.O., Brentjens, R.J., 2016. Armored CAR T-cells: utilizing cytokines and pro-inflammatory ligands to enhance CAR T-cell anti-tumour efficacy. Biochem Soc Trans 44, 412–418.
Yoon, C., Johnston, S.C., Tang, J., Stahl, M., Tobin, J.F., Somers, W.S., 2000. Charged residues dominate a unique interlocking topography in the heterodimeric cytokine interleukin-12. EMBO J 19, 3530–3541.
Yoshida, H., Hunter, C.A., 2015. The immunobiology of interleukin-27. Annu Rev Immunol 33, 417–443.
Zhang, Z., Shah, B., Richardson, J., 2019. Impact of Fc N-glycan sialylation on IgG structure. MAbs 11, 1381–1390.

### 2.2.3 Supplementary material to the manuscript

# Influence of glycosylation on IL-12 family cytokine biogenesis and function

**Supplementary Figures S1-S4**

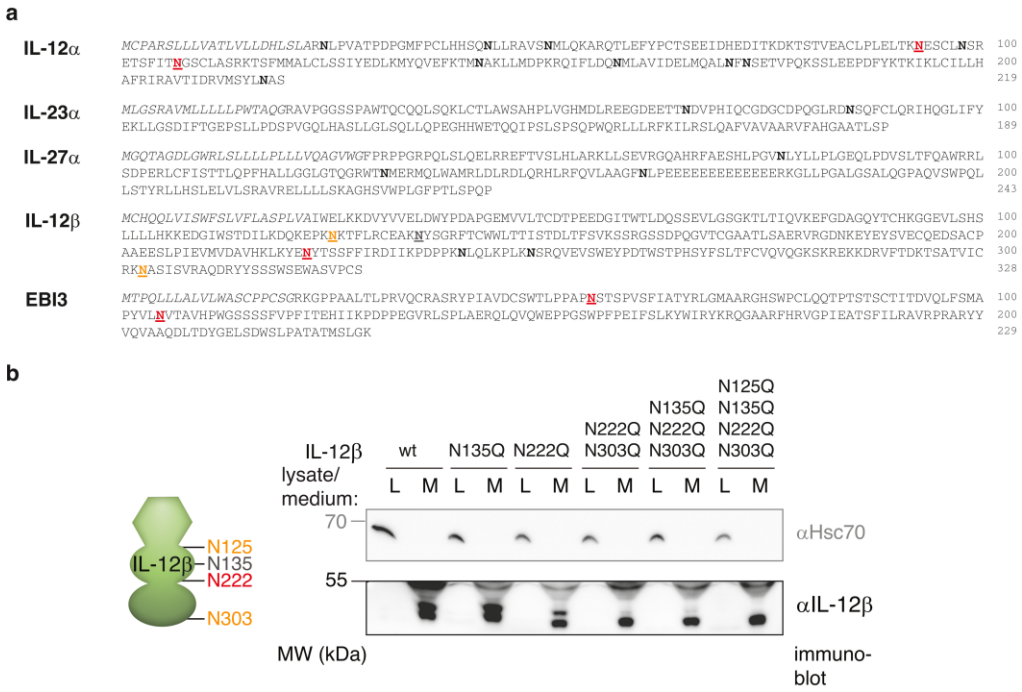


**Fig. S1.** Prediction and verification of IL-12 family subunit *N*-glycosylation. (a) Sequences of IL-12 family cytokine subunits show potential *N*-glycosylation sites. All Asn residues are highlighted in bold, predicted and experimentally verified *N*-glycosylation sites in red. For IL-12β, a predicted but not experimentally verified *N*-glycosylation site (N135) is shown in gray and not predicted (below the threshold) but experimentally detected *N*-glycosylation sites (N125, N303) are colored in orange. All relevant and mutated Asn residues are underlined. ER import sequences are shown in italic. (b) Sequential mutation of Asn residues in IL-12β enables identification of *N*-glycosylation sites (N125, N222, N303) *via* electrophoretic mobility shifts. The schematic shows the Ig domain (hexamer) and FnIII domains (ellipses) of the IL-12β subunit. L, lysate. M, medium. MW, molecular weight. 4% L/M were applied to the gel and blotted with antibodies against IL-12β. Hsc70 served as a loading control.

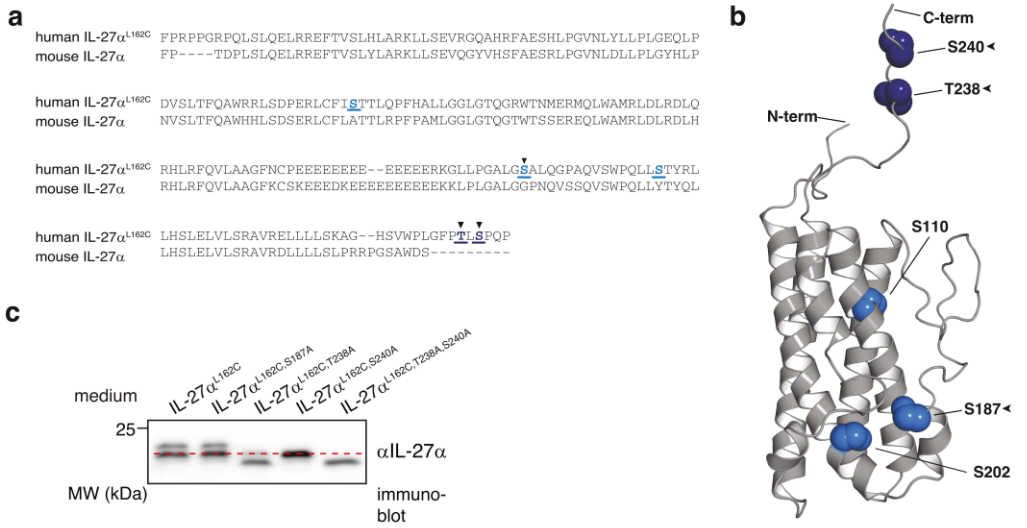


**Fig. S2.** C-terminal *O*-glycosylation sites of IL-27α were determined by sequence alignment, structural assessment and verification by mutation. (a) Sequence alignment of human, *O*-glycosylated IL-27α$^{L162C}$ (Muller et al., 2019b), with murine, non-glycosylated IL-27α and (b) homology model of human IL-27α (Muller et al., 2019a) show Thr and Ser residues (blue) only existing in the human protein and not in murine IL-27α. Of these, surface-exposed residues are highlighted with an arrowhead and experimentally confirmed *O*-glycosylation sites are colored in dark blue. Predicted *O*-glycosylation sites are underlined. (c) Mutation of potential *O*-glycosylation sites in human IL-27α$^{L162C}$ identifies T238 and S240 as *O*-glycosylated residues. Electrophoretic shifts indicate lacking *O*-glycosylation due to residue exchange to Ala. Mutation of both T238 and S240 results in only one protein species which shifts to a lower molecular weight than other mutants due to completely missing *O*-glycosylation (as also verified by absence of any shift upon treatment with *O*-Glycosidase, see Fig. 1b). MW, molecular weight. 2% medium was applied to the gel and blotted with antibodies against IL-27α.

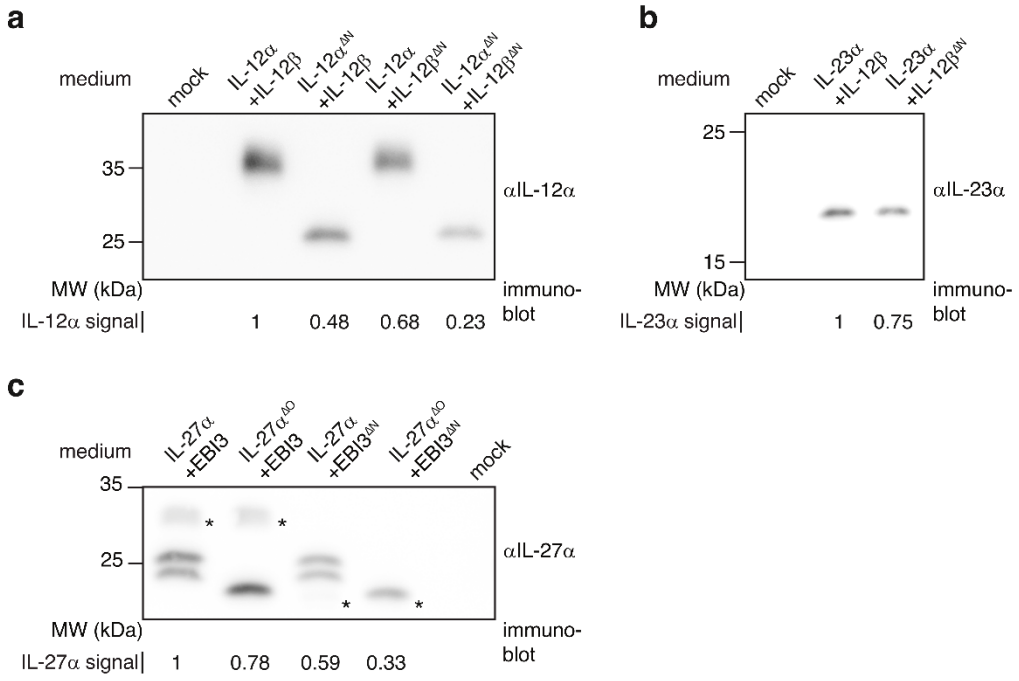


**Fig. S3.** Quantification of IL-12 family cytokine variant secretion. (a) Secretion of IL-12, (b) IL-23 and (c) IL-27 was quantified *via* immunoblotting of medium samples from transiently transfected HEK293T cells relative to the wild type. IL-23 wild type was additionally quantified in comparison to recombinant IL-23 (data not shown). Antibodies against IL-12α, IL-23α or IL-27α, respectively, were used as the α-subunits are not secreted in isolation and thus report on secretion of the heterodimers. The asterisks indicate EBI3 detected by the αIL-27α antibody. MW, molecular weight.

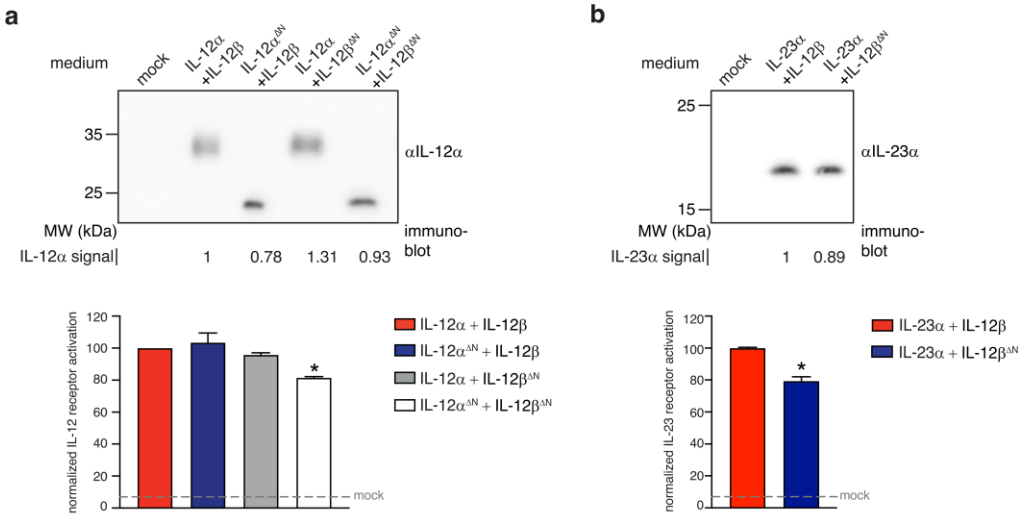


**Fig. S4.** Receptor activation assays. (a) Secretion of IL-12 and (b) IL-23 were quantified *via* immunoblotting of medium samples from transiently transfected HEK293T cells relative to the wild type, which was additionally quantified in comparison to recombinant IL-12/IL-23 (data not shown). MW, molecular weight. (a) Induction of IL-12 and (b) IL-23 signaling by the indicated glycosylation mutants (10 ng/ml final concentration each) were assessed with a receptor activation assay (iLite®). Receptor activation was measured in duplicates (shown ± SEM) and normalized to the wild-type signal, which was set to 100%. Statistical significance was calculated using one-way ANOVA. (a-b) *$p<0.05$, indicates statistical significance.

### 2.2.4 Permission to reprint the manuscript

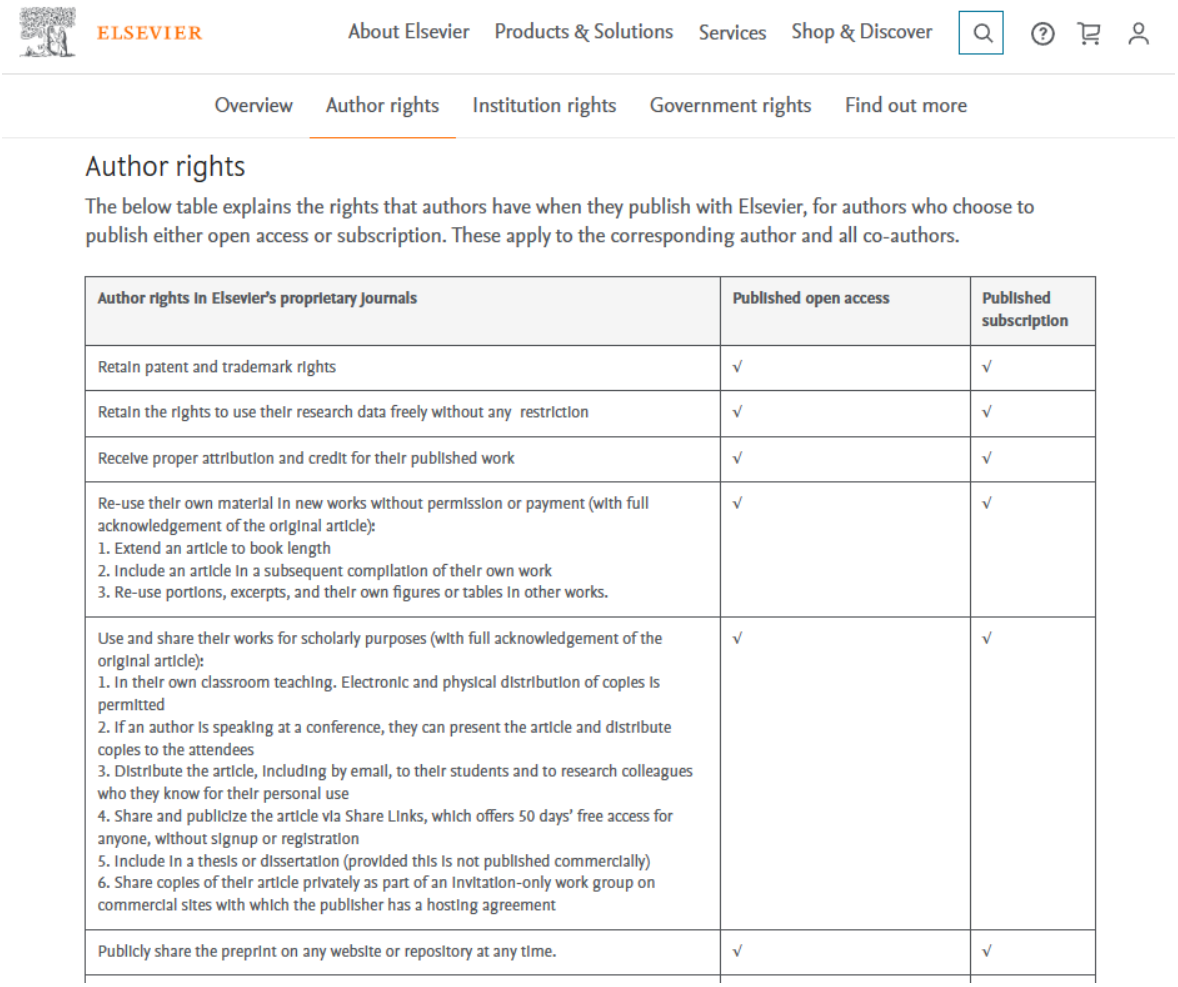

ELSEVIER About Elsevier Products & Solutions Services Shop & Discover

Overview Author rights Institution rights Government rights Find out more

## Author rights

The below table explains the rights that authors have when they publish with Elsevier, for authors who choose to publish either open access or subscription. These apply to the corresponding author and all co-authors.

| Author rights in Elsevier's proprietary journals | Published open access | Published subscription |
|---|---|---|
| Retain patent and trademark rights | √ | √ |
| Retain the rights to use their research data freely without any restriction | √ | √ |
| Receive proper attribution and credit for their published work | √ | √ |
| Re-use their own material in new works without permission or payment (with full acknowledgement of the original article):<br>1. Extend an article to book length<br>2. Include an article in a subsequent compilation of their own work<br>3. Re-use portions, excerpts, and their own figures or tables in other works. | √ | √ |
| Use and share their works for scholarly purposes (with full acknowledgement of the original article):<br>1. In their own classroom teaching. Electronic and physical distribution of copies is permitted<br>2. If an author is speaking at a conference, they can present the article and distribute copies to the attendees<br>3. Distribute the article, including by email, to their students and to research colleagues who they know for their personal use<br>4. Share and publicize the article via Share Links, which offers 50 days' free access for anyone, without signup or registration<br>5. Include in a thesis or dissertation (provided this is not published commercially)<br>6. Share copies of their article privately as part of an invitation-only work group on commercial sites with which the publisher has a hosting agreement | √ | √ |
| Publicly share the preprint on any website or repository at any time. | √ | √ |

## 2.3 A comprehensive set of ER protein disulfide isomerase family members supports the biogenesis of pro-inflammatory interleukin 12 family cytokines

Published by Yonatan G. Mideksa[1], **Isabel Aschenbrenner**[1], Anja Fux, Dinah Kaylani, Caroline A. M. Weiß, Tuan-Anh Nguyen, Nina C. Bach, Kathrin Lang, Stephan A. Sieber, and Matthias J. Feige in *Journal of Biological Chemistry* (2022) 298(12): 102677. DOI: 10.1016/j.jbc.2022.102677

([1] equal contribution)

**Contribution:** Yonatan G. Mideksa, **Isabel Aschenbrenner**, and Matthias J. Feige conceived the study. Yonatan G. Mideksa, **Isabel Aschenbrenner**, Anja Fux, Dinah Kaylani, Caroline A. M. Weiß, Tuan-Anh Nguyen, and Nina C. Bach did the investigation. Yonatan G. Mideksa, **Isabel Aschenbrenner**, Anja Fux, Dinah Kaylani, Tuan-Anh Nguyen, Kathrin Lang, Stephan A. Sieber, and Matthias J. Feige reviewed and edited the original draft. Yonatan G. Mideksa, **Isabel Aschenbrenner**, Anja Fux, and Dinah Kaylani visualized the data.

### 2.3.1 Summary

In humans, α-subunits of IL-12 family members are incompletely structured in isolation and retained in the ER when expressed alone. Thus, they are major targets for chaperoning during their biogenesis and to prevent premature ER exit. In this study, we aimed to analyze which chaperones act on IL-12 and IL-23 α-subunits and what functional roles they have in biogenesis of the key signaling molecules IL-12 and IL-23.

To comprehensively analyze the ER chaperone repertoire acting on IL-12/IL-23 biogenesis, we established a photocrosslinking approach which allowed us to identify chaperone-client interactions also of transient, non-covalent nature. Site-specific incorporation of the diazirine bearing unnatural amino acid DiazK into cell-retained IL-12α or IL-23α by amber suppression resulted in covalently crosslinked complexes upon UV light irradiation, enabling downstream immunoblotting and MS experiments. This method allowed us to detect an extended interactome for cytokine α-subunits.

For IL-12α and IL-23α, we used different surface-exposed positions for incorporation of DiazK. Analysis of expression levels, amber suppression efficiency, and verification of wildtype-like behavior led us to utilize two IL-12α and one IL-23α mutant for MS measurements. Focusing on interactions with PDI family members, we could detect multiple overlapping, but also distinct chaperones significantly involved in IL-12/IL-23 biogenesis.

MS results were verified by co-IP experiments without or, for non-covalent interactions, with addition of the amine-reactive crosslinker dithiobis(succinimidyl propionate) (DSP).

To understand the role of chaperones in cytokine biogenesis in more detail, we assessed the binding preference of selected PDI family members for the cysteines in α-subunits by mutational replacement of cysteines and subsequent co-IP. ERp72, ERp5, and ERp46 bound cysteine pairs of the three intramolecular disulfide bonds in IL-12α to different extents, with the cysteine that forms the interchain disulfide bridge to IL-12β apparently not being bound at all. For IL-23α, ERp5 preferentially bound to its three free cysteines, including the interchain cysteine, but not to the cysteines forming the single intramolecular disulfide bridge.

To test whether PDI family members have a stabilizing effect on unassembled cytokine subunits, a siRNA-mediated knockdown of individual chaperones and subsequent assessment of protein stability under CHX-induced translational shut-off were performed. Knockdown of any interacting PDI chaperone led to accelerated degradation of IL-12α and IL-23α. Heterodimerization of α-subunits with the shared IL-12β was not affected by single PDI knockdown, but multiple PDI depletion reduced IL-12 secretion. This indicates fast and efficient α:β assembly, with chaperones possibly playing a role in the regulation of IL-12 *versus* IL-23 heterodimer assembly, both being highly relevant in human diseases.

Taken together, we could identify a complex network of PDI family members acting on IL-12α and IL-23α subunits to stabilize them when unassembled and incompletely folded during biogenesis. PDI family members recognize different cysteines in the α-subunits, thus acting synergistically but not redundantly on their clients. IL-12 and IL-23, sharing the same β-subunit, prove to be interesting clients for further investigation of yet unknown PDI family member functions and of PDI:client specificity *versus* promiscuity.

## 2.3.2 Manuscript

JBC RESEARCH ARTICLE

# A comprehensive set of ER protein disulfide isomerase family members supports the biogenesis of proinflammatory interleukin 12 family cytokines

Received for publication, August 16, 2021, and in revised form, September 1, 2022 Published, Papers in Press, November 4, 2022,
https://doi.org/10.1016/j.jbc.2022.102677

**Yonatan G. Mideksa[1,‡], Isabel Aschenbrenner[1,‡], Anja Fux[1], Dinah Kaylani[1], Caroline A. M. Weiß[1], Tuan-Anh Nguyen[1], Nina C. Bach[1], Kathrin Lang[1,2], Stephan A. Sieber[1], and Matthias J. Feige[1,*]**

*From the [1]Center for Functional Protein Assemblies (CPA), Department of Bioscience, TUM School of Natural Sciences, Technical University of Munich, Garching, Germany; [2]Laboratory of Organic Chemistry, ETH Zürich, Zurich, Switzerland*

Edited by Ursula Jakob

**Cytokines of the interleukin 12 (IL-12) family are assembled combinatorially from shared α and β subunits. A common theme is that human IL-12 family α subunits remain incompletely structured in isolation until they pair with a designate β subunit. Accordingly, chaperones need to support and control specific assembly processes. It remains incompletely understood, which chaperones are involved in IL-12 family biogenesis. Here, we site-specifically introduce photocrosslinking amino acids into the IL-12 and IL-23 α subunits (IL-12α and IL-23α) for stabilization of transient chaperone–client complexes for mass spectrometry. Our analysis reveals that a large set of endoplasmic reticulum chaperones interacts with IL-12α and IL-23α. Among these chaperones, we focus on protein disulfide isomerase (PDI) family members and reveal IL-12 family subunits to be clients of several incompletely characterized PDIs. We find that different PDIs show selectivity for different cysteines in IL-12α and IL-23α. Despite this, PDI binding generally stabilizes unassembled IL-12α and IL-23α against degradation. In contrast, α:β assembly appears robust, and only multiple simultaneous PDI depletions reduce IL-12 secretion. Our comprehensive analysis of the IL-12/IL-23 chaperone machinery reveals a hitherto uncharacterized role for several PDIs in this process. This extends our understanding of how cells accomplish the task of specific protein assembly reactions for signaling processes. Furthermore, our findings show that cytokine secretion can be modulated by targeting specific endoplasmic reticulum chaperones.**

Mammalian cells dedicate one-third of their genome to secretory pathway proteins, which allow cells to interact with their environment. These proteins generally acquire their native structure in the endoplasmic reticulum (ER), where a comprehensive chaperone machinery supports and controls each molecular step toward the native state (1). Protein maturation in the ER includes post-translational modifications that not only render structure formation more robust and tune functionality but also target proteins to certain chaperone systems. The most prominent modifications are glycosylation and disulfide bond formation, which occur in the majority of ER-produced proteins (2). N-linked glycans target proteins to the calnexin/calreticulin cycle that monitors and supports folding processes in secretory pathway proteins (3, 4). Disulfide bonds stabilize the native structure and, while unpaired, cysteines provide a handle for the ER quality control (ERQC) system (5, 6). Disulfide bond formation, isomerization, and reduction are catalyzed by the ER-resident protein disulfide isomerase (PDI) family. This family comprises a surprisingly large number of approximately 20 members in humans (7, 8). The expansion of the PDI family during evolution of more complex cells can likely be explained by functional specialization of certain family members. While PDI is a generic oxidoreductase with additional chaperone functions (9–11), other family members are more restricted in their clientele and functionalities. For some family members, insights into their specializations have been obtained: ERp57 interacts with calnexin and calreticulin and is thus mostly recruited to glycoproteins (12, 13), whereas the membrane integral PDI family member TMX1 prefers membrane proteins as clients (14). The PDI ERp5 interacts with the ER Hsp70 immunoglobulin binding protein (BiP) and thus may have a preference for BiP clients (15). TMX4 and ERdj5, the latter being another BiP cochaperone, are involved in not only reducing disulfide bonds for ER-associated degradation (ERAD) (16, 17) but also dissolving incorrectly formed disulfide bonds (18). ERp44, on the other hand, serves as a recruitment factor for immature proteins that leave the ER while their native disulfide bonds have not formed yet (19, 20). In addition to their role in catalyzing redox reactions in their clients, PDI family members are key regulators of ER stress responses and thus have further broadened their functional spectrum during evolution (11, 21).

The large variety of PDI family members combined with their different roles not only complicates their functional analysis in the native cellular context but also renders it particularly relevant to decipher the working principles of the

‡ These authors contributed equally to this work.
* For correspondence: Matthias J. Feige, matthias.feige@tum.de.

### *Oxidoreductases in IL-12/23 biogenesis*

ER folding environment. Previous studies often focused on certain PDI family members and analyzed the fate of selected clients in their absence (22). Alternatively, substrate-trapping mutants of PDI family members were used to define their clients (15), which may miss chaperone or oxidase functions of the respective PDI family member. Here, we complement these studies by a client-centric crosslinking approach. We focus on key signaling molecules in the immune system, the interleukin (IL) 12 family members IL-12 and IL-23, which both coordinate innate and adaptive immune responses (23, 24). These two cytokines are ideally suited to further dissect PDI family member functions in the cell. Our recent work has shown that oxidative folding governs the biogenesis of these cysteine-rich cytokines (25–27). Furthermore, these heterodimeric cytokines form intramolecular as well as intermolecular disulfide bonds and populate misoxidized species during their biogenesis, which strongly demands for support by PDI family members (25, 27–29). Since IL-12 and IL-23 both share the same β subunit (IL-12β) (30–32), an analysis of the redox machinery that acts on IL-12 *versus* IL-23 can provide insights into PDI family member client specificity *versus* promiscuity. Accordingly, these studies may point toward possible specific ways of modulating IL-12 *versus* IL-23 assembly, which are both highly relevant molecules for human disease (24).

## Results

### *Establishment of a photocrosslinking approach to identify IL-12/IL-23 chaperones*

Chaperones and folding enzymes generally only transiently interact with their clients. This is a prerequisite for their function but complicates analyses of chaperone–client complexes, in particular in the biologically relevant context of cells. To analyze the ER chaperone machinery that acts on the different steps of IL-12 and IL-23 biogenesis (Fig. 1*A*), we thus decided to covalently crosslink chaperone–client complexes for downstream analyses. Toward this end, we site-specifically incorporated the diazirine bearing unnatural amino acid DiazK (Fig. 1*B*) into various positions of the α subunits of IL-12 and IL-23 (IL-12α and IL-23α, respectively). For this, we used an efficient pyrrolysyl-tRNA synthetase variant together with its amber-suppressor tRNA, a setup that has been thoroughly characterized in very recent studies (33, 34). Upon irradiation with UV light (365 nm), DiazK forms a carbene (Fig. 1*B*) that readily reacts with adjacent proteins to stabilize transient protein–protein complexes for analyses, by for example, immunoblotting and mass spectrometry (MS; Fig. 1*C*). In this study, we specifically focused on IL-12α and IL-23α since these subunits remain incompletely structured in isolation and are retained in cells until they pair with their shared IL-12β subunit (25, 27, 30, 31, 35). They are thus prime targets for molecular chaperoning. To comprehensively analyze the chaperone repertoire that acts on IL-12α and IL-23α, we selected 14 or nine positions within each subunit, respectively, where we individually introduced an amber stop codon to be suppressed by incorporation of DiazK (Fig. 1, *D* and *E*, *left panels*). We focused on positions that were surface exposed, not predicted to destabilize the respective protein upon mutation and not in the interface with IL-12β (28, 29). For each construct, we observed expression upon transient transfection into human embryonic kidney 293T (HEK293T) cells in not only the presence of DiazK but also the presence of polypeptide chains truncated at the intrinsic amber stop codon, as expected for amber suppression (Fig. S1, *A* and *B*). We thus fused a C-terminal FLAG tag to the constructs (Fig. S1, *C* and *D*), which allows for the specific immunoprecipitation (IP) only of completely translated polypeptide chains containing the DiazK moiety. Since IL-12α and IL-23α can form homodimers in cells (25, 27), some truncated proteins could still be observed if rather C-terminally located amber codons were used, which give rise to almost fully translated homodimerization-competent polypeptide chains if a truncation occurs (*e.g.*, in Fig. S1, *C* and *D*). In general, amber suppression was efficient, and ∼20% to 80% of expression of the nonsuppressed wild-type (wt) constructs was obtained (Fig. S1, *C* and *D*).

For a subset of constructs, we in addition tested wt-like behavior in terms of ERQC. Normally, IL-12α and IL-23α are retained in the ER in isolation and can only pass ERQC and become secreted upon coexpression of IL-12β, including further modification of sugar moieties for IL-12α (25, 27, 30, 31, 35, 36). The same behavior was observed for IL-12α and IL-23α containing DiazK at different positions. When expressed alone in HEK293T cells, subunits were retained in cells. When IL-12β was cotransfected, IL-12α and IL-23α were secreted together with IL-12β (Fig. 1, *D* and *E*, *right panels*), showing that DiazK incorporation for photocrosslinking is a suitable tool to query their chaperone repertoire.

Using this approach, we could detect several crosslinked species for IL-12α containing a DiazK moiety, which were present exclusively if the cells were UV irradiated and independent of the presence of the C-terminal FLAG epitope tag (Figs. 2, *A* and *B*, S2, *A–C* and S3*A*). Importantly, some distinct crosslinked species could be detected for different positions of DiazK incorporation. Amber suppression did not interfere with IP, and the crosslinked species could generally be coimmunoprecipitated (Figs. 2, *A* and *B*, S2, *B* and *C* and S3*A*). A similar behavior was observed for IL-23α (Figs. 2, *C* and *D* and S2, *D–F*). Together, this setup should thus allow downstream MS analyses. For IL-12α, we focused on two constructs that showed the presence of a significant number of crosslinks and covered different positions, whereas for IL-23α, one crosslinking position within its first α-helix was used (Figs. 2, *A–D* and S3*A*) since this first α-helix has been shown to serve as a chaperone recognition site (25). MS analyses revealed a large number of proteins in the immunoprecipitated samples of IL-12α and IL-23α (Figs. 2, *E* and *F* and S3*B*; Table S1). Some interactions were dependent on photocrosslinking, showing that this approach extends the interactome that can be detected by MS (Fig. S3, *C–E*). To identify IL-12α and IL-23α ER chaperones and quality control factors among the identified proteins, we used suitable Gene Ontology (GO) term annotations to filter the interactomes (for details, see the Experimental procedures section).

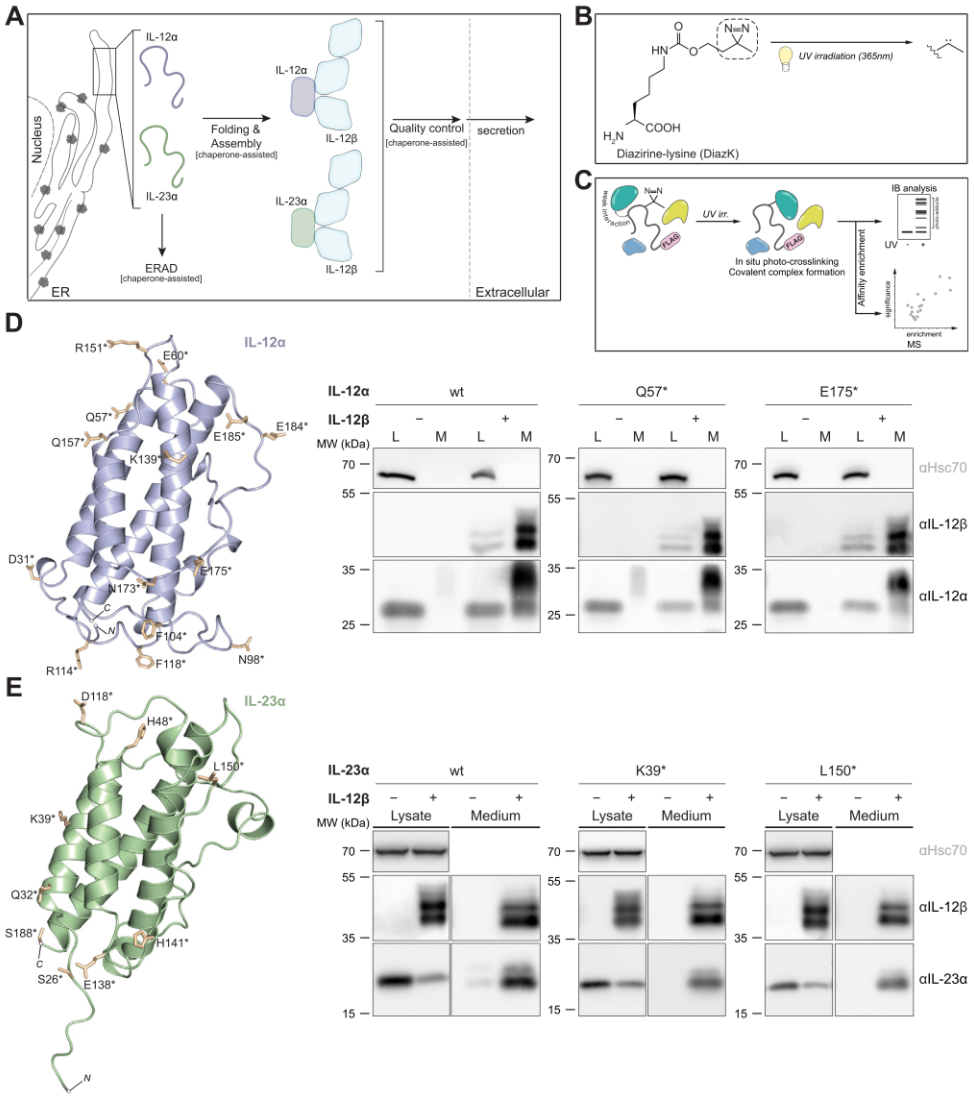


**Figure 1. Establishment of amber suppression for site-specific photocrosslinking of IL-12α and IL-23α.** *A*, the biogenesis of IL-12 and IL-23 involves assembly induced folding reactions of IL-12α/IL-23α by IL-12β, which are coupled to quality control processes. If misfolding occurs or assembly does not take place, ERAD (ER-associated degradation) targets IL-12α/IL-23α for degradation. Each process is dependent on chaperones. *B* and *C*, schematic of our *in situ* photocrosslinking approach to query weak and transient protein–protein interactions. DiazK forms a highly reactive carbene intermediate upon photoactivation by UV irradiation, which can insert readily into nearby C–H and heteroatom–H bonds or react with Asp and Glu residues of proximal proteins. Analysis of UV-crosslinked adducts can be performed by immunoblots (IBs) and mass spectrometry (MS). *D* and *E*, design of positions for amber suppression (*left panel*) in IL-12α and IL-23α subunits, respectively. Selected constructs were tested for assembly induced secretion upon coexpression of IL-12β (*right panel*). HEK293T cells were transiently cotransfected with the indicated constructs in the presence of DiazK, and samples were analyzed by IBs. An *asterisk* denotes the site of stop codon introduction and amber suppression. The upward shift of IL-12α upon secretion into the medium (M: medium; L: cell lysate) is caused by modifications of its sugar moieties in the Golgi (36). IL-12β populates two species differing in the use of N-glycosylation sites (36). HEK293T, human embryonic kidney 293T cell line; IL, interleukin.

***Not only multiple overlapping but also distinct ER PDI family members are involved in IL-12 and IL-23 biogenesis***

Our MS analyses identified several ER chaperones interacting with IL-12α and IL-23α, including, for example, the ER Hsp70 chaperone BiP, the Hsp90 chaperone Grp94 (*ENPL*), and the lectin chaperones calreticulin (*CALR*) and calnexin (*CALX*) (Figs. 2, *E* and *F* and S3, *B–E*). Among the IL-12α or IL-23α interactors, we decided to focus on ER oxidoreductases because of the key role of oxidative folding in IL-12/IL-23 biogenesis (25–27). We found not only several overlapping

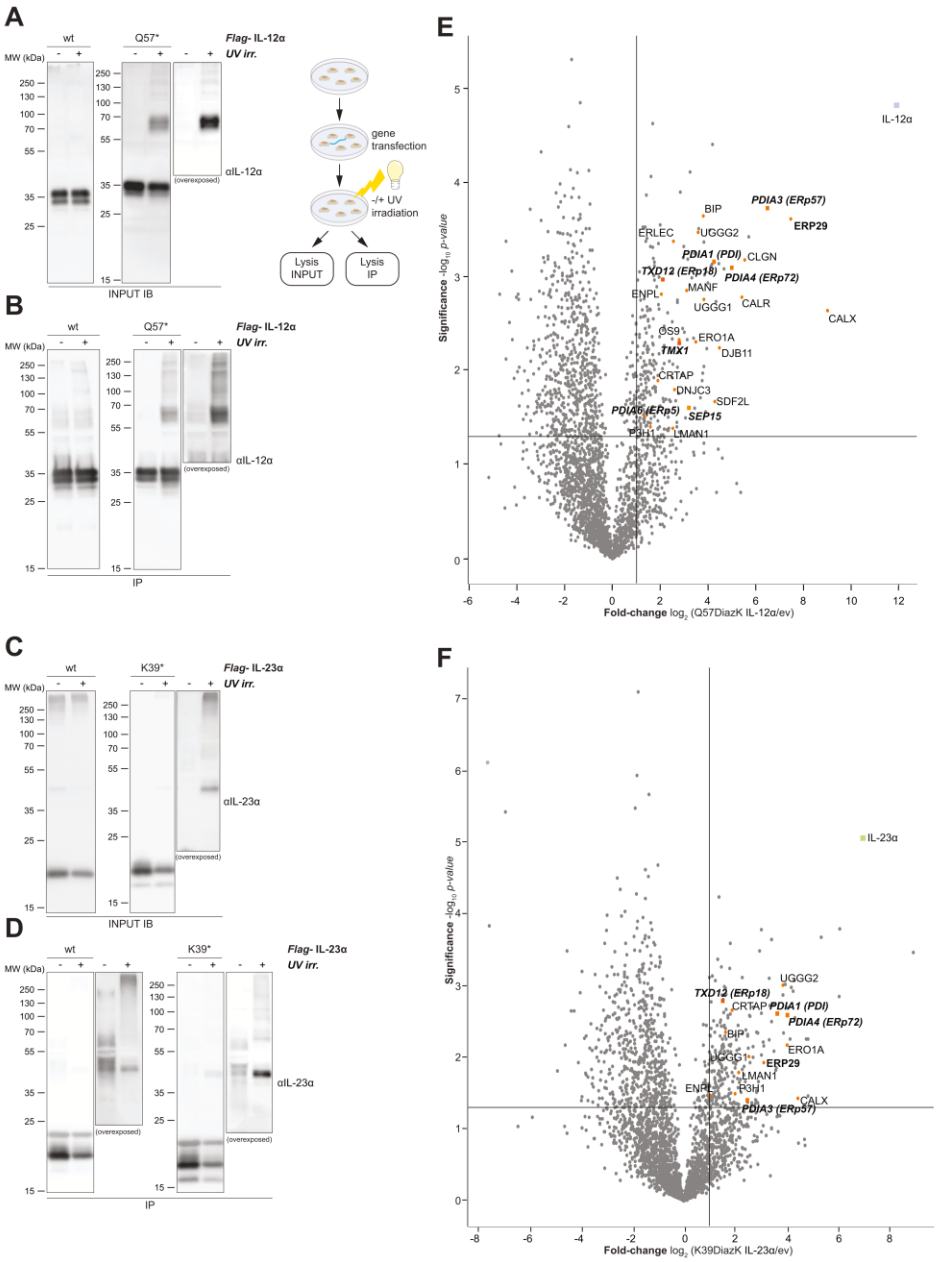


**Figure 2. Photocrosslinking allows to capture IL-12α and IL-23α interaction partners for mass spectrometry.** *A–D*, immunoblot verification of UV-crosslinked complexes before and after immunoprecipitation (IP) with FLAG beads. The orthogonal DiazKRS/$tRNA_{CUA}$ pair was coexpressed in all panels in the presence of DiazK, for site-specific modification of the α subunits. Where indicated, cells were irradiated with UV light (UV irr.) to induce photo-crosslinking of DiAzK to adjacent residues. Overexposed blots are shown to highlight weak signals for high molecular weight species; the schematic summarizes the workflow. Truncated protein species for FLAG-immunoprecipitated IL-12α/IL-23α likely originate from homodimerization as previously reported (27). *E* and *F*, volcano plots derived from LC–MS/MS analysis of the indicated IL constructs compared with control FLAG co-IPs using cells transfected with empty vector (ev), carried out in three replicates. The *top-right* quadrants list significant hits with cutoff values defined as $\log_2 = 1$ (twofold enrichment) and $-\log_{10}$ (*p* value) of 1.3 ($p < 0.05$). ER chaperones and quality control proteins are depicted as *orange circles*. Those with a possible additional PDI molecular function are shown as *orange squares* and labeled in *bold*. Hits were labeled with respective UniProt entry names, and for possible PDIs, protein names are in addition given in brackets. IL-12α and IL-23α are shown in *violet* or *green*, respectively. ER, endoplasmic reticulum; IL, interleukin; PDI, protein disulfide isomerase.

but also distinct PDI family members to interact with IL-12α or IL-23α (Fig. 2, *E* and *F*). To validate and extend our MS data, for each of the identified interacting PDI family members, we next assessed interaction with wt IL-12α or IL-23α by co-IP experiments. In some cases, *N*-ethylmaleimide (NEM), which blocks reshuffling of disulfide bonds, was sufficient to preserve interactions. In other cases, the amine-reactive crosslinker dithiobis(succinimidyl propionate) (DSP) had to be used, suggesting that different interactions between the cytokine subunits and the PDI family members were formed, including noncovalent ones. All significant interactions with PDI family members detected by MS could be verified by co-IP for IL-12α (Fig. 3*A*) as well as for IL-23α (Fig. 3*B*). Underlining the need for confirmatory experiments, ERp57, which is recruited to glycoproteins *via* calnexin/calreticulin, was found to be highly enriched in the interactome of the N-glycoprotein IL-12α but also weakly for IL-23α (Fig. 2, *E* and *F*), which does not contain N-glycosylation sites (36). Interactions with IL-23α were not observed in co-IP experiments (Fig. 3*B*). To further extend our studies, we also included ERp46 into our co-IP experiments because of its recently described role in early protein folding reactions (37) and the fact that we could detect it in the IL-12α

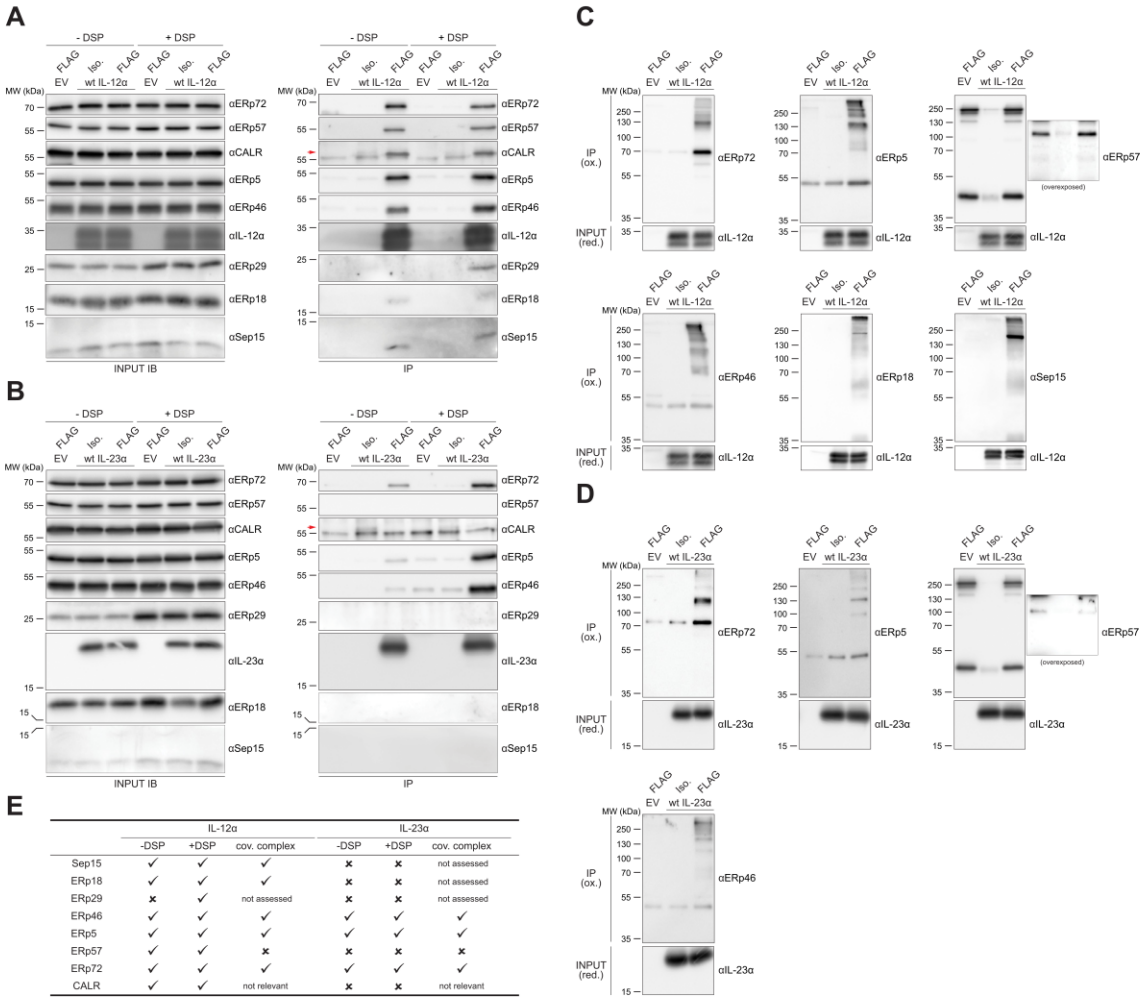


| | IL-12α | | | IL-23α | | |
|---|---|---|---|---|---|---|
| | -DSP | +DSP | cov. complex | -DSP | +DSP | cov. complex |
| Sep15 | ✓ | ✓ | ✓ | × | × | not assessed |
| ERp18 | ✓ | ✓ | ✓ | × | × | not assessed |
| ERp29 | × | ✓ | not assessed | × | × | not assessed |
| ERp46 | ✓ | ✓ | ✓ | ✓ | ✓ | ✓ |
| ERp5 | ✓ | ✓ | ✓ | ✓ | ✓ | ✓ |
| ERp57 | ✓ | ✓ | × | × | × | × |
| ERp72 | ✓ | ✓ | ✓ | ✓ | ✓ | ✓ |
| CALR | ✓ | ✓ | not relevant | × | × | not relevant |

**Figure 3. Analysis of PDI binding partners by coimmunoprecipitations (co-IPs).** *A* and *B*, HEK293T transiently expressing either IL-12α or IL-23α, each C-terminally FLAG-tagged, were subjected to FLAG IP with or without an amine-reactive DSP-crosslinker and analyzed using immunoblots under reducing conditions. CALR (calreticulin), a soluble ER lectin chaperone, was included to benchmark the distinct interaction profile that exists between the N-glycosylated IL-12α *versus* non–N-glycosylated IL-23α. *Arrowheads* point to the top band marking the correct size of the CALR protein. In all cases, interactions with wt IL subunits not containing any UAA were analyzed. *C* and *D*, DSP-independent interactions were further evaluated for covalent complex formation *via* nonreducing co-IPs/SDS-PAGE. Reducing input blots are included to verify the expression of FLAG-tagged IL-12α/23α in whole cell lysates. *E*, each PDI's interaction profile obtained from results in *A–D* is summarized in *E*. DSP, dithiobis(succinimidyl propionate); ER, endoplasmic reticulum; EV, empty vector; HEK293T, human embryonic kidney 293T cell line; IL, interleukin; iso., isotype control beads; PDI, protein disulfide isomerase.

interactome, although not significantly enriched (Table S1). ERp46 interacted with IL-12α independent of the chemical crosslinker DSP (Fig. 3*A*), whereas interaction with IL-23α was strongly increased in the presence of DSP (Fig. 3*B*), showing that although not a significant MS-hit, ERp46 appears to interact with IL-12α and IL-23α and that complementary approaches can further extend the MS interactome.

Of note, for interactions that were observable without DSP as a crosslinker, we could generally detect covalent complexes between IL-12α and the different PDIs (Fig. 3*C*) or IL-23α and the different PDIs (Fig. 3*D*), respectively. Taken together, as intended, our workflow succeeded in identifying covalent and noncovalent chaperone–client complexes (Fig. 3*E*). Of note, among the identified PDIs, our approach revealed not only well-characterized PDI family members (*e.g.*, PDI, ERp57) to interact with IL-12α and/or IL-23α but also less well-understood ones, including ERp72 and Sep15, the latter being a selenoprotein involved in protein quality control (38). The not only overlapping but also partially distinct PDI family repertoire, which contained ill-characterized members, led us to investigate their binding preferences and their role in IL-12/IL-23 biogenesis in more detail.

### *Cysteines in IL-12α and IL-23α are recognized differently by PDI family members*

Our photocrosslinking MS approach and its validation by co-IP experiments revealed multiple PDI family members to interact with IL-12α and IL-23α. This raises the question if the identified PDI family members recognized the same or different cysteines within these clients in cells. To address this question, we generated a panel of IL-12α mutants. We replaced either cysteine 96, which forms an interchain disulfide bond with IL-12β within IL-12, or each pair of cysteines that form one of the three internal disulfide bonds in IL-12α by serines (Fig. 4*A*) (27, 28). In addition, in one mutant, all cysteines were replaced by serines. These mutants were used to analyze interactions with ERp72, ERp5, and ERp46, which all formed covalent complexes with IL-12α (Fig. 3, *C* and *E*) and are thus suitable to assess their cysteine-binding specificities. For the cysteine-free IL-12α mutant, hardly any binding to the three queried PDIs was detectable (Fig. 4*B*). Since no crosslinkers but only NEM to avoid disulfide bond reshuffling was used in this experiment, this finding indicates the absence of any stable chaperone-like interactions between IL-12α and ERp72, ERp5, or ERp46. In contrast, each of the cysteine mutants still bound to the PDIs, but with different effects on binding: ERp72 had a preference for the cysteines forming disulfide bond 1 and 3 within IL-12α, ERp5 preferred cysteines forming disulfide bonds 2 and 3, and ERp46 preferred the cysteines forming disulfide bond 2 (Fig. 4*B*). None of these three PDIs showed reduced binding upon mutation of the interchain disulfide bond–forming cysteine 96 (Fig. 4, *A* and *B*). For IL-23α, we analyzed interaction with ERp5 analogously. In this case, binding was only preserved if the cysteines forming the single disulfide bond in IL-23α were mutated to serines, indicating a preference of ERp5 for the three free cysteines in IL-23α (Fig. 4, *C* and *D*).

### *PDI family members stabilize unassembled cytokine subunits and improve cytokine secretion*

Our comprehensive MS and biochemical analyses revealed not only several overlapping but also distinct ER PDI family members to interact with IL-12α and IL-23α, respectively. To analyze functional effects of these different PDI family members on IL-12 and IL-23 biogenesis, we performed siRNA-mediated knockdowns of the individual PDI family members. None of the knockdowns caused pronounced ER stress as measured by the activation of the unfolded protein response (UPR) (Fig. S4*A*). We thus assessed effects on protein stability in cycloheximide (CHX) translational shut-off experiments, individually knocking down each PDI family member we had found to interact with IL-12α or IL-23α, respectively. Knockdown of any of the PDI family members interacting with IL-12α led to its faster degradation (Fig. 5, *A*, *B* and *D*). For ERp46, however, the effect of knockdown on protein stability was only very weak. For others, for example, ERp5, degradation was accelerated almost twofold (Fig. 5, *A*, *B* and *D*). For IL-23α, we also tested a subset of the PDIs in similar experiments, including not only all those we found to interact with IL-23α (ERp46, ERp5, and ERp72; Fig. 3*E*) but also one that we did not find to strongly associate with this subunit (ERp57; Fig. 3*E*). Similar to what we had observed for IL-12α, knockdown of each of the interacting PDI family members accelerated IL-23α degradation. In contrast, knockdown of ERp57 did not accelerate IL-23α degradation (Fig. 5, *C* and *D*).

Based on these findings, we proceeded to analyze secretion levels of heterodimeric IL-12 or IL-23, respectively, under the same PDI knockdown conditions. In contrast to a more rapid degradation of isolated α subunits, no effect of single PDI knockdown on the secretion of the heterodimeric IL-12 or IL-23 was observed (Figs. 6, *A* and *B* and S5, *A* and *B*). To assess possible compensatory effects of individual PDI members, we thus simultaneously knocked down combinations of three individual PDI family members we had found to interact with IL-12α/IL-23α and assessed secretion of the heterodimeric ILs. Again, no significant ER stress induction was detectable (Fig. S4*B*). In this case, when three PDIs were knocked down simultaneously, although IL-23 remained unaffected, a significant decrease in IL-12 secretion by around 20% could be observed (Fig. 6, *C*–*E*).

## Discussion

IL-12 and IL-23 are key cytokines in the human immune systems and highly relevant molecules in the clinics (24). At the same time, they are demanding clients of the ER folding machinery. The human α subunits, IL-12α and IL-23α, are unfolded in isolation and depend on the shared β subunit IL-12β for structure formation and secretion of the bioactive heterodimeric cytokines (25, 27, 30–32, 35, 39). Both human α subunits contain several cysteine residues, five in the case of IL-23α and seven for IL-12α. In IL-12α, these form three

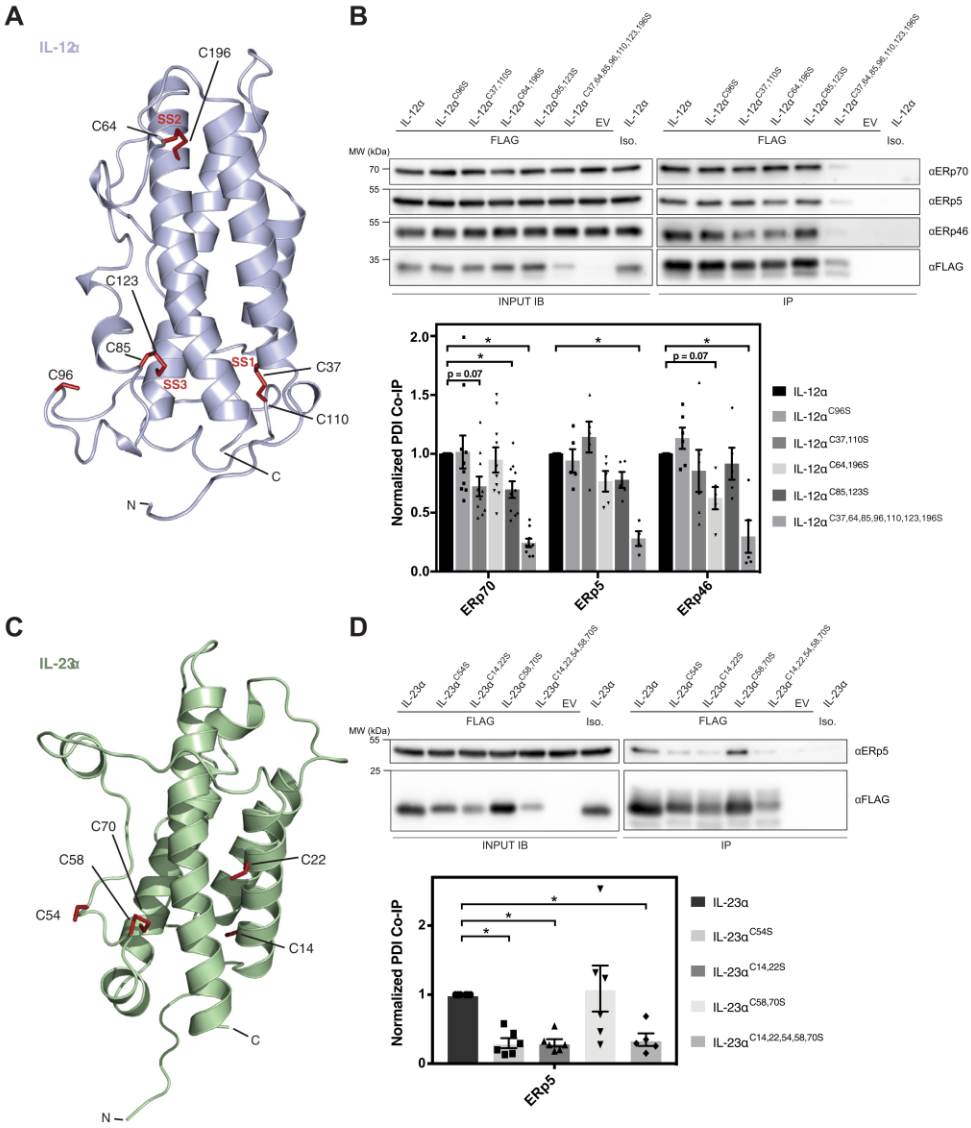


**Figure 4. PDI family members show specificity for distinct cysteines in IL-12α/IL-23α.** *A*, schematic of IL-12α. Cysteines are highlighted in *red* and numbered. Six of the seven cysteines in IL-12α form intramolecular disulfide bonds (denoted as SS1–3, disulfide bonds 1–3), and C96 engages with IL-12β to form an intermolecular disulfide bond. N terminus (N) and C terminus (C) are labeled. *B*, HEK293T cells were transiently transfected with the indicated IL-12α variants in which the indicated cysteines were replaced by serines. Co-IPs of ERp72, ERp5, and ERp46 were analyzed and quantified (n = 4–10 ± SEM, $*p < 0.05$, two-way ANOVA with Dunnett test). *C*, schematic of IL-23α. Cysteines are highlighted in *red* and numbered. C58 and C70 form an intramolecular disulfide bond, and C54 engages with IL-12β to form an intermolecular disulfide bond, and C14 and C22 remain unpaired in IL-23α. N terminus (N) and C terminus (C) are labeled. *D*, HEK293T cells were transiently transfected with the indicated IL-23α variants where the indicated cysteines were replaced by serines. Co-IP of ERp5 was analyzed and quantified (n = 5–6 ± SEM, $*p < 0.05$, one-way ANOVA with Dunnett test). Co-IP, coimmunoprecipitation; HEK293T, human embryonic kidney 293T cell line; IL, interleukin; PDI, protein disulfide isomerase.

intrachain and one interchain disulfide bond to IL-12β (28). In IL-23α, the five cysteines form one intrachain and one interchain disulfide bond, whereas two cysteines remain unpaired (29). Correct disulfide bond formation is important for IL-12/IL-23 to be secreted (25, 27). Their unfolded nature prior to assembly and their complex oxidative folding render IL-12α and IL-23α highly dependent on the ER folding machinery. Using site-specific photocrosslinking coupled to MS, this study is the first comprehensive analysis of the chaperone repertoire that acts on the IL-12 and IL-23 cytokine α subunits,

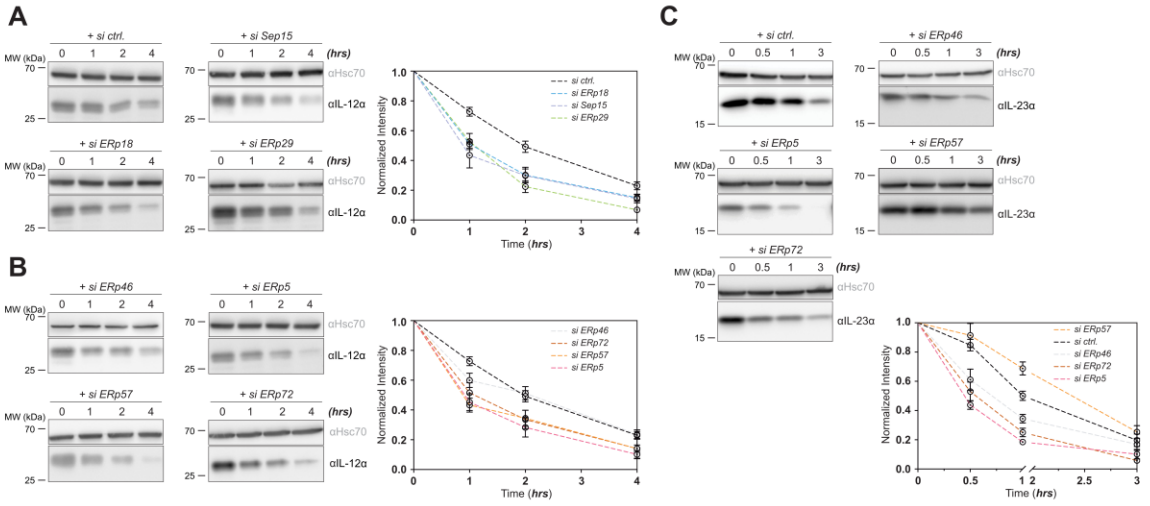


| si PDI | Half-life (*hrs*) ± error | | $R^2$ | |
|---|---|---|---|---|
| | IL-12α | IL-23α | IL-12α | IL-23α |
| *ctrl.* | 1.84 ± 0.11 | 1.18 ± 0.11 | 0.84 | 0.87 |
| *Sep15* | 0.98 ± 0.11 **** | | 0.73 | |
| *ERp18* | 1.07 ± 0.08 **** | | 0.62 | |
| *ERp29* | 0.94 ± 0.06 **** | | 0.87 | |
| *ERp46* | 1.71 ± 0.14 * | 0.83 ± 0.10 ** | 0.71 | 0.83 |
| *ERp5* | 0.94 ± 0.09 **** | 0.38 ± 0.03 **** | 0.78 | 0.76 |
| *ERp57* | 1.12 ± 0.11 **** | 1.51 ± 0.17 ** | 0.82 | 0.84 |
| *ERp72* | 1.09 ± 0.13 **** | 0.53 ± 0.04 **** | 0.61 | 0.90 |

**Figure 5. Effect of PDI knockdowns on IL-12α and IL-23α turnover rates.** *A–C*, cycloheximide (CHX) chases were performed for the indicated periods upon specific depletion of the indicated individual PDIs by siRNA, or with si negative control (*si ctrl.*). The levels of IL-12α or IL-23α were determined from lysate immunoblots relative to the 0 h time point. Representative immunoblots and quantifications are shown (n = 4–7 ± SEM). *D*, summary of protein half-lives and corresponding statistical unpaired *t* test analysis with Welch's corrections for individual PDI knockdowns. Statistical analysis was performed after semilog decay curve fitting to determine protein half-lives, $^*p < 0.05$. A goodness of fit for the linear curve can be assessed based on the given $R^2$ values. CHX, cycloheximide; IL, interleukin; PDI, protein disulfide isomerase.

significantly extending previous studies (25, 40, 41). Among the interacting chaperones, we find not only overlapping but also distinct PDI family members to engage IL-12α or IL-23α (Fig. 6*F*). Of note, our photocrosslinking approach allows to identify interactions with potential PDI family members that do not covalently engage their clients, for example, ERp29, and thus extends the repertoire of interactors that can be identified.

We generally observe a stabilizing effect of PDI family members on the unassembled α subunits, similar to what, for example, had been observed for ERp57 and the prion protein (42). A possible explanation is that PDI binding protects the unfolded α subunits from premature ERAD, a process for which our MS analyses also provide relevant hits, including XTP3B (*ERLEC*) and OS9 for IL-12α (Fig. 2*E* and Table S1). In contrast to the pronounced effects on isolated α subunits, no effects of individual PDI knockdowns on secretion of heterodimeric IL-12/IL-23 was observed when IL-12β was coexpressed (Fig. 6*F*). Although this may depend on relative expression levels of individual subunits, it argues that α:β assembly is a fast and efficient process; hence, the role of the β subunit as a folding matrix may overcome the need for stabilizing unassembled α subunits for IL-12 and IL-23. For the more labile IL-35, that is not disulfide-linked (43), this may be different. Our findings are in agreement with the observation that although IL-12α and IL-23α misfold in isolation and form incorrect disulfide bonds, misfolding is not observed upon coexpression of IL-12β (25, 27). Even though our work was performed by transient transfections in nonimmune cells and thus awaits further studies in endogenous producers, this raises the question of why such a complex network of chaperones caters for IL-12α and IL-23α if heterodimerization appears to be highly efficient. One explanation may be not only the ubiquitous expression of IL-12α (44) and its pairings with other subunits, for example, EBI3 to form IL-35 (43, 45) but possibly also autonomous functions of IL-12α as an anti-inflammatory molecule (46), together requiring a tight regulation of secretion. Another likely explanation is that immune cells must regulate IL-12 *versus* IL-23 assembly. Since IL-12 and IL-23 share the same β subunit, and some cells express all three proteins (see *e.g.*, (47)), their biogenesis has to be chaperoned in the ER to allow for specific downstream immune responses. The large number of ER chaperones, and in particular ER PDI family members our study identifies, testifies to this notion. Our work also shows that combined depletion of several PDI family members can selectively reduce IL-12

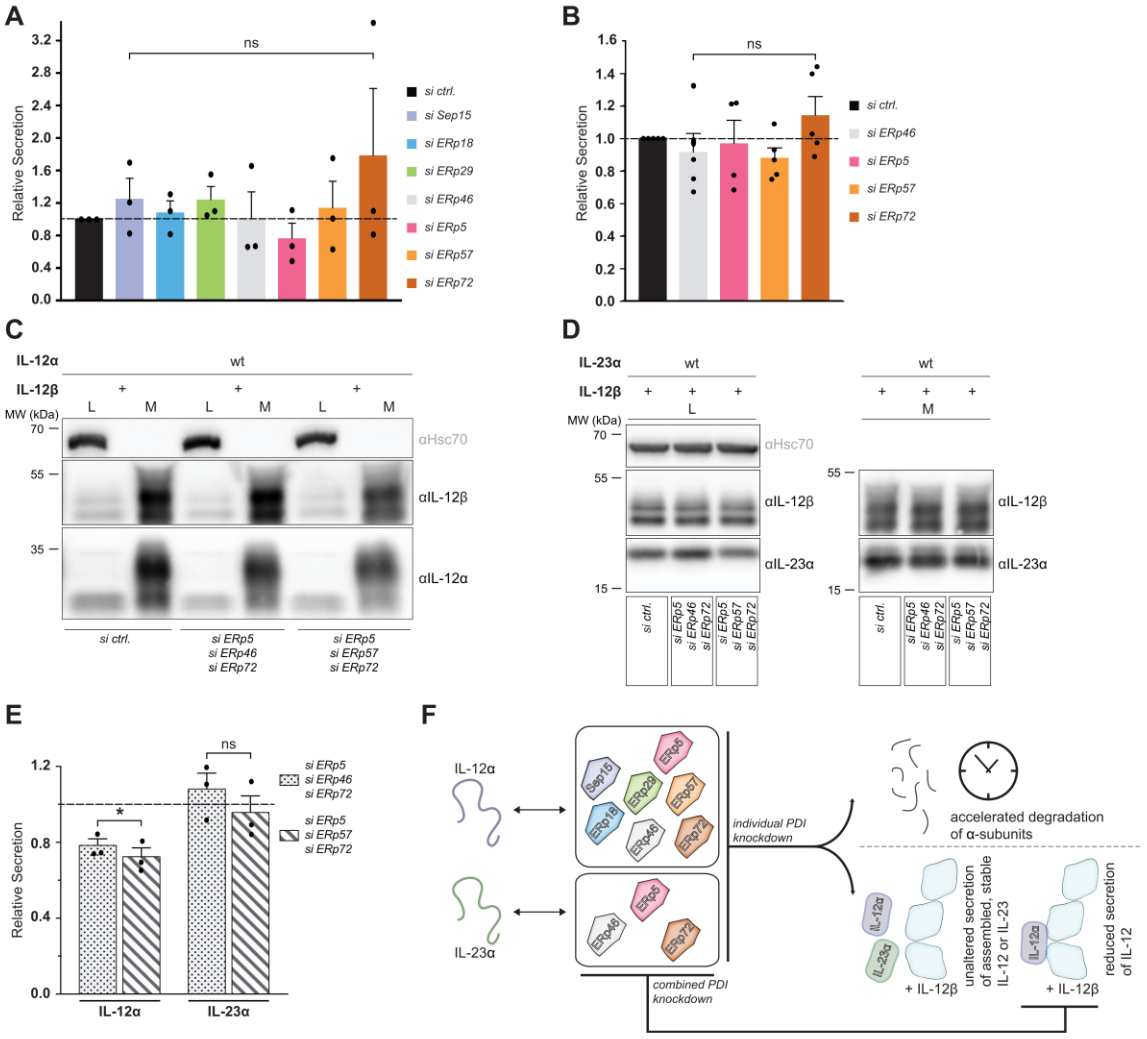


**Figure 6. Effect of PDI knockdowns on IL-12 and IL-23 cytokine secretion.** *A*, graph depicting IL-12α secretion levels upon coexpression of IL-12β, that is, secretion of the heterodimeric cytokine, in HEK293T cells treated with the respective PDI siRNAs relative to those in *si ctrl* (set to 1, *dashed line*). *B*, the same as in (*A*) for IL-23α. *C–E*, similar analyses as in *A* and *B*, but with siRNA-mediated knockdown of the indicated combination of PDIs. Representative immunoblots on IL-12 secretion (*C*) and IL-23 secretion (*D*) are shown. In the quantifications, the *dashed line* corresponds to *si ctrl* sample treatment. *$p < 0.05$ for multiple knockdowns *versus si ctrl* (unpaired two-tailed Student's *t* test). *F*, model for the role of PDIs in the biogenesis of the proinflammatory cytokines IL-12 and IL-23. Each α subunit physically associates with overlapping but also distinct PDI family members (only ER-lumenal, soluble PDIs are shown). Knockdowns of individual interacting PDIs generally led to a faster degradation of the unfolded and unpaired α subunits *via* ERAD. However, no change in secretion levels was observed after assembly with the β subunit. Combined siRNA knockdown, in contrast, leads to reduced secretion of heterodimeric IL-12 but not IL-23. ER, endoplasmic reticulum; ERAD, ER-associated degradation; HEK293T, human embryonic kidney 293T cell line; IL, interleukin; ns, not significant; PDI, protein disulfide isomerase.

secretion without affecting IL-23 secretion (Fig. 6*F*). It may be explained by the larger number of disulfide bonds IL-12α has to form in comparison to IL-23α (25, 27), and its dependency on different branches of the ER folding machinery, IL-12α being an N-glycoprotein, whereas IL-23α is not (36).

In addition to insights into the chaperoning of immune signaling proteins, our study contributes to our understanding of the ER PDI family. A surprising finding we make is that most PDI family members seem to have a stabilizing effect on our two investigated client proteins, arguing against a possible mutual compensation in this function. This is in agreement with recent insights into different binding characteristics of PDI family members (37) and synergistic functions in protein folding (48). A possible explanation is that different folding states, each prone to ERAD, are recognized by the different PDIs or that binding to multiple PDIs shifts the competition between ERAD and stabilizing unfolded proteins toward the latter. This notion, that different PDIs recognize different

features of their clients, is in agreement with our findings that mutating cysteines individually or pairwise within IL-12α or IL-23α differentially affects binding to ERp72, ERp5, and ERp46. Protein folding itself also modulates PDI dependency (49). The fact that IL-12α and IL-23α cannot fold to a native state autonomously may thus contribute to their strong PDI dependency in isolation, where misfolding and mispairing of cysteines are to be chaperoned, and multiple folding intermediates exist in cells (25, 27, 49). For IL-23α, it is noteworthy that ERp44, an ER–Golgi intermediate compartment PDI, can recognize the same free cysteines in IL-23α, which our study reveals to be bound by ERp5—and which are close to a BiP-binding site (25). These free cysteines in IL-23α become buried upon folding (25), together highlighting these as important molecular motifs of folding and assembly control for IL-23. Despite these insights, it should be noted that for several of the PDI family members, we find to interact with IL-12α or IL-23α, functions yet remain to be determined. IL-12α or IL-23α may prove to be very valuable and medically relevant clients for this. One example is Sep15, an interactor of UGGT (50), that has been described as a gatekeeper not only to maintain misfolded immune proteins in the ER (38) but also has redox activity (51). Of note, our data show that IL-12α interacts with both, Sep15 and UGGT1/2, which qualifies it as an interesting client to further define the functions of Sep15.

Taken together, our study reveals a complex network of PDI family members that act on the highly disulfide-bonded glycoprotein IL-12α. The less disulfide-bonded non-glycosylated IL-23α interacts with significantly less PDI family members. The PDI family members recognize different cysteines in their clients and thus seem to act synergistically, not redundantly, when it comes to stabilizing the unassembled incompletely folded cytokine subunits. Despite this, only when multiple PDIs are depleted is the secretion of heterodimeric IL-12, but not IL-23, selectively affected, which may be relevant in the light of PDI inhibitors entering the clinic (52–54).

## Experimental procedures

### *Cloning, DNA constructs, and siRNA*

The piggybac (pPB) vector containing DiazKRS with mutations (*Methanosarcina mazei*: Y306M, L309A, and C348A) (55) has been described previously (33). Amber suppression sites were inserted in IL-12α/23α constructs by site-directed mutagenesis PCR using Pfu (Promega) DNA polymerase in a pSVL vector backbone. "TAG"-replaced coding sequences were subcloned into the pPB vector as reported previously (56) in-frame downstream of the EF-1 promoter. Constructs equipped with a C-terminal FLAG tag were subcloned in a similar approach separated by four (IL-12α) or five (IL-23α) GS-linker repeats. Other plasmids used in this study were an IL-12β construct in the pcDNA3.1(+) vector (56) and immunoglobulin $\gamma_1$ heavy chain in pSVL, a kind gift from Linda M. Hendershot, St Jude Children's Research Hospital. All constructs were verified by sequencing. Custom oligos (Sigma–Aldrich) were designed using the SnapGene tool fulfilling optimal parameters for PCR mutagenesis.

The following human gene-directed Silencer Select siRNAs were purchased from Thermo Fisher Scientific.

**List of siRNAs used in this study**

| siRNA | ID/catalog no. |
|---|---|
| si negative control #1 | 4390843 |
| si Sep15/SEP15 | s17999 |
| si ERp18/TXNDC12 | s27323 |
| si ERp29/PDIA9 | AM16708 |
| si ERp46/TXNDC5 | s37649 |
| si ERp5/PDIA6 | s531609 |
| si ERp57/PDIA3 | s6227 |
| si ERp72/PDIA4 | s225165 |

### *Mammalian cell culture*

HEK293T cells were subcultured every 2-3 days in Dulbecco's modified Eagle's medium containing L-Ala-L-Gln (AQ; Sigma–Aldrich) supplemented with 10% v/v fetal bovine serum (Gibco) and 1% v/v antibiotic/antimycotic solution (25 μg/ml amphotericin B, 10 mg/ml streptomycin, and 10,000 units of penicillin; Sigma–Aldrich) under standard conditions (37 °C and 5% $CO_2$ in a humidified incubator). Cells were routinely tested by PCR for the absence of mycoplasma contamination.

### *Transient transfections*

Transient transfections were carried out using GeneCellin (BioCellChallenge) or Lipofectamine 3000 (Thermo Fisher) according to the manufacturers' instructions. Cells were grown in poly-D-lysine-coated 35 mm dishes (Corning) to a confluency of 60 to 70%. About 1 μg of IL-12α or IL-23α construct in combination with 1 μg of DiazKRS or 1 μg of the α subunits alone were delivered to cells for expression tests and CHX chase experiments, respectively. For PDI co-IP (4 μg of IL-12α or IL-23α) or MS analysis (1 μg of pPB IL-12α or IL-23α "TAG"-replaced constructs or pPB empty vector and 1 μg of DiazKRS), cells were seeded on poly-D-lysine-coated 60 mm. About 2 μg of total DNA in a 1:2 ratio (α subunit:IL-12β) in the presence of 0.5 μg DiazKRS, where indicated, was transfected for *in cellulo* secretion and assembly tests. Cells were lysed 24 to 48 h post-transfection.

For siRNA-mediated knockdown experiments, 25 nM of each individual siRNA was added to cells using Lipofectamine's RNAiMAX (Thermo Fisher) protocol and incubated for another 24 h prior to DNA transfection. Combined knockdowns were achieved by adding three different siRNAs to a final concentration of 50 nM. siRNA stocks at 10 μM were prepared using nuclease-free water.

### *Cell harvesting and immunoblotting*

Cells were washed in ice-cold PBS (Sigma–Aldrich) and lysed in an appropriate amount of radioimmunoprecipitation assay buffer (50 mM Tris–HCl [pH 7.5], 150 mM NaCl, 1% NP-40, 0.1% SDS, 0.5% NaDOC, 1× Roche complete protease inhibitor without EDTA) for 20 to 30 min on ice. For UPR activation tests, cell lysis was performed using either Triton

lysis buffer (50 mM Tris–HCl, pH 7.4, 150 mM NaCl, 1 mM EDTA, 1% Triton X-100, 1× Roche complete protease inhibitor without EDTA, and 1× SERVA phosphatase inhibitor mix) or NP-40 lysis buffer (50 mM Tris–HCl, pH 7.5, 150 mM NaCl, 0.5% NaDOC, 0.5% NP-40 substitute, 1× Roche complete protease inhibitor without EDTA, and 1× SERVA phosphatase inhibitor mix). About 20 mM NEM (Sigma–Aldrich) was added to lysis steps where indicated. Cell debris was pelleted by centrifugation at 20,000*g* at 4 °C for 15 min. Whole cell lysate/input or immunoprecipitated samples were supplemented with Laemmli containing either 10% β-mercaptoethanol (β-Me; reducing) or 100 mM NEM (nonreducing) and heated to 95 °C for 5 min or, in the case of activating transcription factor 6 (ATF6) sample processing, to 37 °C for 30 min. Proteins were then separated using SDS-polyacrylamide gels and transferred to polyvinylidene difluoride membranes (Bio-Rad) by wet electroblotting (overnight at 30 V and 4 °C). Thereafter, membranes were blocked for at least 3 h (at room temperature) with MTBST (25 mM Tris–HCl [pH 7.5], 150 mM NaCl, 5% skim milk powder, and 0.1% Tween) or 5% w/v bovine serum albumin (BSA) in Tris-buffered saline with Tween-20 under constant agitation. Proteins of interest were detected using anti-IL-12α (Abcam; catalog no.: ab133751, 1:500/1:1000 dilution in MTBST), anti-IL-23α (BioLegend; catalog no.: 511202, 1:500 dilution in MTBST), anti-IL-12β (Abcam; catalog no.: ab133752, 1:500 dilution in MTBST), anti-Hsc70 (Santa Cruz; catalog no.: sc-7298, 1:1000 dilution in MTBST), anti-Sep15 (Abcam; catalog no.: ab124840, 1:200 dilution in MTBST), anti-ERp18 (Abcam; catalog no.: ab134938, 1:500 dilution in MTBST), anti-ERp29 (Abcam; catalog no.: ab11420, 1:1000 dilution in MTBST), anti-ERp46 (Proteintech; catalog no.: 19834-1-AP, 1:1000 dilution in MTBST), anti-PDIA6 (Proteintech; catalog no.: 18233-1-AP, 1:1000 dilution in MTBST), anti-ERp57 (Abcam; catalog no.: ab13506, 1:1000 dilution in MTBST), anti-CALR (Abcam; 1:1000 dilution in MTBST), anti-ERp72 (Proteintech; catalog no.: 14712-1-AP, 1:1000 dilution in MTBST), anti-ATF6 (Abcam; catalog no.: ab122897, 1:500 dilution in MTBST), anti–eukaryotic translation initiation factor 2α (eIF2α; Cell Signaling; catalog no.: 9722, 1:1000 dilution in BSA), anti-phospho-eIF2α (Cell Signaling; catalog no.: 9721, 1:500 in BSA), and anti-BiP (Cell Signaling; catalog no.: 3177, 1:500 dilution in MTBST). Membranes were next probed with species-specific secondary antibodies coupled to horseradish peroxidase: goat antimouse immunoglobulin G (IgG) (Santa Cruz; catalog no.: sc-2031), mouse-IgGκ BP (Santa Cruz; catalog no.: sc-516102), or goat anti-rabbit IgG (Santa Cruz; catalog no.: sc-2054/sc-2357). Bands were detected by enhanced chemiluminescence (ECL Prime) on a Fusion Pulse 6 imager (Vilber Lourmat).

### *Incorporation of DiazK*

Where specified, $N^6$-((2-(3-methyl-3*H*-diazirin-3-yl)ethoxy) carbonyl)-L-lysine (DiazK, (33)) was added to the complete Dulbecco's modified Eagle's medium at a concentration of 0.25 mM (MS experiments) or 1 mM during DNA transfections. A 100 mM DiazK stock solution was prepared by dissolving powder form of DiazK in 100 mM TFA/$H_2O$, sterile filtered, and stored at −20 °C. Before incubations, an equivalent amount of NaOH was added to the cell culture medium to neutralize pH.

### *Determination of protein removal rates*

Translational arrest (chase) was carried out 24 to 48 h post-gene transfection with 50 μg/ml CHX (Sigma–Aldrich) added to cells for the indicated time points. Linear regression fittings on semilog curves were used to calculate protein half-lives using plots of protein abundance over time (0 h set to 100%).

### In situ *photocrosslinking/chemical crosslinking, pull-down and co-IP workflows*

Cells expressing the desired constructs for DiazK incorporation were washed twice with PBS and subjected to a broad-emitting UV lamp (Vilber VL-215.L; 2 × 15 W, 365 nm) for 30 min in PBS. During this procedure, culture plates were placed on ice under cardboard covers with occasional swirling. Reactions without irradiation served as negative controls. Thiol-cleavable DSP (Thermo Fisher) crosslinks were also performed in intact cells. A 25 mM stock solution was prepared by reconstituting 1 mg of desiccated DSP in 100 μl dry dimethyl sulfoxide. In brief, cells were first washed in PBS and then in crosslinking buffer (25 mM Hepes–KOH, pH 8.3, 125 mM KCl) on ice before incubation with 0.8 mM DSP in the same buffer for 1 h 20 min and quenched using 100 mM glycine for 20 min on ice checking for even dispersion. Cell lysis was performed as described previously.

To study interactors of IL-12α/23α *via* enrichment of cell lysates, purification from photocrosslinked/chemically crosslinked samples was performed using anti-FLAG affinity gel (Sigma). The same amount of isotype control slurry (mouse IgG-Agarose; Sigma) was used to discriminate positive hits from unspecific binding to antibody and beads. Alternatively, ATF6 samples were initially precleared for 30 min and pulled down overnight using 2 μg of antibody followed by immobilization on protein A/G agarose beads (Thermo Fisher) for 1 h at 4 °C, while rotating and eluted with 2× Laemmli with 10% v/v β-Me after washing three times with NP-40 wash buffer (50 mM Tris–HCl, pH 7.5, 400 mM NaCl, 0.5% NaDOC, and 0.5% NP-40 substitute) and centrifugation in each round (7000*g*, 1 min at 4 °C). Of note, in covalent complex (nonreducing IP) SDS-PAGE, 10% v/v NEM was added instead of β-Me. Beads were washed twice with radioimmunoprecipitation assay buffer and three times with PBS in the case of MS measurements.

### *Sample preparation for MS*

After enrichment, proteins were reduced and digested on-beads in 25 μl 50 mM Tris–HCl, pH 8.0 containing 5 ng/μl sequencing grade trypsin (Promega), 2 M urea, and 1 mM DTT for 30 min at 25 °C and with shaking at 600 rpm. Next, 100 μl 50 mM Tris–HCl, pH 8.0 containing 2 M urea, and alkylating 5 mM iodoacetamide were added (30 min incubation at 25 °C under shaking at 600 rpm). Digestion took place overnight at 37 °C with shaking 600 rpm. The following day, digestion was stopped by addition of formic acid (FA, 0.5% v/v

final amount). The beads were pelleted, and the supernatant was desalted using double layer C18-stage tips (Agilent Technologies, Empore disk-C18, 47 mm) equilibrated with 70 µl methanol and three times aqueous 0.5% v/v FA. Samples were loaded and washed three times with 70 µl aqueous 0.5% v/v FA and eluted three times with 30 µl 80% v/v acetonitrile (ACN), 20% v/v $H_2O$, and 0.5% v/v FA. The eluate was lyophilized *in vacuo*, resuspended in 25 µl aqueous 1% v/v FA, pipetted up and down, vortexed, and sonicated for 15 min. Finally, the peptide solution was passed through a polyvinylidene difluoride filter (Millipore; 0.22 µm pore size).

#### *MS analysis*

Three replicates of photocrosslink/co-IP samples on mutants and wt IL-12α/23α as well as controls transfected with empty vectors were analyzed *via* LC–MS/MS using an UltiMate 3000 nano HPLC system (Thermo Fisher) equipped with an Acclaim C18 PepMap100 75 µm ID × 2 cm trap (Thermo Fisher) and an Aurora C18 separation column (75 µm ID × 25 cm, 1.6 µm; IonOpticks) coupled to a CaptiveSpray source equipped TimsTOF Pro mass spectrometer (Bruker). Samples were loaded onto the trap column at a flow rate of 5 µl/min with aqueous 0.1% TFA and then transferred onto the separation column at 0.4 µl/min. Buffers for the nanochromatography pump were aqueous 0.1% FA (buffer A) and 0.1% FA in ACN (buffer B). The gradient length on the TimsTOF Pro was 73 min, whereas ACN in 0.1% FA was stepwise increased from 5% to 28% in 60 min and from 28% to 40% in 13 min, followed by a washing and equilibration step of the column. The TimsTOF Pro was operated in parallel accumulation–serial fragmentation (PASEF) mode. Mass spectra for MS and MS/MS scans were recorded between 100 and 1700 *m/z*. Ion mobility resolution was set to 0.85 to 1.40 V s/cm over a ramp time of 100 ms. Data-dependent acquisition was performed using ten PASEF MS/MS scans per cycle with a near 100% duty cycle. A polygon filter was applied in the *m/z* and ion mobility space to exclude low *m/z*, singly charged ions from PASEF precursor selection. An active exclusion time of 0.4 min was applied to precursors that reached 20,000 intensity units. Collisional energy was ramped stepwise as a function of ion mobility (57). The acquisition of all MS spectra on the TimsTOF instrument was performed with the Compass HyStar software, version 6.0 (Bruker).

#### *UPR activation tests*

To observe possible effect of PDI siRNAs on ER stress, cells transfected with each siRNA were checked for upregulation of intracellular BiP levels, phosphorylation of eIF2α (protein kinase R-like ER kinase branch) and ATF6 N-terminal cleavage (ATF6 branch) using immunoblots. HEK293T cells incubated with 10 mM DTT (Sigma, 1 h) or 5 µg/ml tunicamycin (Sigma, 4–6 h) before cell lysis served as positive controls.

#### *Software and statistical analyses*

IL-12 and IL-23 structures were modeled *in silico* with YASARA Structure (58) for missing loops and energy minimized (steepest descent). Sites for replacement to amber codons were selected on the basis of residue solvent accessibility (PDBePISA server (59)), mutation stability prediction (SDM (60) and DynaMut servers (61)), and interfaces with the IL-12β subunit and/or IL-23 receptor (28, 29, 62). Other known experimental constraints like secondary structure flexibility/lesions/chaperone-binding sites (25) were also taken into account. Available crystal structural data (Protein Data Bank codes: 3HMX, 1F45, 3DUH, 5MXA, and 5MZV) were inputs for the aforementioned analyses and visualized with PyMOL (www.pymol.org). Western blot raw images were processed for brightness and contrast in ImageJ (63) or Adobe Photoshop. Chemiluminescence band intensity quantifications were performed using the Bio-1D (Vilber Lourmat) software. For normalization of PDI co-IP, IP signals were background subtracted if unspecific signals were detected for empty vector controls. IP signals of wt were set to 1, and chaperone IP was divided by respective FLAG signals, thus amount of IL subunit, to obtain normalized PDI co-IP ratios. Statistical analyses and graph fittings were performed with Prism 7 (GraphPad) software as stated in the figure legends.

#### *Statistical analyses of MS data*

MS raw files were analyzed with MaxQuant software (version 2.1.0.0), and the default settings for TimsTOF files were applied except that the TOF MS/MS match tolerance was set to 0.05 Da. Searches were performed with the Andromeda search engine embedded in the MaxQuant environment against the UniProt human protein database (taxon identifier: 9606; downloaded September 2021; number of entries: 20,371). The following parameter settings were used: peptide spectrum match and protein false discovery rate 1%; enzyme specificity trypsin/P; minimal peptide length: 7; variable modifications: methionine oxidation, N-terminal acetylation; and fixed modification: carbamidomethylation. The minimal number of unique peptides for protein identification was set to 2. For label-free protein quantification, the MaxLFQ algorithm was used as part of the MaxQuant environment: (label-free quantitation) minimum ratio count: 2; peptides for quantification: unique. Resulting data were further analyzed using Perseus software, version 1.6.15.0 (64). The rows were filtered (only identified by site, potential contaminant, reverse), and label-free quantitation intensities were $\log_2$ transformed. Replicates (n = 3) were grouped, filtered for at least two valid values in at least one group, and missing values were imputed for total matrix using default settings. A both sided, two-sample Student's *t* test was performed, and derived *p* values were corrected for multiple testing by the method of Benjamini and Hochberg with a significance level of $p = 0.05$. Volcano plots were generated by plotting $\log_2$ (fold change) against $-\log_{10}$ (*p* value). ER chaperones were detected searching for GO terms cellular compartment = ER, biological process = protein folding (GO numbers: 0006457, 0071712, 0006986, 0030433, 0034975, and 0061077) and molecular function = PDI activity with the help of the GO annotation file

for *Homo sapiens* downloaded from UniProt (August 2022) (65). In addition, all ER proteins were manually scrutinized for possible PDI family members that have not been annotated as such with the suitable GO terms. This further added ERp18, Sep15, and TMX1 to the list.

## Data availability

The MS proteomics data have been deposited to the ProteomeXchange Consortium *via* the PRIDE (66) partner repository with the dataset identifier PXD036463.

*Supporting information*—This article contains supporting information.

*Acknowledgments*—We are grateful to Annina Steinbach for excellent support in MS experiments. This work was supported by the German Research Foundation DFG (Sonderforschungsbereich 1035; project number: 201302640, projects A09, B10, and B11).

*Author contributions*—Y. G. M., I. A., and M. J. F. conceptualization; Y. G. M., A. F., D. K., T.-A. N., N. C. B., K. L., S. A. S., and M. J. F. methodology; Y. G. M. and M. J. F. validation; Y. G. M., I. A., A. F., D. K., C. A. M. W., T.-A. N., and N. C. B. investigation; A. F., D. K., and N. C. B. data curation; M. J. F. writing–original draft; Y. G. M., I. A., A. F., D. K., T.-A. N., K. L., S. A. S., and M. J. F. writing–review & editing; Y. G. M., I. A., A. F., and D. K. visualization; M. J. F. supervision; K. L., S. A. S., and M. J. F. funding acquisition.

*Funding and additional information*—Y. G. M. gratefully acknowledges support by a PhD scholarship by the German Academic Exchange Service (DAAD), I. A. and D. K. by the German Academic Scholarship Foundation (Studienstiftung des Deutschen Volkes), and I. A. by the Marianne-Plehn Program. This work was supported by SPP1623 (to K. L.) and the German Research Foundation DFG (Sonderforschungsbereich 1035, Projektnummer 201302640, projects A09, B10, and B11).

*Conflict of interest*—The authors declare that they have no conflicts of interest with the contents of this article.

*Abbreviations*—The abbreviations used are: ACN, acetonitrile; ATF6, activating transcription factor 6; BiP, immunoglobulin binding protein; BSA, bovine serum albumin; CHX, cycloheximide; co-IP, coimmunoprecipitation; DSP, dithiobis(succinimidyl propionate); eIF2α, eukaryotic translation initiation factor 2α; ERAD, ER-associated degradation; ERQC, ER quality control; FA, formic acid; GO, Gene Ontology; HEK293T, human embryonic kidney 293T cell line; IgG, immunoglobulin G; IL, interleukin; IP, immunoprecipitation; β-Me, β-mercaptoethanol; MS, mass spectrometry; NEM, *N*-ethylmaleimide; PASEF, parallel accumulation–serial fragmentation; PDI, protein disulfide isomerase; pPB, piggybac; UPR, unfolded protein response.

## References

1. Braakman, I., and Hebert, D. N. (2013) Protein folding in the endoplasmic reticulum. *Cold Spring Harb. Perspect. Biol.* **5**, a013201
2. Braakman, I., and Bulleid, N. J. (2011) Protein folding and modification in the mammalian endoplasmic reticulum. *Annu. Rev. Biochem.* **80**, 71–99
3. Tannous, A., Pisoni, G. B., Hebert, D. N., and Molinari, M. (2015) N-linked sugar-regulated protein folding and quality control in the ER. *Semin. Cell Dev. Biol.* **41**, 79–89
4. Kozlov, G., and Gehring, K. (2020) Calnexin cycle - structural features of the ER chaperone system. *FEBS J.* https://doi.org/10.1111/febs.15330
5. Feige, M. J. (2018) *Oxidative Folding of Proteins: Basic Principles, Cellular Regulation and Engineering*, RSC Publishing
6. Anelli, T., and Sitia, R. (2008) Protein quality control in the early secretory pathway. *EMBO J.* **27**, 315–327
7. Appenzeller-Herzog, C., and Ellgaard, L. (2008) The human PDI family: versatility packed into a single fold. *Biochim. Biophys. Acta* **1783**, 535–548
8. Kanemura, S., Matsusaki, M., Inaba, K., and Okumura, M. (2020) PDI family members as guides for client folding and assembly. *Int. J. Mol. Sci.* **21**, 9351
9. Freedman, R. B., Klappa, P., and Ruddock, L. W. (2002) Protein disulfide isomerases exploit synergy between catalytic and specific binding domains. *EMBO Rep.* **3**, 136–140
10. Wilson, R., Lees, J. F., and Bulleid, N. J. (1998) Protein disulfide isomerase acts as a molecular chaperone during the assembly of procollagen. *J. Biol. Chem.* **273**, 9637–9643
11. Yu, J., Li, T., Liu, Y., Wang, X., Zhang, J., Wang, X., *et al.* (2020) Phosphorylation switches protein disulfide isomerase activity to maintain proteostasis and attenuate ER stress. *EMBO J.* **39**, e103841
12. Molinari, M., and Helenius, A. (1999) Glycoproteins form mixed disulphides with oxidoreductases during folding in living cells. *Nature* **402**, 90–93
13. Frickel, E. M., Frei, P., Bouvier, M., Stafford, W. F., Helenius, A., Glockshuber, R., *et al.* (2004) ERp57 is a multifunctional thiol-disulfide oxidoreductase. *J. Biol. Chem.* **279**, 18277–18287
14. Pisoni, G. B., Ruddock, L. W., Bulleid, N., and Molinari, M. (2015) Division of labor among oxidoreductases: TMX1 preferentially acts on transmembrane polypeptides. *Mol. Biol. Cell* **26**, 3390–3400
15. Jessop, C. E., Watkins, R. H., Simmons, J. J., Tasab, M., and Bulleid, N. J. (2009) Protein disulphide isomerase family members show distinct substrate specificity: p5 is targeted to BiP client proteins. *J. Cell Sci.* **122**, 4287–4295
16. Ushioda, R., Hoseki, J., Araki, K., Jansen, G., Thomas, D. Y., and Nagata, K. (2008) ERdj5 is required as a disulfide reductase for degradation of misfolded proteins in the ER. *Science* **321**, 569–572
17. Sugiura, Y., Araki, K., Iemura, S., Natsume, T., Hoseki, J., and Nagata, K. (2010) Novel thioredoxin-related transmembrane protein TMX4 has reductase activity. *J. Biol. Chem.* **285**, 7135–7142
18. Oka, O. B., Pringle, M. A., Schopp, I. M., Braakman, I., and Bulleid, N. J. (2013) ERdj5 is the ER reductase that catalyzes the removal of non-native disulfides and correct folding of the LDL receptor. *Mol. Cell* **50**, 793–804
19. Vavassori, S., Cortini, M., Masui, S., Sannino, S., Anelli, T., Caserta, I. R., *et al.* (2013) A pH-regulated quality control cycle for surveillance of secretory protein assembly. *Mol. Cell* **50**, 783–792
20. Anelli, T., Alessio, M., Mezghrani, A., Simmen, T., Talamo, F., Bachi, A., *et al.* (2002) ERp44, a novel endoplasmic reticulum folding assistant of the thioredoxin family. *EMBO J.* **21**, 835–844
21. Oka, O. B., van Lith, M., Rudolf, J., Tungkum, W., Pringle, M. A., and Bulleid, N. J. (2019) ERp18 regulates activation of ATF6α during unfolded protein response. *EMBO J.* **38**, e100990
22. Rutkevich, L. A., Cohen-Doyle, M. F., Brockmeier, U., and Williams, D. B. (2010) Functional relationship between protein disulfide isomerase family members during the oxidative folding of human secretory proteins. *Mol. Biol. Cell* **21**, 3093–3105
23. Vignali, D. A., and Kuchroo, V. K. (2012) IL-12 family cytokines: immunological playmakers. *Nat. Immunol.* **13**, 722–728
24. Tait Wojno, E. D., Hunter, C. A., and Stumhofer, J. S. (2019) The immunobiology of the interleukin-12 family: room for discovery. *Immunity* **50**, 851–870
25. Meier, S., Bohnacker, S., Klose, C. J., Lopez, A., Choe, C. A., Schmid, P. W. N., *et al.* (2019) The molecular basis of chaperone-mediated interleukin 23 assembly control. *Nat. Commun.* **10**, 4121
26. Muller, S. I., Aschenbrenner, I., Zacharias, M., and Feige, M. J. (2019) An interspecies analysis reveals molecular construction principles of interleukin 27. *J. Mol. Biol.* **431**, 2383–2393

27. Reitberger, S., Haimerl, P., Aschenbrenner, I., Esser-von Bieren, J., and Feige, M. J. (2017) Assembly-induced folding regulates interleukin 12 biogenesis and secretion. *J. Biol. Chem.* **292**, 8073–8081
28. Yoon, C., Johnston, S. C., Tang, J., Stahl, M., Tobin, J. F., and Somers, W. S. (2000) Charged residues dominate a unique interlocking topography in the heterodimeric cytokine interleukin-12. *EMBO J.* **19**, 3530–3541
29. Lupardus, P. J., and Garcia, K. C. (2008) The structure of interleukin-23 reveals the molecular basis of p40 subunit sharing with interleukin-12. *J. Mol. Biol.* **382**, 931–941
30. Oppmann, B., Lesley, R., Blom, B., Timans, J. C., Xu, Y., Hunte, B., *et al.* (2000) Novel p19 protein engages IL-12p40 to form a cytokine, IL-23, with biological activities similar as well as distinct from IL-12. *Immunity* **13**, 715–725
31. Gubler, U., Chua, A. O., Schoenhaut, D. S., Dwyer, C. M., McComas, W., Motyka, R., *et al.* (1991) Coexpression of two distinct genes is required to generate secreted bioactive cytotoxic lymphocyte maturation factor. *Proc. Natl. Acad. Sci. U. S. A.* **88**, 4143–4147
32. Wolf, S. F., Temple, P. A., Kobayashi, M., Young, D., Dicig, M., Lowe, L., *et al.* (1991) Cloning of cDNA for natural killer cell stimulatory factor, a heterodimeric cytokine with multiple biologic effects on T and natural killer cells. *J. Immunol.* **146**, 3074–3081
33. Bartoschek, M. D., Ugur, E., Nguyen, T. A., Rodschinka, G., Wierer, M., Lang, K., *et al.* (2021) Identification of permissive amber suppression sites for efficient non-canonical amino acid incorporation in mammalian cells. *Nucleic Acids Res.* **49**, e62
34. Nguyen, T. A., Gronauer, T., Nast-Kolb, T., Sieber, S., and Lang, K. (2022) Substrate profiling of mitochondrial caseinolytic protease P via a site-specific photocrosslinking approach. *Angew. Chem. Int. Ed. Engl.* **61**, e202111085
35. Jalah, R., Rosati, M., Ganneru, B., Pilkington, G. R., Valentin, A., Kulkarni, V., *et al.* (2013) The p40 subunit of interleukin (IL)-12 promotes stabilization and export of the p35 subunit: implications for improved IL-12 cytokine production. *J. Biol. Chem.* **288**, 6763–6776
36. Bohnacker, S., Hildenbrand, K., Aschenbrenner, I., Müller, S. I., Bieren, J. E., and Feige, M. J. (2020) Influence of glycosylation on IL-12 family cytokine biogenesis and function. *Mol. Immunol.* **126**, 120–128
37. Hirayama, C., Machida, K., Noi, K., Murakawa, T., Okumura, M., Ogura, T., *et al.* (2021) Distinct roles and actions of protein disulfide isomerase family enzymes in catalysis of nascent-chain disulfide bond formation. *iScience* **24**, 102296
38. Yim, S. H., Everley, R. A., Schildberg, F. A., Lee, S. G., Orsi, A., Barbati, Z. R., *et al.* (2018) Role of selenof as a gatekeeper of secreted disulfide-rich glycoproteins. *Cell Rep.* **23**, 1387–1398
39. Hildenbrand, K., Aschenbrenner, I., Franke, F. C., Devergne, O., and Feige, M. J. (2022) Biogenesis and engineering of interleukin 12 family cytokines. *Trends Biochem. Sci.* **47**, 936–949
40. Alloza, I., Martens, E., Hawthorne, S., and Vandenbroeck, K. (2004) Cross-linking approach to affinity capture of protein complexes from chaotrope-solubilized cell lysates. *Anal. Biochem.* **324**, 137–142
41. McLaughlin, M., Alloza, I., Quoc, H. P., Scott, C. J., Hirabayashi, Y., and Vandenbroeck, K. (2010) Inhibition of secretion of interleukin (IL)-12/IL-23 family cytokines by 4-trifluoromethyl-celecoxib is coupled to degradation via the endoplasmic reticulum stress protein HERP. *J. Biol. Chem.* **285**, 6960–6969
42. Torres, M., Medinas, D. B., Matamala, J. M., Woehlbier, U., Cornejo, V. H., Solda, T., *et al.* (2015) The protein-disulfide isomerase ERp57 regulates the steady-state levels of the prion protein. *J. Biol. Chem.* **290**, 23631–23645
43. Devergne, O., Birkenbach, M., and Kieff, E. (1997) Epstein-Barr virus-induced gene 3 and the p35 subunit of interleukin 12 form a novel heterodimeric hematopoietin. *Proc. Natl. Acad. Sci. U. S. A.* **94**, 12041–12046
44. Liu, J., Cao, S., Kim, S., Chung, E. Y., Homma, Y., Guan, X., *et al.* (2005) Interleukin-12: an update on its immunological activities, signaling and regulation of gene expression. *Curr. Immunol. Rev.* **1**, 119–137
45. Collison, L. W., Workman, C. J., Kuo, T. T., Boyd, K., Wang, Y., Vignali, K. M., *et al.* (2007) The inhibitory cytokine IL-35 contributes to regulatory T-cell function. *Nature* **450**, 566–569
46. Dambuza, I. M., He, C., Choi, J. K., Yu, C. R., Wang, R., Mattapallil, M. J., *et al.* (2017) IL-12p35 induces expansion of IL-10 and IL-35-expressing regulatory B cells and ameliorates autoimmune disease. *Nat. Commun.* **8**, 719
47. Dixon, K. O., van der Kooij, S. W., Vignali, D. A., and van Kooten, C. (2015) Human tolerogenic dendritic cells produce IL-35 in the absence of other IL-12 family members. *Eur. J. Immunol.* **45**, 1736–1747
48. Sato, Y., Kojima, R., Okumura, M., Hagiwara, M., Masui, S., Maegawa, K., *et al.* (2013) Synergistic cooperation of PDI family members in peroxiredoxin 4-driven oxidative protein folding. *Sci. Rep.* **3**, 2456
49. Robinson, P. J., Kanemura, S., Cao, X., and Bulleid, N. J. (2020) Protein secondary structure determines the temporal relationship between folding and disulfide formation. *J. Biol. Chem.* **295**, 2438–2448
50. Korotkov, K. V., Kumaraswamy, E., Zhou, Y., Hatfield, D. L., and Gladyshev, V. N. (2001) Association between the 15-kDa selenoprotein and UDP-glucose:glycoprotein glucosyltransferase in the endoplasmic reticulum of mammalian cells. *J. Biol. Chem.* **276**, 15330–15336
51. Ferguson, A. D., Labunskyy, V. M., Fomenko, D. E., Araç, D., Chelliah, Y., Amezcua, C. A., *et al.* (2006) NMR structures of the selenoproteins Sep15 and SelM reveal redox activity of a new thioredoxin-like family. *J. Biol. Chem.* **281**, 3536–3543
52. Hoffstrom, B. G., Kaplan, A., Letso, R., Schmid, R. S., Turmel, G. J., Lo, D. C., *et al.* (2010) Inhibitors of protein disulfide isomerase suppress apoptosis induced by misfolded proteins. *Nat. Chem. Biol.* **6**, 900–906
53. Vatolin, S., Phillips, J. G., Jha, B. K., Govindgari, S., Hu, J., Grabowski, D., *et al.* (2016) Novel protein disulfide isomerase inhibitor with anticancer activity in multiple myeloma. *Cancer Res.* **76**, 3340–3350
54. Karatas, E., Raymond, A. A., Leon, C., Dupuy, J. W., Di-Tommaso, S., Senant, N., *et al.* (2021) Hepatocyte proteomes reveal the role of protein disulfide isomerase 4 in alpha 1-antitrypsin deficiency. *JHEP Rep.* **3**, 100297
55. Nödling, A. R., Spear, L. A., Williams, T. L., Luk, L. Y. P., and Tsai, Y. H. (2019) Using genetically incorporated unnatural amino acids to control protein functions in mammalian cells. *Essays Biochem.* **63**, 237–266
56. Mideksa, Y. G., Fottner, M., Braus, S., Weiß, C. A. M., Nguyen, T. A., Meier, S., *et al.* (2020) Site-specific protein labeling with fluorophores as a tool to monitor protein turnover. *Chembiochem* **21**, 1861–1867
57. Meier, F., Brunner, A. D., Koch, S., Koch, H., Lubeck, M., Krause, M., *et al.* (2018) Online parallel accumulation-serial fragmentation (PASEF) with a novel trapped ion mobility mass spectrometer. *Mol. Cell. Proteomics* **17**, 2534–2545
58. Land, H., and Humble, M. S. (2018) YASARA: a tool to obtain structural guidance in biocatalytic investigations. *Methods Mol. Biol.* **1685**, 43–67
59. Krissinel, E., and Henrick, K. (2007) Inference of macromolecular assemblies from crystalline state. *J. Mol. Biol.* **372**, 774–797
60. Pandurangan, A. P., Ochoa-Montano, B., Ascher, D. B., and Blundell, T. L. (2017) SDM: a server for predicting effects of mutations on protein stability. *Nucleic Acids Res.* **45**, W229–w235
61. Rodrigues, C. H., Pires, D. E., and Ascher, D. B. (2018) DynaMut: predicting the impact of mutations on protein conformation, flexibility and stability. *Nucleic Acids Res.* **46**, W350–W355
62. Bloch, Y., Bouchareychas, L., Merceron, R., Skladanowska, K., Van den Bossche, L., Detry, S., *et al.* (2018) Structural activation of pro-inflammatory human cytokine IL-23 by cognate IL-23 receptor enables recruitment of the shared receptor IL-12Rbeta1. *Immunity* **48**, 45–58.e6
63. Schindelin, J., Arganda-Carreras, I., Frise, E., Kaynig, V., Longair, M., Pietzsch, T., *et al.* (2012) Fiji: an open-source platform for biological-image analysis. *Nat. Methods* **9**, 676–682
64. Tyanova, S., Temu, T., Sinitcyn, P., Carlson, A., Hein, M. Y., Geiger, T., *et al.* (2016) The Perseus computational platform for comprehensive analysis of (prote)omics data. *Nat. Methods* **13**, 731–740
65. Ashburner, M., Ball, C. A., Blake, J. A., Botstein, D., Butler, H., Cherry, J. M., *et al.* (2000) Gene ontology: tool for the unification of biology. The Gene Ontology Consortium. *Nat. Genet.* **25**, 25–29
66. Vizcaíno, J. A., Csordas, A., del-Toro, N., Dianes, J. A., Griss, J., Lavidas, I., *et al.* (2016) 2016 update of the PRIDE database and its related tools. *Nucleic Acids Res.* **44**, D447–456

### 2.3.3 Supplementary material to the manuscript

# A comprehensive set of ER protein disulfide isomerase family members supports the biogenesis of pro-inflammatory interleukin 12 family cytokines

Yonatan G. Mideksa[‡,*], Isabel Aschenbrenner[‡,*], Anja Fux[‡], Dinah Kaylani[‡], Caroline A.M. Weiß[‡], Tuan-Anh Nguyen[‡], Nina C. Bach[‡], Kathrin Lang[‡§], Stephan A. Sieber[‡] and Matthias J. Feige[‡§1]

[‡] Center for Functional Protein Assemblies (CPA), Department of Bioscience, TUM School of Natural Sciences, Technical University of Munich, Germany

[§] Laboratory of Organic Chemistry, ETH Zürich, Zurich, Switzerland

* these authors contributed equally to this work

[1] To whom correspondence may be addressed: Tel: 49-89-28913667; Fax: 49-89-28910698; Email: matthias.feige@tum.de

**Running title: oxidoreductases in IL-12/23 biogenesis**

## – Supplemental Data –

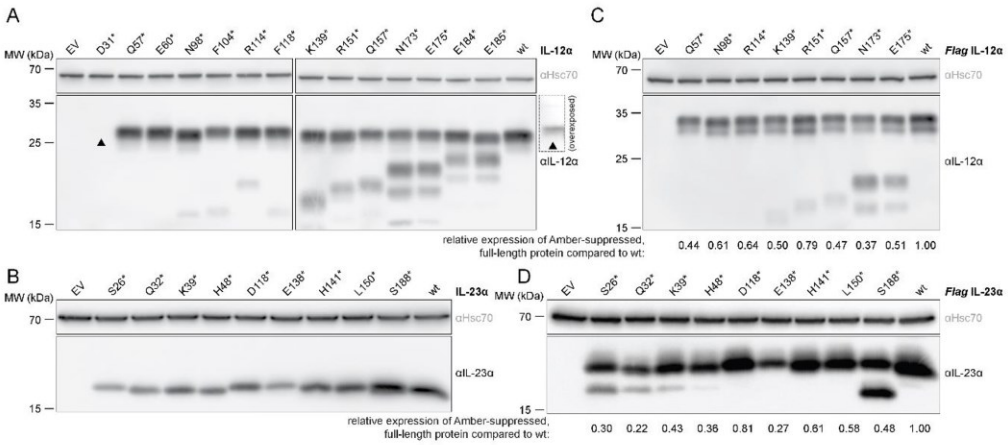


**Fig. S1**: Expression profile of amber stop codon-replaced constructs.

A, B) Representative immunoblots comparing expression levels of untagged, amber stop codon-mutated IL-12α and IL-23α constructs described in Fig. 1, *D* and *E* versus wild-type (wt) protein in the presence of DiazK. The competition of amber codon decoding with intrinsic eRF1 yields lower molecular weight truncated products.

C, D) Same as in A and B, but with C-terminally FLAG-tagged constructs. Introduction of a FLAG-tag causes the observed double band pattern. Truncated protein species for FLAG-immunoprecipitated IL-12α/IL-23α likely originate from homo-dimerization as previously reported (27). Quantification of full-length protein resulting from Amber suppression is shown below the blots. Signals were normalized to the wt signal, which was set to 1.

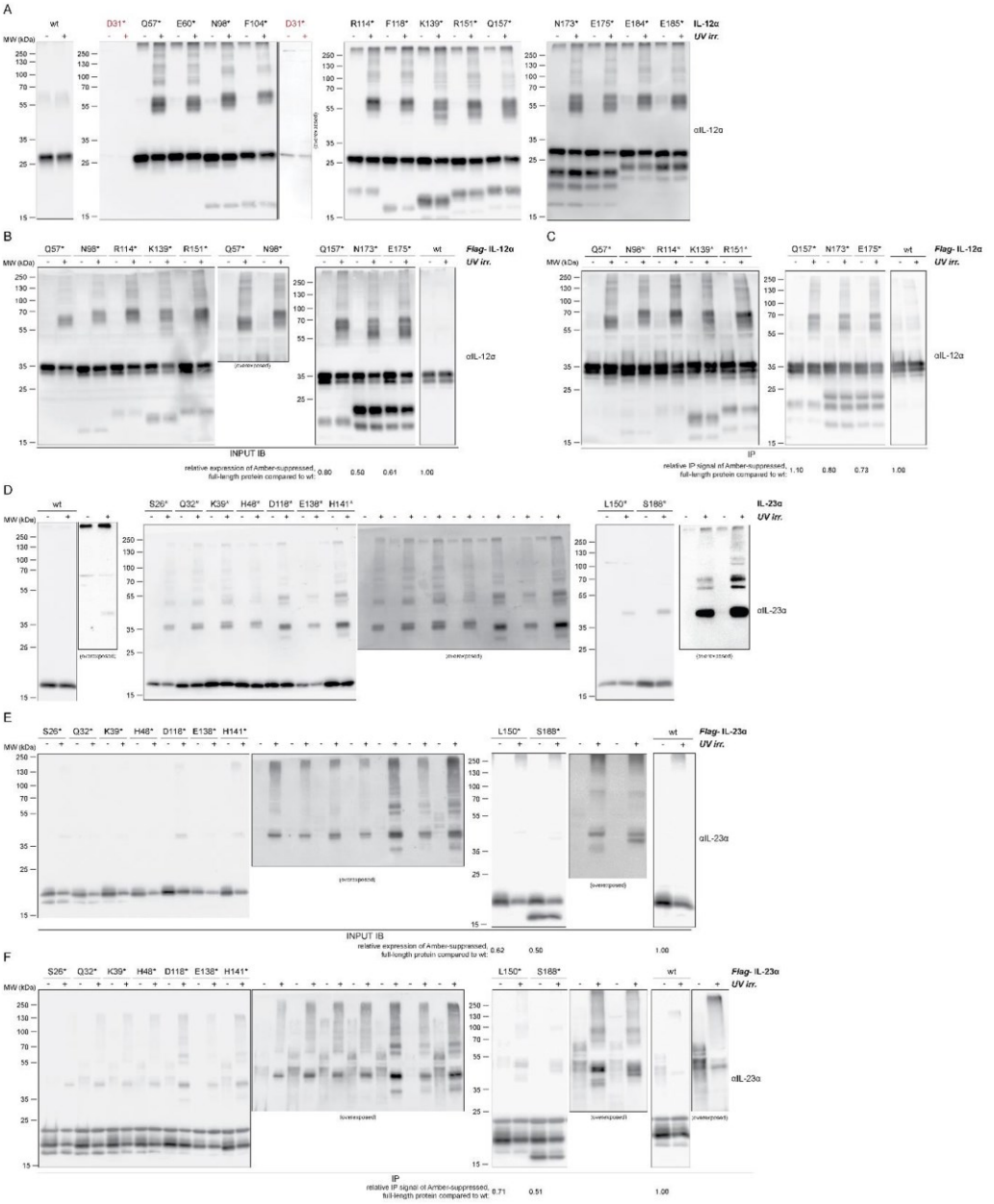

**Fig. S2**: Photoactivation of DiazK at different positions within IL-12α or IL-23α generates protein-protein adducts to varying degrees.

A-F) Same as in Fig. 2*A-D* tested for the remaining positions of IL-12α or IL-23α before and after immunoprecipitation with anti-FLAG beads. For better comparison, input and

IP blots of wt IL-12α as well as the Q57* mutant shown in SI2B and SI2C are the same as shown in Fig. 2*A* and 2*B*.Truncated protein species for FLAG-immunoprecipitated IL-12α/IL-23α likely originate from homo-dimerization as previously reported (27).

B, E) Quantification of full-length protein resulting from Amber suppression is shown below the blots. Signals were normalized to the wild-type signal, which was set to 1.

C, F) Quantification of full-length protein resulting from Amber suppression, which was immunoprecipitated by FLAG-IP is shown below the respective blots. Signals were normalized to wt signal, which was set to 1. Quantifications are only shown for samples from the same immunoblot.

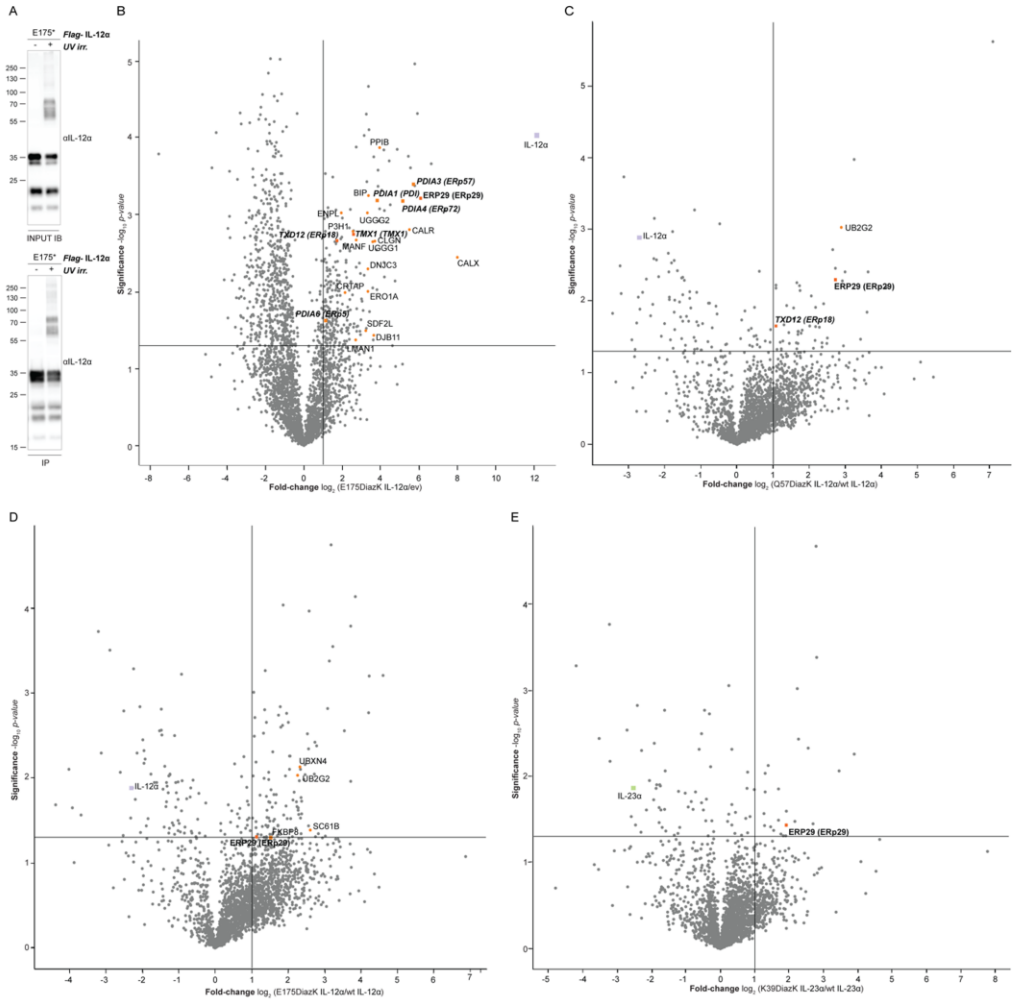


**Fig. S3**: Cellular protein disulfide isomerase (PDI) targets enriched upon photo-crosslinking expand the detectable chaperone repertoire for pro-inflammatory IL-12 cytokines.

A) Immunoblot verification of UV-crosslinked complexes before and after immunoprecipitation (IP) with FLAG beads as in Fig. 2*A* and *B*.

B) Volcano plots, as in Fig. 2*E*, derived from LC-MS/MS analysis of the indicated IL-12α construct compared to control FLAG co-IPs using cells transfected with empty vector (ev), carried out in three replicates.

C-E) Volcano plots as in Fig. 2*E* and *F* compared to wt, without UAA, co-IPs revealing interactions enriched upon photo-crosslinking. The un-/modified α-subunits were all expressed in the presence of DiazK followed by UV-irradiation.

B-E) The top-right quadrants list significant hits with cut-off values defined as $\log_2 = 1$ (2-fold enrichment) and $-\log_{10}$ (*p-value*) of 1.3 ($p<0.05$). ER chaperones and quality control proteins are depicted as orange circles. Those with a possible additional PDI molecular function are shown as orange squares and labeled in bold. Hits were labeled with respective UniProt entry names and for possible PDIs, protein names are additionally given in brackets. IL-12α and IL-23α are shown in violet or green, respectively.

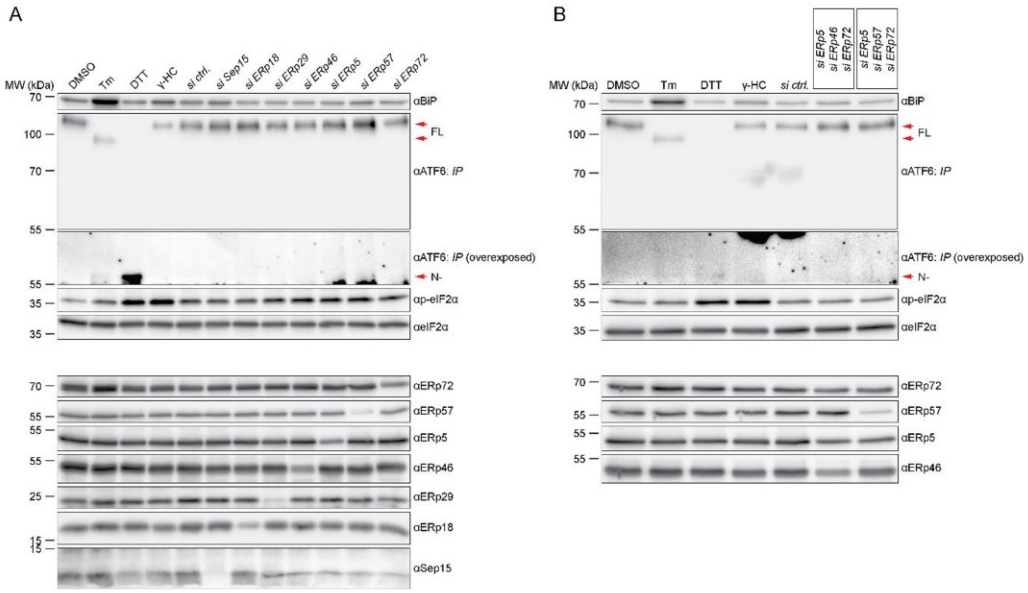


**Fig. S4:** Investigation of unfolded protein response (UPR) induction upon PDI depletion.

A, B) Representative blots of ER stress markers from UPR branches in individual (A) and combined (B) RNAi treated samples compared to chemical (Tm, Tunicamycin or DTT, Dithiothreitol) or protein (IgG, gamma (γ)-HC) positive controls as well as DMSO negative control; FL – full length, N- – N-terminal cleavage. All knockdowns were verified in immunoblots as shown below with antibodies against specific PDIs.

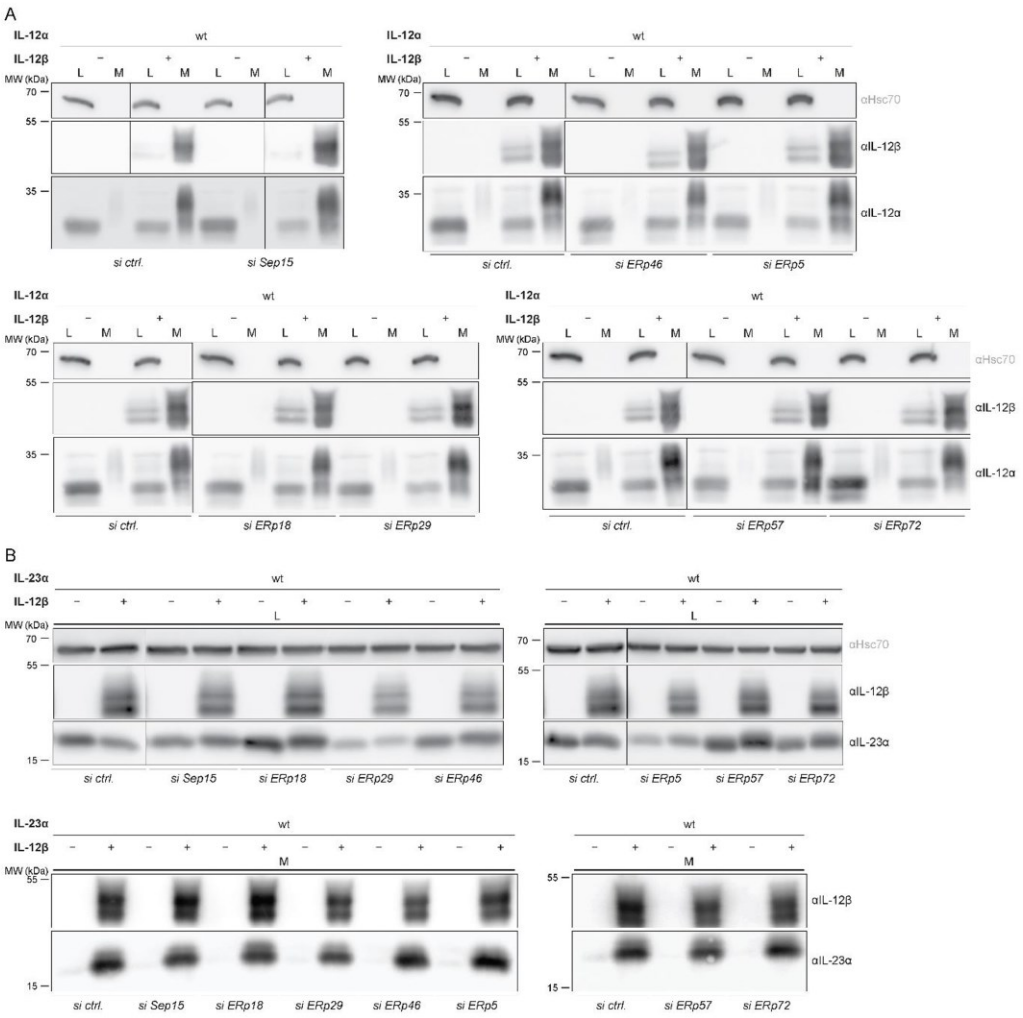


**Fig. S5:** Changes in secretion and assembly status of IL-12 pro-inflammatory cytokines after treatment of cells with relevant PDI siRNAs.

A, B) Secretion behavior of pro-inflammatory IL-12 cytokines in HEK-293T cells was examined where the respective PDI siRNAs were present relative to control siRNA (*si ctrl*). Samples were processed for detection of each of the IL subunits in lysates (L) and medium (M). Hsc70 served as loading control.

### 2.3.4 Permission to reprint the manuscript

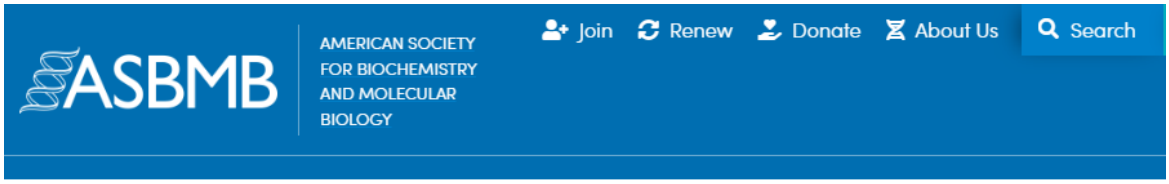


Home > Journals and news > Editorial Policies

# Copyright and license to publish

The text below explains the process for reusing content that was originally published in an ASBMB journal. If you want to reuse previously published content in a new submission to an ASBMB journal and need guidance regarding permissions, please click here.

## For authors:

Effective with initial submissions from January 1, 2018, authors must agree that if their manuscript is accepted, they will grant ASBMB an exclusive, irrevocable License to Publish their work; the copyright remains with the authors.

For an example of a License to Publish, click here.

Manuscripts initially submitted prior to January 1, 2018 are subject to ASBMB's former policy whereby, as a condition of publication, authors transfer copyright to ASBMB upon acceptance.

Authors of manuscripts, submitted at any time, need not contact the journal to request permission to reuse their own material. Authors are allowed to do the following:

1. to use all or part of the work in compilations or other publications of the Authors' own commercial and noncommercial works (includes theses/dissertations), to use figures, photos, and tables created by them and contained in the work, to present the work orally in its entirety, and to make copies of all or part of the work for the Authors' use for lectures, classroom instruction or similar uses. If the author is employed by an academic institution, that institution also may reproduce the article for teaching purposes.
2. to post the accepted manuscript version of the work, the "Paper in Press," on the author's personal web page, their personal or institutional repository, or their funding body's archive or designated noncommercial repository, provided that a link to the article on the journal site is included.
3. to post a manuscript version of the work on not-for-profit preprint servers provided that the Authors retain distribution rights to the work, that ASBMB formatted final files are not posted, and that a link to the article on the journal site is included.
4. to post the final edited PDFs, created by ASBMB, to their own departmental/university websites, provided that the posting does not happen until 12 months after publication of the work, and that a link to the article on the journal site is included.

Reuse of JBC content must include the following: This research was originally published in the Journal of Biological Chemistry. Author(s). Title. J Biol Chem. Year; Vol:pp-pp. © the American Society for Biochemistry and Molecular Biology *or* © the Author(s).

# 3 Discussion and outlook

In this dissertation, the multifaceted and multilayered cellular mechanisms of interleukin biogenesis in the ER were examined. Comprising all IL-12 family members, analyses were performed based on the molecular and structural characteristics, often involving also evolutionary analyses. Light was shed on the role of intramolecular disulfide bond formation and glycosylation for ERQC and signaling, general IL construction principles, key residues for an α:β interface, the chaperone repertoire and its functions in α-subunit biogenesis as well as the role of autonomous α-subunit folding for IL assembly.

The first study covered the biogenesis of IL-27α and assembly of heterodimeric IL-27 throughout species, and a mutagenesis-validated molecular docking to reveal the structural composition of the human IL-27 α:β interface (Figure 12).

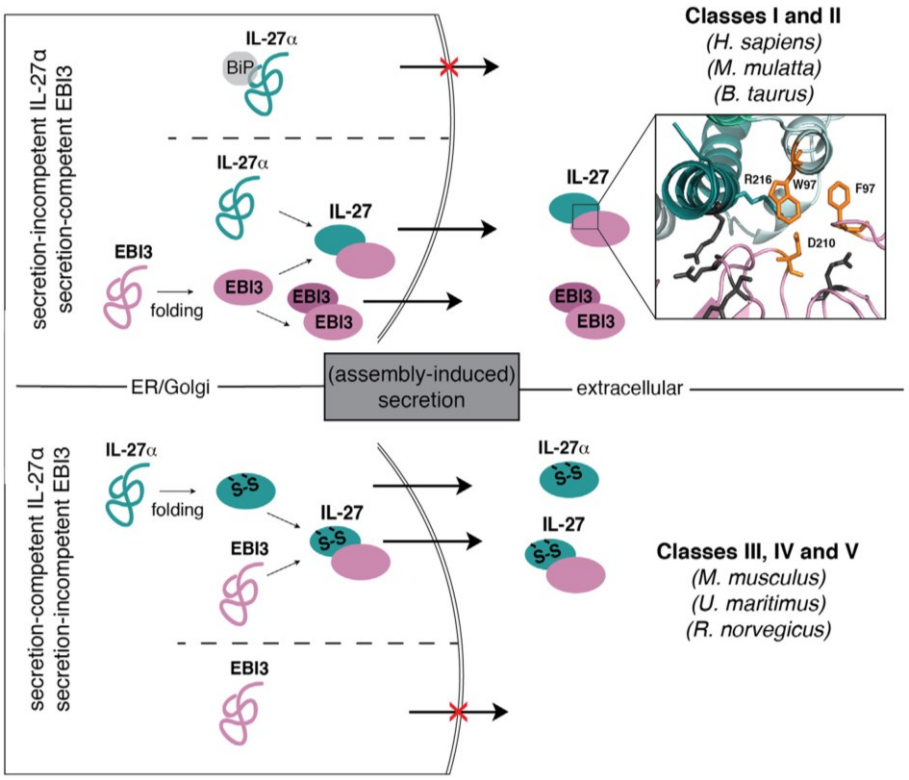


**Figure 12. Model for IL-27 biogenesis taken from the study of Müller, Aschenbrenner, et al. [250].** The common IL-27 construction principle of pairing of a secretion-incompetent subunit with a secretion-competent subunit is conserved throughout species. For IL-27α, disulfide bond formation (S-S) determines folding and secretion, after passing the ER quality control. BiP binding to unfolded human IL-27α, lacking the disulfide bridge, leads to subunit retention in the cell [121]. Secretion-competent human EBI3 can form homodimers. The human IL-27 heterodimerization interface (box) with key residues, shown as orange sticks, was determined by mutagenesis-guided molecular docking.

First uncovered for human IL-27α, a single amino acid switch rendered this cytokine subunit secretion-competent [121]. For IL-27α, we could show that intramolecular disulfide bond formation is the conserved structural basis that determines its secretion-competency throughout species. By a sequence alignment of IL-27α from 15 different species and

subsequent classification based on the number and position of cysteine residues, we experimentally confirmed the evolutionary conserved relation between cysteines and secretion-competency for IL-27α of representative species. Two or more adequately located cysteines qualified the subunit to fold autonomously by intramolecular disulfide bond formation, whereas none or a single cysteine made IL-27α folding-dependent on EBI3. In humans, IL-27α is retained in the cell by BiP binding to exposed hydrophobic regions [121]. As BiP plays essential roles in Ig assembly [49, 52, 65, 251] and thus should be highly conserved among mammals, it would be also of interest to confirm the molecular reason for ER retention *versus* secretion throughout species. If this chaperone interaction turns out to be conserved, BiP interaction with exposed hydrophobic stretches should be concomitantly diminished for secretion-competent IL-27α of other species, whereas cellular retention of IL-27α lacking an intramolecular disulfide should be mediated by BiP.

For human IL-12 family members, the α-subunit relies on the β-subunit for secretion [132]. The conservation of this construction principle, that one secretion-competent pairs with one secretion-incompetent subunit, was confirmed for IL-27 of different species. This provides a layer of cellular regulation on cytokine subunit assembly and secretion, but also confines the cytokine repertoire acting in the immune system, as only one IL-27 subunit can possibly signal independently as cytokine or antagonize heterodimer functions. For humans, EBI3 functions independent from its pairing partner IL-27α were reported [116, 226], and also murine IL-30 expands cytokine functions of heterodimeric IL-12 family members in mice [187, 249]. One known exception to this rule is the murine IL-23 heterodimer for which secretion of both subunits, IL-23α and IL-12β, in isolation was revealed [173]. Nevertheless, secretion levels especially of murine IL-23α seem to be increased by IL-12β co-expression. From an evolutionary point of view, it is intriguing that the coevolution of subunits with such composite natures is not a prerequisite for a subunit to have the ability to induce folding of the pairing partner. This was verified by co-expression of IL-27 α- and β-subunits from different species, both being secretion-incompetent in isolation, which led to secretion of both. Maybe not that obvious, as human EBI3 can be secreted on its own albeit rather inefficiently [124], but mutual induction of secretion was also revealed for human IL-35 subunits IL-12α and EBI3 (data not shown) despite of IL-12α misfolding in isolation [78]. Since the IL-27 structure has been a longstanding puzzle, we approached the human IL-27 interface by mutagenesis-validated molecular docking (Figure 12, box). IL-27 does not only differ from IL-12 and IL-23, for which crystal structures have already been solved [136, 142], by its non-covalent binding of IL-27α and EBI3, but also by a slightly differing subunit orientation towards each other. We found human IL-27 α:β interface disruption by IL-27α$^{W97R}$, EBI3$^{F97R}$, and EBI3$^{D210R}$ mutants, but could not detect other previously stated

residues as critical, possibly due to differences in assays or subunit species used [146, 160]. Human EBI3 could induce secretion of all tested assembly-dependent IL-27α species, suggesting an inter-species conservation of IL-27 interface residues. This comprehensive structural analysis contributed to a better characterization of site 1 interactions in IL-27 and opened up possibilities to covalently link the IL-27 subunits for structure determination or therapeutic applications. Approaches to engineer a biologically active, disulfide bridged IL-27 (IL-27α$^{G235C}$ + EBI3$^{E159C}$) were successful but not further pursued due to sample inhomogeneity with only 70% dimeric species (data not shown). Nevertheless, lack of an intermolecular disulfide bond was unlikely the only reason why IL-27 is more challenging to produce [252], as the crystal structure of human IL-27 was successfully resolved in 2022 by utilizing the antigen-binding fragment (Fab) of the neutralizing monoclonal antibody SRF388 [133]. When comparing our refined model with this solved structure (Figure 13), in both heterodimer structures site 1 interactions mainly involve the AB-loop, which forms a short α-helical motif, of IL-27α packing against EBI3. Interactions of a positively charged dipole of IL-27α with a negatively charged patch of EBI3 are complemented by aromatic stacking contacts involving IL-27α$^{W97}$, IL-27α$^{F94}$, and EBI3$^{F97}$. The hydrophobic nature of interface surfaces for IL-27α and EBI3 conforms with the dependence of subunit interaction for efficient secretion, which we could assess in this study in more detail [124, 148].

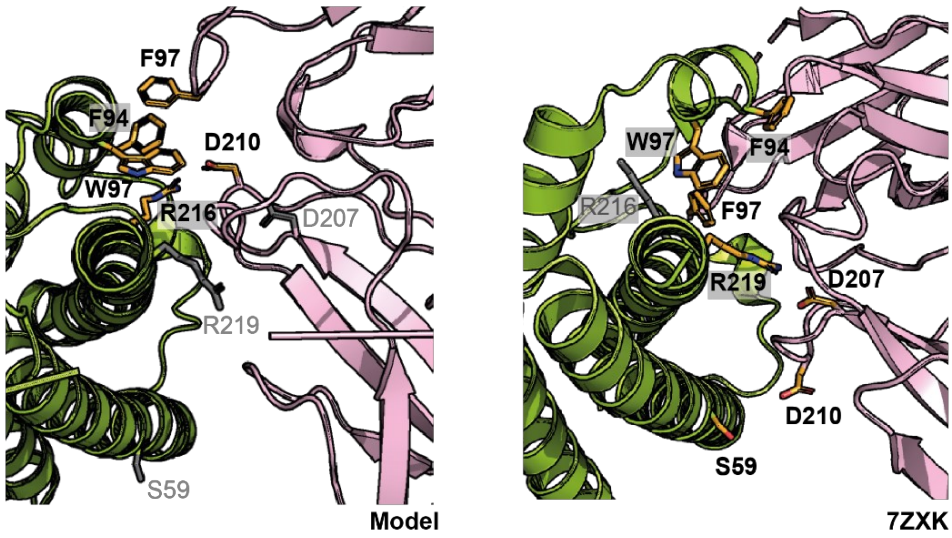


**Figure 13. Comparison of human IL-27 site 1 interactions in our model and the recently resolved crystal structure (PDB: 7ZXK).** Left: Mutagenesis-guided and -validated interface residues were used as basis for a molecular dynamics simulation and molecular docking to obtain the IL-27 heterodimer model [250]. Interface residues are depicted as orange sticks and labeled in bold. Besides aromatic residue interactions, a salt bridge between IL-27α Arg216 and EBI3 Asp210 was predicted. Amino acid residues that were involved in interface interactions according to the crystal structure [133] are shown as gray sticks and are labeled in gray. Right: Crystal structure of IL-27 with key interacting residues for site 1 (orange sticks, labeled in bold) and not directly involved residues that were of importance in the modeled structure (gray). In contrast to the modeled structure, EBI3 Asp210 is involved in a water-mediated interaction with IL-27α Ser59, whereas EBI3 Asp207 and IL-27α Arg219 form a charge interaction. Amino acids are numbered including the ER import sequence.

A structural deviation of the crystal structure from our model, illustrated in Figure 13, can be localized to the charged interaction of IL-27α Arg216 and EBI3 Asp210, which do not directly interact according to the crystal structure [133]. IL-27α Arg216 seems negligible for site 1 interactions, and EBI3 Asp210 is involved in a water-mediated interaction with IL-27α Ser59, explaining its rather outward-facing orientation compared to our modelled structure. Nevertheless, this serine residue is reported to be affected by polymorphisms of human IL-27α, so that the exchange to an alanine residue might negatively affect cytokine stability in nature [133]. In agreement with the cryo-EM structure of the human IL-27 quaternary complex, a salt bridge stabilizing the α:β interface is mediated by IL-27α Arg219 and EBI3 D207 [148], which were not positioned correctly to really interact in our model.

Lastly, by co-IP we could show that human EBI3 forms homodimers in the cell and in the medium. This aspect might be of importance as the cognate IL-12β shows similar behavior in absence of its α-subunit, IL-12α or IL-23α [129, 177], even though functionalities mediated by monomeric *versus* homodimeric IL-12β are not comprehensively explored for humans. Likewise, for IL-35 it was reported by Hildenbrand et al. that IL-35 subunits, IL-12α and EBI3, are not necessarily secreted as heterodimeric proteins and act independently (manuscript in revision). Also the receptor chain repertoire for this special cytokine extends to many possible combinations [110], possibly also including a receptor dimer which responds to EBI3 homodimers. Despite of secretion of the human IL-27 β-subunit, the molecular mechanisms of EBI3 retention, e.g., in mice, remain unexplored. Secretion-competency would argue for negligible or transient chaperone binding, like for CNX which is involved in folding of the *N*-glycosylated human EBI3 [163, 253]. And despite of two disulfide bonds in the N-terminal FnIII domain of the human subunit, no free cysteine could act as ER chaperone handle. Further exploration of the relevance of homodimerization, maybe to mask the rather hydrophobic interface else buried by IL-27α to pass ERQC[148], or a comparative study of chaperone binding of human *versus* murine EBI3 would help to investigate secretion *versus* retention, respectively. These insights, together with the rationally engineered, secretion-competent IL-27α [121], would allow to create a fully human-like mouse model concerning the IL-27 system and to study cytokine functions and pathologies.

The second study presented within this dissertation allowed us to characterize glycosylation of the human IL-12 family and its impact on biogenesis and function (Figure 14)

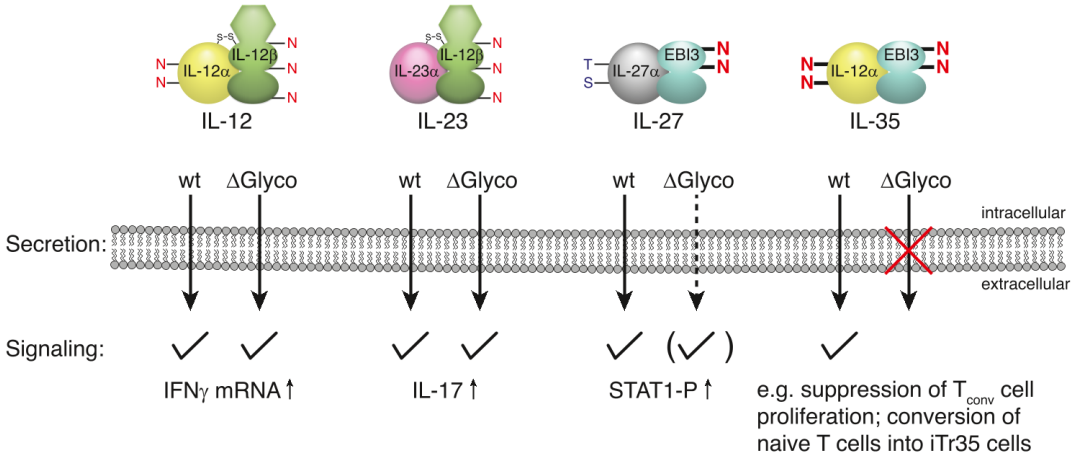


**Figure 14. Schematic illustration of the impact of glycosylation on the human IL-12 family taken from the study of Bohnacker, Hildenbrand, Aschenbrenner, et al. [253].** At least one subunit of the heterodimeric IL-12 family members is glycosylated (red, *N*-glycosylation; blue, *O*-glycosylation). Secretion and biological functions of IL-12 and IL-23 are not affected if glycosylation is absent (ΔGlyco), whereas secretion and signaling are both decreased in case of lacking glycosylation of heterodimeric IL-27. Only for IL-35, secretion strongly depends on subunit glycosylation, as lacking sugar moieties result in complete cellular retention.

Previous studies only incompletely described glycosylation for IL-12 family cytokines [153-155, 161], even though *N*-linked glycosylation of secretory proteins is one of the most prevalent modifications undertaken in the ER [12]. In this study, enzymatic treatment and mutagenesis-based analyses allowed us to identify new glycosylation sites within IL-12 family members. Surprisingly, the impact of glycosylation on the biogenesis and signaling of the investigated cytokines was very diverse, varying from no effect for IL-12 and IL-23 to diminished secretion/function for IL-27 to complete cellular retention in the case of IL-35. Generally, it could be observed that whenever lacking glycosylation impairs β-subunit secretion, as for EBI3, it also negatively affects heterodimer biogenesis and secretion. Thus, IL-27 secretion was significantly reduced, and IL-35 secretion was abrogated. This can be attributed to assembly-dependent folding and secretion of human α-subunits [124, 159]. However, that non-glycosylated IL-27 is secreted at all, is quite interesting. EBI3 lacking both *N*-glycans cannot pass ERQC and is retained in the cell in isolation, whereas co-expression of non-glycosylated IL-27α, which depends on EBI3 for secretion, results in co-secretion. This implies subunit interaction, which then allows mutually enhanced secretion of both subunits. Similarly, in an inter-species analysis the pairing of two secretion-incompetent IL-27 subunits from different species resulted in induction of secretion [250]. This might be explained by partial subunit folding even when the subunit is secretion-incompetent and exposes structural features, which are recognized by the ERQC and prevent it to further traverse the secretory pathway in isolation. To explain impaired IL-27 signaling, measured by STAT1 phosphorylation of the BL-2 immune cell line, from a

structural perspective, one can analyze the orientation and possible interactions of glycans with receptor chains based on the recently resolved quaternary IL-27 receptor complex structure (Figure 15) [148]. Focusing on EBI3, as non-glycosylated EBI3 results in decreased receptor binding, Asn55 is peripheral to receptor chains, whereas Asn105 is facing towards the N-terminal domain of gp130 (site 3). This might be a structural explanation why IL-27 signaling is reduced and would speak for a supportive role of the Asn105-linked glycosylation in gp130 D1 packing against the top of EBI3 D1. This is further underscored by the findings of Caveney et al., that EBI3 Phe118 is the center of this site 3 interface of EBI3, which is located right next to the Asn105 residue. Nevertheless, which role this Asn105-linked glycosylation has on EBI3 biogenesis, remains open.

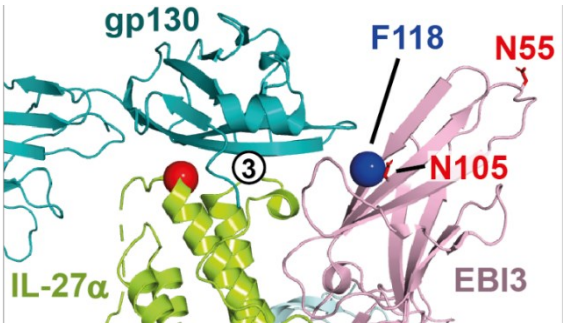


**Figure 15. Structure of the quaternary IL-27 receptor complex reveals orientation of *N*-glycosylation sites.** Site 3 interactions (circled number) are mediated by IL-27α (lime), EBI3 (light pink), and gp130 (teal) (PDB: 7U7N). According to Caveney et al. [148], EBI3 Phe118 (blue sphere) is a central residue of the contact site between gp130 and the β-subunit. The *N*-glycosylation sites of EBI3 are represented as red sticks, with Asn55 located rather at the periphery and Asn105 located right next to Phe118, facing the receptor chain gp130.

With this study, the differences between IL-12β and EBI3 again become clear: IL-12β is efficiently secreted, even in excess over IL-12/IL-23 [162], its stability is irrespective of glycosylation, and it can be easily produced and purified from medium of transfected mammalian cells [79]. In contrast, EBI3 is rather inefficiently secreted, its stability is severely affected by loss of glycosylation, and its purification is challenging, even as heterodimeric IL-27 or IL-35. Especially for IL-35, whose biogenesis most strongly depends on glycosylation, a possible compensation when stabilizing glycan-modifications are lacking could be a covalent intersubunit disulfide bridge, as for IL-12 and IL-23 [78, 79, 136]. If this would allow IL-35 secretion without glycosylation, the impact of glycosylation on receptor interaction and signaling could be assessed. At the same time, one could extend this study by exploring the impact of glycosylation on IL-12 and IL-23 with their intermolecular disulfide bridge between α- and β-subunit being removed by cysteine to serine mutation. Taken together, this study extends our understanding on the influence of the modification glycosylation on IL biogenesis and allows us to selectively remove individual IL-12 cytokines from the organism's repertoire despite of subunit sharing among IL-12 family members. Especially in the context of cancer, targeting of the immunosuppressive IL-35 is a promising strategy for future immunotherapies [254-256].

The third study allowed us to comprehensively assess the chaperone repertoire acting on IL-12 and IL-23 α-subunits and the role of PDIs in their biogenesis (Figure 16).

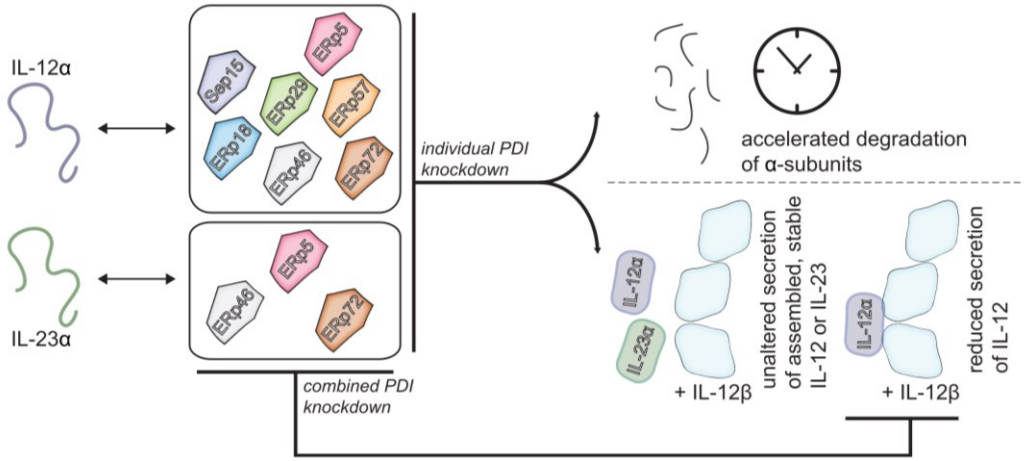


**Figure 16. Model for the role of PDIs in α-subunit biogenesis taken from the study of Mideksa, Aschenbrenner, et al. [257].** IL-12α and IL-23α both interact with overlapping, but also distinct PDI family members, which prevent ER exit of immature cytokine subunits and stabilize subunits to prevent premature degradation by ERAD. Knockdown of individual chaperones led to accelerated degradation of α-subunits if unassembled but did not impair heterodimerization with IL-12β and subsequent secretion of IL-12 or IL-23. Only a combined PDI knockdown reduced secretion of IL-12, but not of IL-23.

A site-specific photocrosslinking approach based on introducing the unnatural amino acid DiazK into IL-12α and IL-23α by amber suppression, allowed us to reveal (transiently) interacting ER-resident chaperones by MS and immunoblotting. With the focus on PDI family members, we could detect PDIs acting on both α-subunits, but also PDIs binding specifically to one of the subunits. As both IL-12α and IL-23α rely on oxidative folding [78, 79], containing seven or five cysteine residues, respectively, significant co-IP and MS hits for interacting PDIs were expected. ERp72, ERp5, and ERp46 interacted with both α-subunits. ERp72 is less well-characterized, whereas for ERp5 its interaction with BiP clients [81] and for ERp46 its role in early protein folding [258] is known. Specific interactors of IL-12α were Sep15, ERp18, non-covalently binding ERp29, and ERp57, the latter acting as prominent oxidoreductase for glycoproteins (like IL-12α, but not IL-23α; see Figure 14), as it gets recruited by lectin chaperones [31, 75].

We could confirm their stabilizing effect on unfolded α-subunits by siRNA-mediated knockdown, which resulted in higher protein turnover rates. We could also show that single PDI knockdown did not affect ERQC of the α-subunits. Instead, both subunits behaved like their wildtype and were not secreted, indicating that none of the tested PDIs is exclusively involved in α-subunit cell retention. For IL-23α, the study of Meier et al. highlighted the role of BiP and ERp44 in recognition of the unpaired subunit [79] and for IL-12α, interactions with lectin chaperone CRT, BiP cochaperone ERdj5, and the ER stress protein HERP were detected [78, 151, 259]. These other interactors point towards an even more complex

ERQC process, exceeding PDI family members. Nevertheless, as nearly every interacting PDI family member, except of ERp46 for IL-12α, showed client protein stabilization, a mutual compensation in this function seems unlikely. This can be underlined by the specificity of different PDIs for distinct cysteine residues in IL-12α/IL-23α. Hence, those oxidoreductases might be involved in interaction with different folding intermediates of the α-subunits, maybe occurring in a sequential order. This would explain why not only one PDI, but a whole repertoire of chaperones is required for α-subunit biogenesis. The rescue by the cognate β-subunit, IL-12β, is an efficient process and not influenced by individual PDIs. IL-12β acts as folding matrix for both IL-12α and IL-23α [152, 157]. How this IL-12β-mediated rescue and complete folding is induced by only likely weak engagement with the partially folded α-subunit in the IL interface remains poorly understood. Only for IL-12, a combined PDI depletion of three representatives impaired heterodimer secretion by 20%. The reason for these differences between IL-12 and IL-23 heterodimer biogenesis might lie in IL-12α and IL-23α: IL-12α is a rather sophisticated chaperone client protein, as it has two *N*-glycosylation sites and several cysteines, which need to correctly form three intramolecular disulfides [78, 253]. In contrast, non-glycosylated IL-23α only needs to form one intramolecular disulfide bond [79, 253], which seems rather independent of chaperoning, as ERp5 only shows binding preference for the two free cysteines and the cysteine for the bridge to IL-12β. In summary, a comprehensive PDI chaperone repertoire caters for IL-12α and IL-23α biogenesis, possibly allowing intervention in the assembly process of one specific IL, based on distinct chaperone interactions. Further experimental investigation in endogenous IL-producing immune cells is needed to confirm this chaperone-dependency of IL-12 family α-subunits.

The reason why chaperones are required even if IL-12β acts as folding matrix for IL-12α and IL-23α is still unknown. It also remains open which characteristics or factors determine whether IL-12 or IL-23, relying on the same β-subunit, is assembled within the cell. To address these remaining questions, we conducted a fourth study (see Appendix: II. Assembly-dependent structure formation determines the human interleukin-12/interleukin-23 secretion ratio). Here we utilized rational engineering of IL-23α to design an autonomously folding-competent α-subunit, which allowed us to assess the tight regulation of IL-12 *versus* IL-23 secretion in cells expressing subunits for both IL-12 family members. This IL-23α variant proved to be not only structurally stabilized by introduction of an extra intramolecular disulfide bridge, but also secretion-competent in isolation. We could show that this cytokine subunit interacts significantly less with ER chaperones, including BiP and PDI family members, compared to the wildtype. Heterodimerization with its partner subunit was affected in that way, that structural stabilization of our so-called IL-23α$^{stabilized}$ mutant

even strengthened β-subunit interaction. The assembled IL-23$^{stabilized}$ proved to be signaling-competent, whereas the single α-subunit showed no independent signaling. However, we could show that this engineered subunit significantly influences the human IL-23/IL-12 secretion ratio by its assembly-independent structure formation. Taken together, this study provides insights into how IL-12β might distinguish between its pairing partners IL-12α and IL-23α, which has a fundamental impact on the diverging immunity mediated by cytokine secretion: IL-12 signaling results in naïve T lymphocyte differentiation to the pro-inflammatory, IFNγ-secreting Th1 subset, whereas IL-23 induces the highly pro-inflammatory, IL-17-producing Th17 cell type [108, 112, 157, 198].

With these studies we covered not only the impact of regulating modifications, like disulfide bonds or glycosylation, but also of α-subunits' chaperone-dependency and folding-competency on IL-12 family cytokine biogenesis and assembly. Besides these molecular insights into IL-12 family biogenesis, the biological functionalities of the family members are also of high interest. IL-12 cytokines act as regulators of inflammation, can recruit, activate, or dampen immune signaling, and regulate immune cell proliferation and differentiation. Therefore, they are attractive therapeutic targets or represent potential therapeutics in a variety of pathologies. As a short outlook, I here want to summarize some advances in cytokine engineering for cancer immunotherapy, as I also could contribute to two translational IL-12-related projects during my doctoral studies.

The IL-12 family members all have their roles in cancer [120, 256, 260, 261], but IL-12 is of special interest for the treatment of solid tumors due to its cytotoxic effects mediated by IFNγ-producing Th1 and CD8+ T cells and potent inhibition of angiogenesis [108, 262]. In fact, a key protective role of IL-12 could be shown by mice lacking IL-12 or its receptor, which led to a higher chance of tumor development [112]. Nevertheless, severe drawbacks on the way towards IL-12 application as anti-cancer drug were the deaths of two patients, because of cytokine storm after its intravenous administration, and toxic adverse effects with accompanying disappointing responses in a phase I and II clinical trial in the mid-1990s [263, 264]. Even though subcutaneous IL-12 injection was well tolerated, no tumor response could be observed with this type of application [265, 266]. The need for targeted, non-toxic therapies to reach high local IL-12 concentrations in the tumor but concurrently prevent lethal, systemic side effects resulted in the development of novel strategies [267, 268]. One approach are immunocytokines. Targeting moieties like antibody fragments fused to IL-12 should allow specific delivery to the tumor. In case of NHS-IL12, two single chain IL-12 molecules were fused to the human IgG1 NHS76 antibody, which recognizes DNA/histone complexes in necrotic tumor portions [269]. Improved targeting and a longer half-life of this immunocytokine, compared to recombinant IL-12, resulted in a more robust T cell-driven

immune response. Synergistic effects with other immune-based therapeutics, like the anti-PD-L1 monoclonal antibody Avelumab, are now being assessed in clinical trials [270, 271]. Other approaches are plasmid-based delivery of IL-12, e.g., by intratumoral injection of naked plasmids and electroporation or as lipopolymer-DNA complex, mRNA-based delivery, or virus-based delivery for gene therapy [152, 268]. To prevent adverse effects by systemic IL-12 dissemination a layer of regulation was added by anchoring of IL-12 to the tumor surface or transcriptional regulation of IL-12 expression [272, 273].

To utilize the patient's own cellular immune system to recognize and defeat cancer, adoptive T cell transfer has been widely investigated. By anchoring IL-12 to the cell surface of engineered lymphocytes, a strategy to target tumors with increased safety and superior antitumor efficacy compared to systemic IL-12 coadministration could be developed [274, 275]. Nevertheless, such lymphocytes might show effects only in their direct surrounding and penetration of the tumor tissue is unlikely. A hallmark strategy for specific immunotherapies are T cells equipped with a chimeric antigen receptor (CAR). This CAR allows T cells to target tumor surface-associated antigens, commonly by a single-chain variable fragment, and get activated by an intracellular CD3ζ and co-stimulation domains, independent of endogenous TCR interactions [267]. Local IL-12 administration seems to be an effective adjuvant in CAR T cell therapy, as the highly suppressive tumor microenvironment leads to CAR T cell dysfunction and can be overcome by the stimulating, pro-inflammatory cytokine [276]. Moreover, inducible IL-12 expression in CAR T cells represents another advancement. Here, IL-12 expression is dependent on a nuclear factor of activated T cells (NFAT)-responsive promotor which enables IL-12 translation only upon CAR-mediated T cell activation resulting in nuclear translocation of the transcription factor NFAT [277, 278]. The advantage of inducible IL-12 release is prevention of systemic toxicity while still reaching the therapeutically required concentration. This is opposed by the possibility of on-target off-tumor activation of those CAR T cells with severe effects of IL-12-mediated immune reactions on healthy tissue (Figure 17, current approach) [278]. To address this shortcoming and improve safety, we rationally destabilized IL-12, which would further improve such inducible systems (Figure 17, our approach). The rationale behind this destabilization is the preserved on-target functionality but rapid dissociation into its subunits IL-12α and IL-12β at distal sites, which limits the radius of action and therefore reduces systemic side-effects of IL-12.

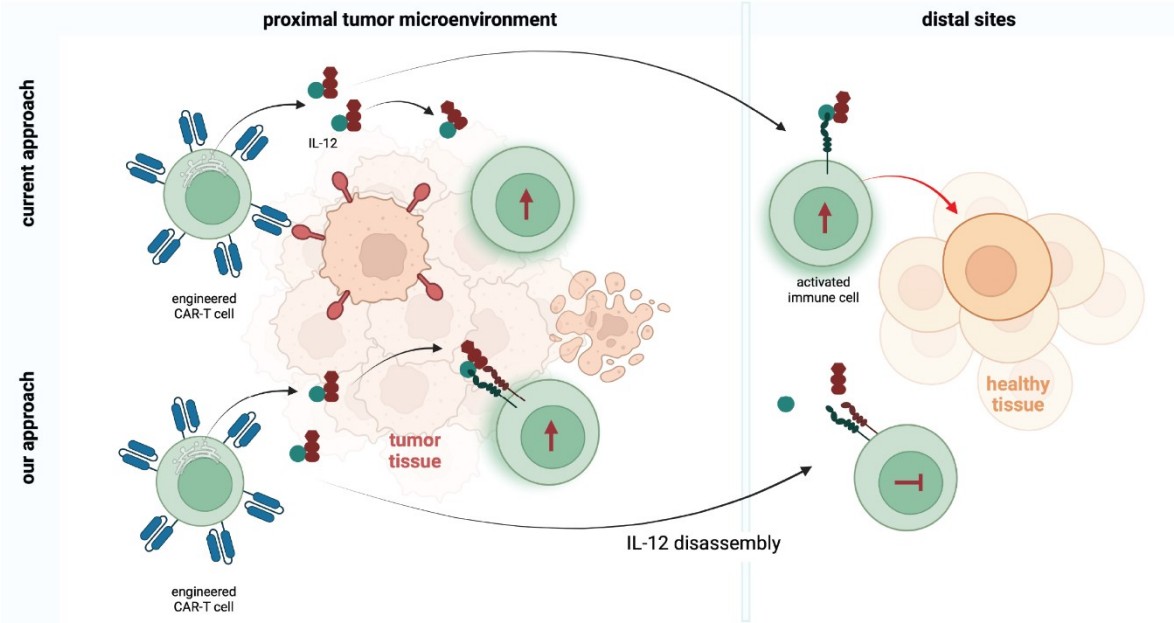


**Figure 17. Self-inactivating IL-12 renders a local tumor therapy possible by reducing systemic side effects.** In contrast to current tumor therapy approaches, our approach allows secretion of self-inactivating IL-12 by engineered chimeric antigen receptor (CAR) T cells in the tumor tissue inducing tumor cell killing by activated immune cells. Once IL-12 diffuses away from the site of action, the heterodimer disassembles into its subunits, thus self-inactivates it. This prevents undesired immune cell activation at distal sites and reduces toxic side effects on healthy tissue.

Interleukin engineering can also directly target cytokine:receptor interactions. Recently, a mutant IL-12 could be engineered for lower receptor affinity. While still showing T cell-mediated antitumor activity, this partial agonist reduced NK cell-mediated IFNγ release, which limits systemic toxicity of IL-12 [170]. The reason for this immunological effect is the constant level of IL-12 receptor on NK cells, whereas receptor expression on T cells is increased upon activation. Using this, we could structurally assess IL-12 receptor binding and engineer attenuated IL-12 variants which preferentially activate T cells and elicit anti-tumor immunity. Interestingly, a similar engineering approach towards a partial agonist acting cell type-specifically was conducted for IL-10 and successfully deconvoluted its pleiotropy [279].

These described immune-engineering approaches are just a selection of manifold strategies to tune cytokine axes for therapeutics. Especially for the heterodimeric IL-12 family, tailor-made cytokines or synthetic subunit combinations might extend the biology of the IL-12 family. Together with the design of synthetic receptors, novel functionalities and bio-orthogonal regulation of lymphocyte functions will be pursued in future research.

Taken together, studies performed during my doctorate expanded our knowledge on which structural characteristics and chaperone interactions determine protein folding, subunit assembly and quality control in the ER. These insights pave the way towards a better understanding of molecular and immunological interrelations and towards novel routes for translational cytokine engineering.

# Bibliography


1. Anfinsen, C.B., et al., *The kinetics of formation of native ribonuclease during oxidation of the reduced polypeptide chain.* Proc Natl Acad Sci U S A, 1961. **47**(9): p. 1309-14.
2. Anfinsen, C.B., *Principles that govern the folding of protein chains.* Science, 1973. **181**(4096): p. 223-30.
3. Levinthal, C., *Are there pathways for protein folding?* J. Chim. Phys., 1968. **65**: p. 44-45.
4. Dill, K.A. and H.S. Chan, *From Levinthal to pathways to funnels.* Nat Struct Biol, 1997. **4**(1): p. 10-9.
5. Dill, K.A. and J.L. MacCallum, *The protein-folding problem, 50 years on.* Science, 2012. **338**(6110): p. 1042-6.
6. Karplus, M., *Behind the folding funnel diagram.* Nat Chem Biol, 2011. **7**(7): p. 401-4.
7. Balchin, D., M. Hayer-Hartl, and F.U. Hartl, *Recent advances in understanding catalysis of protein folding by molecular chaperones.* FEBS Letters, 2020. **594**(17): p. 2770-2781.
8. Jumper, J., et al., *Highly accurate protein structure prediction with AlphaFold.* Nature, 2021. **596**(7873): p. 583-589.
9. Burley, S.K., et al., *RCSB Protein Data Bank: powerful new tools for exploring 3D structures of biological macromolecules for basic and applied research and education in fundamental biology, biomedicine, biotechnology, bioengineering and energy sciences.* Nucleic Acids Research, 2020. **49**(D1): p. D437-D451.
10. Cross, B.C., et al., *Delivering proteins for export from the cytosol.* Nat Rev Mol Cell Biol, 2009. **10**(4): p. 255-64.
11. Baum, D.A. and B. Baum, *An inside-out origin for the eukaryotic cell.* BMC Biology, 2014. **12**(1): p. 76.
12. Braakman, I., Bulleid, N.J., *Protein folding and modification in the mammalian endoplasmic reticulum.* Annu Rev Biochem, 2011. **80**: p. 71-99.
13. Ellgaard, L., Helenius, A., *Quality control in the endoplasmic reticulum.* Nat Rev Mol Cell Biol, 2003. **4**(3): p. 181-91.
14. Wu, X. and T.A. Rapoport, *Mechanistic insights into ER-associated protein degradation.* Curr Opin Cell Biol, 2018. **53**: p. 22-28.
15. Csala, M., et al., *The endoplasmic reticulum as the extracellular space inside the cell: role in protein folding and glycosylation.* Antioxid Redox Signal, 2012. **16**(10): p. 1100-8.
16. Hwang, C., A.J. Sinskey, and H.F. Lodish, *Oxidized redox state of glutathione in the endoplasmic reticulum.* Science, 1992. **257**(5076): p. 1496-502.
17. Appenzeller-Herzog, C., *Glutathione- and non-glutathione-based oxidant control in the endoplasmic reticulum.* J Cell Sci, 2011. **124**(Pt 6): p. 847-55.
18. Flohé, L., *The fairytale of the GSSG/GSH redox potential.* Biochim Biophys Acta, 2013. **1830**(5): p. 3139-42.
19. Tsunoda, S., et al., *Intact protein folding in the glutathione-depleted endoplasmic reticulum implicates alternative protein thiol reductants.* Elife, 2014. **3**: p. e03421.
20. Papp, S., et al., *Is all of the endoplasmic reticulum created equal? The effects of the heterogeneous distribution of endoplasmic reticulum Ca2+-handling proteins.* J Cell Biol, 2003. **160**(4): p. 475-9.
21. Meldolesi, J. and T. Pozzan, *The endoplasmic reticulum Ca2+ store: a view from the lumen.* Trends Biochem Sci, 1998. **23**(1): p. 10-4.
22. Halic, M., et al., *Following the signal sequence from ribosomal tunnel exit to signal recognition particle.* Nature, 2006. **444**(7118): p. 507-11.
23. Wiedmann, M., et al., *A signal sequence receptor in the endoplasmic reticulum membrane.* Nature, 1987. **328**(6133): p. 830-3.

24. Rapoport, T.A., L. Li, and E. Park, *Structural and Mechanistic Insights into Protein Translocation.* Annu Rev Cell Dev Biol, 2017. **33**: p. 369-390.
25. Johnson, N., K. Powis, and S. High, *Post-translational translocation into the endoplasmic reticulum.* Biochim Biophys Acta, 2013. **1833**(11): p. 2403-9.
26. Liaci, A.M., et al., *Structure of the human signal peptidase complex reveals the determinants for signal peptide cleavage.* Mol Cell, 2021. **81**(19): p. 3934-3948.e11.
27. Bause, E., *Structural requirements of N-glycosylation of proteins. Studies with proline peptides as conformational probes.* Biochem J, 1983. **209**(2): p. 331-6.
28. Kornfeld, R. and S. Kornfeld, *Assembly of asparagine-linked oligosaccharides.* Annu Rev Biochem, 1985. **54**: p. 631-64.
29. Stanley, P., N. Taniguchi, and M. Aebi, *N-Glycans*, in *Essentials of Glycobiology*, A. Varki, et al., Editors. 2017, Cold Spring Harbor (NY): Cold Spring Harbor Laboratory Press; 2015-2017.
30. Hammond, C., I. Braakman, and A. Helenius, *Role of N-linked oligosaccharide recognition, glucose trimming, and calnexin in glycoprotein folding and quality control.* Proc Natl Acad Sci U S A, 1994. **91**(3): p. 913-7.
31. Ellgaard, L. and E.M. Frickel, *Calnexin, calreticulin, and ERp57: teammates in glycoprotein folding.* Cell Biochem Biophys, 2003. **39**(3): p. 223-47.
32. Huppa, J.B. and H.L. Ploegh, *The eS-Sence of -SH in the ER.* Cell, 1998. **92**(2): p. 145-8.
33. Cannon, K.S. and A. Helenius, *Trimming and readdition of glucose to N-linked oligosaccharides determines calnexin association of a substrate glycoprotein in living cells.* J Biol Chem, 1999. **274**(11): p. 7537-44.
34. Suh, K., J.E. Bergmann, and C.A. Gabel, *Selective retention of monoglucosylated high mannose oligosaccharides by a class of mutant vesicular stomatitis virus G proteins.* J Cell Biol, 1989. **108**(3): p. 811-9.
35. Jelinek-Kelly, S. and A. Herscovics, *Glycoprotein biosynthesis in Saccharomyces cerevisiae. Purification of the alpha-mannosidase which removes one specific mannose residue from Man9GlcNAc.* J Biol Chem, 1988. **263**(29): p. 14757-63.
36. Hosokawa, N., et al., *EDEM1 accelerates the trimming of alpha1,2-linked mannose on the C branch of N-glycans.* Glycobiology, 2010. **20**(5): p. 567-75.
37. Helenius, A., Aebi, M., *Intracellular functions of N-linked glycans.* Science, 2001. **291**(5512): p. 2364-9.
38. Hiller, M.M., et al., *ER degradation of a misfolded luminal protein by the cytosolic ubiquitin-proteasome pathway.* Science, 1996. **273**(5282): p. 1725-8.
39. Zhang, X. and Y. Wang, *Glycosylation Quality Control by the Golgi Structure.* J Mol Biol, 2016. **428**(16): p. 3183-3193.
40. Helenius, A., *How N-linked oligosaccharides affect glycoprotein folding in the endoplasmic reticulum.* Mol Biol Cell, 1994. **5**(3): p. 253-65.
41. Van den Steen, P., et al., *Concepts and principles of O-linked glycosylation.* Crit Rev Biochem Mol Biol, 1998. **33**(3): p. 151-208.
42. McKay, D.B., *Structure and mechanism of 70-kDa heat-shock-related proteins.* Adv Protein Chem, 1993. **44**: p. 67-98.
43. Wiseman, R.L., J.S. Mesgarzadeh, and L.M. Hendershot, *Reshaping endoplasmic reticulum quality control through the unfolded protein response.* Mol Cell, 2022. **82**(8): p. 1477-1491.
44. Fourie, A.M., J.F. Sambrook, and M.J. Gething, *Common and divergent peptide binding specificities of hsp70 molecular chaperones.* J Biol Chem, 1994. **269**(48): p. 30470-8.
45. Marcinowski, M., et al., *Substrate discrimination of the chaperone BiP by autonomous and cochaperone-regulated conformational transitions.* Nat Struct Mol Biol, 2011. **18**(2): p. 150-8.
46. Shen, Y., L. Meunier, and L.M. Hendershot, *Identification and characterization of a novel endoplasmic reticulum (ER) DnaJ homologue, which stimulates ATPase activity of BiP in vitro and is induced by ER stress.* J Biol Chem, 2002. **277**(18): p. 15947-56.

47. Andréasson, C., et al., *The endoplasmic reticulum Grp170 acts as a nucleotide exchange factor of Hsp70 via a mechanism similar to that of the cytosolic Hsp110.* J Biol Chem, 2010. **285**(16): p. 12445-53.
48. Meunier, L., et al., *A subset of chaperones and folding enzymes form multiprotein complexes in endoplasmic reticulum to bind nascent proteins.* Mol Biol Cell, 2002. **13**(12): p. 4456-69.
49. Feige, M.J., L.M. Hendershot, and J. Buchner, *How antibodies fold.* Trends Biochem Sci, 2010. **35**(4): p. 189-98.
50. Lee, Y.K., et al., *BiP and immunoglobulin light chain cooperate to control the folding of heavy chain and ensure the fidelity of immunoglobulin assembly.* Mol Biol Cell, 1999. **10**(7): p. 2209-19.
51. Hendershot, L., et al., *Assembly and secretion of heavy chains that do not associate posttranslationally with immunoglobulin heavy chain-binding protein.* J Cell Biol, 1987. **104**(3): p. 761-7.
52. Hendershot, L.M., *The ER function BiP is a master regulator of ER function.* Mt Sinai J Med, 2004. **71**(5): p. 289-97.
53. Bertolotti, A., et al., *Dynamic interaction of BiP and ER stress transducers in the unfolded-protein response.* Nat Cell Biol, 2000. **2**(6): p. 326-32.
54. Argon, Y. and B.B. Simen, *GRP94, an ER chaperone with protein and peptide binding properties.* Semin Cell Dev Biol, 1999. **10**(5): p. 495-505.
55. Schaiff, W.T., et al., *HLA-DR associates with specific stress proteins and is retained in the endoplasmic reticulum in invariant chain negative cells.* J Exp Med, 1992. **176**(3): p. 657-66.
56. Melnick, J., J.L. Dul, and Y. Argon, *Sequential interaction of the chaperones BiP and GRP94 with immunoglobulin chains in the endoplasmic reticulum.* Nature, 1994. **370**(6488): p. 373-5.
57. Marzec, M., D. Eletto, and Y. Argon, *GRP94: An HSP90-like protein specialized for protein folding and quality control in the endoplasmic reticulum.* Biochim Biophys Acta, 2012. **1823**(3): p. 774-87.
58. Biswas, C., et al., *The N-terminal fragment of GRP94 is sufficient for peptide presentation via professional antigen-presenting cells.* Int Immunol, 2006. **18**(7): p. 1147-57.
59. Lev, A., et al., *Efficient cross-priming of antiviral CD8+ T cells by antigen donor cells is GRP94 independent.* J Immunol, 2009. **183**(7): p. 4205-10.
60. Jin, Y., et al., *Regulated release of ERdj3 from unfolded proteins by BiP.* Embo j, 2008. **27**(21): p. 2873-82.
61. Genereux, J.C., et al., *Unfolded protein response-induced ERdj3 secretion links ER stress to extracellular proteostasis.* Embo j, 2015. **34**(1): p. 4-19.
62. Rutkowski, D.T., et al., *The role of p58IPK in protecting the stressed endoplasmic reticulum.* Mol Biol Cell, 2007. **18**(9): p. 3681-91.
63. Fanghänel, J. and G. Fischer, *Insights into the catalytic mechanism of peptidyl prolyl cis/trans isomerases.* Front Biosci, 2004. **9**: p. 3453-78.
64. Zhang, X., et al., *The mouse FKBP23 binds to BiP in ER and the binding of C-terminal domain is interrelated with Ca2+ concentration.* FEBS Lett, 2004. **559**(1-3): p. 57-60.
65. Feige, M.J., et al., *An unfolded CH1 domain controls the assembly and secretion of IgG antibodies.* Mol Cell, 2009. **34**(5): p. 569-79.
66. Feige, M.J., I. Braakman, and L. Hendershot, *Disulfide Bonds in Protein Folding and Stability*, in *Oxidative Folding of Proteins*, M.J. Feige, Editor. 2018, Royal Society of Chemistry. p. 3-33.
67. Creighton, T.E., *A three-disulphide intermediate in refolding of reduced ribonuclease A with a folded conformation.* FEBS Lett, 1980. **118**(2): p. 283-8.
68. Wilkinson, B. and H.F. Gilbert, *Protein disulfide isomerase.* Biochim Biophys Acta, 2004. **1699**(1-2): p. 35-44.
69. Ellgaard, L., *Catalysis of disulphide bond formation in the endoplasmic reticulum.* Biochem Soc Trans, 2004. **32**(Pt 5): p. 663-7.

70. Appenzeller-Herzog, C. and L. Ellgaard, *The human PDI family: versatility packed into a single fold.* Biochim Biophys Acta, 2008. **1783**(4): p. 535-48.
71. Kanai, S., et al., *Molecular evolution of the domain structures of protein disulfide isomerases.* J Mol Evol, 1998. **47**(2): p. 200-10.
72. Ellgaard, L. and L.W. Ruddock, *The human protein disulphide isomerase family: substrate interactions and functional properties.* EMBO Rep, 2005. **6**(1): p. 28-32.
73. Alanen, H.I., et al., *ERp27, a new non-catalytic endoplasmic reticulum-located human protein disulfide isomerase family member, interacts with ERp57.* J Biol Chem, 2006. **281**(44): p. 33727-38.
74. Givol, D., R.F. Goldberger, and C.B. Anfinsen, *OXIDATION AND DISULFIDE INTERCHANGE IN THE REACTIVATION OF REDUCED RIBONUCLEASE.* J Biol Chem, 1964. **239**: p. Pc3114-16.
75. Oliver, J.D., et al., *Interaction of the thiol-dependent reductase ERp57 with nascent glycoproteins.* Science, 1997. **275**(5296): p. 86-8.
76. Antoniou, A.N., et al., *The oxidoreductase ERp57 efficiently reduces partially folded in preference to fully folded MHC class I molecules.* Embo j, 2002. **21**(11): p. 2655-63.
77. Tempio, T. and T. Anelli, *The pivotal role of ERp44 in patrolling protein secretion.* J Cell Sci, 2020. **133**(21).
78. Reitberger, S., et al., *Assembly-induced folding regulates interleukin 12 biogenesis and secretion.* J Biol Chem, 2017. **292**(19): p. 8073-8081.
79. Meier, S., et al., *The molecular basis of chaperone-mediated interleukin 23 assembly control.* Nat Commun, 2019. **10**(1): p. 4121.
80. Cunnea, P.M., et al., *ERdj5, an endoplasmic reticulum (ER)-resident protein containing DnaJ and thioredoxin domains, is expressed in secretory cells or following ER stress.* J Biol Chem, 2003. **278**(2): p. 1059-66.
81. Jessop, C.E., et al., *Protein disulphide isomerase family members show distinct substrate specificity: P5 is targeted to BiP client proteins.* J Cell Sci, 2009. **122**(Pt 23): p. 4287-95.
82. Eletto, D., et al., *Protein disulfide isomerase A6 controls the decay of IRE1α signaling via disulfide-dependent association.* Mol Cell, 2014. **53**(4): p. 562-576.
83. Appenzeller-Herzog, C., et al., *A novel disulphide switch mechanism in Ero1alpha balances ER oxidation in human cells.* Embo j, 2008. **27**(22): p. 2977-87.
84. Zito, E., *ERO1: A protein disulfide oxidase and H2O2 producer.* Free Radic Biol Med, 2015. **83**: p. 299-304.
85. Hatahet, F. and L.W. Ruddock, *Protein disulfide isomerase: a critical evaluation of its function in disulfide bond formation.* Antioxid Redox Signal, 2009. **11**(11): p. 2807-50.
86. Soares Moretti, A.I. and F.R. Martins Laurindo, *Protein disulfide isomerases: Redox connections in and out of the endoplasmic reticulum.* Archives of Biochemistry and Biophysics, 2017. **617**: p. 106-119.
87. Braakman, I., Hebert, D.N., *Protein folding in the endoplasmic reticulum.* Cold Spring Harb Perspect Biol, 2013. **5**(5): p. a013201.
88. Tsai, B., Y. Ye, and T.A. Rapoport, *Retro-translocation of proteins from the endoplasmic reticulum into the cytosol.* Nature Reviews Molecular Cell Biology, 2002. **3**(4): p. 246-255.
89. Sun, Z. and J.L. Brodsky, *Protein quality control in the secretory pathway.* J Cell Biol, 2019. **218**(10): p. 3171-3187.
90. Brodsky, J.L., *Cleaning up: ER-associated degradation to the rescue.* Cell, 2012. **151**(6): p. 1163-7.
91. Strzyz, P., *Foundations of ER-phagy regulation.* Nature Reviews Molecular Cell Biology, 2020. **21**(5): p. 251-251.
92. Ron, E., et al., *Bypass of glycan-dependent glycoprotein delivery to ERAD by up-regulated EDEM1.* Mol Biol Cell, 2011. **22**(21): p. 3945-54.
93. Ron, D. and P. Walter, *Signal integration in the endoplasmic reticulum unfolded protein response.* Nat Rev Mol Cell Biol, 2007. **8**(7): p. 519-29.

94. Dempsey, P.W., S.A. Vaidya, and G. Cheng, *The Art of War: Innate and adaptive immune responses.* Cellular and Molecular Life Sciences CMLS, 2003. **60**(12): p. 2604-2621.
95. Janeway, C.A., Jr. and R. Medzhitov, *Innate immune recognition.* Annu Rev Immunol, 2002. **20**: p. 197-216.
96. Janeway, C.A., Jr., *Approaching the asymptote? Evolution and revolution in immunology.* Cold Spring Harb Symp Quant Biol, 1989. **54 Pt 1**: p. 1-13.
97. Relja, B. and W.G. Land, *Damage-associated molecular patterns in trauma.* European Journal of Trauma and Emergency Surgery, 2020. **46**(4): p. 751-775.
98. Thomas, C.J. and K. Schroder, *Pattern recognition receptor function in neutrophils.* Trends Immunol, 2013. **34**(7): p. 317-28.
99. Akira, S., *Mammalian Toll-like receptors.* Curr Opin Immunol, 2003. **15**(1): p. 5-11.
100. Sarma, J.V. and P.A. Ward, *The complement system.* Cell Tissue Res, 2011. **343**(1): p. 227-35.
101. Medzhitov, R., *Toll-like receptors and innate immunity.* Nat Rev Immunol, 2001. **1**(2): p. 135-45.
102. Bonilla, F.A. and H.C. Oettgen, *Adaptive immunity.* J Allergy Clin Immunol, 2010. **125**(2 Suppl 2): p. S33-40.
103. Catalán, D., et al., *Immunosuppressive Mechanisms of Regulatory B Cells.* Frontiers in Immunology, 2021. **12**.
104. Vignali, D.A.A., L.W. Collison, and C.J. Workman, *How regulatory T cells work.* Nature Reviews Immunology, 2008. **8**(7): p. 523-532.
105. Vivier, E., et al., *Innate or adaptive immunity? The example of natural killer cells.* Science, 2011. **331**(6013): p. 44-9.
106. Brocker, C., Thompson, D., Matsumoto, A., Nebert, D.W., Vasiliou, V., *Evolutionary divergence and functions of the human interleukin (IL) gene family.* Hum Genomics, 2010. **5**(1): p. 30-55.
107. Akdis, M., et al., *Interleukins (from IL-1 to IL-38), interferons, transforming growth factor β, and TNF-α: Receptors, functions, and roles in diseases.* J Allergy Clin Immunol, 2016. **138**(4): p. 984-1010.
108. Vignali, D.A., Kuchroo, V.K., *IL-12 family cytokines: immunological playmakers.* Nat Immunol, 2012. **13**(8): p. 722-8.
109. Leonard, W.J. and J.J. O'Shea, *Jaks and STATs: biological implications.* Annu Rev Immunol, 1998. **16**: p. 293-322.
110. Collison, L.W., et al., *The composition and signaling of the IL-35 receptor are unconventional.* Nat Immunol, 2012. **13**(3): p. 290-9.
111. Wang, R.X., et al., *Interleukin-35 induces regulatory B cells that suppress autoimmune disease.* Nat Med, 2014. **20**(6): p. 633-41.
112. Tait Wojno, E.D., C.A. Hunter, and J.S. Stumhofer, *The Immunobiology of the Interleukin-12 Family: Room for Discovery.* Immunity, 2019. **50**(4): p. 851-870.
113. Wang, R.X., et al., *Novel IL27p28/IL12p40 cytokine suppressed experimental autoimmune uveitis by inhibiting autoreactive Th1/Th17 cells and promoting expansion of regulatory T cells.* J Biol Chem, 2012. **287**(43): p. 36012-21.
114. Bridgewood, C., et al., *The IL-23p19/EBI3 heterodimeric cytokine termed IL-39 remains a theoretical cytokine in man.* Inflamm Res, 2019. **68**(6): p. 423-426.
115. Ecoeur, F., et al., *Lack of evidence for expression and function of IL-39 in human immune cells.* PLoS One, 2020. **15**(12): p. e0242329.
116. Chehboun, S., et al., *Epstein-Barr virus-induced gene 3 (EBI3) can mediate IL-6 trans-signaling.* J Biol Chem, 2017. **292**(16): p. 6644-6656.
117. Garbers, C., et al., *An interleukin-6 receptor-dependent molecular switch mediates signal transduction of the IL-27 cytokine subunit p28 (IL-30) via a gp130 protein receptor homodimer.* J Biol Chem, 2013. **288**(6): p. 4346-54.
118. Gerber, A.N., K. Abdi, and N.J. Singh, *The subunits of IL-12, originating from two distinct cells, can functionally synergize to protect against pathogen dissemination in vivo.* Cell Rep, 2021. **37**(2): p. 109816.

119. Kundu, M., A. Roy, and K. Pahan, *Selective neutralization of IL-12 p40 monomer induces death in prostate cancer cells via IL-12-IFN-γ.* Proc Natl Acad Sci U S A, 2017. **114**(43): p. 11482-11487.
120. Trinchieri, G., *Interleukin-12 and the regulation of innate resistance and adaptive immunity.* Nat Rev Immunol, 2003. **3**(2): p. 133-46.
121. Müller, S.I., et al., *A folding switch regulates interleukin 27 biogenesis and secretion of its α-subunit as a cytokine.* Proc Natl Acad Sci U S A, 2019. **116**(5): p. 1585-1590.
122. Mideksa, Y.G., et al., *Site-Specific Protein Labeling with Fluorophores as a Tool To Monitor Protein Turnover.* Chembiochem, 2020. **21**(13): p. 1861-1867.
123. Feige, M.J., et al., *Dimerization-dependent folding underlies assembly control of the clonotypic αβT cell receptor chains.* J Biol Chem, 2015. **290**(44): p. 26821-31.
124. Pflanz, S., et al., *IL-27, a heterodimeric cytokine composed of EBI3 and p28 protein, induces proliferation of naive CD4+ T cells.* Immunity, 2002. **16**(6): p. 779-90.
125. Russell, T.D., et al., *IL-12 p40 homodimer-dependent macrophage chemotaxis and respiratory viral inflammation are mediated through IL-12 receptor beta 1.* J Immunol, 2003. **171**(12): p. 6866-74.
126. Jana, M. and K. Pahan, *IL-12 p40 homodimer, but not IL-12 p70, induces the expression of IL-16 in microglia and macrophages.* Mol Immunol, 2009. **46**(5): p. 773-83.
127. Jana, M., et al., *IL-12 p40 homodimer, the so-called biologically inactive molecule, induces nitric oxide synthase in microglia via IL-12R beta 1.* Glia, 2009. **57**(14): p. 1553-65.
128. Mondal, S., et al., *IL-12 p40 monomer is different from other IL-12 family members to selectively inhibit IL-12Rβ1 internalization and suppress EAE.* Proc Natl Acad Sci U S A, 2020. **117**(35): p. 21557-21567.
129. Cooper, A.M. and S.A. Khader, *IL-12p40: an inherently agonistic cytokine.* Trends Immunol, 2007. **28**(1): p. 33-8.
130. Mattner, F., et al., *The interleukin-12 subunit p40 specifically inhibits effects of the interleukin-12 heterodimer.* Eur J Immunol, 1993. **23**(9): p. 2202-8.
131. Shimozato, O., et al., *The secreted form of the p40 subunit of interleukin (IL)-12 inhibits IL-23 functions and abrogates IL-23-mediated antitumour effects.* Immunology, 2006. **117**(1): p. 22-8.
132. Hildenbrand, K., et al., *Biogenesis and engineering of interleukin 12 family cytokines.* Trends Biochem Sci, 2022. **47**(11): p. 936-949.
133. Składanowska, K., et al., *Structural basis of activation and antagonism of receptor signaling mediated by interleukin-27.* Cell Rep, 2022. **41**(3): p. 111490.
134. Boulay, J.L., J.J. O'Shea, and W.E. Paul, *Molecular phylogeny within type I cytokines and their cognate receptors.* Immunity, 2003. **19**(2): p. 159-63.
135. Bazan, J.F., *Neuropoietic cytokines in the hematopoietic fold.* Neuron, 1991. **7**(2): p. 197-208.
136. Yoon, C., et al., *Charged residues dominate a unique interlocking topography in the heterodimeric cytokine interleukin-12.* Embo j, 2000. **19**(14): p. 3530-3541.
137. Wells, J.A. and A.M. de Vos, *Hematopoietic receptor complexes.* Annu Rev Biochem, 1996. **65**: p. 609-34.
138. Boulanger, M.J. and K.C. Garcia, *Shared cytokine signaling receptors: structural insights from the gp130 system.* Adv Protein Chem, 2004. **68**: p. 107-46.
139. Bazan, J.F., *Structural design and molecular evolution of a cytokine receptor superfamily.* Proc Natl Acad Sci U S A, 1990. **87**(18): p. 6934-8.
140. Cosman, D., et al., *A new cytokine receptor superfamily.* Trends Biochem Sci, 1990. **15**(7): p. 265-70.
141. de Vos, A.M., M. Ultsch, and A.A. Kossiakoff, *Human growth hormone and extracellular domain of its receptor: crystal structure of the complex.* Science, 1992. **255**(5042): p. 306-12.
142. Lupardus, P.J. and K.C. Garcia, *The structure of interleukin-23 reveals the molecular basis of p40 subunit sharing with interleukin-12.* J Mol Biol, 2008. **382**(4): p. 931-41.

143. Jones, L.L. and D.A. Vignali, *Molecular interactions within the IL-6/IL-12 cytokine/receptor superfamily.* Immunol Res, 2011. **51**(1): p. 5-14.
144. Wang, X., et al., *Structural biology of shared cytokine receptors.* Annu Rev Immunol, 2009. **27**: p. 29-60.
145. Boulanger, M.J., et al., *Hexameric structure and assembly of the interleukin-6/IL-6 alpha-receptor/gp130 complex.* Science, 2003. **300**(5628): p. 2101-4.
146. Rousseau, F., et al., *IL-27 structural analysis demonstrates similarities with ciliary neurotrophic factor (CNTF) and leads to the identification of antagonistic variants.* Proc Natl Acad Sci U S A, 2010. **107**(45): p. 19420-5.
147. Jin, Y., et al., *Structural insights into the assembly and activation of the IL-27 signaling complex.* EMBO Rep, 2022. **23**(10): p. e55450.
148. Caveney, N.A., et al., *Structure of the IL-27 quaternary receptor signaling complex.* Elife, 2022. **11**.
149. Kobayashi, M., et al., *Identification and purification of natural killer cell stimulatory factor (NKSF), a cytokine with multiple biologic effects on human lymphocytes.* J Exp Med, 1989. **170**(3): p. 827-45.
150. Alloza, I., et al., *Cross-linking approach to affinity capture of protein complexes from chaotrope-solubilized cell lysates.* Anal Biochem, 2004. **324**(1): p. 137-42.
151. Alloza, I., et al., *Celecoxib inhibits interleukin-12 alphabeta and beta2 folding and secretion by a novel COX2-independent mechanism involving chaperones of the endoplasmic reticulum.* Mol Pharmacol, 2006. **69**(5): p. 1579-87.
152. Jalah, R., Rosati, M., Ganneru, B., Pilkington, G.R., Valentin, A., Kulkarni, V., Bergamaschi, C., Chowdhury, B., Zhang, G.M., Beach, R.K., Alicea, C., Broderick, K.E., Sardesai, N.Y., Pavlakis, G.N., Felber, B.K., *The p40 subunit of interleukin (IL)-12 promotes stabilization and export of the p35 subunit: implications for improved IL-12 cytokine production.* J Biol Chem, 2013. **288**(9): p. 6763-76.
153. Carra, G., F. Gerosa, and G. Trinchieri, *Biosynthesis and posttranslational regulation of human IL-12.* J Immunol, 2000. **164**(9): p. 4752-61.
154. Podlaski, F.J., et al., *Molecular characterization of interleukin 12.* Arch Biochem Biophys, 1992. **294**(1): p. 230-7.
155. Ha, S.J., et al., *Engineering N-glycosylation mutations in IL-12 enhances sustained cytotoxic T lymphocyte responses for DNA immunization.* Nat Biotechnol, 2002. **20**(4): p. 381-6.
156. Jana, M. and K. Pahan, *Induction of lymphotoxin-alpha by interleukin-12 p40 homodimer, the so-called biologically inactive molecule, but not IL-12 p70.* Immunology, 2009. **127**(3): p. 312-25.
157. Oppmann, B., Lesley, R., Blom, B., Timans, J.C., Xu, Y., Hunte, B., Vega, F., Yu, N., Wang, J., Singh, K., Zonin, F., Vaisberg, E., Churakova, T., Liu, M., Gorman, D., Wagner, J., Zurawski, S., Liu, Y., Abrams, J.S., Moore, K.W., Rennick, D., de Waal-Malefyt, R., Hannum, C., Bazan, J.F., Kastelein, R.A., *Novel p19 protein engages IL-12p40 to form a cytokine, IL-23, with biological activities similar as well as distinct from IL-12.* Immunity, 2000. **13**(5): p. 715-25.
158. Rousseau, F., et al., *Ciliary neurotrophic factor, cardiotrophin-like cytokine, and neuropoietin share a conserved binding site on the ciliary neurotrophic factor receptor alpha chain.* J Biol Chem, 2008. **283**(44): p. 30341-50.
159. Devergne, O., M. Birkenbach, and E. Kieff, *Epstein-Barr virus-induced gene 3 and the p35 subunit of interleukin 12 form a novel heterodimeric hematopoietin.* Proc Natl Acad Sci U S A, 1997. **94**(22): p. 12041-6.
160. Jones, L.L., Chaturvedi, V., Uyttenhove, C., Van Snick, J., Vignali, D.A., *Distinct subunit pairing criteria within the heterodimeric IL-12 cytokine family.* Mol Immunol, 2012. **51**(2): p. 234-44.
161. Aparicio-Siegmund, S., et al., *Recombinant p35 from bacteria can form Interleukin (IL-)12, but Not IL-35.* PLoS One, 2014. **9**(9): p. e107990.
162. Heinzel, F.P., et al., *In vivo production and function of IL-12 p40 homodimers.* J Immunol, 1997. **158**(9): p. 4381-8.

163. Devergne, O., et al., *A novel interleukin-12 p40-related protein induced by latent Epstein-Barr virus infection in B lymphocytes.* J Virol, 1996. **70**(2): p. 1143-53.
164. Hebert, D.N. and M. Molinari, *Flagging and docking: dual roles for N-glycans in protein quality control and cellular proteostasis.* Trends Biochem Sci, 2012. **37**(10): p. 404-10.
165. Mizoguchi, I., et al., *EBV-induced gene 3 augments IL-23Rα protein expression through a chaperone calnexin.* J Clin Invest, 2020. **130**(11): p. 6124-6140.
166. Skiniotis, G., et al., *Structural organization of a full-length gp130/LIF-R cytokine receptor transmembrane complex.* Mol Cell, 2008. **31**(5): p. 737-48.
167. Ward, L.D., et al., *High affinity interleukin-6 receptor is a hexameric complex consisting of two molecules each of interleukin-6, interleukin-6 receptor, and gp-130.* J Biol Chem, 1994. **269**(37): p. 23286-9.
168. Stahl, N., et al., *Association and activation of Jak-Tyk kinases by CNTF-LIF-OSM-IL-6 beta receptor components.* Science, 1994. **263**(5143): p. 92-5.
169. Georgy, J., et al., *Tryptophan (W) at position 37 of murine IL-12/IL-23 p40 is mandatory for binding to IL-12Rβ1 and subsequent signal transduction.* J Biol Chem, 2021. **297**(5): p. 101295.
170. Glassman, C.R., et al., *Structural basis for IL-12 and IL-23 receptor sharing reveals a gateway for shaping actions on T versus NK cells.* Cell, 2021. **184**(4): p. 983-999.e24.
171. Bloch, Y., et al., *Structural Activation of Pro-inflammatory Human Cytokine IL-23 by Cognate IL-23 Receptor Enables Recruitment of the Shared Receptor IL-12Rβ1.* Immunity, 2018. **48**(1): p. 45-58.e6.
172. Presky, D.H., et al., *A functional interleukin 12 receptor complex is composed of two beta-type cytokine receptor subunits.* Proc Natl Acad Sci U S A, 1996. **93**(24): p. 14002-7.
173. Schröder, J., et al., *Non-canonical interleukin 23 receptor complex assembly: p40 protein recruits interleukin 12 receptor β1 via site II and induces p19/interleukin 23 receptor interaction via site III.* J Biol Chem, 2015. **290**(1): p. 359-70.
174. Esch, A., et al., *Deciphering site 3 interactions of interleukin 12 and interleukin 23 with their cognate murine and human receptors.* J Biol Chem, 2020. **295**(30): p. 10478-10492.
175. Yao, B.B., et al., *Direct interaction of STAT4 with the IL-12 receptor.* Arch Biochem Biophys, 1999. **368**(1): p. 147-55.
176. Bacon, C.M., et al., *Interleukin 12 induces tyrosine phosphorylation and activation of STAT4 in human lymphocytes.* Proc Natl Acad Sci U S A, 1995. **92**(16): p. 7307-11.
177. Gillessen, S., et al., *Mouse interleukin-12 (IL-12) p40 homodimer: a potent IL-12 antagonist.* Eur J Immunol, 1995. **25**(1): p. 200-6.
178. Presky, D.H., et al., *Analysis of the multiple interactions between IL-12 and the high affinity IL-12 receptor complex.* J Immunol, 1998. **160**(5): p. 2174-9.
179. Lay, C.S., et al., *Probing the binding of interleukin-23 to individual receptor components and the IL-23 heteromeric receptor complex in living cells using NanoBRET.* Cell Chem Biol, 2022. **29**(1): p. 19-29.e6.
180. Machleidt, T., et al., *NanoBRET--A Novel BRET Platform for the Analysis of Protein-Protein Interactions.* ACS Chem Biol, 2015. **10**(8): p. 1797-804.
181. Lay, C.S., et al., *Use of NanoBiT and NanoBRET to characterise interleukin-23 receptor dimer formation in living cells.* Br J Pharmacol, 2022.
182. Reich, K., et al., *A 52-week trial comparing briakinumab with methotrexate in patients with psoriasis.* N Engl J Med, 2011. **365**(17): p. 1586-96.
183. Luo, J., et al., *Structural basis for the dual recognition of IL-12 and IL-23 by ustekinumab.* J Mol Biol, 2010. **402**(5): p. 797-812.
184. Eldirany, S.A., M. Ho, and C.G. Bunick, *Structural Basis for How Biologic Medicines Bind their Targets in Psoriasis Therapy.* Yale J Biol Med, 2020. **93**(1): p. 19-27.
185. Jin, Y., et al., *Structural insights into the assembly and activation of IL-27 signalling complex.* bioRxiv, 2022: p. 2022.02.18.481027.

186. Sprecher, C.A., et al., *Cloning and characterization of a novel class I cytokine receptor.* Biochem Biophys Res Commun, 1998. **246**(1): p. 82-90.
187. Stumhofer, J.S., et al., *A role for IL-27p28 as an antagonist of gp130-mediated signaling.* Nat Immunol, 2010. **11**(12): p. 1119-26.
188. Moritz, R.L., et al., *The N-terminus of gp130 is critical for the formation of the high-affinity interleukin-6 receptor complex.* Growth Factors, 1999. **16**(4): p. 265-78.
189. Pflanz, S., et al., *WSX-1 and glycoprotein 130 constitute a signal-transducing receptor for IL-27.* J Immunol, 2004. **172**(4): p. 2225-31.
190. Wilmes, S., et al., *Competitive binding of STATs to receptor phospho-Tyr motifs accounts for altered cytokine responses.* Elife, 2021. **10**.
191. Floss, D.M., et al., *IL-6/IL-12 Cytokine Receptor Shuffling of Extra- and Intracellular Domains Reveals Canonical STAT Activation via Synthetic IL-35 and IL-39 Signaling.* Sci Rep, 2017. **7**(1): p. 15172.
192. Stern, A.S., et al., *Purification to homogeneity and partial characterization of cytotoxic lymphocyte maturation factor from human B-lymphoblastoid cells.* Proc Natl Acad Sci U S A, 1990. **87**(17): p. 6808-12.
193. Wolf, S.F., et al., *Cloning of cDNA for natural killer cell stimulatory factor, a heterodimeric cytokine with multiple biologic effects on T and natural killer cells.* J Immunol, 1991. **146**(9): p. 3074-81.
194. D'Andrea, A., et al., *Production of natural killer cell stimulatory factor (interleukin 12) by peripheral blood mononuclear cells.* J Exp Med, 1992. **176**(5): p. 1387-98.
195. Sypek, J.P., et al., *Resolution of cutaneous leishmaniasis: interleukin 12 initiates a protective T helper type 1 immune response.* J Exp Med, 1993. **177**(6): p. 1797-802.
196. Tripp, C.S., et al., *Neutralization of IL-12 decreases resistance to Listeria in SCID and C.B-17 mice. Reversal by IFN-gamma.* J Immunol, 1994. **152**(4): p. 1883-7.
197. Gazzinelli, R.T., et al., *Interleukin 12 is required for the T-lymphocyte-independent induction of interferon gamma by an intracellular parasite and induces resistance in T-cell-deficient hosts.* Proc Natl Acad Sci U S A, 1993. **90**(13): p. 6115-9.
198. Trinchieri, G., Pflanz, S., Kastelein, R.A., *The IL-12 family of heterodimeric cytokines: new players in the regulation of T cell responses.* Immunity, 2003. **19**(5): p. 641-4.
199. Fukao, T., et al., *Inducible expression of Stat4 in dendritic cells and macrophages and its critical role in innate and adaptive immune responses.* J Immunol, 2001. **166**(7): p. 4446-55.
200. McKenzie, B.S., Kastelein, R. A., Cua, D. J., *Understanding the IL-23-IL-17 immune pathway.* Trends Immunol, 2006. **27**(1): p. 17-23.
201. Park, A.Y., B.D. Hondowicz, and P. Scott, *IL-12 is required to maintain a Th1 response during Leishmania major infection.* J Immunol, 2000. **165**(2): p. 896-902.
202. Hsieh, C.S., et al., *Development of TH1 CD4+ T cells through IL-12 produced by Listeria-induced macrophages.* Science, 1993. **260**(5107): p. 547-9.
203. Wills-Karp, M., *IL-12/IL-13 axis in allergic asthma.* J Allergy Clin Immunol, 2001. **107**(1): p. 9-18.
204. Cooper, A.M., et al., *Mice lacking bioactive IL-12 can generate protective, antigen-specific cellular responses to mycobacterial infection only if the IL-12 p40 subunit is present.* J Immunol, 2002. **168**(3): p. 1322-7.
205. Becher, B., B.G. Durell, and R.J. Noelle, *Experimental autoimmune encephalitis and inflammation in the absence of interleukin-12.* J Clin Invest, 2002. **110**(4): p. 493-7.
206. Cua, D.J., et al., *Interleukin-23 rather than interleukin-12 is the critical cytokine for autoimmune inflammation of the brain.* Nature, 2003. **421**(6924): p. 744-8.
207. Langrish, C.L., et al., *IL-23 drives a pathogenic T cell population that induces autoimmune inflammation.* J Exp Med, 2005. **201**(2): p. 233-40.
208. Aggarwal, S., et al., *Interleukin-23 promotes a distinct CD4 T cell activation state characterized by the production of interleukin-17.* J Biol Chem, 2003. **278**(3): p. 1910-4.
209. Murphy, C.A., et al., *Divergent pro- and antiinflammatory roles for IL-23 and IL-12 in joint autoimmune inflammation.* J Exp Med, 2003. **198**(12): p. 1951-7.

210. Yen, D., et al., *IL-23 is essential for T cell-mediated colitis and promotes inflammation via IL-17 and IL-6.* J Clin Invest, 2006. **116**(5): p. 1310-6.
211. Chabaud, M., et al., *Human interleukin-17: A T cell-derived proinflammatory cytokine produced by the rheumatoid synovium.* Arthritis Rheum, 1999. **42**(5): p. 963-70.
212. Teunissen, M.B., et al., *Interleukin-17 and interferon-gamma synergize in the enhancement of proinflammatory cytokine production by human keratinocytes.* J Invest Dermatol, 1998. **111**(4): p. 645-9.
213. Homey, B., et al., *Up-regulation of macrophage inflammatory protein-3 alpha/CCL20 and CC chemokine receptor 6 in psoriasis.* J Immunol, 2000. **164**(12): p. 6621-32.
214. Kurasawa, K., et al., *Increased interleukin-17 production in patients with systemic sclerosis.* Arthritis Rheum, 2000. **43**(11): p. 2455-63.
215. Christophers, E., *Psoriasis--epidemiology and clinical spectrum.* Clin Exp Dermatol, 2001. **26**(4): p. 314-20.
216. Zheng, Y., et al., *Interleukin-22, a T(H)17 cytokine, mediates IL-23-induced dermal inflammation and acanthosis.* Nature, 2007. **445**(7128): p. 648-51.
217. Codarri, L., et al., *RORγt drives production of the cytokine GM-CSF in helper T cells, which is essential for the effector phase of autoimmune neuroinflammation.* Nat Immunol, 2011. **12**(6): p. 560-7.
218. Noster, R., et al., *IL-17 and GM-CSF expression are antagonistically regulated by human T helper cells.* Sci Transl Med, 2014. **6**(241): p. 241ra80.
219. Langowski, J.L., R.A. Kastelein, and M. Oft, *Swords into plowshares: IL-23 repurposes tumor immune surveillance.* Trends Immunol, 2007. **28**(5): p. 207-12.
220. Langowski, J.L., Zhang, X., Wu, L., Mattson, J.D., Chen, T., Smith, K., Basham, B., McClanahan, T., Kastelein, R.A., Oft, M., *IL-23 promotes tumour incidence and growth.* Nature, 2006. **442**(7101): p. 461-5.
221. Wight, A.E., et al., *Antibody-mediated blockade of the IL23 receptor destabilizes intratumoral regulatory T cells and enhances immunotherapy.* Proc Natl Acad Sci U S A, 2022. **119**(18): p. e2200757119.
222. Yeilding, N., et al., *Development of the IL-12/23 antagonist ustekinumab in psoriasis: past, present, and future perspectives.* Ann N Y Acad Sci, 2011. **1222**: p. 30-9.
223. Hawkes, J.E., et al., *Discovery of the IL-23/IL-17 Signaling Pathway and the Treatment of Psoriasis.* J Immunol, 2018. **201**(6): p. 1605-1613.
224. Villegas, J.A., et al., *Blocking interleukin-23 ameliorates neuromuscular and thymic defects in myasthenia gravis.* J Neuroinflammation, 2023. **20**(1): p. 9.
225. Gaignage, M., et al., *Novel antibodies that selectively block mouse IL-12 enable the re-evaluation of the role of IL-12 in immune protection and pathology.* Eur J Immunol, 2021. **51**(6): p. 1482-1493.
226. Devergne, O., et al., *Expression of Epstein-Barr virus-induced gene 3, an interleukin-12 p40-related molecule, throughout human pregnancy: involvement of syncytiotrophoblasts and extravillous trophoblasts.* Am J Pathol, 2001. **159**(5): p. 1763-76.
227. Larousserie, F., et al., *Frontline Science: Human bone cells as a source of IL-27 under inflammatory conditions: role of TLRs and cytokines.* J Leukoc Biol, 2017. **101**(6): p. 1289-1300.
228. Hibbert, L., et al., *IL-27 and IFN-alpha signal via Stat1 and Stat3 and induce T-Bet and IL-12Rbeta2 in naive T cells.* J Interferon Cytokine Res, 2003. **23**(9): p. 513-22.
229. Chen, Q., et al., *Development of Th1-type immune responses requires the type I cytokine receptor TCCR.* Nature, 2000. **407**(6806): p. 916-20.
230. Yoshida, H., et al., *WSX-1 is required for the initiation of Th1 responses and resistance to L. major infection.* Immunity, 2001. **15**(4): p. 569-78.
231. Mayer, K.D., et al., *Cutting edge: T-bet and IL-27R are critical for in vivo IFN-gamma production by CD8 T cells during infection.* J Immunol, 2008. **180**(2): p. 693-7.
232. Villarino, A., et al., *The IL-27R (WSX-1) is required to suppress T cell hyperactivity during infection.* Immunity, 2003. **19**(5): p. 645-55.

233. Hamano, S., et al., *WSX-1 is required for resistance to Trypanosoma cruzi infection by regulation of proinflammatory cytokine production.* Immunity, 2003. **19**(5): p. 657-67.
234. Fitzgerald, D.C., et al., *Suppression of autoimmune inflammation of the central nervous system by interleukin 10 secreted by interleukin 27-stimulated T cells.* Nat Immunol, 2007. **8**(12): p. 1372-9.
235. Fitzgerald, D.C., et al., *Independent and interdependent immunoregulatory effects of IL-27, IFN-β, and IL-10 in the suppression of human Th17 cells and murine experimental autoimmune encephalomyelitis.* J Immunol, 2013. **190**(7): p. 3225-34.
236. Hirahara, K., et al., *Interleukin-27 priming of T cells controls IL-17 production in trans via induction of the ligand PD-L1.* Immunity, 2012. **36**(6): p. 1017-30.
237. Stumhofer, J.S., et al., *Interleukins 27 and 6 induce STAT3-mediated T cell production of interleukin 10.* Nat Immunol, 2007. **8**(12): p. 1363-71.
238. Casella, G., et al., *IL-27, but not IL-35, inhibits neuroinflammation through modulating GM-CSF expression.* Sci Rep, 2017. **7**(1): p. 16547.
239. Villarino, A.V., et al., *IL-27 limits IL-2 production during Th1 differentiation.* J Immunol, 2006. **176**(1): p. 237-47.
240. Wirtz, S., et al., *Protection from lethal septic peritonitis by neutralizing the biological function of interleukin 27.* J Exp Med, 2006. **203**(8): p. 1875-81.
241. Aparicio-Siegmund, S. and C. Garbers, *The biology of interleukin-27 reveals unique pro- and anti-inflammatory functions in immunity.* Cytokine Growth Factor Rev, 2015. **26**(5): p. 579-86.
242. Hu, P., et al., *Expression of interleukins-23 and 27 leads to successful gene therapy of hepatocellular carcinoma.* Mol Immunol, 2009. **46**(8-9): p. 1654-62.
243. Collison, L.W., Workman, C.J., Kuo, T.T., Boyd, K., Wang, Y., Vignali, K.M., Cross, R., Sehy, D., Blumberg, R.S., Vignali, D.A., *The inhibitory cytokine IL-35 contributes to regulatory T-cell function.* Nature, 2007. **450**(7169): p. 566-9.
244. Collison, L.W., et al., *IL-35-mediated induction of a potent regulatory T cell population.* Nat Immunol, 2010. **11**(12): p. 1093-101.
245. Li, S., et al., *STING-induced regulatory B cells compromise NK function in cancer immunity.* Nature, 2022. **610**(7931): p. 373-380.
246. Turnis, M.E., et al., *Interleukin-35 Limits Anti-Tumor Immunity.* Immunity, 2016. **44**(2): p. 316-29.
247. Wiekowski, M.T., et al., *Ubiquitous transgenic expression of the IL-23 subunit p19 induces multiorgan inflammation, runting, infertility, and premature death.* J Immunol, 2001. **166**(12): p. 7563-70.
248. Espígol-Frigolé, G., et al., *Identification of IL-23p19 as an endothelial proinflammatory peptide that promotes gp130-STAT3 signaling.* Sci Signal, 2016. **9**(419): p. ra28.
249. Shimozato, O., et al., *The secreted form of p28 subunit of interleukin (IL)-27 inhibits biological functions of IL-27 and suppresses anti-allogeneic immune responses.* Immunology, 2009. **128**(1 Suppl): p. e816-25.
250. Müller, S.I., et al., *An Interspecies Analysis Reveals Molecular Construction Principles of Interleukin 27.* J Mol Biol, 2019. **431**(12): p. 2383-2393.
251. Hendershot, L., et al., *Inhibition of immunoglobulin folding and secretion by dominant negative BiP ATPase mutants.* Proc Natl Acad Sci U S A, 1996. **93**(11): p. 5269-74.
252. Detry, S., et al., *Revisiting the combinatorial potential of cytokine subunits in the IL-12 family.* Biochem Pharmacol, 2019. **165**: p. 240-248.
253. Bohnacker, S., et al., *Influence of glycosylation on IL-12 family cytokine biogenesis and function.* Mol Immunol, 2020. **126**: p. 120-128.
254. Lee, C.C., et al., *Macrophage-secreted interleukin-35 regulates cancer cell plasticity to facilitate metastatic colonization.* Nat Commun, 2018. **9**(1): p. 3763.
255. Sawant, D.V., et al., *Adaptive plasticity of IL-10(+) and IL-35(+) T(reg) cells cooperatively promotes tumor T cell exhaustion.* Nat Immunol, 2019. **20**(6): p. 724-735.

256. Mirlekar, B. and Y. Pylayeva-Gupta, *IL-12 Family Cytokines in Cancer and Immunotherapy.* Cancers (Basel), 2021. **13**(2).
257. Mideksa, Y.G., et al., *A comprehensive set of ER protein disulfide isomerase family members supports the biogenesis of proinflammatory interleukin 12 family cytokines.* J Biol Chem, 2022. **298**(12): p. 102677.
258. Hirayama, C., et al., *Distinct roles and actions of protein disulfide isomerase family enzymes in catalysis of nascent-chain disulfide bond formation.* iScience, 2021. **24**(4): p. 102296.
259. McLaughlin, M., et al., *Inhibition of secretion of interleukin (IL)-12/IL-23 family cytokines by 4-trifluoromethyl-celecoxib is coupled to degradation via the endoplasmic reticulum stress protein HERP.* J Biol Chem, 2010. **285**(10): p. 6960-9.
260. Briukhovetska, D., et al., *Interleukins in cancer: from biology to therapy.* Nat Rev Cancer, 2021. **21**(8): p. 481-499.
261. Kourko, O., et al., *IL-27, IL-30, and IL-35: A Cytokine Triumvirate in Cancer.* Front Oncol, 2019. **9**: p. 969.
262. Tannenbaum, C.S., et al., *The CXC chemokines IP-10 and Mig are necessary for IL-12-mediated regression of the mouse RENCA tumor.* J Immunol, 1998. **161**(2): p. 927-32.
263. Atkins, M.B., et al., *Phase I evaluation of intravenous recombinant human interleukin 12 in patients with advanced malignancies.* Clin Cancer Res, 1997. **3**(3): p. 409-17.
264. Leonard, J.P., et al., *Effects of single-dose interleukin-12 exposure on interleukin-12-associated toxicity and interferon-gamma production.* Blood, 1997. **90**(7): p. 2541-8.
265. Motzer, R.J., et al., *Phase I trial of subcutaneous recombinant human interleukin-12 in patients with advanced renal cell carcinoma.* Clin Cancer Res, 1998. **4**(5): p. 1183-91.
266. Bajetta, E., et al., *Pilot study of subcutaneous recombinant human interleukin 12 in metastatic melanoma.* Clin Cancer Res, 1998. **4**(1): p. 75-85.
267. Cirella, A., et al., *Novel strategies exploiting interleukin-12 in cancer immunotherapy.* Pharmacol Ther, 2022. **239**: p. 108189.
268. Nguyen, K.G., et al., *Localized Interleukin-12 for Cancer Immunotherapy.* Front Immunol, 2020. **11**: p. 575597.
269. Greiner, J.W., Y.M. Morillon, 2nd, and J. Schlom, *NHS-IL12, a Tumor-Targeting Immunocytokine.* Immunotargets Ther, 2021. **10**: p. 155-169.
270. Xu, C., et al., *Combination Therapy with NHS-muIL12 and Avelumab (anti-PD-L1) Enhances Antitumor Efficacy in Preclinical Cancer Models.* Clin Cancer Res, 2017. **23**(19): p. 5869-5880.
271. Strauss, J., et al., *1224P - Phase Ib, open-label, dose-escalation study of M9241 (NHS-IL12) plus avelumab in patients (pts) with advanced solid tumours.* Annals of Oncology, 2019. **30**: p. v500-v501.
272. Nagarajan, S. and P. Selvaraj, *Glycolipid-anchored IL-12 expressed on tumor cell surface induces antitumor immune response.* Cancer Res, 2002. **62**(10): p. 2869-74.
273. Barrett, J.A., et al., *Regulated intratumoral expression of IL-12 using a RheoSwitch Therapeutic System(®) (RTS(®)) gene switch as gene therapy for the treatment of glioma.* Cancer Gene Ther, 2018. **25**(5-6): p. 106-116.
274. Hu, J., et al., *Cell membrane-anchored and tumor-targeted IL-12 (attIL12)-T cell therapy for eliminating large and heterogeneous solid tumors.* J Immunother Cancer, 2022. **10**(1).
275. Jones, D.S., 2nd, et al., *Cell surface-tethered IL-12 repolarizes the tumor immune microenvironment to enhance the efficacy of adoptive T cell therapy.* Sci Adv, 2022. **8**(17): p. eabi8075.
276. Agliardi, G., et al., *Intratumoral IL-12 delivery empowers CAR-T cell immunotherapy in a pre-clinical model of glioblastoma.* Nat Commun, 2021. **12**(1): p. 444.

277. Zhang, L., et al., *Improving adoptive T cell therapy by targeting and controlling IL-12 expression to the tumor environment.* Mol Ther, 2011. **19**(4): p. 751-9.
278. Chmielewski, M. and H. Abken, *TRUCKs: the fourth generation of CARs.* Expert Opin Biol Ther, 2015. **15**(8): p. 1145-54.
279. Saxton, R.A., et al., *Structure-based decoupling of the pro- and anti-inflammatory functions of interleukin-10.* Science, 2021. **371**(6535).

Figure 5 and Figure 14 were created with BioRender.com.

# Acknowledgment

Als Erstes möchte ich mich ganz herzlich bei meinem Doktorvater, Prof. Dr. Matthias J. Feige bedanken: *Danke* Matthias, für die exzellente fachliche Betreuung meiner spannenden Promotionsprojekte über die letzten 44 Monate hinweg. Deine kreativen Ideen, Dein Input und Deine Führung haben mich in meiner Promotion geleitet und unterstützt. Ich habe dank Deiner wertschätzenden Art (fast) nie die Motivation verloren, und bin durch meinen, aber auch Deinen Anspruch über mich und meine Grenzen (häufiger als Du eventuell vermutest) hinausgewachsen. *Danke* auch dafür, dass Du mir die Freiheiten gegeben hast, auch während meiner Promotion über den Tellerrand zu schauen und mich auszuprobieren. Das macht unglaublich viel aus und ich bin sehr froh, dass ich in Deiner Arbeitsgruppe promoviert habe.

Ebenso ist es mir wichtig allen kollaborierenden KollegInnen zu danken, ohne welche die in dieser Dissertation veröffentlichten Publikationen und facettenreichen molekularen Einblicke in die IL-12 Zytokinfamilie nicht möglich gewesen wären. Wenn auch nur zeitweise, aber meine Studierenden Sarah, Silvia, Konstantin, Philipp, Anna und Maxi haben mich bei kleinen und großen Schritten der Projekte tatkräftig unterstützt. Es hat mir viel Spaß gemacht mit Euch im Team zu arbeiten!

Herzlichen Dank auch an die Studienstiftung des deutschen Volkes, welche mich mit einem Promotionsstipendium finanziell unterstützt hat, und an das Marianne-Plehn Programm, durch das ich am Lehrstuhl für Zelluläre Proteinbiochemie angestellt sein konnte.

Als Nächstes möchte ich dem gesamten CPBlab *Danke* sagen! Ich bin richtig froh, mit all den tollen Menschen, die ab Beginn des Labors ein Teil der CPBlab Family waren oder sind, zusammen gearbeitet zu haben und weiterhin arbeiten zu dürfen. Ich durfte sowohl Freunde aus dem Studium mitnehmen als auch neue Freunde dazugewinnen – das ist wirklich, wirklich schön. Dadurch hat das Arbeiten einfach eine Menge Spaß gebracht, sodass es sich ab und zu wie ein Sommerurlaub (Aloha Hawaii!), warme Sonnenstrahlen im Frühling (oder einfach eine Umarmung), ein ausgiebiger Spaziergang (oder Laufrunde) in der Natur, ein harmonisches (Nasenflöten-)Konzert, ein Kaffee am Morgen (um Punkt 7 Uhr im Seminarraum) oder der Duft von frisch gebackenem Kuchen (Kuchääään, ich raste aus!) angefühlt hat. Ich könnte diese Liste noch ellenlang weiterführen! Ihr habt mir emotionalen Halt gegeben und ich konnte wunderbar mit Euch lachen. Ohne Euch hätte ich das nicht geschafft, deswegen *Danke*!

Zuletzt möchte ich mich noch bei meinen Eltern bedanken, die wirklich immer für mich da sind, wenn ich sie brauche. Das ist ein wunderbares Privileg, dass ich nicht missen will. Aber auch *Danke* an meine große Schwester Jasmin, auf die ich sehr stolz bin.

Ich bin sehr froh, dass mich noch viele weitere, nicht weniger wichtige Freunde und Familienmitglieder, KollegInnen und meine Mentorin Sabine Höppner begleitet haben.

Und als Letztes noch ein liebevolles *Mahalo* an Dich, Jonas!

## Declaration

I hereby declare that this thesis has been written only by the undersigned and without any assistance from third parties. Furthermore, I confirm that no sources have been used in preparation of this thesis other than those indicated in the thesis itself.

Munich, March 01, 2023

Isabel Aschenbrenner

# Appendix

## I. Biogenesis and engineering of interleukin 12 family cytokines

Published by Karen Hildenbrand[1], **Isabel Aschenbrenner**[1], Fabian C. Franke, Odile Devergne, and Matthias J. Feige in *Trends in Biochemical Sciences* (2022) 47(11): 936-949.
DOI: 10.1016/j.tibs.2022.05.005

([1] equal contribution)

CellPress

Trends in Biochemical Sciences

Review

# Biogenesis and engineering of interleukin 12 family cytokines

Karen Hildenbrand,[1,3] Isabel Aschenbrenner,[1,3] Fabian C. Franke,[1,3] Odile Devergne,[2,*] and Matthias J. Feige[1,*]

Interleukin 12 (IL-12) family cytokines are secreted proteins that regulate immune responses. Each family member is a heterodimer and nature uses shared building blocks to assemble the functionally distinct IL-12 cytokines. In recent years we have gained insights into the molecular principles and cellular regulation of IL-12 family biogenesis. For each of the family members, generally one subunit depends on its partner to acquire its native structure and be secreted from immune cells. If unpaired, molecular chaperones retain these subunits in cells. This allows cells to regulate and control secretion of the highly potent IL-12 family cytokines. Molecular insights gained into IL-12 family biogenesis, structure, and function now allow us to engineer IL-12 family cytokines to develop novel immunotherapeutic approaches.

## Highlights

Interleukin 12 (IL-12) family cytokines connect innate and adaptive immunity and are key signaling molecules in the immune system.

Nature uses shared building blocks to assemble the functionally distinct family members.

In recent years, we have gained detailed mechanistic insights into IL-12 cytokine biogenesis on the transcriptional, translational, and post-translational level, as well as structural insights into receptor binding.

Currently, IL-12 family members are (re-)emerging as very attractive molecules for immunotherapeutic approaches.

## IL-12 family cytokines: demanding but capable

The human immune system can adapt, learn, and memorize. It is a network of billions of cells that have to be regulated and controlled in order for immune reactions to be efficient while protecting the host. This immense complexity is, among others, regulated by secreted signaling proteins, the **interleukins (ILs)** (see Glossary). In humans, around 40 different ILs are known to date [1]. ILs are classified into structurally related protein families and, among those, one family stands out: the IL-12 family. Generally, human ILs are monomeric or homooligomeric proteins, but members of the IL-12 family are heterodimers. Furthermore, all family members are made up of a limited set of shared subunits [2]. This complexity poses significant challenges during the biogenesis of IL-12 family **cytokines**. At the same time, due to their key role in connecting innate and adaptive immunity and thus shaping immune responses, IL-12 family cytokine biogenesis has to be tightly regulated and controlled. This review summarizes our current understanding of how cells produce IL-12 family cytokines, a field in which many new insights have been obtained during recent years, and how this may be translated into new therapeutic approaches that harness the power of our immune system.

## Structural and functional principles of IL-12 cytokines: it runs in the family

Each IL-12 family member consists of an α and a β subunit. The α subunits possess a four-helical bundle structure typical for many human cytokines, including IL-2 and IL-4 [3]. The four α-helices are arranged in an 'up-up-down-down' fashion, which originates from the antiparallel orientation of two consecutive pairs of helices first described for porcine growth hormone [4] (Figure 1A). The β subunits, by contrast, have an all-β structure that is similar to the one found in cell-surface type I and II cytokine receptors and comprises fibronectin and immunoglobulin domains (Figure 1A). This heterodimeric nature of IL-12 cytokines reflects their evolutionary history. The current heterodimers have likely evolved from 'classical' cytokines and their receptors, the latter of which have become soluble components of the cytokines themselves during evolution [5]. This is reminiscent of proteolytic shedding of cell-surface cytokine receptors, where shed receptor subunits pair with their cytokine partner to act as one signaling entity [6].

[1]Department of Chemistry, Technical University of Munich, 85748 Garching, Germany
[2]Sorbonne Université, INSERM, CNRS, Centre d'Immunologie et des Maladies Infectieuses (Cimi-Paris), 75 013 Paris, France
[3]These authors contributed equally to this work

*Correspondence:
odile.devergne@inserm.fr (O. Devergne) and matthias.feige@tum.de (M.J. Feige).

 https://doi.org/10.1016/j.tibs.2022.05.005

Trends in Biochemical Sciences

CellPress

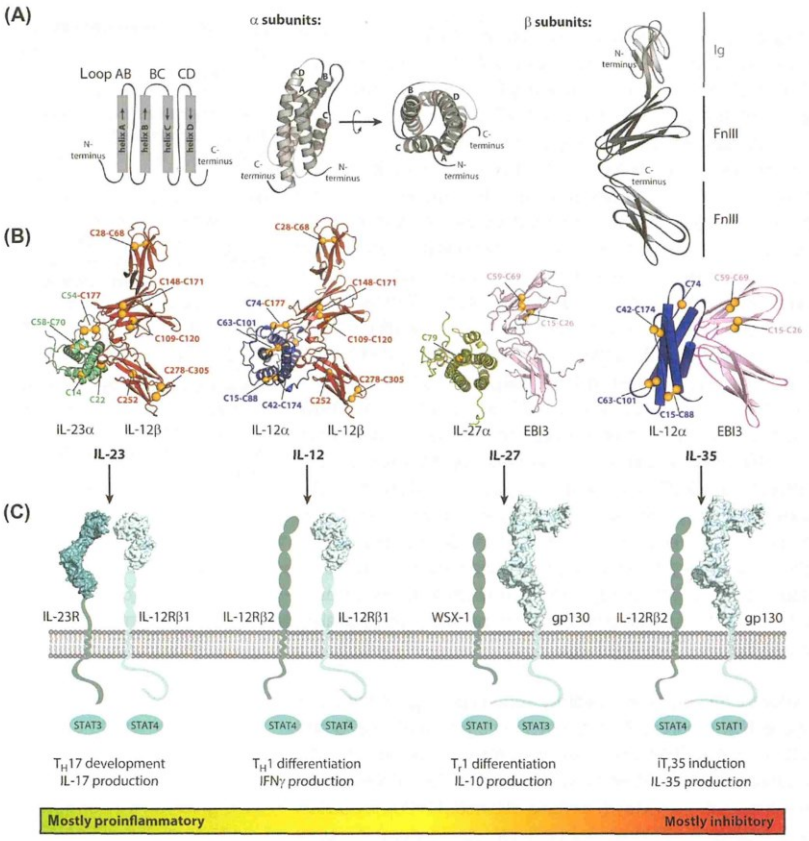


(D) Exceptions from the rule:

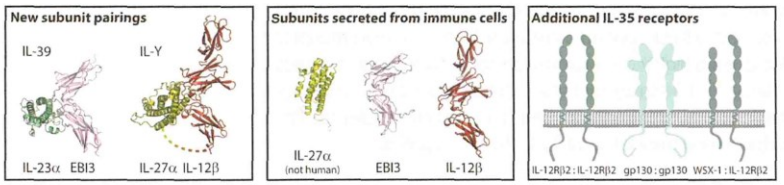


Figure 1. Setup of the human interleukin (IL)-12 family. (A) Schematics of IL-12 family cytokine subunits. All α subunits possess a four-helical bundle structure with an 'up-up-down-down' topology (arrows) of helix A to helix D connected via loops. β subunits contain two **fibronectin type III (FnIII) domains** and, in the case of IL-12β, an additional N-terminal immunoglobulin (Ig)-like domain. (B) The four IL-12 family members are made up of five different subunits: IL-23α, IL-12α, IL-27α, IL-12β, and EBI3. One α subunit pairs with one β subunit to form the respective heterodimeric cytokine IL-23, IL-12, IL-27, or IL-35. Crystal structures of IL-23 (PDB: 3D87) and IL-12 (PDB: 3HMX), a modeled structure of IL-27 [65], and a hypothetical model for IL-35 are depicted, since the IL-35 AlphaFold model is not in agreement with available experimental data on the heterodimerization interface [69]. Positions of free cysteines and disulfide bonds are indicated as orange spheres, numbering of residues begins after the signal sequence. (C) IL-12 family receptors pair to form functional receptors and are shared

*(Figure legend continued at the bottom of the next page.)*

## Glossary

**B cell:** a lymphocyte that produces antibodies and expresses B cell receptors on the plasma membrane as part of the adaptive humoral immune system.

**BiP:** *immunoglobulin* heavy chain binding protein; a Hsp70 molecular chaperone in the ER that interacts with incompletely folded proteins, originally discovered to bind antibody heavy chains.

**Calnexin (CNX):** a membrane-integrated lectin chaperone of the ER that interacts with newly synthesized glycoproteins as part of the ER quality control.

**Chimeric antigen receptor (CAR) T cell:** transgenic T cell that produces an artificial T cell receptor, mediating antigen-binding and T cell activation, for use in immunotherapy.

**Cytokine:** a protein that acts as a cell signaling molecule and induces and/or regulates differentiation and proliferation of cell populations through binding of cell surface receptors (e.g., an interleukin).

**Epstein-Barr virus-induced gene 3 (EBI3):** one of the five cytokine subunits of the IL-12 family that pairs as a soluble cytokine receptor homolog with IL-27α to form IL-27 and with IL-12α to form IL-35.

**ER-associated degradation (ERAD):** pathway for protein quality control in the ER, targeting proteins for dislocation and proteasomal degradation.

**Fibronectin type III (FnIII) domain:** a conserved protein domain, historically originating from the glycoprotein fibronectin, with a β sandwich fold.

**Interleukin (IL):** a cytokine that is secreted by immune cells and regulates immune responses (e.g., IL-12).

**Jak/STAT:** Janus kinase-signal transducer and activator of transcription pathway; cytoplasmic tyrosine kinase Jak family that activates the intracellular transcription factor STAT family via phosphorylation as a result of cytokine signaling with effects on cell growth, differentiation, and survival.

**Matrix metallopeptidase 9 (MMP-9):** zinc-metalloproteinase that is involved in degradation of the extracellular matrix and plays a role during tumor progression in several cancer entities, in which it is frequently overexpressed.

**Molecular chaperone:** a protein that aids in proper folding or refolding of (partially) unfolded or misfolded proteins into their native, functional structure.

Nature uses extensive subunit sharing to build the different IL-12 heterodimers. Three α and two β subunits form the different heterodimers, with IL-12α (also named IL-12p35) and IL-12β (IL-12p40) constituting IL-12; IL-23α (IL-23p19) and IL-12β forming IL-23; IL-27α (IL-27p28) and **Epstein-Barr virus-induced gene 3 (EBI3)** constituting IL-27; and IL-12α and EBI3 forming IL-35 (Figure 1B). This combinatorial complexity also applies to IL-12 family receptors, which are generally also heterodimers, formed by five different shared chains (Figure 1C). Binding of the corresponding IL induces receptor chain heterodimerization, thereby activating **Jak/STAT** signaling pathways [2]. Subunit sharing on the level of cytokines and receptors may suggest closely related functions of IL-12 family cytokines, but this notion is misleading. The founding member of the IL-12 family, IL-12 itself, is a key immune-activating cytokine that is secreted from antigen-presenting cells and regulates proinflammatory functions of **T cells**, for example, by inducing T helper 1 ($T_H1$) cells and CD8+ cytotoxic T cells that are key for inflammatory reactions in fighting infections but also tumors [7]. IL-23 is the most proinflammatory IL-12 family member and plays a crucial role in inducing and maintaining $T_H17$ cell populations that secrete the strongly proinflammatory cytokine IL-17 [8]. As such, several IL-23-blocking antibodies have entered the clinics for inflammatory diseases [9]. IL-27 is an immune-modulatory cytokine, which on the one hand is able to promote $T_H1$ differentiation and on the other hand suppresses proinflammatory $T_H17$ cells and induces anti-inflammatory IL-10-producing T regulatory 1 ($T_r1$) cells [10]. IL-35 is the only strictly immune-inhibitory family member. It suppresses conventional T cells and induces their conversion into suppressive regulatory T cells called iTr35 [11] (Figure 1C). Taken together, IL-12 family cytokines have very distinct, and even opposing immune functions, which are summarized in excellent reviews [2,12,13]. IL-12 cytokines thus encompass a key concept in immunology within one family: that pro- and anti-inflammatory signaling molecules are needed for a balanced immune reaction [14].

In addition to the four core IL-12 family members, new intrafamily subunit pairings termed IL-Y and IL-39 have been reported (Figure 1D). Whereas IL-Y is a synthetic fusion of IL-27α and IL-12β [15], IL-39 (composed of IL-23α and EBI3) has been described to be secreted by **B cells** in mice and to induce inflammatory reactions [16]. However, no indication for IL-39 existence in humans is available yet and the existence of IL-39 generally remains debated [17–20]. In addition to the heterodimeric family members, isolated IL-12 family subunits can also perform immune-regulatory functions. Unpaired forms of IL-12β, IL-27α, and EBI3 are secreted from certain cell populations and in certain species, and free IL-12β and EBI3 are often secreted in excess over IL-12, IL-23, and IL-27 heterodimers [10,21–23] (Figure 1D). Once secreted, isolated subunits can either act by themselves or pair with circulating cytokine subunits or shed receptor chains [23–28]. Together, this establishes a highly complex molecular network that underlies IL-12 family cytokine functions. Since IL-12 family members have very potent immune-regulatory functions, their biogenesis and secretion thus need to be tightly regulated. The first layer of regulation is the transcription and translation of IL-12 family subunits.

## Regulation of IL-12 family transcription and translation

In inflammatory settings, cells of the myeloid lineage, such as monocytes, macrophages, dendritic cells, microglia, or neutrophils, are major sources of IL-12, IL-23, or IL-27. Other cell

**Protein disulfide isomerase (PDI):** oxidoreductase protein family catalyzing oxidative protein folding via disulfide bond formation/reduction/isomerization using catalytic thioredoxin-like domains.
**Single chain variable fragment (scFv):** artificial antibody fragment containing the antigen-binding variable domains of the light and heavy chains fused together via a short linker to generate a single chain protein.
**T cell:** a lymphocyte as part of the adaptive immune system recognizing antigen peptides via the cell surface T cell receptor and being responsible for cell-mediated immunity (e.g., $T_H1$, $T_H17$, $T_r1$, iT$_r$35).
**Toll-like receptor (TLR):** a protein of the innate immune system recognizing structurally conserved molecules of microbes, thus activating immune cell responses.

between ILs. High resolution structures for IL-23R (PDB: 5MZV), gp130 (PDB: 3L5H), and IL-12Rβ1 (PDB: 6WDP) are shown in surface representation, unresolved/low-resolution structures are depicted as schematic. Divergent immunological functions are mediated via different Janus kinase (Jak1, Jak2, Tyk2)-signal transducers and activators of transcription (STAT) pathways [2,12]. (D) Left: new IL-12 family members IL-39 and IL-Y (covalently linked) are depicted as AlphaFold models. Middle: single subunits IL-27α, EBI3, and IL-12β were reported to be secreted independent of their partner subunits. Right: in murine T and B cells, additional IL-35 receptor pairings in addition to IL-12Rβ2/gp130 (C) have been reported [99,100]. Abbreviations: IFN, interferon; $T_H$, T helper; $T_r$, T regulatory; iT$_r$35, suppressive regulatory T cell induced by IL-35.

types such as epithelial, endothelial, or tumor cells can additionally account for their production [23,29]. IL-35 stands out from other IL-12 family members as it appears to be primarily expressed by specific subsets of regulatory T and B lymphocytes and by tumor cells, even though myeloid cells such as tolerogenic dendritic cells and tumor-associated macrophages also express it [30].

In myeloid cells, transcription of the genes encoding IL-12α, IL-12β, IL-23α, IL-27α, or EBI3 is triggered through activation by microbial products of pattern recognition receptors, such as **Toll-like receptors (TLR)**-3, -4, -7, or -9, as well as by ligation of the co-stimulatory cell surface molecules CD40 or 4-1BB. Further contributing to gene transcription are proinflammatory cytokines, especially type I and II interferons. These stimuli act in concert to initiate downstream signaling cascades that ultimately result in the activation and binding of transcription factors, such as NF-κB (RelA, RelB, and c-Rel), interferon regulatory factors (IRFs; IRF-1, IRF-3, IRF-8, and IRF-9), c-EBP, or Ets family members (PU-1 and Ets-2), to the promoter regions of IL-12 family genes [23,29,31]. Of note, although common pathways induce transcription of both α and β subunits in myeloid cells, the magnitude and kinetics of the transcriptional responses often vary for each subunit. In human activated dendritic cells, for example, expression of *EBI3* transcripts is longer lasting than that of *IL12α* and *IL27α* transcripts [10]. In addition to immune signals, metabolism also controls IL-12 family transcription, as shown by the glycolytic enzyme PKM2, which partners with c-Rel to induce *IL12α* transcription in dendritic cells [32]. In regulatory T cells, the transcription factor Foxp3 is required for *EBI3* expression, while IRF-4 and IRF-8, together with the transcription factor BATF, are involved in transactivation of *EBI3* and *IL12α* promoters in regulatory B cells [30,33]. Counteracting IL-12 family cytokine production, several factors negatively regulate IL-12 family transcription, such as purinergic receptors and the complement product C5a [23,29].

Expression of IL-12 family cytokines is also regulated at a post-transcriptional level by different mechanisms. Early work had shown that murine IL-12α expression can be controlled through the use of alternative transcription start sites that could lead to inhibition of its translation [34]. Expression of IL-12 family cytokines is further controlled through mRNA degradation. As an example, the endoribonuclease Regnase-1 has been reported to degrade *IL12β* mRNA [35], while the RNA-binding protein tristetraprolin promotes the decay of both *IL23α* and *IL27α* mRNAs [36,37]. In addition, several miRNAs, such as *miR-21* that bind to the 3′ untranslated region (UTR) of *IL12α*, negatively regulate IL-12 expression [38–40]. By contrast, the long noncoding intergenic RNA, *lincRNA-Cox2*, that is induced in macrophages upon TLR activation, appears to positively regulate *IL23α* transcription [41].

Collectively, these studies highlight the complexity of IL-12 family cytokine expression and the fact that for a given member, the expression of its α or β subunit is not always coregulated, both at the transcriptional and post-transcriptional level. This points out that cytokine formation also needs to be tightly controlled at the protein level.

## Biogenesis of IL-12 family cytokines: structural insights and cellular regulation

Once translated, IL-12 family cytokines need to assemble to form bioactive αβ heterodimers. This assembly occurs in the endoplasmic reticulum (ER), the central hub for protein biogenesis of the eukaryotic secretory pathway. Nature has evolved intricate mechanisms and machineries that support IL-12 cytokine formation (Box 1). This is highly relevant due to the shared subunits IL-12 family cytokines use and the autonomous functions some unpaired subunits possess. At the same time, it provides another layer of control for immune system functions, the basis of which we are just beginning to understand. Biogenesis in the ER will be described in the following paragraphs for each of the four established IL-12 family members, with a focus on human cytokines.

CellPress Trends in Biochemical Sciences

### Box 1. General principles of IL-12 family cytokine biogenesis

For human IL-12 family cytokines, a clear principle has emerged in recent years to underlie their biogenesis: α subunits are incompletely structured in isolation and hardly, if at all, secreted by themselves. Instead, isolated α subunits are targeted for degradation. By contrast, human β subunits are secretion-competent on their own, induce structure formation in their designate partner α subunit, and thus regulate trafficking and export of the heterodimeric cytokine. Interestingly, in other species this behavior is reversed, for example, mouse IL-27α is readily secreted, but mouse EBI3 depends on IL-27α coexpression for secretion [10,65]. Notwithstanding these differences, we generally have one secretion-competent and one assembly-dependent subunit, with murine IL-23 potentially being an exception [8]. Assembly-induced secretion/transport is a principle also found for antibodies and the T cell receptor, other key immune proteins [97,98]. For IL-12 family cytokines, however, this principle becomes biologically even more interesting: the secretion competent IL-12 family subunits, be it the α or the β subunit, often perform autonomous immune-modulatory functions. This argues that this behavior has likely evolved due to functional needs of, for example, maintaining balanced immune reactions. Due to our recent molecular insights into IL-12 family folding and assembly, animal studies where both subunits are secretion-incompetent and thus need each other for secretion now become possible and will reveal if this hypothesis is valid.

A further general principle that emerges from recent studies on IL-12 family cytokines is that, quite unusual for secreted proteins, they have several disulfide bonds (Figure 1B) that are dispensable for secretion (IL-12α, [53]) or even free cysteines (IL-27α, [63] and IL-23α, [60]). These cysteines may thus be present to engage cellular chaperone machineries to regulate and control IL-12 family cytokine assembly, which is crucial in the light of distinct biological functions but subunit sharing. Glycosylation of IL-12 family cytokines [64] further allows recruitment of the lectin-based chaperone systems of the ER, providing another layer of support and control for IL-12 family cytokine assembly.

## Biogenesis of IL-12

IL-12, the founding member of the family, consists of the subunits IL-12α and IL-12β [7]. IL-12α secretion depends on its pairing with a partner subunit, IL-12β in the case of IL-12 [42,43]. By contrast, IL-12β can also be secreted in isolation as a monomer and homodimer with likely autonomous and distinct immunological functions. These include inhibiting IL-12 signaling and also regulating airway and other inflammatory responses, as shown by the ability of IL-12β to act as a chemoattractant for macrophages and to regulate nitric oxide synthase expression, downstream cytokine induction, and IL-12 receptor expression [24,27,44–52]. Structural insights into IL-12β homodimer assembly are lacking. Hence, we are still at early stages in dissecting the different IL-12β functions. Since IL-12α is expressed in many cell types [23], the dependency on a partner subunit generally allows regulation of IL-12 secretion. Recent work has revealed the molecular basis of this behavior (Figure 2A). If unpaired, IL-12α fails to acquire its native structure and forms non-native disulfide bonds and various molecular species, including homodimers and oligomers. Due to this incomplete folding in isolation, unpaired IL-12α is recognized and retained in the cell by the ER chaperone machinery [53,54], including members of the **protein disulfide isomerase (PDI)** family [53,55]. In the light of this finding, it is interesting to note that IL-12α has three intramolecular disulfide bonds (Figure 1B), two of which are dispensable for assembly-induced folding and formation of IL-12 [53]. This may argue that cysteine:PDI interactions play a role in regulating the secretion of IL-12 family members. The same applies to the disulfide bond that covalently stabilizes the interaction between IL-12α and IL-12β: it is dispensable for secretion of the heterodimer [56] but may stabilize the heterodimer against dissociation once secreted and might play a role in assembly control. If no pairing with IL-12β occurs, IL-12α will ultimately be degraded via **ER-associated degradation (ERAD)** [57], which involves the ERAD factor HERP [58] and potentially also the PDI ERdj5 to reduce wrong disulfide bonds [53]. By contrast, if pairing with IL-12β occurs, IL-12α correctly folds and is efficiently secreted as heterodimeric IL-12 [43,53]. The complex chaperone repertoire that caters for IL-12 assembly might also be sensitive to drugs that affect the ER folding environment [55], which may impact IL-12 secretion and thus contribute to some of the drugs (side) effects.

Since the IL-12 cytokine family subunits are shared and structural changes occur upon heterodimer formation, the dimerization interface is of particular interest. The interlocking topography of IL-12α and IL-12β is mediated by several charged residues via the helical face of the A and D

Trends in Biochemical Sciences

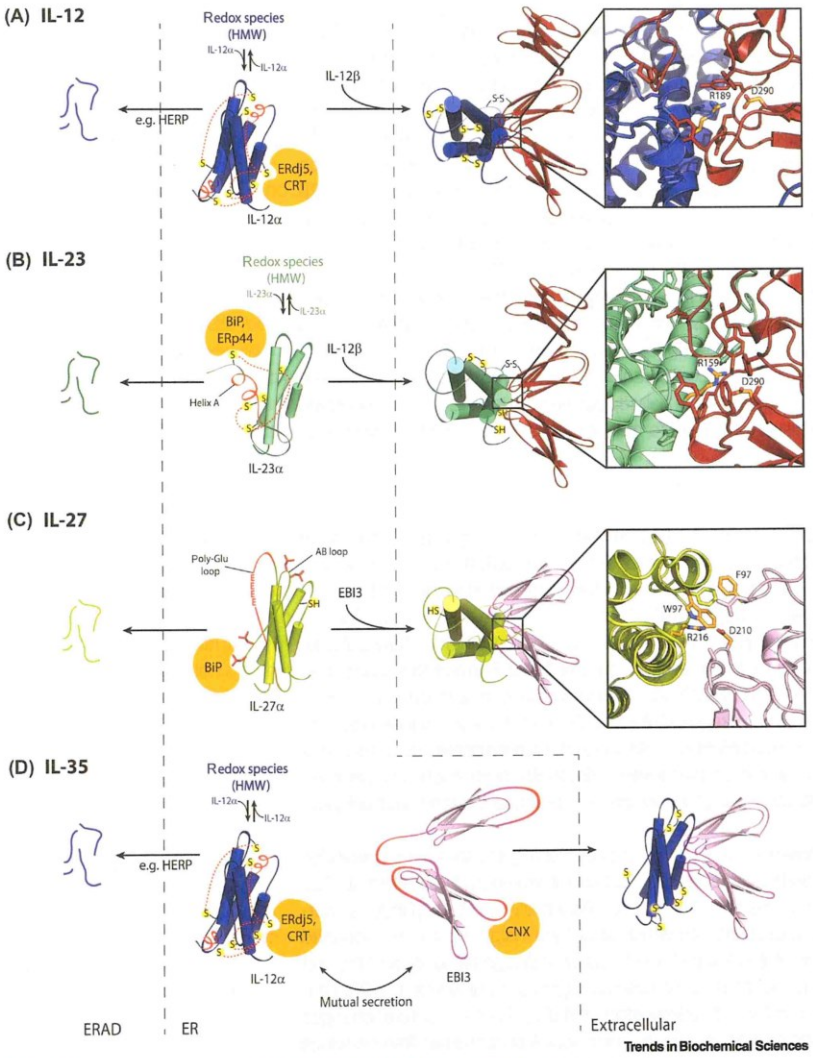


Figure 2. Molecular mechanisms of interleukin (IL)-12 cytokine biogenesis. Critical elements (highlighted in red) and **molecular chaperones** involved in IL-12 family endoplasmic reticulum (ER) quality control are depicted for each member. Successful biogenesis of heterodimeric ILs leads to secretion (Extracellular), otherwise subunits are degraded via ER-associated degradation (ERAD). Interfaces are shown as magnified images (boxes) (IL-12, PDB: 3HMX; IL-23, PDB: 3D87; IL-27 model, [65]). Critical interface residues are labeled and marked in orange. Residues forming salt-bridges or hydrophobic interactions in the direct surrounding of the core are shown as sticks. Details on the subunit pairings: (A) in isolation, IL-12α forms non-native disulfide bonds (red broken lines), thus misfolds and forms redox species of high molecular weight (HMW), including dimers. Upon pairing with IL-12β, the correctly folded, disulfide-linked IL-12 is secreted. The arginine-binding pocket with its charged interaction is highlighted in the interface structure. (B) Helix A of IL-23α is unstructured, highly flexible and erroneous disulfide-linked redox species of IL-23α are formed in absence of IL-12β. The interface of the covalently linked IL-23 heterodimer with its charged interaction is magnified. (C) Hydrophobic residues of IL-27α are exposed in the absence of EBI3 due to the flexibility of the AB and poly-Glu

*(Figure legend continued at the bottom of the next page.)*

helices and the AB-loop of IL-12α packing against loops 1 and 3 from domain 2 and loops 5 and 6 from domain 3 of IL-12β. Characteristic is the central Arg189 residue of IL-12α helix D reaching into a deep arginine-binding pocket of IL-12β with Asp290 at its base to form an Arg–Asp salt bridge. Hydrogen bonds and hydrophobic interactions line the pocket, completing the interface [56] (Figure 2A). Considering this complex interface, it is noteworthy that, whereas isolated IL-12α has a strong tendency to misfold, no misfolding is observed in model cell lines upon coexpression of IL-12β [53]. This argues for efficient and/or rapid IL-12α assembly with IL-12β in cells that either inhibits or corrects IL-12α misfolding. Furthermore, it is unusual for a misfolded protein that normally lacks well-formed interaction interfaces to populate such a well-defined homodimeric species in cells as IL-12α does even in the absence of IL-12β [53]. This may argue for a substantial amount of structure also in unpaired IL-12α, where parts of the dimerization interface outlined earlier may be present. Such species could potentially form a reservoir for assembly with IL-12β, once expression of IL-12β begins, allowing for rapid proinflammatory responses. In further support of this idea, a pool of assembly-competent IL-12α may more efficiently compete with secretion of IL-12β, that has distinct and potentially opposing effects to IL-12 once secreted [44–46]. Other modes of IL-12α secretion and IL-12 formation are discussed, but their mechanistic basis remains to be defined [26].

### Biogenesis of IL-23

The IL-23 heterodimer comprises IL-23α and IL-12β [8]. Although IL-12 and IL-23 share the same β subunit, the interactions between IL-23α and IL-12β are somewhat different compared with IL-12. In comparison to IL-12α, the IL-23α subunit is tilted and rotated within the heterodimeric structure. As a consequence, IL-23α Arg159 of helix D forms the critical salt bridge to Asp290 of the IL-12β arginine-binding pocket and is surrounded by different hydrophobic contacts and polar interactions at the interface periphery than for IL-12. Furthermore, compared with the largely disordered AB-loop in IL-12α, IL-12β forms several more contacts with the AB-loop of IL-23α near its interchain disulfide bond linkage [59] (Figure 2B). IL-12β thus engages in at least two, and possibly more [24], heterodimeric cytokines. Although the nature of the interactions that constitute the interface (i.e., charged interactions lined with hydrophobic and peripheral polar interactions) is conserved in IL-12 and IL-23, most of the interface is structurally distinct and unique.

Like IL-12α, IL-23α depends on assembly with IL-12β for secretion [8] and forms multiple redox species via non-native disulfide bonds in its absence [53,60]. Interestingly, like IL-12α, IL-23α populates dimeric species in the absence of IL-12β [53,60]. Assembly with IL-12β induces correct folding of the IL-23α subunit, a process into which structural insights could be obtained recently (Figure 2B). In the absence of IL-12β, IL-23α shows overall high flexibility and the first of its four helices (helix A) appears to be mostly unstructured. Upon assembly with IL-12β, helix A becomes structured and the remainder of IL-23α is stabilized [60]. These structural changes are coupled to an intricate chaperone recognition mechanism: helix A contains two free cysteines and binding sites for the major ER chaperone **BiP**. While unpaired, the sites are free to engage PDIs, including ERp44 as well as BiP [60]. This confers ER retention of unassembled IL-23α. Once assembled with IL-12β, due to the folding of helix A, the chaperone binding sites are buried within the native structure, allowing release from the ER. The single internal disulfide bond within IL-23α is needed for IL-23 secretion, whereas, like for IL-12, the covalent disulfide linkage of IL-23α with IL-12β is dispensable for subunit interaction and secretion [60]. IL-23 has

loops [63]. Subunit interactions of the noncovalently linked IL-27 are mediated via aromatic and charged residues. (D) For IL-35, IL-12α and EBI3 mutually enhance their secretion. IL-12α in isolation behaves as described in (A). EBI3 is bound by the chaperone calnexin (CNX). For IL-35, depicted as hypothetical model, neither its structure nor the interface is known. Abbreviations: BiP, immunoglobulin heavy chain binding protein; CRT, calreticulin.

thus developed an intricate mechanism that allows the ER chaperone machinery to oversee its assembly and which likely plays an active role in tuning it. In the light of this complex assembly control it is noteworthy that biological functions for unpaired IL-23α have also been described [61]. It will be important to reveal how IL-23α in this case obtains a biologically active structure.

### Biogenesis of IL-27

IL-27 is composed of IL-27α and EBI3, which form a noncovalent heterodimer [10]. IL-27α shows structural homology to the aforementioned α subunits, with one exception being a unique glutamic acid stretch (poly-Glu loop) in the CD loop [62]. In isolation, human IL-27α is not secreted but requires interaction with EBI3 for assembly-induced secretion as part of the heterodimeric IL-27 complex [10]. The underlying mechanisms were recently revealed (Figure 2C). Structural dynamics of the poly-Glu loop and exposed hydrophobic residues cause IL-27α to bind the chaperone BiP, which results in ER retention and rapid degradation of the unassembled IL-27α subunit via ERAD [63]. Only upon coexpression of EBI3, IL-27α is stabilized and hydrophobic regions are buried within the helical structure, which releases it from chaperone-mediated retention [63]. Once assembled, the heterodimeric complex further traverses through the Golgi, where human IL-27α becomes *O*-glycosylated before secretion [10,64]. Unlike IL-12α and IL-23α, human IL-27α has only one single cysteine residue located in helix B (Figure 1B). It therefore lacks an internal disulfide bond [63]. Available structural models reveal similarities of IL-27α to the ciliary neurotrophic factor cytokine, suggesting an evolutionary relationship. Within the IL-27 interface, the conserved and solvent-exposed Trp97 of IL-27α interacts with Phe97 of EBI3. This aromatic interaction is further supported by salt bridges between the rather positively charged surface of IL-27α (e.g., Arg216) and the negatively charged surface of EBI3 (e.g., Glu159, Asp210) [65,66] (Figure 2C). Although an IL-27 crystal structure is not yet available, critical interface residues could be verified via mutation and the slightly rotated conformation of α and β subunits compared with IL-12 and IL-23 could be confirmed by molecular docking [65], further extending the structural setups found for IL-12 cytokine heterodimerization. Very recent studies [67,68], in particular the first high-resolution cryogenic electron microscopy analyses on the structure of the IL-27:receptor complex [67], are in agreement with the available IL-27 models and significantly extend our understanding of its receptor engagement.

### Biogenesis of IL-35

EBI3 is not an exclusive component of IL-27 but also forms a noncovalent heterodimer with IL-12α, termed IL-35 [22]. In contrast to IL-12, IL-23, and IL-27, for which detailed structural insights into the heterodimerization interface are available, the IL-35 interface remains completely undefined (Figure 2D). Furthermore, IL-35 is largely unaffected by amino acid substitutions that affect other IL-12 family members [69]. IL-35 thus seems to have a distinct pairing interface compared with all other IL-12 family members. In agreement with this notion, bacterially produced IL-12α could form IL-12 but not IL-35 [70], which may be due to the lack of glycosylation in bacterially produced proteins, as recent data suggest glycosylation to be important for IL-35 formation [64]. Together, these findings indicate that complex formation of IL-12α and EBI3 might be weaker and that it clearly differs from the other family members.

Despite these differences and analogous to IL-12β, EBI3 is required to release IL-12α from ER retention and for subsequent secretion of the heterodimeric complex [22] (Figure 2D). In contrast to IL-12, IL-35 secretion is by far less efficient, which might be due to the inefficient secretion of EBI3 itself compared with IL-12β [22] and likely due to differences in complex formation [69]. Furthermore, EBI3 not only induces secretion of IL-12α but is itself more efficiently secreted in the presence of IL-12α, although the effect is less pronounced [22]. This mutual secretion of an α and β subunit can further be observed for IL-27, arguing that for human IL-27 and IL-35,

both the α and the β subunit are labile in isolation and need each other for stabilization and efficient export. In agreement with this, the lectin chaperone **calnexin (CNX)**, which is involved in the folding of newly synthesized glycoproteins in the ER [71], associates with EBI3 [72]. Normally, CNX mostly acts on membrane-associated proteins [71]. It is thus interesting to note that, although lacking a membrane anchor, EBI3 has been described to localize to the cell surface [72], potentially also in a complex with IL-23R [73]. Furthermore, colocalization of IL-12α and EBI3 on the surface of tolerogen-specific regulatory T cells has been reported [74]. In agreement with a somewhat special role of EBI3 in the IL-12 family, EBI3 itself seems to have chaperone-like functions on other proteins. By binding of EBI3 to CNX and IL-23R, IL-23R expression is augmented and degradation is reduced [73]. Even though CNX is necessary for this EBI3-mediated folding, and further data to back up these ideas are needed, EBI3 may thus perform intracellular roles independent of the cytokines to which it contributes.

## IL-12 family cytokines: new opportunities for immune engineering

The pivotal roles IL-12 family cytokines play in regulating immune responses is underlined by many severe pathologies, including cancer and immune-mediated inflammatory diseases, in which they are involved [13,75]. Accordingly, IL-12 family cytokines are promising targets but also candidates as immune-modulatory agents for therapeutic interventions [12]. Many intrinsic features of therapeutic cytokines, however, such as poor manufacturability, stability, short plasma half-life, and poor selectivity, demand further developments [76]. To improve cytokine-based therapeutics, several protein engineering strategies have been employed. These include sequence alterations to optimize protein folding, stability, or activity, as well as the generation of cytokine fusion proteins to increase plasma half-life or to equip the engineered cytokine with additional functions [76]. Poor selectivity has been tackled by modulation of receptor binding interfaces [77–80]. The design of synthetic cytokines in turn not only offers the opportunity to improve selectivity but also to activate novel receptor combinations [81].

Many of the aforementioned approaches have been used to improve IL-12 family cytokines as therapeutic agents or to generate completely novel immune-modulatory activities within this already diverse cytokine family (Figure 3). Subunit and receptor chain sharing renders this family particularly attractive for the design of new cytokine pairs, but also for improving selectivity. IL-12 is a potent proinflammatory cytokine with remarkable antitumor effects in several cancer entities. However, its systemic administration is associated with severe toxicities, so far limiting its clinical use [13]. Engineering of IL-12 thus primarily focused on improving selectivity or attenuating its activity. Toward this aim, cytokine protein fusions proved to be a flexible toolbox. Fusion of IL-12 to tumor-directed moieties, such as the tumor necrosis targeting antibody NHS76 or the von Willebrand factor A3 collagen binding domain, resulted in reduced toxicity due to local accumulation of the cytokine fusion in the tumor [82–84]. Besides tumor-targeting moieties, IL-12 was also fused as single chain variant to an IL-12 binding **single chain variable fragment (scFv)** via a **matrix metallopeptidase 9 (MMP-9)**-cleavable linker. This attenuated its activity until cleavage by MMP-9 (which is overexpressed in cancerous tissues) occurs [85] and shows that attenuation combined with local activation is a promising avenue to develop IL-12-based therapeutics. Other approaches, in which IL-12 is not directly modified, include the use of nucleic acids, viruses, and transgenic cells [such as **chimeric antigen receptor (CAR) T cells**] for local IL-12 production, or local injection of sustained release platforms [84]. Biochemical and structural insights into IL-12 family cytokine receptor binding [86–88] provide a further avenue for rational engineering. Focusing on the structural properties of IL-12, a recent study showed that modification of the receptor binding interface of the IL-12β subunit reduced its affinity to IL-12Rβ1 and thus improved selectivity of CD8+ T cell over natural killer cell activation. This

Trends in Biochemical Sciences

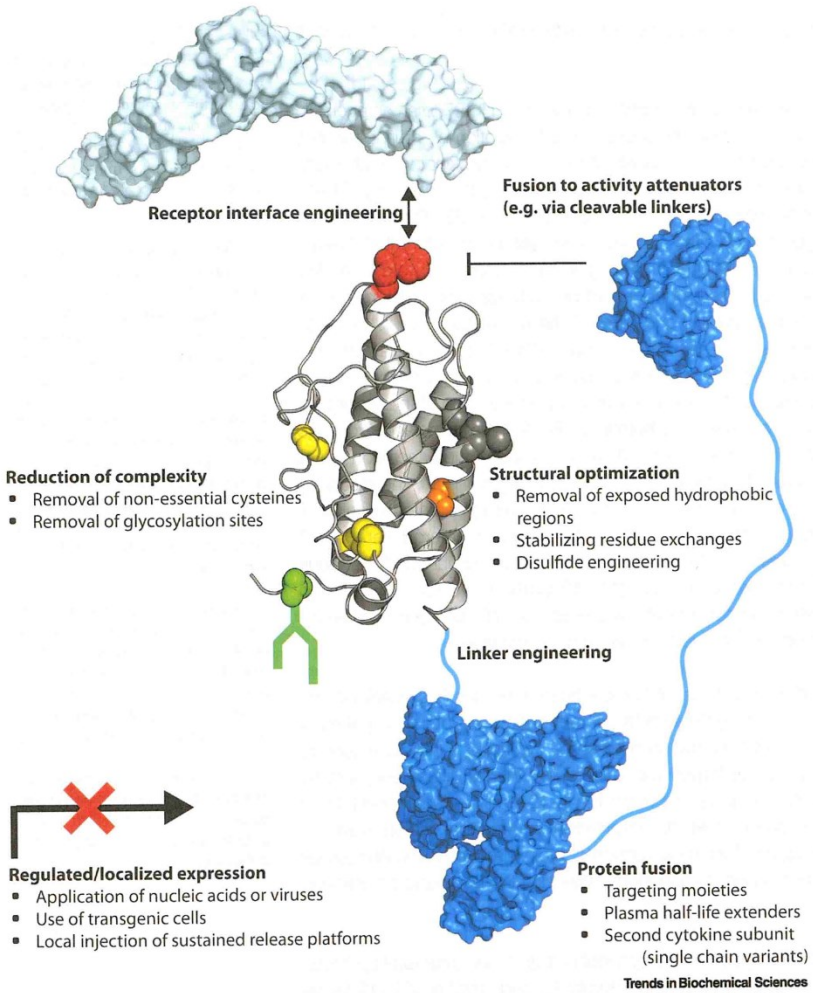


Figure 3. Engineering strategies for interleukin (IL)-12 family cytokines. Functionality and selectivity of IL-12 family cytokines can be directly enhanced by changes in the receptor binding interface (highlighted by red residue), by regulated and/or localized expression of the cytokine at the target site, or by protein fusion (highlighted in blue) to targeting moieties such as antibodies, as well as to cleavable activity attenuators. Protein fusion technology also allows the extension of the half-life of biologics during circulation and can be used to generate single chain cytokine variants. The activity and functionality of cytokines can be affected by the fusion partner, highlighting the importance of identifying optimal linkers for each cytokine fusion protein (highlighted in blue). Furthermore, the complexity of cytokines can be reduced by deletion of glycosylation sites (highlighted in green) and removal of nonessential cysteine residues, which could otherwise promote misfolding and, as well as glycosylation, increase heterogeneity during protein production (cysteine residues highlighted in yellow). Protein stability and possibly secretion can be improved by removal of surface exposed hydrophobic patches (highlighted in dark gray), exchanging destabilizing residues (highlighted in orange), or by introducing additional disulfides (cysteine residues highlighted in yellow). The protein structures shown here are only exemplary for the strategies employed and are modified for this purpose based on PDB identifiers 3D87, 5Z0B, 4RZC, and 6WDQ.

way, the engineered IL-12 variant still elicited antitumor immunity, while toxicity was reduced in murine models [88].

Beyond IL-12, engineering receptor binding also allowed the conversion of IL-27 to an antagonistic variant, binding to IL-27Rα but not to gp130, which decreased liver inflammation in a murine hepatitis model [66]. Besides selectivity, manufacturability and stability of IL-12 family cytokines were also subject to optimization, focusing on their secretion-limiting α subunits. Reducing the complexity of IL-12 by deletion of nonessential disulfide bridges in IL-12α is one such approach [53]. Further, with the exception of IL-35, deletion of glycosylation sites resulted in secretion-competent IL-12 family cytokines with functionalities maintained [64,70], thus opening doors to simplified cytokines and/or expression systems. In a rational approach based on insights into IL-23 biogenesis, structural optimization of helix A of IL-23α improved its stability and allowed the engineered subunit to pass chaperone-based ER quality control, thus being secreted in isolation [60]. Interestingly, the optimized IL-23α subunit still exhibited biological activity even in the absence of IL-12β, highlighting the potential design of single subunit cytokine variants with biological effects by optimization of their structural features. A related strategy was used for engineering of human IL-27α. A single amino acid exchange within human IL-27α, which enabled intramolecular disulfide formation, allowed secretion of the biologically active human IL-27α subunit in the absence of EBI3 [63]. Of note, the disulfide-containing murine IL-27α, which is, in contrast to the human variant, naturally secreted in isolation, performs immune-balancing roles and shows functional differences to heterodimeric IL-27 [63,65,89–92]. This potentially indicates a similar role for the engineered human IL-27α subunit and opens up another opportunity for therapeutic use of IL-12 family cytokines: in addition to focusing on family members with strong effects but also systemic side effects, novel engineered immune-modulatory family members may prove useful for systemic applications.

The advent of genetically engineered immune cells for therapeutic interventions (e.g., CAR T cells), gave rise to the need of specifically targeting these cells without directly affecting the patient's immune system. Therefore, instead of solely relying on engineered cytokines, synthetic receptors can be utilized for selective modulation of target cells expressing the modified receptors as transgenes [81,93]. Examples of synthetic receptors within the IL-12 family include constitutively active IL-23R homodimers via deletion of a membrane-proximal extracellular region, chimeric receptors, in which the extracellular region of one IL-12 family receptor was fused to the intracellular region of another IL-12 family receptor, as well as nanobody-based synthetic receptors mimicking IL-23 signaling [94–96].

In summary, receptor interface engineering, protein fusion technologies, and structural optimizations are currently used to optimize selectivity, manufacturability, and stability of IL-12 family cytokines, as well as to introduce novel functions. Molecular engineering, based on insights into IL-12 family biogenesis, additionally allowed the production of single subunit variants with biological activity and potentially distinct immune-modulatory effects compared with the naturally produced dimeric variants. Cytokine engineering thus offers many opportunities for a better understanding and targeting of the immune system. These may be combined with other strategies that do not directly involve modification of the cytokine, but use local cytokine production or release at the target site to improve selectivity. Synthetic receptors will likely accompany engineering of IL-12 family cytokines for optimized immunotherapeutics in the future.

## Concluding remarks

Cytokines of the IL-12 family are structurally unique and functionally of immense importance for the proper functioning of our immune system. Recent years have provided insights into how cells specifically assemble and control the various IL-12 family members as well as structural

### Outstanding questions

IL-35 is structurally not understood and has an unusual receptor repertoire. At the same time, it may constitute a very attractive therapeutic target (e.g., in cancer immunotherapy). New insights into the molecular setup of IL-35 and its receptor repertoire are urgently needed.

Most studies on IL-12 family cytokine biogenesis have been performed in model cell lines. How these translate into immune and tumor cells, with possibly unique chaperones, differing redox conditions, and sometimes ER stress being present remains unknown.

In cells that express different subunits and can thus assemble different IL-12 family members, what governs relative secretion of the pairs and subunits is still not clear. Relative expression, chaperone interactions, or both and potentially even further aspects may impact assembly.

Do further subunit pairings/secreted subunits within the IL-12 family exist of which we do not know yet? And, related to this question, it remains unknown which of the new pairings/secreted subunits do exist in humans and what their biological functions are.

Using molecular engineering approaches, it remains to be seen which are the best possible ways to move forward to bring IL-12 family cytokine-based approaches to the clinics.

insights into receptor engagement by IL-12 cytokines. Together, this provides an ideal basis to begin to translate these insights into new approaches for immunotherapies, for which IL-12 family cytokines are uniquely suited. Despite this major progress, many important questions remain surrounding the IL-12 family, providing exciting opportunities for future research (see Outstanding questions).

## Acknowledgments

We thank Dr Korbinian Liebl, Technical University of Munich, for support with structural modeling. K.H. gratefully acknowledges a PhD scholarship from the Cusanuswerk and I.A. from the German Academic Scholarship Foundation and the Marianne-Plehn-Program of the Elite Network of Bavaria. M.J.F. gratefully acknowledges funding of our work on interleukin biogenesis and engineering by the German Research Foundation DFG (Sonderforschungsbereich 1035, project number 201302640, project B11 and Transregio 338, project number 452881907, project A04), by the BMBF VIP+ grant 03VP08300 and the EKFS ForTra grant number 2020_EKTP26. O.D. is supported by grants from the Ligue Nationale contre le Cancer (Comité de Paris). Reference [67] was published after the acceptance of this manuscript so that the first structure of IL-27 with its receptor and major conclusions from this study could not be included into Figure 1 and the text of this review.

## Declaration of interests

No interests are declared.

## References

1. Akdis, M. *et al.* (2016) Interleukins (from IL-1 to IL-38), interferons, transforming growth factor beta, and TNF-alpha: receptors, functions, and roles in diseases. *J. Allergy Clin. Immunol.* 138, 984–1010
2. Vignali, D.A. and Kuchroo, V.K. (2012) IL-12 family cytokines: immunological playmakers. *Nat. Immunol.* 13, 722–728
3. Leonard, W.J. *et al.* (2019) The γ(c) family of cytokines: basic biology to therapeutic ramifications. *Immunity* 50, 832–850
4. Abdel-Meguid, S.S. *et al.* (1987) Three-dimensional structure of a genetically engineered variant of porcine growth hormone. *Proc. Natl. Acad. Sci. U. S. A.* 84, 6434–6437
5. Boulay, J.L. *et al.* (2003) Molecular phylogeny within type I cytokines and their cognate receptors. *Immunity* 19, 159–163
6. Lokau, J. *et al.* (2017) Proteolytic control of interleukin-11 and interleukin-6 biology. *Biochim. Biophys. Acta Mol. Cell Res.* 1864, 2105–2117
7. Wolf, S.F. *et al.* (1991) Cloning of cDNA for natural killer cell stimulatory factor, a heterodimeric cytokine with multiple biologic effects on T and natural killer cells. *J. Immunol.* 146, 3074–3081
8. Oppmann, B. *et al.* (2000) Novel p19 protein engages IL-12p40 to form a cytokine, IL-23, with biological activities similar as well as distinct from IL-12. *Immunity* 13, 715–725
9. Ghoreschi, K. *et al.* (2021) Therapeutics targeting the IL-23 and IL-17 pathway in psoriasis. *Lancet* 397, 754–766
10. Pflanz, S. *et al.* (2002) IL-27, a heterodimeric cytokine composed of EBI3 and p28 protein, induces proliferation of naive CD4(+) T cells. *Immunity* 16, 779–790
11. Collison, L.W. *et al.* (2007) The inhibitory cytokine IL-35 contributes to regulatory T-cell function. *Nature* 450, 566–569
12. Tait Wojno, E.D. *et al.* (2019) The immunobiology of the interleukin-12 family: room for discovery. *Immunity* 50, 851–870
13. Mirlekar, B. and Pylayeva-Gupta, Y. (2021) IL-12 family cytokines in cancer and immunotherapy. *Cancers (Basel)* 13, 167
14. Medzhitov, R. (2021) The spectrum of inflammatory responses. *Science* 374, 1070–1075
15. Wang, R.X. *et al.* (2012) Novel IL27p28/IL12p40 cytokine suppressed experimental autoimmune uveitis by inhibiting autoreactive Th1/Th17 cells and promoting expansion of regulatory T cells. *J. Biol. Chem.* 287, 36012–36021
16. Wang, X. *et al.* (2016) A novel IL-23p19/Ebi3 (IL-39) cytokine mediates inflammation in lupus-like mice. *Eur. J. Immunol.* 46, 1343–1350
17. Bridgewood, C. *et al.* (2019) The IL-23p19/EBI3 heterodimeric cytokine termed IL-39 remains a theoretical cytokine in man. *Inflamm. Res.* 68, 423–426
18. Cassatella, M.A. *et al.* (2020) Human neutrophils activated by TLR8 agonists, with or without IFNγ, synthesize and release EBI3, but not IL-12, IL-27, IL-35, or IL-39. *J. Leukoc. Biol.* 108, 1515–1526
19. Ecoeur, F. *et al.* (2020) Lack of evidence for expression and function of IL-39 in human immune cells. *PLoS One* 15, e0242329
20. Detry, S. *et al.* (2019) Revisiting the combinatorial potential of cytokine subunits in the IL-12 family. *Biochem. Pharmacol.* 165, 240–248
21. Coulomb-L'Herminé, A. *et al.* (2007) Expression of interleukin-27 by human trophoblast cells. *Placenta* 28, 1133–1140
22. Devergne, O. *et al.* (1997) Epstein-Barr virus-induced gene 3 and the p35 subunit of interleukin 12 form a novel heterodimeric hematopoietin. *Proc. Natl. Acad. Sci. U. S. A.* 94, 12041–12046
23. Trinchieri, G. (2003) Interleukin-12 and the regulation of innate resistance and adaptive immunity. *Nat. Rev. Immunol.* 3, 133–146
24. Abdi, K. *et al.* (2014) Free IL-12p40 monomer is a polyfunctional adaptor for generating novel IL-12-like heterodimers extracellularly. *J. Immunol.* 192, 6028–6036
25. Chehboun, S. *et al.* (2017) Epstein-Barr virus-induced gene 3 (EBI3) can mediate IL-6 trans-signaling. *J. Biol. Chem.* 292, 6644–6656
26. Gerber, A.N. *et al.* (2021) The subunits of IL-12, originating from two distinct cells, can functionally synergize to protect against pathogen dissemination in vivo. *Cell Rep.* 37, 109816
27. Kundu, M. *et al.* (2017) Selective neutralization of IL-12 p40 monomer induces death in prostate cancer cells via IL-12-IFN-γ. *Proc. Natl. Acad. Sci. U. S. A.* 114, 11482–11487
28. Garbers, C. *et al.* (2013) An interleukin-6 receptor-dependent molecular switch mediates signal transduction of the IL-27 cytokine subunit p28 (IL-30) via a gp130 protein receptor homodimer. *J. Biol. Chem.* 288, 4346–4354
29. Yoshida, H. and Hunter, C.A. (2015) The immunobiology of interleukin-27. *Annu. Rev. Immunol.* 33, 417–443
30. Ye, C. *et al.* (2021) Interleukin-35: structure, function and its impact on immune-related diseases. *J. Interf. Cytokine Res.* 41, 391–406
31. Ma, X. *et al.* (2015) Regulation of IL-10 and IL-12 production and function in macrophages and dendritic cells. *F1000Res* 4, 1465
32. Jin, X. *et al.* (2020) Pyruvate kinase M2 promotes the activation of dendritic cells by enhancing IL-12p35 expression. *Cell Rep.* 31, 107690

33. Yu, C.R. *et al.* (2018) Production of IL-35 by Bregs is mediated through binding of BATF-IRF-4-IRF-8 complex to il12a and ebi3 promoter elements. *J. Leukoc. Biol.* 104, 1147–1157
34. Babik, J.M. *et al.* (1999) Expression of murine IL-12 is regulated by translational control of the p35 subunit. *J. Immunol.* 162, 4069–4078
35. Uehata, T. and Akira, S. (2013) mRNA degradation by the endoribonuclease Regnase-1/ZC3H12a/MCPIP-1. *Biochim. Biophys. Acta* 1829, 708–713
36. Qian, X. *et al.* (2011) Posttranscriptional regulation of IL-23 expression by IFN-gamma through tristetraprolin. *J. Immunol.* 186, 6454–6464
37. Wang, Q. *et al.* (2017) Tristetraprolin inhibits macrophage IL-27-induced activation of antitumour cytotoxic T cell responses. *Nat. Commun.* 8, 867
38. Lu, T.X. *et al.* (2009) MicroRNA-21 is up-regulated in allergic airway inflammation and regulates IL-12p35 expression. *J. Immunol.* 182, 4994–5002
39. Cui, B. *et al.* (2017) Brucella Omp25 upregulates miR-155, miR-21-5p, and miR-23b to inhibit interleukin-12 production via modulation of programmed death-1 signaling in human monocyte/macrophages. *Front. Immunol.* 8, 708
40. Varikuti, S. *et al.* (2021) MicroRNA-21 deficiency promotes the early Th1 immune response and resistance toward visceral leishmaniasis. *J. Immunol.* 207, 1322–1332
41. Carpenter, S. *et al.* (2013) A long noncoding RNA mediates both activation and repression of immune response genes. *Science* 341, 789–792
42. Gubler, U. *et al.* (1991) Coexpression of two distinct genes is required to generate secreted bioactive cytotoxic lymphocyte maturation factor. *Proc. Natl. Acad. Sci. U. S. A.* 88, 4143–4147
43. Jalah, R. *et al.* (2013) The p40 subunit of interleukin (IL)-12 promotes stabilization and export of the p35 subunit: implications for improved IL-12 cytokine production. *J. Biol. Chem.* 288, 6763–6776
44. Mondal, S. *et al.* (2020) IL-12 p40 monomer is different from other IL-12 family members to selectively inhibit IL-12Rβ1 internalization and suppress EAE. *Proc. Natl. Acad. Sci. U. S. A.* 117, 21557–21567
45. Jana, M. and Pahan, K. (2009) IL-12 p40 homodimer, but not IL-12 p70, induces the expression of IL-16 in microglia and macrophages. *Mol. Immunol.* 46, 773–783
46. Lee, S.Y. *et al.* (2015) IL-12p40 homodimer ameliorates experimental autoimmune arthritis. *J. Immunol.* 195, 3001–3010
47. Jana, M. *et al.* (2009) IL-12 p40 homodimer, the so-called biologically inactive molecule, induces nitric oxide synthase in microglia via IL-12R beta 1. *Glia* 57, 1553–1565
48. Walter, M.J. *et al.* (2001) Interleukin 12 p40 production by barrier epithelial cells during airway inflammation. *J. Exp. Med.* 193, 339–351
49. Cooper, A.M. and Khader, S.A. (2007) IL-12p40: an inherently agonistic cytokine. *Trends Immunol.* 28, 33–38
50. Gately, M.K. *et al.* (1996) Interleukin-12 antagonist activity of mouse interleukin-12 p40 homodimer in vitro and in vivo. *Ann. N. Y. Acad. Sci.* 795, 1–12
51. Ling, P. *et al.* (1995) Human IL-12 p40 homodimer binds to the IL-12 receptor but does not mediate biologic activity. *J. Immunol.* 154, 116–127
52. Mattner, F. *et al.* (1993) The interleukin-12 subunit p40 specifically inhibits effects of the interleukin-12 heterodimer. *Eur. J. Immunol.* 23, 2202–2208
53. Reitberger, S. *et al.* (2017) Assembly-induced folding regulates interleukin 12 biogenesis and secretion. *J. Biol. Chem.* 292, 8073–8081
54. Alloza, I. *et al.* (2004) Cross-linking approach to affinity capture of protein complexes from chaotrope-solubilized cell lysates. *Anal. Biochem.* 324, 137–142
55. Alloza, I. *et al.* (2006) Celecoxib inhibits interleukin-12 alphabeta and beta2 folding and secretion by a novel COX2-independent mechanism involving chaperones of the endoplasmic reticulum. *Mol. Pharmacol.* 69, 1579–1587
56. Yoon, C. *et al.* (2000) Charged residues dominate a unique interlocking topography in the heterodimeric cytokine interleukin-12. *EMBO J.* 19, 3530–3541
57. Mideksa, Y.G. *et al.* (2020) Site-specific protein labeling with fluorophores as a tool to monitor protein turnover. *Chembiochem* 21, 1861–1867
58. McLaughlin, M. *et al.* (2010) Inhibition of secretion of interleukin (IL)-12/IL-23 family cytokines by 4-trifluoromethyl-celecoxib is coupled to degradation via the endoplasmic reticulum stress protein HERP. *J. Biol. Chem.* 285, 6960–6969
59. Lupardus, P.J. and Garcia, K.C. (2008) The structure of interleukin-23 reveals the molecular basis of p40 subunit sharing with interleukin-12. *J. Mol. Biol.* 382, 931–941
60. Meier, S. *et al.* (2019) The molecular basis of chaperone-mediated interleukin 23 assembly control. *Nat. Commun.* 10, 4121
61. Espigol-Frigolé, G. *et al.* (2016) Identification of IL-23p19 as an endothelial proinflammatory peptide that promotes gp130-STAT3 signaling. *Sci. Signal.* 9, ra28
62. Tormo, A.J. *et al.* (2013) A polyglutamic acid motif confers IL-27 hydroxyapatite and bone-binding properties. *J. Immunol.* 190, 2931–2937
63. Muller, S.I. *et al.* (2019) A folding switch regulates interleukin 27 biogenesis and secretion of its alpha-subunit as a cytokine. *Proc. Natl. Acad. Sci. U. S. A.* 116, 1585–1590
64. Bohnacker, S. *et al.* (2020) Influence of glycosylation on IL-12 family cytokine biogenesis and function. *Mol. Immunol.* 126, 120–128
65. Muller, S.I. *et al.* (2019) An interspecies analysis reveals molecular construction principles of interleukin 27. *J. Mol. Biol.* 431, 2383–2393
66. Rousseau, F. *et al.* (2010) IL-27 structural analysis demonstrates similarities with ciliary neurotrophic factor (CNTF) and leads to the identification of antagonistic variants. *Proc. Natl. Acad. Sci. U. S. A.* 107, 19420–19425
67. Caveney, N.A. *et al.* (2022) Structure of the IL-27 quaternary receptor signaling complex. *Elife* 11, e78463
68. Jin, Y. *et al.* (2022) Structural insights into the assembly and activation of IL-27 signalling complex. *bioRxiv* Published online March 3, 2022. https://doi.org/10.1101/2022.02.18.481027
69. Jones, L.L. *et al.* (2012) Distinct subunit pairing criteria within the heterodimeric IL-12 cytokine family. *Mol. Immunol.* 51, 234–244
70. Aparicio-Siegmund, S. *et al.* (2014) Recombinant p35 from bacteria can form interleukin (IL-)12, but not IL-35. *PLoS One* 9, e107990
71. Hebert, D.N. and Molinari, M. (2012) Flagging and docking: dual roles for N-glycans in protein quality control and cellular proteostasis. *Trends Biochem. Sci.* 37, 404–410
72. Devergne, O. *et al.* (1996) A novel interleukin-12 p40-related protein induced by latent Epstein-Barr virus infection in B lymphocytes. *J. Virol.* 70, 1143–1153
73. Mizoguchi, I. *et al.* (2020) EBV-induced gene 3 augments IL-23Rα protein expression through a chaperone calnexin. *J. Clin. Invest.* 130, 6124–6140
74. Sullivan, J.A. *et al.* (2020) Treg-cell-derived IL-35-coated extracellular vesicles promote infectious tolerance. *Cell Rep.* 30, 1039–1051
75. Teng, M.W. *et al.* (2015) IL-12 and IL-23 cytokines: from discovery to targeted therapies for immune-mediated inflammatory diseases. *Nat. Med.* 21, 719–729
76. Pires, I.S. *et al.* (2021) Engineering strategies for immunomodulatory cytokine therapies: challenges and clinical progress. *Adv. Ther.* 4, 2100035
77. Mo, F. *et al.* (2021) An engineered IL-2 partial agonist promotes CD8(+) T cell stemness. *Nature* 597, 544–548
78. Glassman, C.R. *et al.* (2021) Calibration of cell-intrinsic interleukin-2 response thresholds guides design of a regulatory T cell biased agonist. *Elife* 10, e65777
79. Saxton, R.A. *et al.* (2021) The tissue protective functions of interleukin-22 can be decoupled from pro-inflammatory actions through structure-based design. *Immunity* 54, 660–672
80. Saxton, R.A. *et al.* (2021) Structure-based decoupling of the pro- and anti-inflammatory functions of interleukin-10. *Science* 371, eabc8433
81. Scheller, J. *et al.* (2019) Immunoreceptor engineering and synthetic cytokine signaling for therapeutics. *Trends Immunol.* 40, 258–272

82. Mansurov, A. *et al.* (2020) Collagen-binding IL-12 enhances tumour inflammation and drives the complete remission of established immunologically cold mouse tumours. *Nat. Biomed. Eng.* 4, 531–543
83. Fallon, J. *et al.* (2014) The immunocytokine NHS-IL12 as a potential cancer therapeutic. *Oncotarget* 5, 1869–1884
84. Nguyen, K.G. *et al.* (2020) Localized interleukin-12 for cancer immunotherapy. *Front. Immunol.* 11, 575597
85. Skrombolas, D. *et al.* (2019) Development of an interleukin-12 fusion protein that is activated by cleavage with matrix metalloproteinase 9. *J. Interf. Cytokine Res.* 39, 233–245
86. Bloch, Y. *et al.* (2017) Structural activation of pro-inflammatory human cytokine IL-23 by cognate IL-23 receptor enables recruitment of the shared receptor IL-12Rbeta1. *Immunity* 48, 45–58
87. Schroder, J. *et al.* (2015) Non-canonical interleukin 23 receptor complex assembly: p40 protein recruits interleukin 12 receptor beta1 via site II and induces p19/interleukin 23 receptor interaction via site III. *J. Biol. Chem.* 290, 359–370
88. Glassman, C.R. *et al.* (2021) Structural basis for IL-12 and IL-23 receptor sharing reveals a gateway for shaping actions on T versus NK cells. *Cell* 184, 983–999
89. Yan, J. *et al.* (2016) Interleukin-30 (IL27p28) alleviates experimental sepsis by modulating cytokine profile in NKT cells. *J. Hepatol.* 64, 1128–1136
90. Shimozato, O. *et al.* (2009) The secreted form of p28 subunit of interleukin (IL)-27 inhibits biological functions of IL-27 and suppresses anti-allogeneic immune responses. *Immunology* 128, e816–e825
91. Stumhofer, J.S. *et al.* (2010) A role for IL-27p28 as an antagonist of gp130-mediated signaling. *Nat. Immunol.* 11, 1119–1126
92. Mitra, A. *et al.* (2014) IL-30 (IL27p28) attenuates liver fibrosis through inducing NKG2D-rae1 interaction between NKT and activated hepatic stellate cells in mice. *Hepatology* 60, 2027–2039
93. Floss, D.M. and Scheller, J. (2019) Naturally occurring and synthetic constitutive-active cytokine receptors in disease and therapy. *Cytokine Growth Factor Rev.* 47, 1–20
94. Hummel, T.M. *et al.* (2017) Synthetic deletion of the interleukin 23 receptor (IL-23R) stalk region led to autonomous IL-23R homodimerization and activation. *Mol. Cell. Biol.* 37, e00014-17
95. Floss, D.M. *et al.* (2017) IL-6/IL-12 cytokine receptor shuffling of extra- and intracellular domains reveals canonical STAT activation via synthetic IL-35 and IL-39 signaling. *Sci. Rep.* 7, 15172
96. Engelowski, E. *et al.* (2018) Synthetic cytokine receptors transmit biological signals using artificial ligands. *Nat. Commun.* 9, 2034
97. Feige, M.J. *et al.* (2010) How antibodies fold. *Trends Biochem. Sci.* 35, 189–198
98. Alcover, A. *et al.* (2018) Cell biology of T cell receptor expression and regulation. *Annu. Rev. Immunol.* 36, 103–125
99. Collison, L.W. *et al.* (2012) The composition and signaling of the IL-35 receptor are unconventional. *Nat. Immunol.* 13, 290–299
100. Wang, R.X. *et al.* (2014) Interleukin-35 induces regulatory B cells that suppress autoimmune disease. *Nat. Med.* 20, 633–641

## II. Assembly-dependent structure formation determines the human interleukin-12/interleukin-23 secretion ratio

by **Isabel Aschenbrenner**[1], Abraham Lopez, Till Siebenmorgen, Marina Parr, Philipp Ruckgaber, Anna Miesl, Florian Rührnößl, Dragana Catici, Martin Haslbeck, Michael Sattler, Dimitri Frishman, Martin Zacharias, and Matthias J. Feige

Manuscript in preparation.

### Manuscript draft

# Assembly-dependent structure formation determines the human interleukin-12/interleukin-23 secretion ratio

Isabel Aschenbrenner[1], Till Siebenmorgen[1], Abraham Lopez[2,3], Marina Parr[4], Philipp Ruckgaber[1], Anna Miesl[1], Florian Rührnößl[1], Dragana Catici[1], Martin Haslbeck[1], Dmitrij Frishman[4], Michael Sattler[2,3], Martin Zacharias[1], Matthias J. Feige[1,*]

[1] Center for Functional Protein Assemblies (CPA), Department of Bioscience, TUM School of Natural Sciences, Technical University of Munich, Garching, Germany

[2] Department of Bioscience, TUM School of Natural Sciences, Technical University of Munich, Garching, Germany

[3] Institute of Structural Biology, Helmholtz Zentrum München, Neuherberg, Germany

[4] Department of Bioinformatics, TUM School of Life Sciences, Technical University of Munich, Freising, Germany

* To whom correspondence may be addressed: Tel: +49-89-28913667; Fax: +49-89-28910698; E-mail: matthias.feige@tum.de

## Abstract

Interleukin 12 (IL-12) family cytokines regulate immune responses and connect the innate and adaptive branches of the immune system. Each IL-12 family member is an α:β heterodimer. For human α subunits it has been shown that they depend on their β subunit for structure formation. Furthermore, subunits are shared within the family and IL-12 as well as IL-23 use the same β subunit despite distinct immunological functions. It remains unclear, what biological advantage this confers.

Here, we rationally design and comprehensively analyze a folding-competent human IL-23α subunit. This engineered variant still forms a functional heterodimeric cytokine but shows less chaperone dependency and stronger affinity in assembly with its β subunit. As such, it more efficiently forms IL-23 than its natural counterpart, skewing the balance of IL-12 and IL-23 towards more IL-23 formation.

Together, our study shows that folding-competent IL-12 family α subunits are possible and compatible with assembly and function of the cytokine. These findings suggest that nature has evolved human α subunits for assembly-dependent folding to maintain and regulate correct IL-12 family member ratios in the light of subunit competition.

## Introduction

The human immune system uses secreted proteins, interleukins, to regulate immune cell functions. Among those, the interleukin 12 (IL-12) family has a particularly broad range of biological activities with pro- and anti-inflammatory family members [1]. Since ILs are secretory proteins, they are produced in the endoplasmic reticulum (ER) where they undergo folding and, in the case of IL-12 family members, assembly into their heterodimeric structure. In recent years, key steps in IL-12 family member biogenesis have been revealed [2].

It could be shown that all human IL-12 family α subunits, IL-12 α, IL-23α, and IL-27α, are unstructured in isolation and depend on their suitable partner β subunit to adopt their native structures [3-6]. As such, structure formation of IL-12 cytokines can be quite complex, thus requiring chaperones and folding enzymes to support and control the outcomes. Among others, the lectin chaperone calreticulin assists in folding of *N*-glycosylated IL-12α and the Hsp70 chaperone immunoglobulin heavy-chain binding protein (BiP) supports structure formation of IL-12, IL-23, and IL-27 [3, 5, 7]. Of particular complexity is the repertoire of protein disulfide isomerase (PDI) family members in IL-12 and IL-23 biogenesis [7]. IL-12α has three intramolecular disulfide bonds and misfolds when unassembled [4]. The different PDIs that interact with IL-12α show binding specificity for distinct cysteine residues within the subunit [7]. The same is true for isolated IL-23α, as e.g., the PDI ERp5 seems to prefer binding of only free cysteines over cysteine residues responsible for its single intramolecular disulfide bond [7].

In addition to these intrinsic challenges in α subunit folding, subunit sharing within the IL-12 family adds another layer of complexity. IL-12 and IL-23 share the same β subunit, IL-12β, to form biologically active heterodimers [8-10]. The α:β interface structures have been comparatively explored for the IL-12/IL-23 heterodimers and revealed a common Arg-Asp salt bridge as crucial binding hotspot but unique pairwise contacts in the surrounding [11, 12]. Despite the sharing of IL-12β as a common building block for both heterodimeric cytokines, even down to certain molecular details of the interface, the biological effects of IL-23 *versus* IL-12 signaling are highly distinct [13] and thus their relative secretion needs to be tightly regulated to ensure proper immune reactions.

Molecular determinants of this regulation still remain unclear, in particular on the post-transcriptional level [2]. An important open question is what governs the relative secretion of heterodimers from cells that express multiple subunits which can in principle assemble different IL-12 family members due to chain pairing promiscuity. And related to this, it remains unclear why nature has evolved such a complex molecular setup for IL-12 family

cytokines. To address these questions, in this study we designed a structurally stabilized IL-23α variant using a computational engineering approach. This variant proved to be folding-competent in isolation but could still assemble with its partner β subunit. It thus allowed us to assess the impact of assembly-induced folding on IL-12 *versus* IL-23 biogenesis. Together, our study provides insights into how immunological functions and their balance can be regulated on the cellular level despite of extensive chain sharing between IL-12 family members.

## Results

### *In silico* analyses enable rational engineering of an autonomously folded IL-23α.

A common theme within the human IL-12 family is that α subunits are unstructured in isolation and depend on their β subunit for proper structure formation and secretion from cells. Which impact this dependence has on regulating secretion of IL-12 cytokines remains incompletely explored. To investigate this, α subunit variants are needed that structure autonomously. Previous work has suggested the first α helix of the IL-23α four-helix bundle fold to be incompletely structured and thus be critical for chaperone-mediated retention of unassembled IL-23α [5]. However, further structural instabilities within IL-23α likely contribute to its assembly-dependent secretion and thus may provide opportunities for rational engineering of an autonomously folded IL-23α. To define these, we performed hydrogen/deuterium exchange (HDX) mass spectrometry (MS) measurements of the purified IL-23α subunit, using a variant devoid of free cysteines (C14V,C22V,C54S; IL-23α$^{\Delta\text{free cys}}$) that can be purified without aggregation (Supplementary Fig. 1A-D, [5]). Our findings confirmed structural instability of helix 1 in IL-23α (Fig. 1A), which remains quite flexible even in the assembled state (Fig. 1B), but also revealed that the protein becomes globally stabilized upon correct assembly with IL-12β (Fig. 1A, B and Supplementary Fig. 1E). Regions that became stabilized upon IL-12β assembly included the N-terminus, the long AB loop, which also contains the residue Cys54 for covalent heterodimerization, the BC loop, and helix 4, constituting the α:β interface together with helix 1 [11] (Fig. 1B, C).

Having defined these weak spots of IL-23α, we used *in silico* analyses by molecular dynamics (MD) simulations to provide a starting point for rational engineering of mutants aiming to stabilize this subunit. Additionally, we took the native structure of IL-23α in the context of IL-23 and an evolutionary analysis of IL-23α into account. The evolutionary analysis revealed that the free cysteines Cys14 and Cys22, located in the first α helix of IL-23α, are well-conserved in IL-23α of other species (Supplementary Fig. 1F). Furthermore, such free cysteines can be found in ~12% of human four-helix bundle

cytokines (4 out of 33 proteins) in the N-terminal helix (Supplementary Fig. 1G). This is relevant, since previous work has shown these two free cysteines to be hotspots of IL-23 assembly control and recognition of unpaired IL-23α by chaperones [5, 14], together qualifying them as targets for engineering.

To decrease the flexibility and concomitantly increase stability of IL-23α, a single cysteine residue introduced into helix 4 at position Phe161 (IL-23α$^{F161C}$) should facilitate internal disulfide bond formation with one of these free cysteines, in this case Cys14, in helix 1 (Fig. 1D, E: second panel). Another approach emerging from the structural analysis of IL-23α was the rearrangement of the helix sequence to helix 2-3-4-1 (IL-23α$^{helix2341}$; Fig. 1D, E: third panel). Fusing helix 1 to the C-terminus of helix 4 by a short loop should possibly result in less structural flexibility and allow more efficient attachment of helix 1 to helix 4, as they are in structural proximity in the native state. RS-REMD simulations confirmed increased stability of the rearranged mutant (-32.3±1.7 kcal/mol) in terms of helix 1 dissociation compared to the wild-type IL-23α (-25.7±1.3 kcal/mol). To possibly improve proper folding, a further approach was to shorten the long unstructured, highly flexible AB loop between helix 1 and helix 2 (Fig. 1A, C) in IL-23α$^{\Delta 40\text{-}48}$ (Fig. 1D, E: fourth panel) for better helix attachment. Lastly, MD simulations revealed that helices 2-4 in IL-23α tend to collapse to a certain extent, so that the first helix may not be able to bind efficiently. Thus, one or more bulky amino acid residues, i.e., Met, were inserted at positions in which helices are facing to each other to form the bundled structure (IL-23α$^{V102M,L150M,A157M}$; Fig. 1 D, E: fifth panel). Cleft expansion between the three helices (helix 2, 3, and 4) could be confirmed by defining distance differences between helices 2-4 in the simulated structure (data not shown). This expansion possibly entropically facilitates helix 1 attachment.

To test these rationally engineered IL-23α variants for improved folding, we assessed their secretion behavior from mammalian cells, since only properly structured IL-23α was expected to pass ER quality control (QC) and be secreted. As previously shown [5, 8], wild-type IL-23α does not fold in isolation and is thus retained in cells, whereas assembly with IL-12β enables efficient secretion of heterodimeric IL-23 into the cell media (Fig. 1F). Among the four engineered mutants, two behaved as intended: IL-23α with an extra intramolecular disulfide bridge as well as the helix-rearranged mutant were both secreted without IL-12β, showing partial *O*-glycosylation [5], indicating their ability to fold and thus pass ERQC. All four mutants were secreted in the presence of IL-12β, showing that also for the remaining two mutants the overall folding and assembly-competency was not compromised (Fig. 1F). Of note, the principle of inserting an additional intramolecular disulfide bond also worked for other amino acid positions in close proximity to the natively free Cys14 or Cys22 in IL-23α, showing that this is a rather robust approach to confer secretion-competency to

isolated IL-23α (Supplementary Fig. 1H, I). For the helix rearrangement mutant, which still contained both free cysteine residues in its now C-terminal helix 1, secretion was less efficient than for the disulfide-stabilized variants and also could not be improved by deleting the now potentially flexible N-terminus (Fig. 1D-F and Supplementary Fig. 1J, K).

Taken together, based on a molecular analysis of the structural weak points in the subunit IL-23α, we could design secretion-competent variants, in some cases by exchanging only a single amino acid of the native protein.

**Introducing an intramolecular disulfide bond in IL-23α provides a stably folded protein.**

Our engineering approach provided us with a point mutant of IL-23α that was predicted to form a stabilizing disulfide bond and was efficiently secreted from cells. To further reduce the risk of covalent misfolding, the other free cysteine Cys22, not involved in the extra intramolecular disulfide bond, as well as Cys54, else responsible for covalent β subunit linkage, were mutated to valine or serine, respectively (Supplementary Fig. 2A). When transiently transfected in HEK 293T cells, the engineered IL-23α$^{C22V,C54S,F161C}$ variant showed efficient secretion as intended (Fig. 2A). Because of its autonomous folding and stabilized nature, this mutant was designated as IL-23α$^{stabilized}$. When co-transfected with IL-12β, with which it cannot interact covalently anymore due to the Cys54Ser replacement, *O*-glycosylation was diminished, which confirms successful but not complete β subunit interaction in the early secretory pathway [5] (Fig. 2A). In comparison to the wildtype, which forms the covalently linked IL-23 heterodimer, secreted IL-23α$^{stabilized}$ has its intramolecular disulfide bonds formed regardless of IL-12β presence (Fig. 2B). To further confirm folding-competency of IL-23α$^{stabilized}$, we analyzed its redox status in cells. Wild-type IL-23α is prone to misfolding when expressed alone and forms various erroneous, disulfide-linked species [5]. In contrast, IL-23α$^{folded}$ equipped with a KDEL-ER retention sequence to maintain it in cells shows 5-fold more correctly oxidized, monomeric protein than the wildtype, with IL-12β co-expression further reducing misoxidation (Fig. 2C and Supplementary Fig. 3). Lastly, we assessed intracellular degradation of IL-23α$^{stabilized}$ *versus* the wild-type protein in cycloheximide (CHX) chase assays. Protein turnover rates were strongly reduced for IL-23α$^{stabilized}$ equipped with a KDEL-sequence in comparison to the wildtype (Fig. 2D), again confirming its correct folding and stabilization.

To further define the structural properties of IL-23α$^{stabilized}$, we performed a suite of biophysical experiments on the variant. IL-23α$^{stabilized}$ could be purified to homogeneity and proved to be a monomeric protein (Supplementary Fig. 2A-D). HDX MS measurements revealed stabilization of IL-23α$^{stabilized}$ around the critical helix 1 as intended (Fig. 3A, B and

Supplementary Fig. 2E) and, like observed in cells, IL-12β assembly led to further structural stabilization (Supplementary Fig. 2F, G). NMR measurements verified stabilizing effects of the mutations in IL-23α$^{stabilized}$ as well, which showed less line broadening than IL-23α$^{\Delta free\ cys}$ in $^{1}H$, $^{15}N$ spectra, indicative of a more rigid α helical structure (Fig. 3C-E), which was confirmed by far-UV circular dichroism (CD) spectroscopy (Supplementary Fig. 2H). Lastly, temperature-dependent unfolding, measured by far-UV CD spectroscopy, confirmed a significant stabilization of IL-23α$^{stabilized}$ over IL-23α$^{\Delta free\ cys}$ by more than 20% (11 °C) (Fig. 3F).

In summary, insertion of an extra intramolecular disulfide bridge renders IL-23α a stably folded and secretion-competent protein that remains assembly-competent with IL-12β. This raises the question of why nature has evolved IL-23α differently, a question IL-23α$^{stabilized}$ now allowed us to assess.

**Autonomous folding of IL-23α strongly affects ER chaperone recruitment and IL-23 heterodimer assembly.**

Key processes in the assembly of human IL-12 family cytokines are chaperone recruitment to unassembled α subunits and their assembly-induced folding [2, 4, 7, 15]. IL-23α$^{stabilized}$ now allowed us to analyze these processes for an autonomously folding-competent variant. To assess how chaperone interactions are influenced when IL-23α is folding-competent on its own, we analyzed the interaction of the wildtype compared to the engineered mutant with relevant chaperones. To do so, we used variants equipped with a KDEL ER-retention sequence, as otherwise IL-23α$^{stabilized}$ becomes secreted. In co-immunoprecipitation (co-IP) experiments we identified endogenous interactions with chaperones by subsequent immunoblotting (Fig. 4A). Chaperone binding to IL-23α$^{stabilized}$ was significantly reduced for the Hsp70 chaperone BiP as well as the PDI family members ERp72, ERp5, and ERp44, which all have been previously shown to bind to IL-23α [5, 7] (Fig. 4B). IL-23α$^{stabilized}$ is thus an engineered cytokine subunit which passes the secretory pathway with significantly less ER chaperone interactions than the wildtype.

Building on this, we next assessed how assembly and interaction with IL-12β was affected by rendering IL-23α folding-competent. Isothermal titration calorimetry (ITC) experiments revealed that IL-23α$^{\Delta free\ cys}$ bound to its pairing partner IL-12β with a $K_D$-value of 9.4 µM (Fig. 4 C). The engineered IL-23α$^{stabilized}$ showed an around 4-fold higher affinity with a $K_D$-value of 2.3 µM (Fig. 4D). These affinity values for IL-23$^{\Delta free\ cys}$ and IL-23α$^{stabilized}$ heterodimerization with IL-12β were further verified by surface plasmon resonance (SPR) measurements, revealing very fast $k_{on}/k_{off}$ rates with comparable $K_D$-values of 11.6 µM and

2.8 µM, respectively (Supplementary Fig. 4). Structural stabilization of IL-23α thus significantly strengthens β subunit interaction.

Together, this now allowed us to investigate which roles these processes, chaperone recruitment and association with IL-12β, play in IL-23 *versus* IL-12 assembly as well as in IL-23 signaling.

**An autonomously folded IL-23α subunit does not interfere with IL-23 signaling but changes the IL-12 *versus* IL-23 secretion ratio.**

Possible hypotheses why nature has evolved assembly-dependent secretion of IL-23α are that a secretion-competent IL-23α is not compatible with - or interferes with IL-23 signaling. Or that this feature is crucial for regulating IL-12 *versus* IL-23 assembly in cells since both cytokines share the same β subunit.

To test the first hypothesis, we used a previously established NanoBRET™ assay (Hildenbrand *et al.*, submitted) which utilizes bioluminescence resonance energy transfer (BRET) to allow detection of receptor chain dimerization by cytokine binding (Fig. 5A). Single IL-23 subunits, no matter whether IL-23$^{\Delta free\ cys}$ or IL-23α$^{stabilized}$ was used, resulted in no significant signals. In contrast, native IL-23 or reconstituted IL-23 proteins induced comparable NanoBRET™ signals independent if IL-23 contained the wild-type α subunit, the one devoid of free cysteines IL-23$^{\Delta free\ cys}$ or IL-23α$^{stabilized}$ (Fig. 5A). Thus, secretion-competent IL-23α$^{stabilized}$ associates with IL-12β to form a heterodimeric, signaling-competent cytokine that induces receptor chain dimerization like native human IL-23. Another possibility is that if IL-23α was secretion-competent in isolation, it could interfere with IL-23 signaling by blocking IL-23 receptor binding. This, however, was hardly the case even up to a 100-fold excess of IL-23α$^{stabilized}$ over IL-23 (Supplementary Fig. 5A).

We thus next assessed the second hypothesis, that IL-12α and IL-23α may compete for the IL-12β subunit within cells expressing both IL-12 and IL-23 and that this might be influenced by the folding state of IL-23α. For this, we used a T2A sequence between genes for IL-23α and IL-12α to allow stoichiometric production of protein subunits (Fig. 5B). By co-expression of FLAG-tagged IL-12β with the T2A construct and subsequent FLAG-IP of medium, we could assess heterodimer formation ratios (Fig. 5B). Of note, the IL-23/IL-12 ratio was significantly shifted towards IL-23 in the presence of IL-23α$^{stabilized}$ compared to IL-23α wildtype, with an increase in IL-23 secretion by almost 100% (Fig. 5C). A similar increase in the IL-23/IL-12 ratio was observed when the T2A construct arrangement was inverted (Supplementary Fig. 5B, C), showing that the folding-competency of IL-23α strongly influences IL-23 *versus* IL-12 assembly and secretion.

Taken together, our data show that engineered, secretion-competent IL-23α does not interfere with IL-23 signaling. However, it significantly influences the human IL-23/IL-12 secretion ratio by its assembly-independent structure formation.

## Discussion

The IL-12 family shows extensive subunit sharing and, for all human members, assembly-induced folding of α subunits to allow secretion of heterodimers. Within this study we aimed to assess the impact of both these characteristics on human IL-12 cytokine assembly and secretion. We focused on IL-12 and IL-23, which both share the same β subunit (IL-12β) but differ in their α subunits (IL-12α *versus* IL-23α) so that cells producing all subunits must regulate and control cytokine assembly in the ER to elicit proper downstream immune reactions.

To dissect the underlying principles, we engineered human IL-23α to fold autonomously based on a comprehensive structural, computational, and evolutionary analysis. We rationally targeted weak points of the four-helix bundle subunit in its unpaired state and could show that either introduction of an additional disulfide bond or a helix rearrangement conferred folding-competency to IL-23α. Addition of the extra disulfide bond targets two weak spots within IL-23α at the same time: its unstructured first helix [5] and its free cysteines within this helix, the first becoming stabilized by the disulfide bond and using one of the free cysteines for this. Indeed, further removal of the remaining free cysteine and Cys54 for the interchain disulfide bond resulted in the mutant IL-23α$^{stabilized}$ for which we could confirm less misfolding in isolation, and a strong reduction of chaperone dependency (Fig. 6). The PDI family members ERp72, ERp5, and ERp44 recognize their clients in a thiol-dependent [16-18] manner, with ERp5 showing a strong association with BiP and its substrates [19], so that less chaperone binding can also be partially caused by the cysteine mutations itself. BiP binding, however, was equally reduced arguing for improved folding as the cause. However, cellular retention due to free cysteines is not a general principle, since other four-helix bundle cytokines, IFNβ, GCSF, and CNTF, contain an N-terminal free cysteine (Supplementary Fig. 1G) but are secreted from cells when bearing an appropriate signal sequence [20-22]. The combination of partial folding and free cysteines is thus critical for IL-23α retention. In agreement with this notion, moving helix 1 to the C-terminus of the native IL-23α sequence leads to secretion although the free Cys14 and Cys22 are still present. This rearrangement may stabilize the structure since helix 1 is now covalently linked to helix 4 by a quite short, engineered DA-loop, which entropically may stabilize the overall structure compared to the long AB-loop in wild-type IL-23α. Still, both free cysteines probably still cause partial recognition and ER retention by PDI family members [5, 7]

explaining its less efficient secretion than the disulfide-bond containing variant. In contrast, truncating flexible loops alone or extending the helical cleft to facilitate docking of the first helix on the bundle failed to stabilize IL-23α sufficiently for autonomous secretion.

All variants, including the disulfide-bonded mutant, remained assembly-competent with IL-12β. Furthermore, recent work has shown that human IL-27α can also be rendered secretion-competent by introducing an additional disulfide bond - which naturally exists in its murine counterpart [3, 23, 24]. Together, this indicates that human IL-12 family α subunits have evolved to become dependent on their β subunit for secretion, that this confers an advantage in producing IL-12 family cytokines and regulating immune responses. Further support of this idea comes from the fact that IL-12 family cytokines seem to have evolved from cytokine:receptor pairs [25], suggesting that back in evolution α and β subunits were folding-competent in isolation. Assembly-induced secretion/transport to the cell surface is a common theme for immune proteins [26-31]. This safeguards correct structure formation of potent molecules in our body. For IL-12 family cytokines, however, there must be additional reasons as chain sharing adds another layer of regulation. We find micromolar affinities between IL-23α and IL-12β, so preventing assembly outside of the cell is an unlikely explanation, since cytokine concentrations are normally orders of magnitude less (IL-12/IL-23: 0.1-3.5 pM; IL-12β: 0.6-37 pM; based on peripheral blood mononuclear cells) [32-34]. Also, we do not detect any strong effect of IL-23α on signaling of IL-23 or strong signaling-competency itself, at least in our assay system (Fig. 5A and Supplementary Fig. 5A). Even though some human IL-12 family subunits can induce signaling on their own [5, 15, 35], our engineered IL-23α$^{stabilized}$ utilizes IL-12β for wildtype-like receptor chain interaction with IL-23R and IL-12Rβ1, respectively [36, 37].

In contrast, our study reveals that rendering IL-23α folding-competent has a strong impact on the relative IL-12/IL-23 ratio, with a folding-competent IL-23α assembling more efficiently with IL-12β, thereby outcompeting IL-12α to a certain extent. Keeping a biologically important balance between IL-23 and IL-12 may thus be one explanation for human α subunits depending on their β subunits for secretion. This is of high importance as IL-12 and IL-23 trigger very distinct immunological pathways: IL-12 drives naïve T lymphocyte differentiation to the pro-inflammatory T helper (Th) 1 subset, which secrete interferon-γ, whereas IL-23 stimulates a highly pro-inflammatory immune response by induction of IL-17-producing Th17 cell populations [1, 38-40].

This outcome, however, could possibly also be achieved by other means, e.g., relative expression levels and evolution of proper affinities/interfaces. For both cysteine-rich α subunits, IL-12α and IL-23α, PDI interactions are of outmost importance for their

biogenesis and might depict a further layer of cytokine assembly regulation [7]. As the interacting chaperone repertoire is not completely overlapping for these pro-inflammatory α subunits, specific interventions in the IL assembly process are possible. For EBI3 comprising IL-27 and IL-35, IL-12α and IL-27α subunit biogenesis and interacting chaperones might also be diverging enough to allow such an assembly-regulation [4, 15]. An intriguing difference between the human α subunits, mediated by stabilizing chaperones, is their turnover rate: IL-12α remains longer than IL-23α in the ER before being ultimately degraded by ERAD [4, 5, 7]. Depending on the cellular expression rates, this might affect the availability of α subunits for assembly with IL-12β, besides differential subunit expression levels. Intracellular roles for pro-inflammatory IL-23α, like induction of leukocyte migration and attachment [42], as well as various functions of IL-12β in isolation have been described [35, 43-47]. Therefore, the IL-12/IL-23 assembly ratio in immune cells might be adapted to match a certain immunological context and allow signaling of single subunits, or *vice versa* could be disturbed in pathologies.

Intriguingly, an analysis of IL-23α from different species revealed that, likewise to our engineering approach, IL-23α of species belonging to the Toxicofera clade are lacking a cysteine residue at the position of human Cys22 but instead contained Cys14 as well as an extra Cys at the position corresponding to human Gly164, according to a sequence alignment (Supplementary Fig. 6A). Strikingly, a secretion test of IL-23α from the corn snake, *P. guttatus*, revealed it to be secretion-competent in isolation (Supplementary Fig. 6B). Derived from the AlphaFold model of IL-23α *P.guttatus* and a structure overlay with human (Supplementary Fig. 6C), Cys143 is in close proximity to human Phe161. This would allow intramolecular disulfide bond formation between Cys143 and Cys14, comparable to Cys14-Cys161 in IL-23α$^{stabilized}$. Some species thus do have a secretion-competent IL-23α, and it will be interesting to see how IL-12β behaves in these species and which impact this has on the biology of the IL-12 system.

Taken together, our study provides molecular insights into the relevance of assembly-induced folding for IL-12 *versus* IL-23 secretion. Chaperone-assisted and β subunit-dependent folding of α subunits turn out to have a major impact on human IL-12/IL-23 cytokine biogenesis and the regulation thereof.

## Material and Methods

**Constructs.** Human interleukin cDNAs (IL-23α, IL-12α, and IL-12β, UniProt accession numbers: Q9NPF7, P29459, and P29460, respectively) were obtained from OriGene and were cloned into the pSVL vector (Amersham) for cell culture experiments, or pcDNA3.4 TOPO vector (Gibco) for mammalian protein expression, or the pET21a expression vector (Novagen) for protein production in *E. coli*. The helix-rearranged IL-23α, a T2A peptide construct (IL-23α-T2A-IL-23α) used for cloning of the desired competition assay constructs as well as IL-23α of *P. guttatus* (UniProt accession number: A0A6P9BFU5) were synthesized human codon-optimized by GeneArt (Thermo Fisher Scientific). Mutants were generated by site-directed mutagenesis PCR using Pfu (Promega) DNA polymerase with the help of custom oligos (Sigma-Aldrich). Restriction-based cloning using restriction enzymes (New England Biolabs), Antarctic Phosphatase (New England Biolabs), and T4 DNA ligase (Promega) was utilized for T2A constructs. Where indicated, IL-23α or IL-12β was equipped with C-terminal $(GS)_2$-linker and FLAG-tag, or myc-tag, respectively. Whenever a KDEL-sequence was used to retain the protein within the cell, it was attached C-terminally separated by a $(GA)_2$-linker. Proteins connected by the T2A peptide contained both an N-terminal HA-tag with $(GA)_2$-linker. For mammalian protein production, IL-23α was equipped with a C-terminal His-tag with TEV cleavage site. For protein production in *E. coli*, an N-terminal His-tag, separated by $(GS)_2$ from the TEV cleavage site, was attached to the IL-23α construct, also separated by a GS-linker. All constructs were sequenced.

**Sequence and evolutionary analyses.** Sequences of IL-23α were obtained from UniProt [48] by searching for the sequences with the gene name “IL23a”. This search brought the set of 253 IL-23α sequences. Annotation of signal peptides and cysteine residues has also been obtained from UniProt. Cysteine residues that were not reported to form any disulfide bonds were marked as free cysteines. Multiple sequence alignments were built using the MUSCLE tool [49] with default parameters and were visualized using the UGENE package [50]. BLAST search [51] in the Toxicofera clade (NCBI taxonomy ID 1329911) was performed with default parameters of the blastp algorithm and with IL-23α sequence from *Notechis scutatus* (UniProt accession number: A0A6J1UXJ1) as query.

**Structural modeling and RS-REMD simulations.** Based on crystal structures from the PDB database (IL-23: 3D87), missing loops were modelled *in silico* using Yasara Structure (www.yasara.org) with a subsequent steepest decent energy minimization for wild-type IL-23α. Structures of other four-helix bundle cytokines were taken from the PDB data base (1CNT, 1RHG, 1AU1) and AlphaFold [52] was used for a structural model of *P. guttatus*

IL-23α. Structures were depicted with PyMOL (PyMOL Molecular Graphics System, Version 2.0 Schrödinger, LLC; www.pymol.org).

The stability of helix 1 for the wild-type protein and mutant proteins was analyzed using molecular dynamics simulations. These simulations were conducted with the amber18 [53] program using ff14SB force field parameters [54]. The proteins were neutralized using $Na^+$ ions and an overall salt concentration of 0.12 M using $Na^+$ and $Cl^-$ ions was achieved. The proteins were solvated in an octahedron box of 15 Å minimum distance between the protein and the box edges. After energy minimization (1000 steps conjugate gradient) the molecules were heated to 300 K (in three steps) and equilibrated in 16 ps. A Langevin thermostat for temperature scaling was used.

In order to calculate the affinity of helix 1 to the protein, the RS-REMD method was conducted [55, 56], which was originally developed to calculate the binding affinity of protein-protein complexes. It is a H-REMD based simulation technique in which a repulsive bias is introduced in different copies (replicas) of the original system. To calculate the helix 1 affinity, the σ and ε parameters of the Lennard-Jones potential between helix 1 (residues 5 to 20) and helix B-D (beginning at residue 55) were altered for each replica according to the scheme given in Table 1 (only the parameters between these parts of the protein not within each part of the protein were altered). The given bias in the higher replicas leads to a dissociation of helix 1 so that a free energy difference between bound and dissociated helix 1 can be calculated using MBAR [57]. In total 5 ns (per replica) of RS-REMD simulations for 16 replicas were performed for each system, the second half was used to calculate the free energy differences. The results were obtained by splitting the simulations in five parts and evaluating the mean affinity with standard deviation.

**Table 1:** The Lennard-Jones parameters for the 16 replicas of the RS-REMD simulations.

| Residue | σ | ε |
|---|---|---|
| 1 | 0.0 | 1.0 |
| 2 | 0.01 | 0.99 |
| 3 | 0.02 | 0.98 |
| 4 | 0.04 | 0.97 |
| 5 | 0.08 | 0.96 |
| 6 | 0.12 | 0.94 |
| 7 | 0.16 | 0.92 |
| 8 | 0.2 | 0.9 |

| | | |
|---|---|---|
| 9 | 0.24 | 0.88 |
| 10 | 0.28 | 0.86 |
| 11 | 0.32 | 0.84 |
| 12 | 0.38 | 0.82 |
| 13 | 0.44 | 0.80 |
| 14 | 0.5 | 0.78 |
| 15 | 0.58 | 0.76 |
| 16 | 0.68 | 0.74 |

**Cell culture and transient transfections.** Human embryonic kidney (HEK) 293T and COS-7 cells were cultured in Dulbecco's modified Eagle's medium (DMEM) containing high glucose (4500 mg/l) and L-Ala-L-Gln (Sigma-Aldrich) supplemented with 10% (v/v) fetal bovine serum (FBS; Gibco) and 1% (v/v) antibiotic-antimycotic solution (25 µg/ml amphotericin B, 10 mg/ml streptomycin and 10,000 units of penicillin; Sigma-Aldrich) at 37 °C and 5% $CO_2$. Transient transfections of HEK 293T cells were carried out either in poly D-lysine coated p35 or p60 dishes (BioCoat, Corning or VWR) using GeneCellin (Eurobio), Lipofectamine 3000 (Thermo Fisher Scientific), or Metafectene PRO (Biontex) according to the manufacturer's instructions. A total DNA amount of 2 µg (p35) or 4 µg (p60) was used, except for degradation-experiments where only 1 µg DNA per p35 was transfected. The $\alpha$ subunit DNA was co-transfected with the $\beta$ subunit DNA or empty pSVL vector in a ratio of 1:2. For chaperone co-immunoprecipitation (co-IP) and degradation-experiments, $\alpha$ subunit DNA was transfected alone.

**Immunoblotting experiments.** For secretion and redox status experiments by immunoblotting, cells were transfected for 8 h in p35 dishes and then supplemented with 0.5 ml fresh medium for another 16 h. For the competition assay of $\alpha$ subunits, p60 dishes were used to analyze secretion into 1 ml medium. For analysis of secreted proteins, the medium was centrifuged for 5 min, 300 g, 4 °C. Subsequently, the supernatant was transferred into a new reaction tube and supplemented with 0.1 volumes of 500 mM Tris/HCl, pH 7.5, 1.5 M NaCl, complemented with 10x Roche complete Protease Inhibitor w/o EDTA (Roche Diagnostics).

For cycloheximide (CHX) chase assay, cells seeded in p35 dishes were treated with 50 µg/ml CHX (Sigma-Aldrich) for times indicated before lysis. For chaperone co-IP experiments, cells in p60 dishes were treated likewise for one hour prior to lysis. If indicated,

10 mM dithiothreitol (DTT, Sigma-Aldrich) was added to the cells in p60 dishes for 15 min in redox-status experiments.

To analyze the cell lysate, cells were washed twice with ice-cold phosphate-buffered saline (PBS, Sigma-Aldrich), supplemented with 20 mM *N*-ethylmaleimide (NEM) if samples were to be analyzed by non-reducing SDS- polyacrylamide gel electrophoresis (PAGE) or for chaperone co-IP experiments, and additional 10 U/ml apyrase (Sigma-Aldrich) was used for BiP interaction studies. Cell lysis was carried out in RIPA buffer (50 mM Tris/HCl, pH 7.5, 150 mM NaCl, 1.0% Nonidet P40 substitute, 0.5% sodium deoxycholate, 0.1% SDS, 1x Roche complete Protease Inhibitor w/o EDTA; Roche Diagnostics) for 20-30 min on ice. Again, buffer was supplemented with 10 U/ml apyrase and/or 20 mM NEM for experimental procedures previously explained.

Both lysate and medium samples were centrifuged for 15 min, 20,000 g, 4 °C. Samples were supplemented with 0.2 volumes of 5x Laemmli buffer (0.3125 M Tris/HCl pH 6.8, 10% SDS, 50% glycerol, bromphenol blue) containing either 10% (v/v) β-mercaptoethanol (β-Me) for reducing SDS-PAGE or 100 mM NEM for non-reducing SDS-PAGE.

Co-IPs were performed with anti-FLAG agarose beads (Sigma-Aldrich, A2220), or mouse IgG-beads (Sigma-Aldrich, A0919) for isotype-control. Harvested cell lysate (chaperone co-IP) or medium (competition co-IP) was supplemented with 30 µl beads, rotated for 1-1,5 hours at 4 °C, and beads were washed three times with RIPA buffer or NP40 wash buffer (50 mM Tris/HCl, pH 7.5, 400 mM NaCl, 0.5% NP40, 0.5% DOC) (5,000 g, 1 min). Elution of immunoprecipitated proteins from beads was performed with 2x Laemmli buffer containing 10% β-Me, boiling the samples for 5 min at 95°C.

For immunoblots, samples were run on 12% or 15% SDS-PAGE gels, transferred to polyvinylidene difluoride (PVDF) membranes by blotting overnight (o/n) at 30 V (4 °C). After blocking the membrane with Tris-buffered saline (25 mM Tris/HCl, pH 7.5, 150 mM NaCl; TBS) containing 5% (w/v) skim milk powder and 0.05% (v/v) Tween-20 (M-TBST), binding of primary antibody was carried out o/n at 4 °C with anti-Hsc70 (Santa Cruz Biotechnology, sc-7298, 1:1,000), anti-IL-12β (abcam, ab133752, 1:500), anti-IL-23α (Santa Cruz Biotechnology, sc-271279, 1:250-1:500), anti-myc-tag (Sigma-Aldrich, clone 4A6, 05-724MG, 1:1,000), anti-FLAG-tag (Sigma-Aldrich, F7425, 1:1,000), anti-HA-tag (Biolegend, 902302 1:500), anti-ERp70 (Proteintech, 14712-1-AP, 1:1,000), anti-PDIA6/ERp5 (Proteintech, 18233-1-AP, 1:1,000), anti-ERp44 (B68 [17], 1:1,000), anti-BiP (Cell Signaling Technology, C50B12, 1:500) in M-TBST containing 0.002% $NaN_3$. Species-specific HRP-conjugated secondary antibodies (Santa Cruz Biotechnology, 1:10,000 in M-TBST or for IL-23α and anti-HA-tag 1:5,000 in M-TBST) were used to detect the proteins. For detection, ECL prime reagent (Cytiva) and Fusion FX7 Edge V0.7 imager (Vilber Lourmat) were used.

**Protein production and purification.** Protein expression of IL-23α subunits in BL21 Star (DE3) *E. coli* (Invitrogen, Thermo Fisher Scientific) was induced at $OD_{600}$ = 0.8 with 1 mM Isopropyl β-D-1-thiogalactopyranoside (IPTG) and performed for 5 h at 37 °C. Expression resulted in inclusion bodies which were isolated by sonication, supplemented with SIGMA*FAST* protease inhibitor cocktail (Sigma-Aldrich), and thereafter solubilized in 50 mM sodium phosphate (pH 7.5), 250 mM NaCl, 10 mM β-Me, and 6 M guanidine hydrochloride. Solubilized inclusion bodies were centrifuged (20,000 g, 30 min, 20 °C) and the supernatant was applied to a HisTrap HP column (Cytiva) in 50 mM sodium phosphate (pH 7.5), 250 mM NaCl, 1 mM β-Me, 6 M guanidine hydrochloride supplemented with 20 mM imidazole. Elution was performed in 50 mM sodium phosphate (pH 4.0), 250 mM NaCl, 1 mM β-Me, and 6 M guanidine hydrochloride. For further purification by gel filtration chromatography, the eluate was supplemented with 100 mM DTT and 10 mM EDTA before applying to a HiPrep 16/60 Sephacryl S-200 HR column (Cytiva) equilibrated in 50 mM sodium phosphate (pH 7.5), 6 M guanidine hydrochloride, 1 mM EDTA and 1 mM DTT. Subsequently, the protein was diluted to <0.1 mg/ml in the same buffer, and then refolded for at least 24 hours or 48 hours, for IL-23$\alpha^{C14VC22VC54S}$ (IL-23$\alpha^{\Delta free\ cys}$) or IL-23$\alpha^{C22V,C54S,F161C}$ (IL-23$\alpha^{stabilized}$), respectively, at 4 °C via dialysis against 250 mM Tris/HCl (pH 8.0), 500 mM L-arginine, 100 mM NaCl, 10 mM EDTA, 0.25 mM GSSG, and 0.25 mM GSH. IL-23$\alpha^{\Delta free\ cys}$ was pre-treated with 20 mM GSSG for at least 4 h before refolding. After refolding, IL-23α proteins were dialyzed against 10 mM potassium phosphate buffer (pH 7.5) and TEV protease was added in a 1:10 ratio (w/w) to cleave the His-tag o/n at 4 °C. After cleavage, the protein was applied to a HisTrap HP column (Cytiva) in 10 mM potassium phosphate (pH 7.5). The flow through was concentrated and applied to an HiLoad 16/60 Superdex 75pg gel filtration column (Cytiva), equilibrated in 10 mM potassium phosphate buffer (pH 7.5). For nuclear magnetic resonance (NMR) experiments, IL-23α proteins were purified following the same protocol except that *E. coli* were cultured in minimal M9 media supplemented with 1 g/l $^{15}$N-ammonium chloride and 2 g/l $^{13}$C-glucose for protein expression.

IL-23 was produced using the ExpiCHO Expression System (Gibco) according to the manufacturer's protocol. His-tagged IL-23α was co-transfected with untagged IL-12β, both expressed from the pcDNA3.4 TOPO vector, in a ratio of 2:1 for five days at 32 °C (max titer protocol). After expression, medium was centrifuged (5,000 g, 30 min, 4 °C), supplemented with SIGMA*FAST* protease inhibitor cocktail (Sigma-Aldrich) and applied to a HisTrap HP column (Cytiva) in 10 mM potassium phosphate (pH 7.5). Elution was performed in 10 mM potassium phosphate (pH 7.5) with 500 mM imidazole. Subsequently, the His-tag was cleaved by addition of TEV protease 1:10 (w/w) o/n at 4 °C and removed by a HisTrap HP column (Cytiva) in 10 mM potassium phosphate (pH 7.5). Final purification

was performed using a HiLoad 26/60 Superdex 200 pg column (Cytiva) in 10 mM potassium phosphate (pH 7.5). Expression and purification of IL-12$\beta^{C177S}$ (with and without His-tag) and IL-23 from mammalian cells is described elsewhere [5].

Purity and redox status of the purified proteins were assessed by non-reducing SDS-PAGE in the presence of 20 mM NEM.

**HDX measurements.** Hydrogen/deuterium exchange (HDX) experiments were performed using an ACQUITY UPLC M-class system equipped with automated HDX technology (Waters, Milford, MA, USA). HDX kinetics were determined in technical triplicates, tacking data points at 0, 10, 60, 600, 1800 and 7200 s at 20 °C. At each data point, 3 µl of a solution of 30 µM protein ($\alpha$ subunit alone or with IL-12$\beta^{C177S}$) were diluted automatically 1:20 into 99.9% $D_2O$-containing 10 mM potassium phosphate, pH 7.5 (titrated with HCl) or the respective $H_2O$-containing reference buffer. The reaction mixture was quenched by the 1:1 addition of 200 mM $KH_2PO_4$, 200 mM $Na_2HPO_4$, pH 2.3 (titrated with HCl), containing 4 M guanidine hydrochloride and 200 mM TCEP at 1 °C and 50 µl of the resulting sample were subjected to on-column peptic digest on a Waters Enzymate BEH pepsin column 2.1 x 30 mm at 20 °C. Peptides were separated by reverse phase chromatography at 0 °C using a Waters Acquity UPLC C18, 1.7 µm, 2.1 x 5.0 mm, 130 Å trapping column and a Waters Acquity UPLC BEH C18, 1.7 µm, 1 x 100 mm, 130 Å separation column. For separation, a gradient increasing the acetonitrile concentration stepwise from 5-35% in 6 min, from 35-40% in 1 min and from 40-95% in 1 min was applied and the eluted peptides were analyzed using an in-line Synapt G2-S QTOF HDMS mass spectrometer (Waters, Milford, MA, USA). UPLC was performed in protonated solvents (0.1% formic acid), allowing deuterium to be replaced with hydrogen from side chains and amino/carboxyl termini that exchange much faster than backbone amide linkages [58]. All experiments were performed in duplicates. deuterium levels were not corrected for back exchange and are therefore reported as relative deuterium levels [59]. The use of an automated system handling all samples at identical conditions avoids the need for back exchange correction. MS data were collected over an m/z range of 100-2000. Mass accuracy was ensured by calibration with Glu-fibrino peptide B (Waters, Milford, MA, USA) and peptides were identified by $MS^E$ ramping the collision energy automatically from 20-50 V. Data were analyzed in PLGS 3.0.3 and DynamX 3.0 software packages (Waters, Milford, MA, USA). For comparative illustration, Deuteros 2.0 was used [60].

**NMR spectroscopy.** Nuclear magnetic resonance (NMR) experiments were performed using $^{15}N$-labeled protein samples at a concentration of 280 µM in 10 mM potassium phosphate buffer (pH 7.5) containing 5% $D_2O$. $^{1}H$, $^{15}N$ heteronuclear single quantum coherence (HSQC) experiments using watergate water flip-back for solvent suppression

were performed at 293 K on a Bruker Avance III spectrometer operating at 800 MHz proton Larmor frequency using a cryogenically cooled probe. Spectra comprised 2046 x 256 complex data points for direct and indirect dimensions, respectively, with a spectral window of 33 ppm centered at 117 ppm for the indirect dimension. All spectra were processed using Bruker Topspin 3.5 software (Bruker, Billerica, USA) using linear prediction and zero filling in the indirect dimension and were analyzed using CcpNmr Analysis [61]. Gaussian distribution was fitted from the histograms using Python.

**CD spectroscopy.** Far-UV circular dichroism (CD) spectra were recorded with a Jasco J-1500 CD spectrophotometer (Jasco) at 20 °C, using a 0.2 mm quartz cuvette at a protein concentration of 50 µM in 10 mM potassium phosphate buffer, pH 7.5. Spectra (197-260 nm) were recorded ten times and averages were analyzed after buffer-correction. For far-UV CD temperature transitions, 8 µM protein in 10 mM potassium phosphate buffer, pH 7.5, was heated in a 1 mm quartz cuvette at a heating rate of 60 °C/h from 20 °C to 90 °C, recorded at 222 nm.

**Analytical ultracentrifugation.** Sedimentation velocity analytical ultracentrifugation (AUC) measurements were performed on a Beckman Coulter Optima™ analytical ultracentrifuge (Beckman Coulter, Brea, CA, USA) using an An-50 Ti rotor at 20 °C, 34,000 rpm, and equipped with absorbance optics (with an initial test run at 3,000 rpm). 350 µl of 10 µM IL-23$\alpha^{\Delta \text{free cys}}$ or IL-23$\alpha^{\text{stabilized}}$ in 10 mM potassium phosphate buffer, pH 7.5, were loaded into a standard 12 mm double-sector epon-filled centerpiece, covered with quartz windows, alongside with the reference buffer solution. Detection was conducted at 230 nm with 500 scans and a radial step size of 0.001 cm. Resulting sedimentation velocity profiles were analyzed using SedFit software with a non-model based continuous Svedberg distribution method (c(s)) [62]. The density (ρ) and viscosity (η) of the potassium phosphate buffer used for data analysis was experimentally determined.

**High Performance Liquid Chromatography.** For quality control of purified IL-23$\alpha$ subunits, high performance liquid chromatography (HPLC) was performed on the AdvanceBio SEC 130 Å, 2.7 µm, 7.8 x 300 mm column together with the AdvanceBio SEC 130 Å, 2.7 µm, 7.8 x 50 mm LC guard column (Agilent) using the AdvanceBio SEC 130 Å Protein Standard (Agilent Technologies). Runs were performed using PBS, pH 7.4, as running buffer and detection at 220 nm. Runs of three standard proteins were used for calibration curve determination. Analysis was performed with the OpenLab Data Analysis (version 2.5, Agilent Technologies) with use of three standard proteins.

**Isothermal titration calorimetry.** Prior to the isothermal titration calorimetry (ITC) measurements, all protein pairs were buffer matched by dialysis in 10 mM potassium phosphate buffer, pH 7.5. Experiments were carried out using a MicroCal PEAQ-ITC

instrument (Malvern Panalytical). Titration of IL-12$\beta^{C177S}$ (500-650 µM) in the syringe to IL-23$\alpha^{\Delta free\ cys}$ (25-40 µM) or IL-23$\alpha^{stabilized}$ (35-38 µM), respectively, in the cell was conducted at 25 °C. Injection spacing was chosen to allow for signal to get back to stable baseline. Data were analyzed using the PEAQ-ITC analysis software v1.41 (Malvern Panalytical).

**Surface Plasmon Resonance.** Surface plasmon resonance (SPR) measurements were performed on a Biacore X100 instrument (Cytiva). His-tagged IL-12$\beta^{C177S}$ was immobilized on a CM5 sensor chip (Cytiva) previously treated with the His Capture Kit (Cytiva) to covalently couple anti-His antibody on the surface. With a low density of captured His-tagged IL-12$\beta^{C177S}$ (≈ 70 responsive units (RU)), binding of IL-23$\alpha^{\Delta free\ cys}$ or IL-23$\alpha^{stabilized}$ was measured at room temperature with a flow rate of 30 µl/min in 10 mM potassium phosphate buffer, pH 7.5. Contact of the ligand was performed for 180 sec followed by a 120 s stabilization phase. Analyte was injected for 120 s and dissociation was performed for 180 s. Following each cycle, the chip was regenerated with 10 mM Glycine-HCl, pH 1.5. Binding curves were fitted to calculate the steady state affinity using BIAevaluation software (Cytiva).

**NanoBRET™ Assay.** Receptor chains were cloned into the pHTC HaloTag® (HT) CMV-neo vector (IL-23R) or the pNLF1-C [CMV/Hygro] NanoLuc® luciferase (NL) protein fusion vector (IL-12R$\beta$1) (Promega). For transient transfection, COS-7 cells were seeded in uncoated tissue culture 6-well plates (VWR) and transfected using GeneCellin (Eurobio) according to manufacturer's protocol. In total, 2 µg receptor chain DNA were transfected per well with a ratio of 100:1 HT:NL. After 16 h, transfected cells were detached by Accutase® solution (Sigma-Aldrich). Cells were resuspended in assay medium (DMEM w/o Phenolred, 4% (v/v) FBS) to a cell number of 2.2 x $10^5$ cells/ml, divided into two pools and 1 µl HaloTag® NanoLuc® 618 Ligand (Promega) or 1 µl DMSO per ml cells were added. 2 x $10^4$ cells were seeded into white bottom 96-well plates and incubated for another 20 h. Reconstituted proteins (1:1), single subunits, or the IL-23 heterodimer were incubated for 60 min at 25 °C and cells were stimulated thereafter with cytokines or PBS for 30 min at a final concentration of 20 nM. For experimentally assessing inhibition, cells were pre-incubated 30 min with indicated concentrations of IL-23$\alpha^{stabilized}$ or Guselkumab and subsequently stimulated with 20 nM IL-23 or 10 mM potassium phosphate (KPi), pH 7.5. Measurement was conducted with the CLARIOstar® platereader (BMG Labtech) after addition of the Nano-Glo® substrate. Bioluminescence resonance energy transfer using the NL, NanoBRET™, ratios were calculated by dividing blank-corrected acceptor emission (610 nm) by blank-corrected donor luminescence (450-480 nm) and subsequent multiplication by 1,000. Mean NanoBRET™ ratios were determined averaging the experimental ratios and subtracting the no-acceptor (DMSO) control mean from the

experimental mean. Samples are measured in technical triplicates and one representative result from biological triplicates is shown.

**Quantification and statistics.** Immunoblots were quantified using the Bio-1D software (Vilber Lourmat). Statistical analyses were performed using Prism (GraphPad Software), with differences considered statistically significant when $p < 0.05$. Applied statistical test types and experimental sample sizes are stated in the figure legends. Where no statistical data are shown, experiments were performed at least two times.

## Acknowledgements

We thank Karen Hildenbrand, TUM, for providing receptor chain constructs and helping with the NanoBRET™ measurement setup. Support with ITC measurement and analyses by Hyun-Seo Kang, and with SPR analysis by Hristo Svilenov is also very much acknowledged. The ERp44 antibody was a kind gift from Tiziana Anelli and Roberto Sitia, Ospedale San Raffaele, Milan, Italy. We acknowledge access to NMR and ITC measurements at the Bavarian NMR Center and to SPR measurements at the CPA, Chair of Biotechnology.

IA gratefully acknowledges a PhD scholarship from the German Academic Scholarship Foundation and the Marianne-Plehn-Program of the Elite Network of Bavaria. MJF gratefully acknowledges funding of our work on interleukin biogenesis by the German Research Foundation DFG (Sonderforschungsbereich 1035, project number 201302640, project B11 and Transregio 338, project number 452881907, project A04).

## Author contributions

MJF conceived the study. NMR experiments were performed by AL and analyzed by AL and MS. TS and MZ did structural modeling and RS-REMD simulations. DC performed ultracentrifugation experiments. HDX experiments were carried out and analyzed by FR and MH. Evolutionary analyses were conducted by MP and DF. All other experiments were performed by IA, PR, and AM. IA and MJF analyzed data. The paper was written by IA and MJF.

## Figures

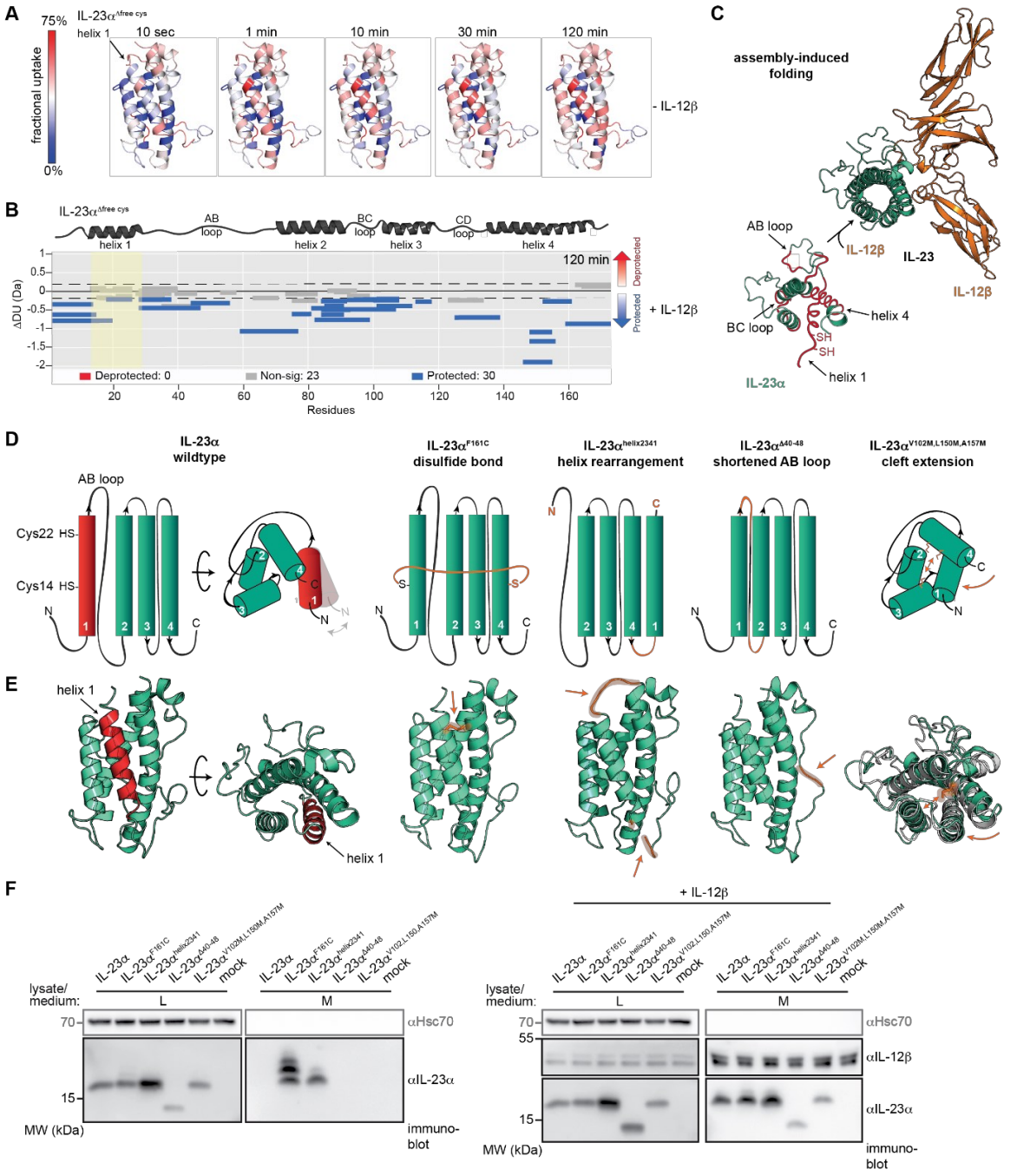


**Fig. 1: Rational engineering of a secretion-competent human IL-23α subunit. A** Hydrogen/deuterium exchange (HDX) experiments of four-helix bundle IL-23$\alpha^{C14V,C22V,C54S}$ (IL-23$\alpha^{\Delta free\ cys}$) reveal flexible regions. Structure of IL-23α (taken from PDB: 3D87) is colored according to the measured HDX rates, with blue corresponding to a lower and red to a higher fractional deuterium uptake/structural flexibility. **B** Differential Wood's plot of IL-23$\alpha^{\Delta free\ cys}$ peptides depicts differential uptake (ΔDU) upon IL-12$\beta^{C177S}$ interaction. Each peptide (bar) is represented with its ΔDU magnitude. Significantly ($p$<0.05, Hybrid method) protected peptides (blue) indicate structural stabilization. Those with no statistical difference in uptake are shown in gray for t = 120 min. Helix 1 is highlighted (yellow) and structural features are indicated. **C** Schematic of IL-23 heterodimerization. IL-23α (cyan) is incompletely structured, particularly helix 1 with two free cysteines (-SH), the AB loop, BC loop, and helix 4, all marked in red, prior to assembly-induced folding by the β subunit IL-12β (orange). In heterodimeric IL-23 (PDB: 3D87), subunits are disulfide-linked. **D-E** Molecular dynamics (MD) simulations provided *in silico* engineered mutants, shown in schematics (**D**) and structures (**E**), aiming on stabilizing the IL-23α structure. The wild-type IL-23α (left) is composed of four helices (cylinder) with its unstructured helix 1 (red) and two free cysteines (-SH). Introduction of a single cysteine residue (IL-23$\alpha^{F161C}$) inducing internal disulfide bond formation with one of the two free cysteines (Cys14) in helix 1, rearrangement

of the helix sequence (IL-23$\alpha^{helix2341}$), shortening of the unstructured AB loop (IL-23$\alpha^{\Delta 40\text{-}48}$), or insertion of one or more bulky amino acids to expand the cleft between helices 2-4 and thereby entropically facilitate helix 1 attachment (IL-23$\alpha^{V102M,L150M,A157M}$) was tested. Structural changes are colored orange with arrows highlighting changes. Helices are numbered according to the wild-type protein. N, N-terminus. C, C-terminus. **F** The human wild-type IL-23 $\alpha$ subunit is secretion-incompetent in isolation and retained in cells (lysate, L). Assembly with the secretion-competent $\beta$ subunit enables formation of the heterodimeric IL-23 and induces secretion into cell media (medium, M). Engineered IL-23$\alpha$ mutants are all expressed in the cell and are secreted (M) when co-transfected with IL-12$\beta$. *O*-glycosylation of IL-23$\alpha$ occurs during secretion and is blocked by assembly with IL-12$\beta$ [5]. Unlike the wildtype, IL-23$\alpha^{F161C}$ and IL-23$\alpha^{helix2341}$ are secreted in isolation. Hsc70 served as loading control. Mock, empty vector transfection. MW, molecular weight.

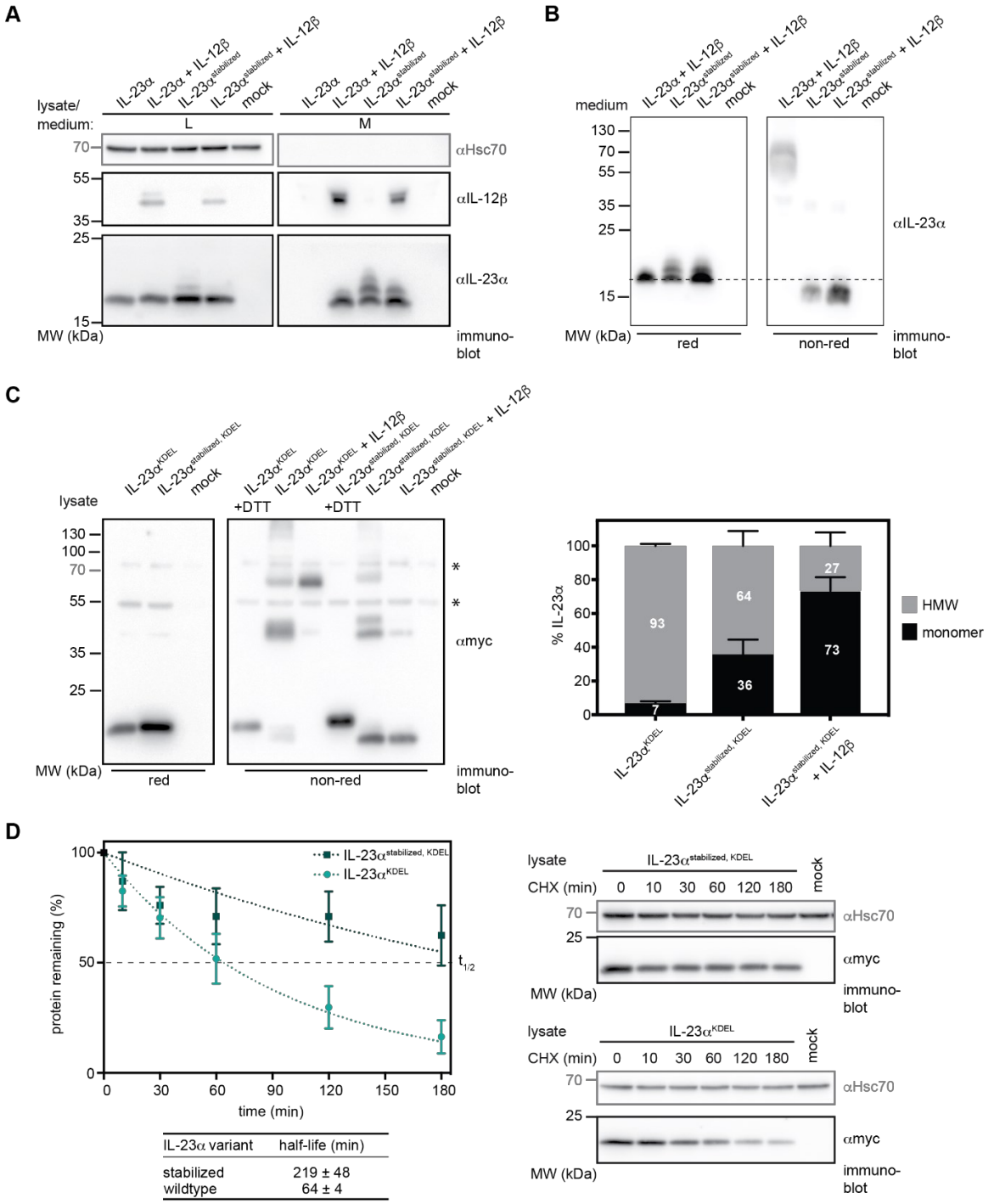


**Fig. 2: An engineered intramolecular disulfide bond stabilizes IL-23α. A** Secretion behavior of wild-type IL-23α and engineered IL-23α$^{C22V,C54S,F161C}$ (IL-23α$^{stabilized}$) in the absence or presence of IL-12β. Based on IL-23α$^{F161C}$, further cysteines (free Cys22, not interacting with Phe161Cys, and Cys54 responsible for covalent IL-12β linkage) were mutated for improved folding. Lysate, L. Medium, M. **B** Redox behavior of the secreted subunits. The engineered IL-23α$^{stabilized}$ gets secreted in isolation, with a further increase in secretion when co-expressed with IL-12β. Oxidative folding of the α subunit is indicated by the mobility shift when comparing reduced (red; β-mercaptoethanol, β-Me) and non-reduced (non-red; *N*-ethylmaleimide, NEM) samples. Wild-type IL-23 shows covalent heterodimer formation under non-reducing conditions. **C** In the cell, IL-23α$^{stabilized}$ shows less misfolded, disulfide-linked species of high-molecular weight (HMW) compared to the wildtype in isolation. Interaction with IL-12β further reduces misfolding of the mutant, indicating folding assistance. IL-12β together with IL-23α wildtype form covalently linked IL-23 in the lysate. Constructs were equipped with a KDEL-sequence to induce ER retention, and a myc-tag for detection. Samples were treated with dithiothreitol (DTT) in cells, where indicated, and post-lysis with β-Me (red) or NEM (non-red). Unspecific bands are marked with asterisks. Bar graphs (right) show the percentage of HMW and monomeric species (n=4, ±SEM). **D** Cycloheximide (CHX) chases for up to 180 min with KDEL-tagged IL-23α constructs show slower protein

degradation for IL-23$\alpha^{stabilized}$ compared to the wildtype. Protein turnover data (n=5-7, ± SD) of quantified lysate signals (right) was fitted as exponential one phase decay (dotted curve). Determination of half-lives $t_{1/2}$ (dashed line) was performed by logarithmic linearization and linear regression (not shown). Constructs were myc-tagged for detection. Hsc70 served as loading control. Mock, empty vector transfection. MW, molecular weight.

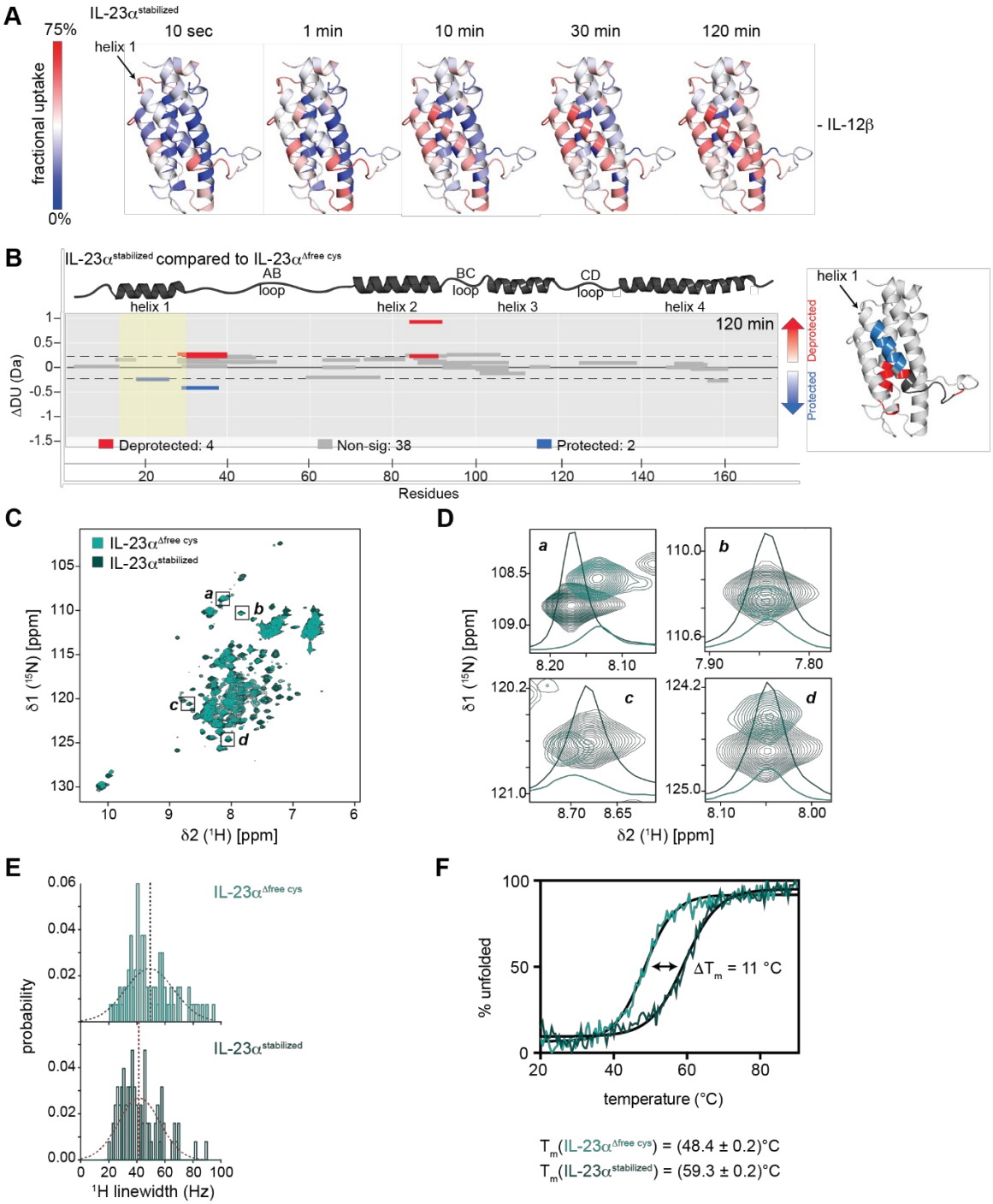


**Fig. 3: Folding and stability of IL-23α$^{stabilized}$. A** HDX experiment, same as in **Fig. 1A**, of IL-23α$^{stabilized}$ shows fractional deuterium uptake of the α subunit in isolation, with blue highlighting more rigid and red more flexible protein regions on the protein structure (adapted from PDB:3D87). **B** Wood's plot like in **Fig. 1B**, with differential deuterium uptake (ΔDU) of IL-23α$^{stabilized}$ compared to IL-23α$^{\Delta free\ cys}$. Significantly ($p$<0.02, Hybrid method) protected peptides (blue), indicating structural stabilization, deprotected peptides (red), or those with no significant difference in uptake (gray) for the two α subunits are marked for t = 120 min. The position of helix 1 (yellow) and structural features are indicated. Significant (de-)protection according to the differential Wood's plot is also mapped on the IL-23α structure (PDB: 3D87) colored in blue or red, respectively. Conflicting effects (significant protection and deprotection for peptides at the same region) are depicted in black. **c** NMR spectroscopy reveals stabilizing effects of mutations in IL-23α by spectra overlay of IL-23α$^{\Delta free\ cys}$ (bright cyan) and stabilized mutant (dark cyan). **D** Zoomed view of selected signals (marked by squares in **c**), showing 1D traces of the $^{1}$H dimension in the corresponding color. Increased line broadening in IL-23α$^{\Delta free\ cys}$ indicates higher dynamics in the µs-ms time scale. **E** Histograms showing distributions of peak width at half-height in the $^{1}$H dimension for the two variants, highlighting the pervasive increase in line broadening in the wildtype-like IL-23α$^{\Delta free\ cys}$ protein. **F** Temperature-dependent unfolding curve by far-UV circular dichroism (CD) measurements at 222 nm. IL-23α$^{stabilized}$ unfolds at a higher melting temperature compared to IL-23α$^{\Delta free\ cys}$.

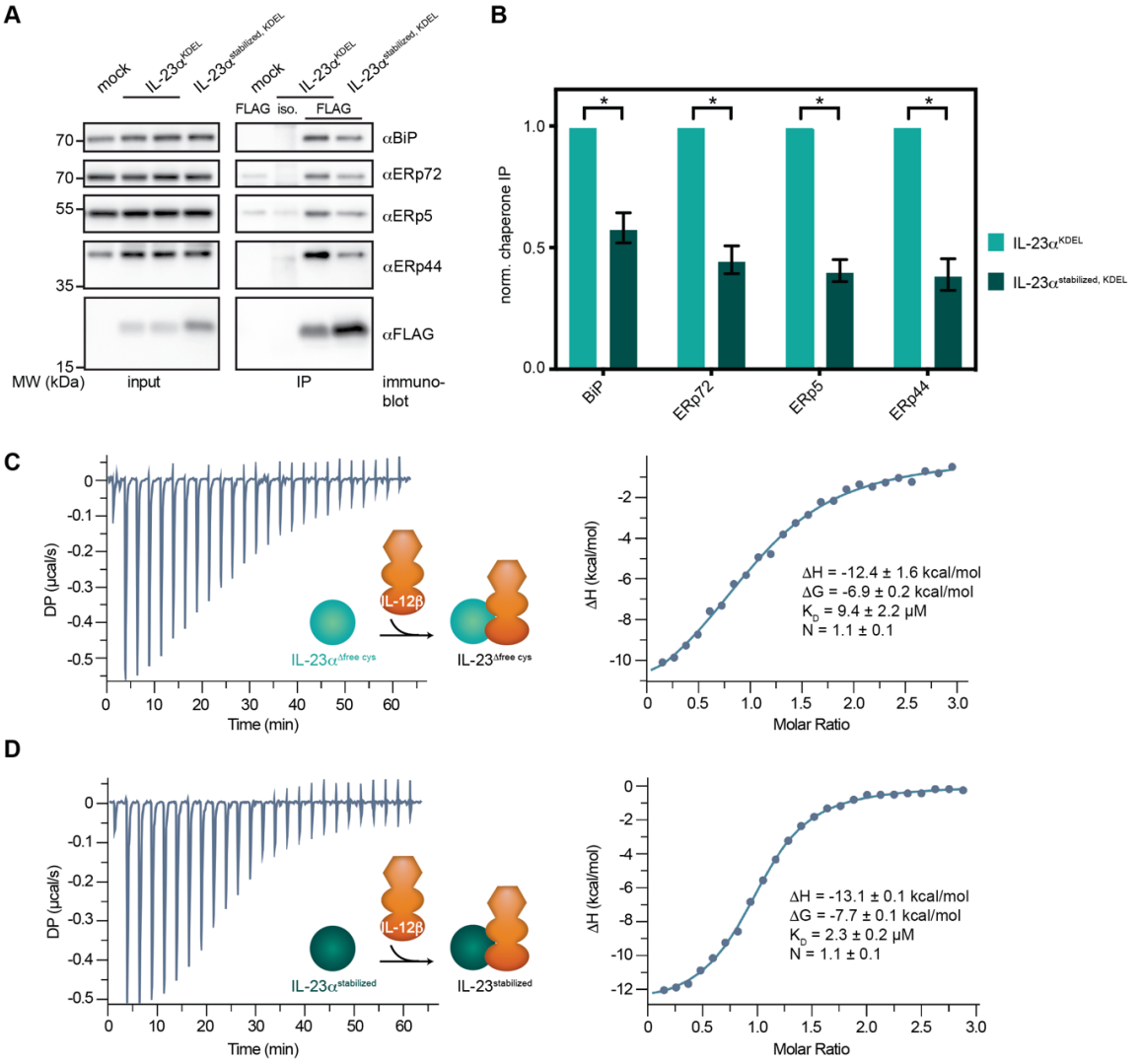


**Fig. 4: Effects of IL-23α structural optimization on chaperone recruitment and IL-23 heterodimer assembly. A** IL-23α proteins were equipped with a KDEL retention signal and FLAG-tag, the latter allowing immunoprecipitation (IP) from the lysate. Interaction with Hsp70 family chaperone immunoglobulin heavy-chain binding protein (BiP) and protein disulfide isomerase (PDI) family members ERp72, ERp5, and ERp44 was analyzed via co-IP and immunoblotting. Mock, empty vector transfection. Iso., isotype control. MW, molecular weight. **B** Quantification of immunoblot IP signals, with unspecific signals subtracted and signal normalization to the wildtype (n=8-12, ±SEM, * $p$<0.05, multiple t-test) shows that chaperones interact differently with IL-23α$^{KDEL}$ variants. **C** Isothermal titration calorimetry (ITC) measurement of purified subunits IL-23α$^{\Delta free\ cys}$ and IL-12β$^{C177S}$ reveals thermodynamic parameters of wildtype-like IL-23 formation. Schematic depicts titration of IL-12β (orange) with its two fibronectin type III domains (ellipses) and the N-terminal immunoglobulin-like domain (hexamer) to the four-helix bundle IL-23α (green circle). **D** ITC measurement like in **C**, with IL-23α$^{stabilized}$ and IL-12β$^{C177S}$, assessing respective thermodynamic parameters of subunit interaction during heterodimer formation. A fourfold lower $K_D$-value for the engineered, stabilized IL-23 depicts higher binding affinity of IL-23α$^{stabilized}$ in assembly with IL-12β compared to IL-23 formation with α subunit IL-23α$^{\Delta free\ cys}$ *in vitro*.

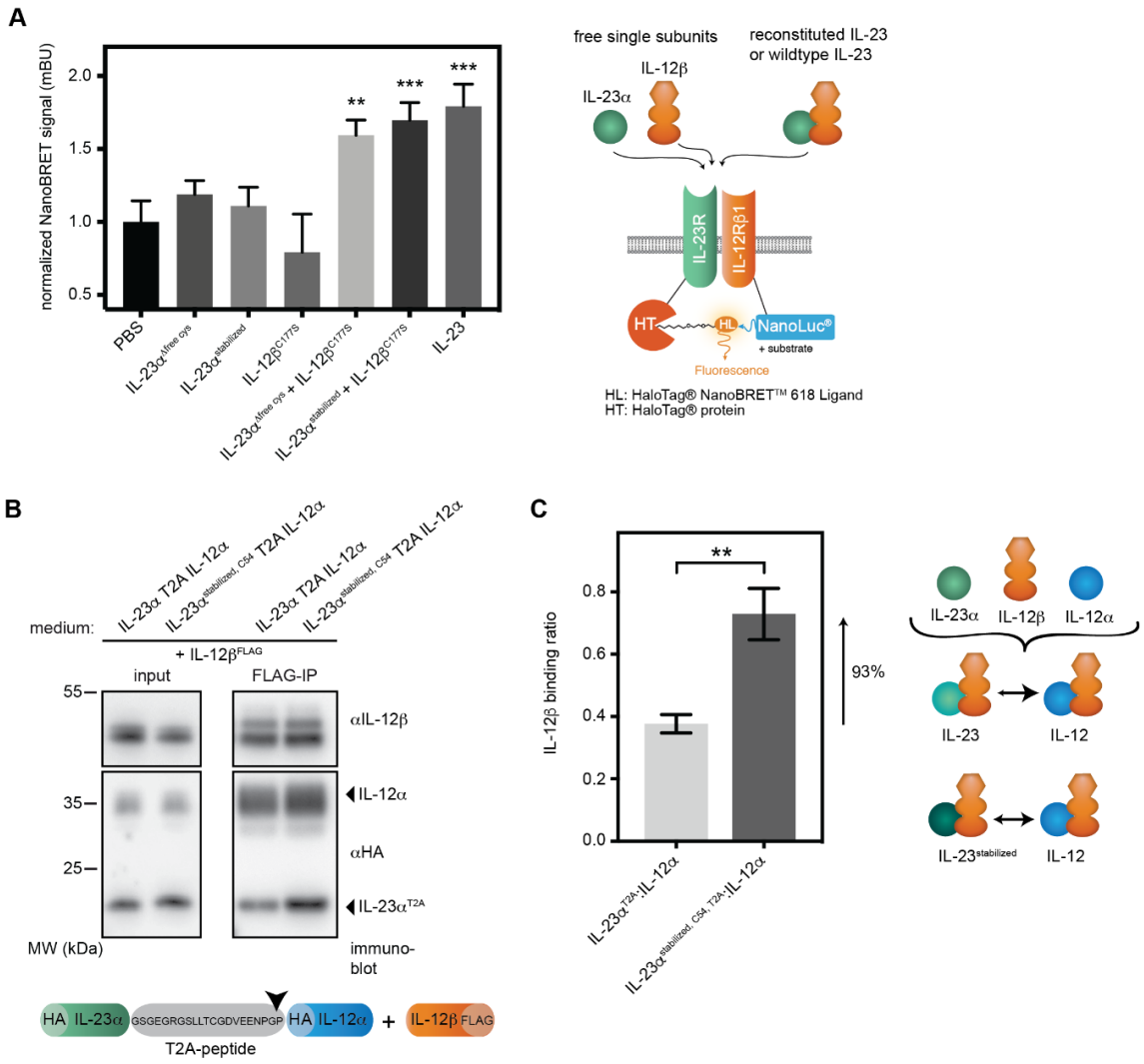


**Fig. 5: IL-23α$^{stabilized}$ can form a functional IL-23 heterodimer and shifts the IL-12/IL-23 secretion ratio. A** *In vitro* reconstituted wildtype-like IL-23 (IL-23α$^{\Delta free\ cys}$ + IL-12β$^{C177S}$) and engineered IL-23 (IL-23α$^{stabilized}$ + IL-12β$^{C177S}$) both induce receptor chain dimerization in a NanoBRET™ assay comparable to the IL-23 heterodimer (n=3, ±SD, ** $p$<0.005, *** $p$<0.0005, One-way ANOVA). Signals were normalized to PBS. Schematic (right) shows experimental setup to assess binding of single IL-23 subunits or heterodimeric IL-23 to IL-23 receptor chains. IL-12Rβ1 is fused to the NanoBRET™ donor NanoLuc® Luciferase and IL-23R to the acceptor HaloTag® 618 Ligand to induce a bioluminescence resonance energy transfer (BRET) upon receptor chain dimerization. **B** The ratio of IL-12/IL-23 heterodimer formation when α subunits are competing for their shared β subunit was analyzed by co-immunoprecipitation (co-IP). HEK 293T cells were transiently transfected with the indicated constructs (schematics below, with T2A cleavage site indicated as arrowhead) and medium was analyzed for secreted FLAG-tagged IL-12β and co-immunoprecipitating HA-tagged IL-12α and IL-23α. For better comparison, α subunits were expressed equimolarly via self-processing T2A-peptide and contained the respective cysteine residues responsible for intermolecular disulfide bond formation with IL-12β. **C** IL-12β binding ratio derived from immunoblot quantification of α subunit IP signals, shown in **B**, differs significantly when IL-23α$^{stabilized,\ C54}$ instead of IL-23α wildtype is competing with IL-12α for IL-12β binding (n=6, ±SEM, ** $p$<0.005, unpaired t test). Schematic depicts analyzed subunits and shifted ratio of IL-12 *versus* IL-23 formation for the two different IL-23α variants involved.

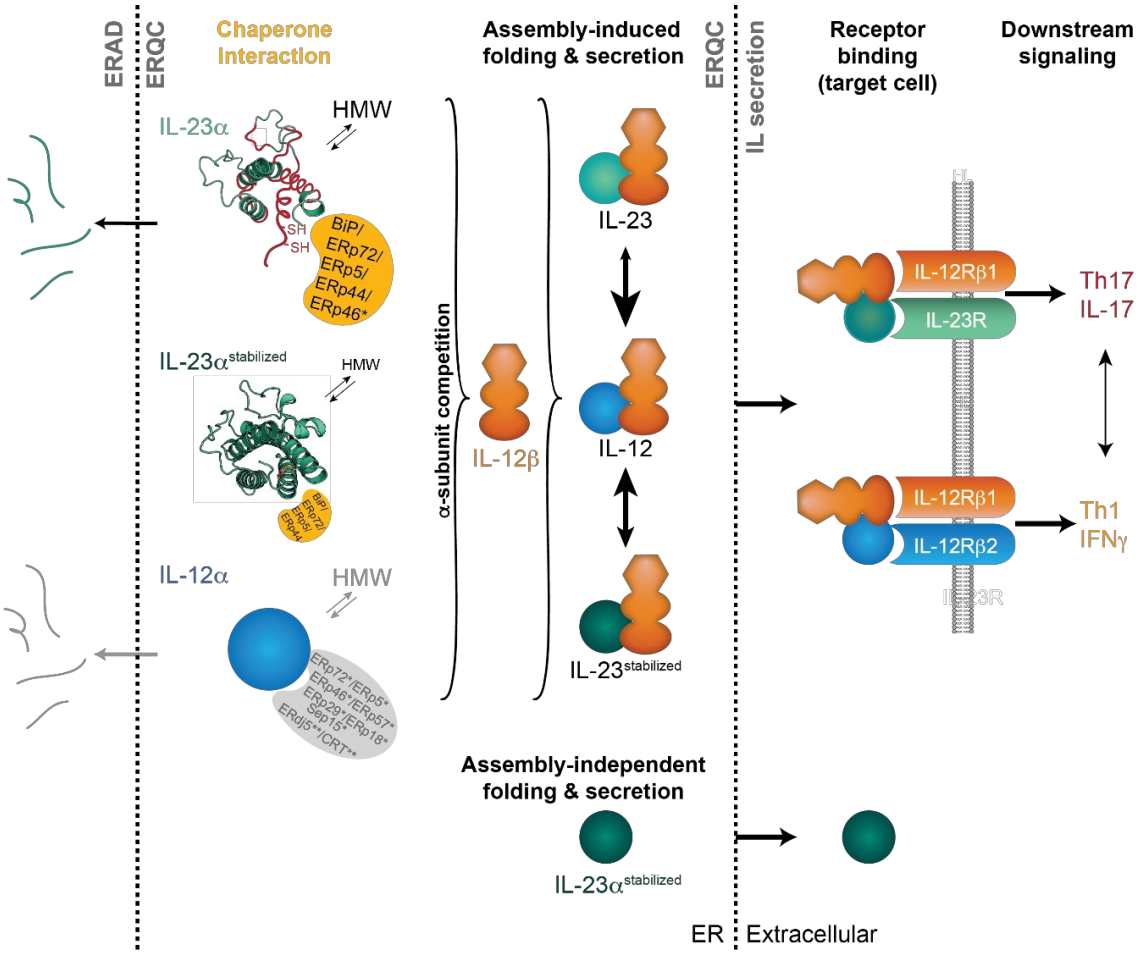


**Fig. 6: Assembly-dependent structure formation impacts interleukin secretion ratio in humans.** IL-23α (bright green) is highly flexible (red regions) with free cysteines (-SH), forming erroneous disulfide-linked species of high molecular weight (HMW) in the endoplasmic reticulum (ER) in isolation. It strongly interacts with a diverse chaperone repertoire (yellow) involved in ER quality control (ERQC) processes. Assembly-induced folding by IL-12β rescues this α subunit from ER-associated degradation (ERAD), resulting in IL-23 heterodimer formation and secretion (Extracellular). For the engineered IL-23α$^{stabilized}$ (dark green), an extra intramolecular disulfide bond structurally stabilizes its fold, leading to reduced chaperone binding and less HMW redox species formation. It can fold and secrete assembly-independent as well as interact with IL-12β with a higher affinity than the wild-type IL-23α to form IL-23$^{stabilized}$. For IL-12α, chaperone interaction, misfolding to HMW species in isolation, and degradation by ERAD are depicted in gray and adopted from [4]. Chaperone interactions not analyzed in this study, but confirmed in other studies, are marked with one [7] or two [2, 4] asterisks. α subunits compete for IL-12β interaction, with arrowhead sizes illustrating the IL-12α:IL-23α binding ratios based on co-immunoprecipitation experiments. Thus, presence of the folding-competent IL-23α$^{stabilized}$ subunit shifts the assembled cytokine ratio. Heterodimeric cytokines can then secrete and induce different signaling in the target cell by receptor binding. IL-12 and IL-23 stimulate distinct immune responses by T helper (Th) subset differentiation (Th1 *versus* Th17) and other cytokine secretion (IFNγ *versus* IL-17), resulting in strong pro-inflammatory (IL-23) or pro-inflammatory (IL-12) immunity.

## References


1. Tait Wojno, E.D., C.A. Hunter, and J.S. Stumhofer, *The Immunobiology of the Interleukin-12 Family: Room for Discovery.* Immunity, 2019. **50**(4): p. 851-870.
2. Hildenbrand, K., et al., *Biogenesis and engineering of interleukin 12 family cytokines.* Trends Biochem Sci, 2022. **47**(11): p. 936-949.
3. Muller, S.I., et al., *A folding switch regulates interleukin 27 biogenesis and secretion of its alpha-subunit as a cytokine.* Proc Natl Acad Sci U S A, 2019. **116**(5): p. 1585-1590.
4. Reitberger, S., et al., *Assembly-induced folding regulates interleukin 12 biogenesis and secretion.* J Biol Chem, 2017. **292**(19): p. 8073-8081.
5. Meier, S., et al., *The molecular basis of chaperone-mediated interleukin 23 assembly control.* Nat Commun, 2019. **10**(1): p. 4121.
6. Jalah, R., et al., *The p40 Subunit of Interleukin (IL)-12 Promotes Stabilization and Export of the p35 Subunit: IMPLICATIONS FOR IMPROVED IL-12 CYTOKINE PRODUCTION.* J Biol Chem, 2013. **288**(9): p. 6763-76.
7. Mideksa, Y.G., et al., *A comprehensive set of ER protein disulfide isomerase family members supports the biogenesis of proinflammatory interleukin 12 family cytokines.* J Biol Chem, 2022. **298**(12): p. 102677.
8. Oppmann, B., et al., *Novel p19 protein engages IL-12p40 to form a cytokine, IL-23, with biological activities similar as well as distinct from IL-12.* Immunity, 2000. **13**(5): p. 715-25.
9. Wolf, S.F., et al., *Cloning of cDNA for natural killer cell stimulatory factor, a heterodimeric cytokine with multiple biologic effects on T and natural killer cells.* J Immunol, 1991. **146**(9): p. 3074-81.
10. Gubler, U., et al., *Coexpression of two distinct genes is required to generate secreted bioactive cytotoxic lymphocyte maturation factor.* Proc Natl Acad Sci U S A, 1991. **88**(10): p. 4143-7.
11. Lupardus, P.J. and K.C. Garcia, *The structure of interleukin-23 reveals the molecular basis of p40 subunit sharing with interleukin-12.* J Mol Biol, 2008. **382**(4): p. 931-41.
12. Yoon, C., et al., *Charged residues dominate a unique interlocking topography in the heterodimeric cytokine interleukin-12.* Embo j, 2000. **19**(14): p. 3530-3541.
13. Floss, D.M., J.M. Moll, and J. Scheller, *IL-12 and IL-23-Close Relatives with Structural Homologies but Distinct Immunological Functions.* Cells, 2020. **9**(10).
14. Mideksa, Y.G., et al., *Site-Specific Protein Labeling with Fluorophores as a Tool To Monitor Protein Turnover.* Chembiochem, 2020. **21**(13): p. 1861-1867.
15. Müller, S.I., et al., *A folding switch regulates interleukin 27 biogenesis and secretion of its α-subunit as a cytokine.* Proc Natl Acad Sci U S A, 2019. **116**(5): p. 1585-1590.
16. Satoh, M., et al., *Functional characterization of 3 thioredoxin homology domains of ERp72.* Cell Stress Chaperones, 2005. **10**(4): p. 278-84.
17. Anelli, T., et al., *ERp44, a novel endoplasmic reticulum folding assistant of the thioredoxin family.* Embo j, 2002. **21**(4): p. 835-44.
18. Anelli, T., et al., *Thiol-mediated protein retention in the endoplasmic reticulum: the role of ERp44.* Embo j, 2003. **22**(19): p. 5015-22.
19. Jessop, C.E., et al., *Protein disulphide isomerase family members show distinct substrate specificity: P5 is targeted to BiP client proteins.* J Cell Sci, 2009. **122**(Pt 23): p. 4287-95.
20. Lin, L.F., et al., *Purification, cloning, and expression of ciliary neurotrophic factor (CNTF).* Science, 1989. **246**(4933): p. 1023-5.
21. Borden, E.C., *Interferons α and β in cancer: therapeutic opportunities from new insights.* Nature Reviews Drug Discovery, 2019. **18**(3): p. 219-234.
22. Nomura, H., et al., *Purification and characterization of human granulocyte colony-stimulating factor (G-CSF).* Embo j, 1986. **5**(5): p. 871-6.
23. Müller, S.I., et al., *An Interspecies Analysis Reveals Molecular Construction Principles of Interleukin 27.* J Mol Biol, 2019. **431**(12): p. 2383-2393.

24. Pflanz, S., et al., *IL-27, a heterodimeric cytokine composed of EBI3 and p28 protein, induces proliferation of naive CD4(+) T cells.* Immunity, 2002. **16**(6): p. 779-90.
25. Boulay, J.L., J.J. O'Shea, and W.E. Paul, *Molecular phylogeny within type I cytokines and their cognate receptors.* Immunity, 2003. **19**(2): p. 159-63.
26. Feige, M.J., L.M. Hendershot, and J. Buchner, *How antibodies fold.* Trends Biochem Sci, 2010. **35**(4): p. 189-98.
27. Feige, M.J. and L.M. Hendershot, *Quality control of integral membrane proteins by assembly-dependent membrane integration.* Mol Cell, 2013. **51**(3): p. 297-309.
28. Christis, C., N.H. Lubsen, and I. Braakman, *Protein folding includes oligomerization - examples from the endoplasmic reticulum and cytosol.* FEBS J, 2008. **275**(19): p. 4700-27.
29. Call, M.E., et al., *The organizing principle in the formation of the T cell receptor-CD3 complex.* Cell, 2002. **111**(7): p. 967-79.
30. Klausner, R.D., J. Lippincott-Schwartz, and J.S. Bonifacino, *The T cell antigen receptor: insights into organelle biology.* Annu Rev Cell Biol, 1990. **6**: p. 403-31.
31. Sitia, R., et al., *Developmental regulation of IgM secretion: the role of the carboxy-terminal cysteine.* Cell, 1990. **60**(5): p. 781-90.
32. Lee, S.M., et al., *Decreased interleukin-12 (IL-12) from activated cord versus adult peripheral blood mononuclear cells and upregulation of interferon-gamma, natural killer, and lymphokine-activated killer activity by IL-12 in cord blood mononuclear cells.* Blood, 1996. **88**(3): p. 945-54.
33. Wang, X., et al., *Expression of IL-23 and IL-17 and effect of IL-23 on IL-17 production in ankylosing spondylitis.* Rheumatol Int, 2009. **29**(11): p. 1343-7.
34. Ethuin, F., et al., *Regulation of Interleukin 12 p40 and p70 Production by Blood and Alveolar Phagocytes During Severe Sepsis.* Laboratory Investigation, 2003. **83**(9): p. 1353-1360.
35. Cooper, A.M. and S.A. Khader, *IL-12p40: an inherently agonistic cytokine.* Trends Immunol, 2007. **28**(1): p. 33-8.
36. Bloch, Y., et al., *Structural Activation of Pro-inflammatory Human Cytokine IL-23 by Cognate IL-23 Receptor Enables Recruitment of the Shared Receptor IL-12Rβ1.* Immunity, 2018. **48**(1): p. 45-58.e6.
37. Glassman, C.R., et al., *Structural basis for IL-12 and IL-23 receptor sharing reveals a gateway for shaping actions on T versus NK cells.* Cell, 2021. **184**(4): p. 983-999.e24.
38. Oppmann, B., Lesley, R., Blom, B., Timans, J.C., Xu, Y., Hunte, B., Vega, F., Yu, N., Wang, J., Singh, K., Zonin, F., Vaisberg, E., Churakova, T., Liu, M., Gorman, D., Wagner, J., Zurawski, S., Liu, Y., Abrams, J.S., Moore, K.W., Rennick, D., de Waal-Malefyt, R., Hannum, C., Bazan, J.F., Kastelein, R.A., *Novel p19 protein engages IL-12p40 to form a cytokine, IL-23, with biological activities similar as well as distinct from IL-12.* Immunity, 2000. **13**(5): p. 715-25.
39. Trinchieri, G., Pflanz, S., Kastelein, R.A., *The IL-12 family of heterodimeric cytokines: new players in the regulation of T cell responses.* Immunity, 2003. **19**(5): p. 641-4.
40. Vignali, D.A., Kuchroo, V.K., *IL-12 family cytokines: immunological playmakers.* Nat Immunol, 2012. **13**(8): p. 722-8.
41. Soares Moretti, A.I. and F.R. Martins Laurindo, *Protein disulfide isomerases: Redox connections in and out of the endoplasmic reticulum.* Archives of Biochemistry and Biophysics, 2017. **617**: p. 106-119.
42. Espígol-Frigolé, G., et al., *Identification of IL-23p19 as an endothelial proinflammatory peptide that promotes gp130-STAT3 signaling.* Sci Signal, 2016. **9**(419): p. ra28.
43. Jana, M. and K. Pahan, *IL-12 p40 homodimer, but not IL-12 p70, induces the expression of IL-16 in microglia and macrophages.* Mol Immunol, 2009. **46**(5): p. 773-83.

44. Jana, M., et al., *IL-12 p40 homodimer, the so-called biologically inactive molecule, induces nitric oxide synthase in microglia via IL-12R beta 1.* Glia, 2009. **57**(14): p. 1553-65.
45. Russell, T.D., et al., *IL-12 p40 homodimer-dependent macrophage chemotaxis and respiratory viral inflammation are mediated through IL-12 receptor beta 1.* J Immunol, 2003. **171**(12): p. 6866-74.
46. Mondal, S., et al., *IL-12 p40 monomer is different from other IL-12 family members to selectively inhibit IL-12Rβ1 internalization and suppress EAE.* Proc Natl Acad Sci U S A, 2020. **117**(35): p. 21557-21567.
47. Mattner, F., et al., *The interleukin-12 subunit p40 specifically inhibits effects of the interleukin-12 heterodimer.* Eur J Immunol, 1993. **23**(9): p. 2202-8.
48. *UniProt: the Universal Protein Knowledgebase in 2023.* Nucleic Acids Res, 2023. **51**(D1): p. D523-d531.
49. Madeira, F., et al., *Search and sequence analysis tools services from EMBL-EBI in 2022.* Nucleic Acids Res, 2022. **50**(W1): p. W276-9.
50. Okonechnikov, K., O. Golosova, and M. Fursov, *Unipro UGENE: a unified bioinformatics toolkit.* Bioinformatics, 2012. **28**(8): p. 1166-7.
51. Altschul, S.F., et al., *Basic local alignment search tool.* J Mol Biol, 1990. **215**(3): p. 403-10.
52. Jumper, J., et al., *Highly accurate protein structure prediction with AlphaFold.* Nature, 2021. **596**(7873): p. 583-589.
53. Case, D., et al., *Amber 2018*. 2018.
54. Hornak, V., et al., *Comparison of multiple Amber force fields and development of improved protein backbone parameters.* Proteins, 2006. **65**(3): p. 712-25.
55. Siebenmorgen, T. and M. Zacharias, *Efficient Refinement and Free Energy Scoring of Predicted Protein-Protein Complexes Using Replica Exchange with Repulsive Scaling.* J Chem Inf Model, 2020. **60**(11): p. 5552-5562.
56. Siebenmorgen, T., M. Engelhard, and M. Zacharias, *Prediction of protein-protein complexes using replica exchange with repulsive scaling.* J Comput Chem, 2020. **41**(15): p. 1436-1447.
57. Shirts, M.R. and J.D. Chodera, *Statistically optimal analysis of samples from multiple equilibrium states.* J Chem Phys, 2008. **129**(12): p. 124105.
58. Englander, S.W. and N.R. Kallenbach, *Hydrogen exchange and structural dynamics of proteins and nucleic acids.* Q Rev Biophys, 1983. **16**(4): p. 521-655.
59. Wales, T.E. and J.R. Engen, *Hydrogen exchange mass spectrometry for the analysis of protein dynamics.* Mass Spectrom Rev, 2006. **25**(1): p. 158-70.
60. Lau, A.M., et al., *Deuteros 2.0: peptide-level significance testing of data from hydrogen deuterium exchange mass spectrometry.* Bioinformatics, 2021. **37**(2): p. 270-272.
61. Vranken, W.F., et al., *The CCPN data model for NMR spectroscopy: development of a software pipeline.* Proteins, 2005. **59**(4): p. 687-96.
62. Dam, J., et al., *Sedimentation velocity analysis of heterogeneous protein-protein interactions: Lamm equation modeling and sedimentation coefficient distributions c(s).* Biophys J, 2005. **89**(1): p. 619-34.

## Supplemental material

# Assembly-dependent structure formation determines the human interleukin-12/interleukin-23 secretion ratio

Isabel Aschenbrenner[1], Abraham Lopez[1,2], Till Siebenmorgen[1], Marina Parr[3], Philipp Ruckgaber[1], Anna Miesl[1], Florian Rührnößl[1], Dragana Catici[1], Martin Haslbeck[1], Michael Sattler[1,2], Dmitrij Frishman[3], Martin Zacharias[1], Matthias J. Feige[1,*]

[1] Center for Functional Protein Assemblies (CPA), Department of Bioscience, TUM School of Natural Sciences, Technical University of Munich, Garching, Germany

[2] Institute of Structural Biology, Helmholtz Zentrum München, Neuherberg, Germany

[3] Department of Bioinformatics, TUM School of Life Sciences, Technical University of Munich, Freising, Germany

* To whom correspondence may be addressed: Tel: +49-89-28913667; Fax: +49-89-28910698; E-mail: matthias.feige@tum.de

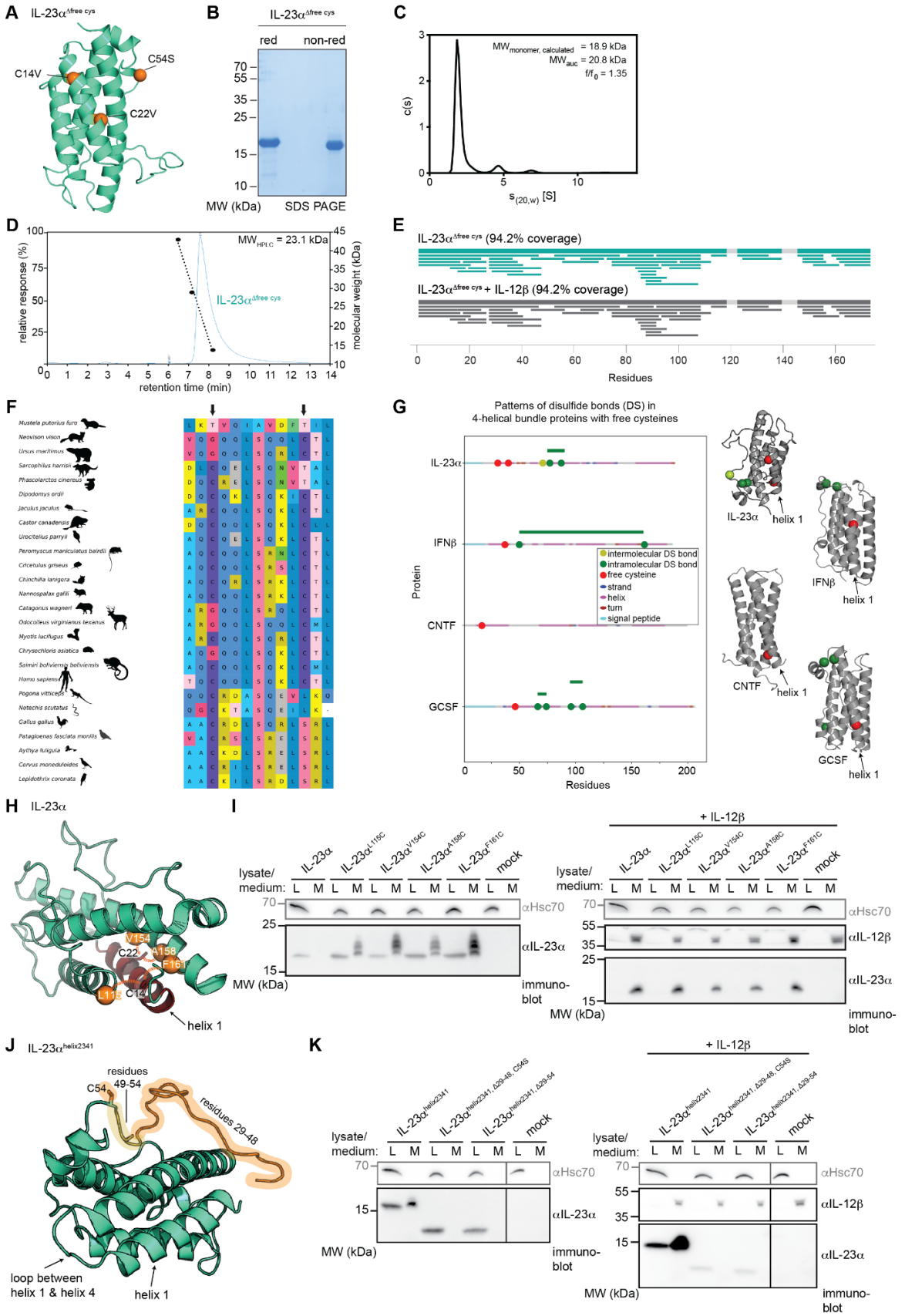


**Supplementary Fig. 1: Purification and basic characterization of IL-23α$^{C14V,C22V,C54S}$ (IL-23α$^{\Delta free\ cys}$) and further rational engineering approaches for IL-23α. A** Structural model of IL-23α$^{\Delta free\ cys}$ based on PDB: 3D87, with mutated free cysteines (Cys14, Cys22) and Cys54, involved in IL-12β binding, colored in orange and shown in CPK representation. **B** SDS-PAGE of IL-23α$^{\Delta free\ cys}$ protein under reducing (red; β-mercaptoethanol) or non-reducing (non-red; *N*-ethylmaleimide) conditions confirms purity and native intramolecular disulfide bridge

formation by mobility shift. **C** Analytical ultracentrifugation (AUC) measurement of IL-23$\alpha^{\Delta free\ cys}$ shows the monomeric status of purified protein. **d** High-performance liquid chromatography (HPLC) run confirms protein integrity of purified IL-23$\alpha^{\Delta free\ cys}$. **E** Coverage plots of $\alpha$ subunit without and with its $\beta$ subunit IL-12$\beta^{C177S}$ based on peptides detected in hydrogen deuterium exchange (HDX) experiments. **F** Sequence alignment of an IL-23$\alpha$ interspecies comparison shows relatively strong conservation of human Cys14 and Cys22 (arrows). **G** N-terminal free cysteines (red dots) can be also found in other four-helix bundle cytokines. Patterns of intramolecular disulfide bonds (dark green bars) in proteins differ strongly in their positions and sequence spanning distance. Only IL-23$\alpha$ pairs covalently (bright green dot) with another subunit to form heterodimeric IL-23. Secondary structure characteristics are colored according to the legend. In structures (adapted from PDB: 1CNT, 1RHG, 1AU1, 3D87) cysteines are marked in CPK representation and respective helix 1 is annotated. **H** Structural model shows cysteine insertion sites (orange; L115C, V154C, A158C, F161C) in CPK representation for internal disulfide bond formation (dashed lines) with one of the free cysteines (sticks; Cys14, Cys22) within helix 1 (red). **I** Human wild-type IL-23$\alpha$ is secretion-incompetent in isolation and retained in cells (lysate, L). Assembly with its $\beta$ subunit enables formation of the heterodimeric IL-23 and induces secretion (medium, M). Engineered IL-23$\alpha$ cysteine mutants are all expressed in the cell, are secretion-competent alone (M) to varying secretion efficiencies, and interact with IL-12$\beta$. Hsc70 served as loading control. Mock, empty vector transfection. MW, molecular weight. **J** Structural model of rearranged mutant IL-23$\alpha^{helix2341}$ with highlighted regions (orange, yellow) of the flexible loop for deletion. **K** Secretion blots of IL-23$\alpha^{helix2341}$ variants show secretion-competency for the rearranged mutant in isolation, but no secretion of the mutants lacking residues of the native AB loop, in absence and presence of IL-12$\beta$. Hsc70 served as loading control. Mock, empty vector transfection. MW, molecular weight.

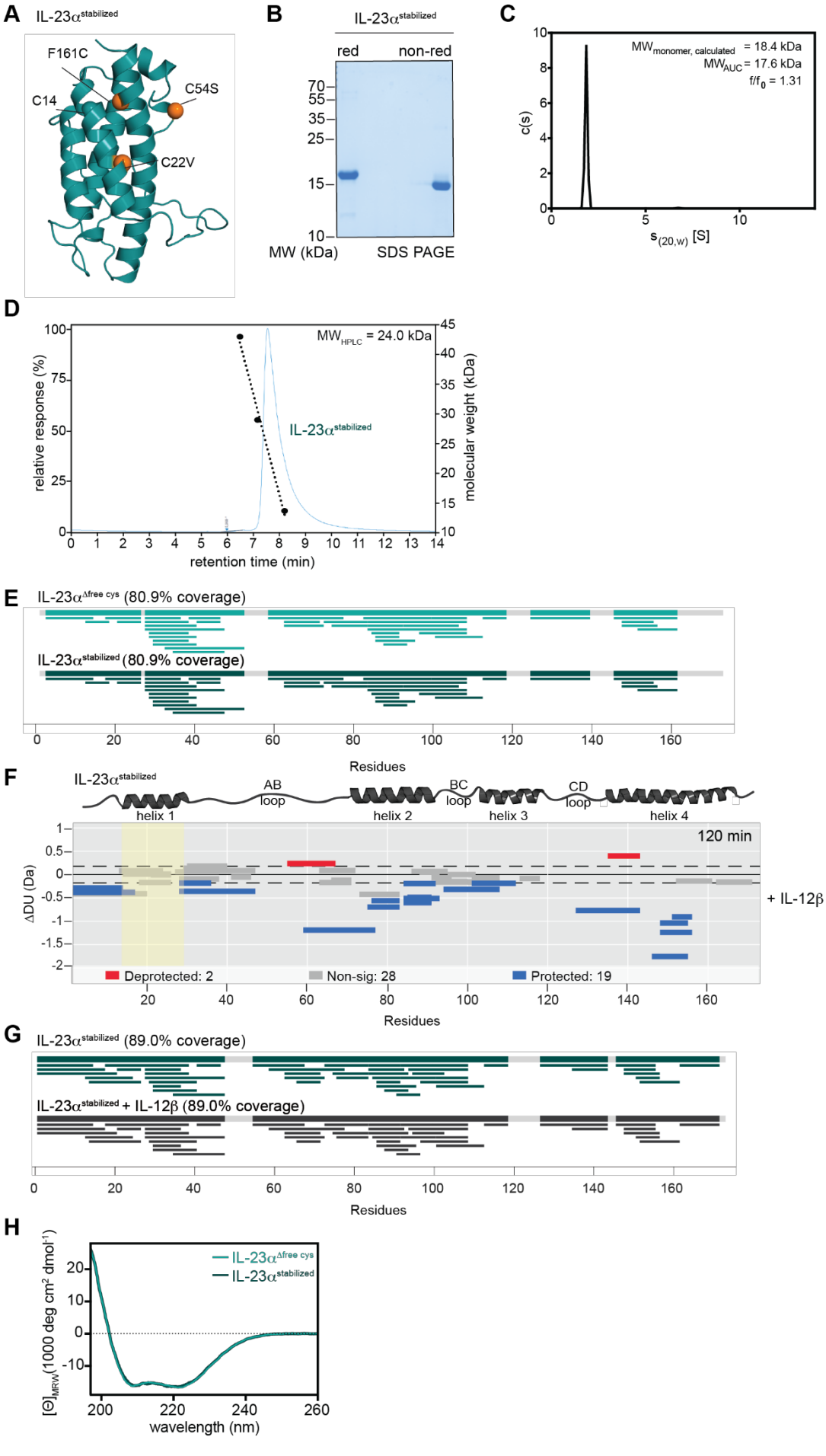
A
IL-23α^stabilized
F161C
C54S
C14
C22V
B
IL-23α^stabilized
red
non-red
70
55
35
25
15
10
MW (kDa)
SDS PAGE
C
MW_monomer, calculated = 18.4 kDa
MW_AUC = 17.6 kDa
f/f_0 = 1.31
c(s)
s_(20,w) [S]
D
MW_HPLC = 24.0 kDa
IL-23α^stabilized
relative response (%)
molecular weight (kDa)
retention time (min)
E
IL-23α^Δfree cys (80.9% coverage)
IL-23α^stabilized (80.9% coverage)
Residues
F
IL-23α^stabilized
AB loop
BC loop
CD loop
helix 1
helix 2
helix 3
helix 4
120 min
ΔDU (Da)
+ IL-12β
Deprotected: 2
Non-sig: 28
Protected: 19
Residues
G
IL-23α^stabilized (89.0% coverage)
IL-23α^stabilized + IL-12β (89.0% coverage)
Residues
H
IL-23α^Δfree cys
IL-23α^stabilized
[Θ]_MRW (1000 deg cm² dmol⁻¹)
wavelength (nm)

**Supplementary Fig. 2: Purification and basic characterization of engineered IL-23α$^{C22V,C54S,F161C}$ (IL-23α$^{stabilized}$) and comparative 23α subunit analyses. A** Structural model of IL-23α$^{stabilized}$ with mutated amino acid residues colored in orange and shown in CPK representation. Cysteine, introduced at position Phe161, enables disulfide bond formation with Cys14. **B** SDS-PAGE confirms protein purity and folding status of purified IL-23α$^{stabilized}$ under reducing (red; β-mercaptoethanol) or non-reducing (non-red; *N*-ethylmaleimide) conditions. Intracellular disulfide bonds (Cys14-Cys161, Cys58-Cys70) induce protein mobility shift. **C** Analytical ultracentrifugation (AUC) measurement of IL-23α$^{stabilized}$ shows monomeric status of purified protein. **D** High-performance liquid chromatography (HPLC) run of engineered α subunit confirms protein integrity. **E** Coverage plots of IL-23 α subunit variants based on peptides detected in hydrogen deuterium exchange (HDX) experiments. **F** Differential Wood's plot shows differential uptake (ΔDU) of IL-23α$^{stabilized}$ peptides, represented as bars, upon IL-12β$^{C177S}$ interaction. Significantly ($p$<0.05, Hybrid method) protected (blue) and deprotected (red) peptides or those with no statistical difference in uptake (gray) between the two states are indicated for t = 120 min. Helix 1 (yellow) is highlighted and structural features are indicated. **G** Coverage plots of IL-23α$^{stabilized}$, without and with IL-12β$^{C177S}$ addition, show peptides detected in HDX experiments. **H** Far-UV circular dichroism (CD) spectra measurements of IL-23α variants confirm overall α helical protein structure for both proteins.

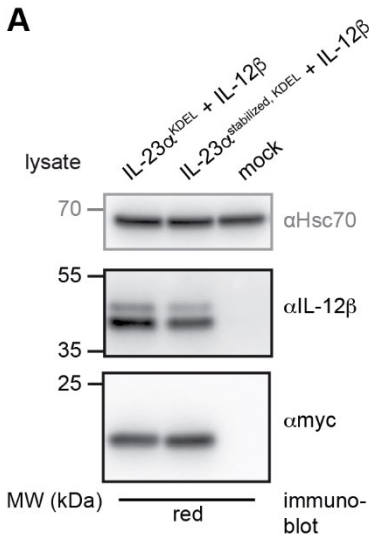


**Supplementary Fig. 3: Protein expression control immunoblot of redox experiment.** Reducing (red; β-mercaptoethanol) immunoblot showing intracellular proteins (lysate) verifies transfection and co-expression of IL-12β with respective KDEL- and myc-tagged IL-23 α subunits. Hsc70 serves as loading control. MW, molecular weight.

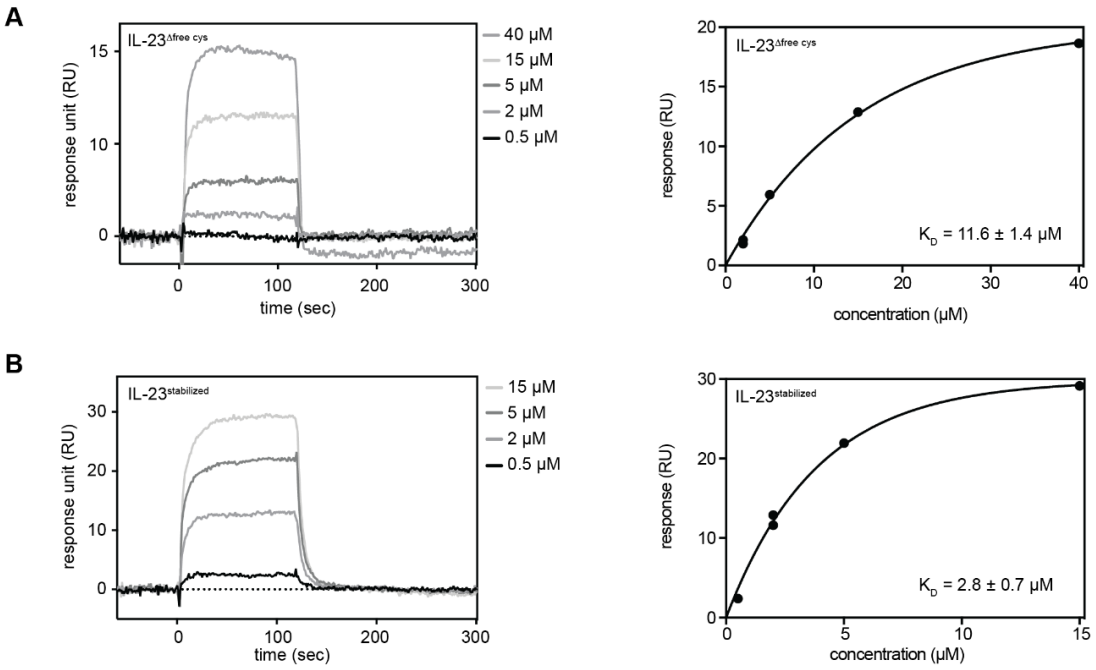


**Supplementary Fig. 4: Effect of structural engineering on IL-23 heterodimer assembly *in vitro*. A** IL-23 subunit binding was assessed by surface plasmon resonance (SPR) with IL-12$\beta^{C177S}$, coupled via its His-tag on the chip surface, using different analyte concentrations of IL-23$\alpha^{\Delta free\ cys}$ (0.5-40 µM). Binding affinity was determined in the steady state with $K_D$ = 11.6±1.4 µM (n=5, ±SD) with a one-site binding fit. **B** Affinity measurement by SPR, same as in **A**, but with IL-23$\alpha^{stabilized}$ (0.5-15 µM) as analyte. The $K_D$-value of 2.8±0.7 µM was determined by fitting steady state responses (n=3, ±SD).

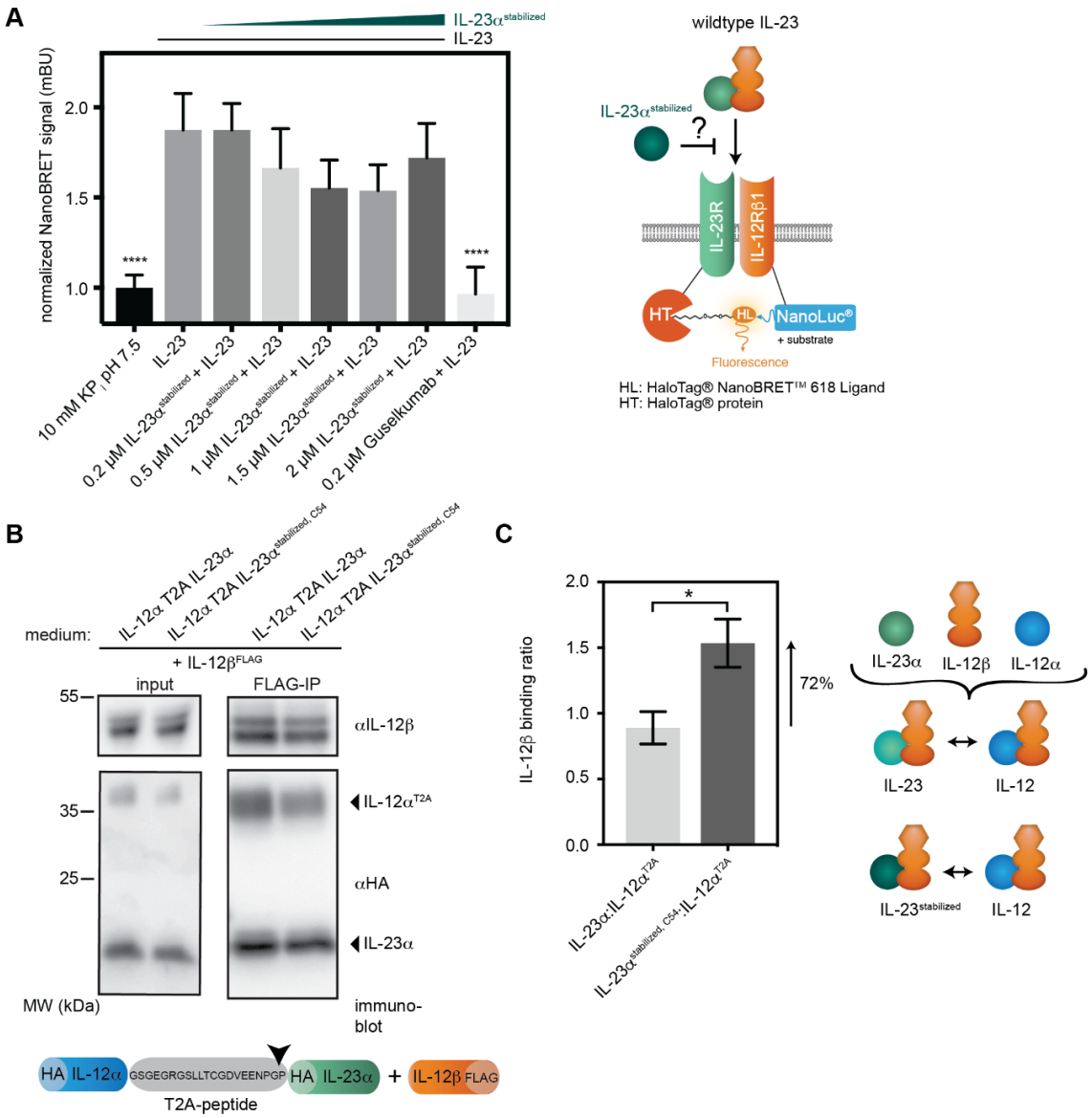


**Supplementary Fig. 5: Approaching the biological implications of rationally engineered IL-23α. A** Engineered IL-23α shows no significant inhibitory effect on IL-23 signaling. Receptor activation measured by NanoBRET™ assay shows no inhibition of receptor dimerization when priorly treated with increasing concentrations of IL-23α$^{stabilized}$. Addition of anti-IL-23 antibody Guselkumab served as positive control for signaling inhibition compared to stimulation with IL-23 alone (n=3, ±SD, **** $p$<0.0001, One-way ANOVA). Signals were normalized to NanoBRET™ signal of stimulation with buffer only (10 mM KPi pH 7.5), which served as negative control. **B** IL-23α$^{stabilized}$ assembles with IL-12β to the IL-23 heterodimer, shifting the IL-12/IL-23 balance within cells as α subunits are competing for their shared β subunit. HEK 293T cells were transiently transfected with the indicated constructs and medium was analyzed for secreted FLAG-tagged IL-12β and co-immunoprecipitation (co-IP) of HA-tagged IL-12α and IL-23α. α subunits were expressed in equimolar ratios via T2A-peptide, here with IL-12α being N-terminally to the T2A sequence, and contained the respective cysteine residue responsible for intermolecular disulfide bond formation with IL-12β. **C** IL-12β binding ratio results from quantification of α subunit IP signals from immunoblots (shown in **B**) and differs significantly when IL-23α$^{stabilized, C54}$ instead of wild-type IL-23α is competing with T2A-tagged IL-12α for IL-12β binding (n=7, ±SEM, * $p$<0.05, unpaired t test). Schematic depicts analyzed subunits and shifted ratio of IL-12 *versus* IL-23 formation.

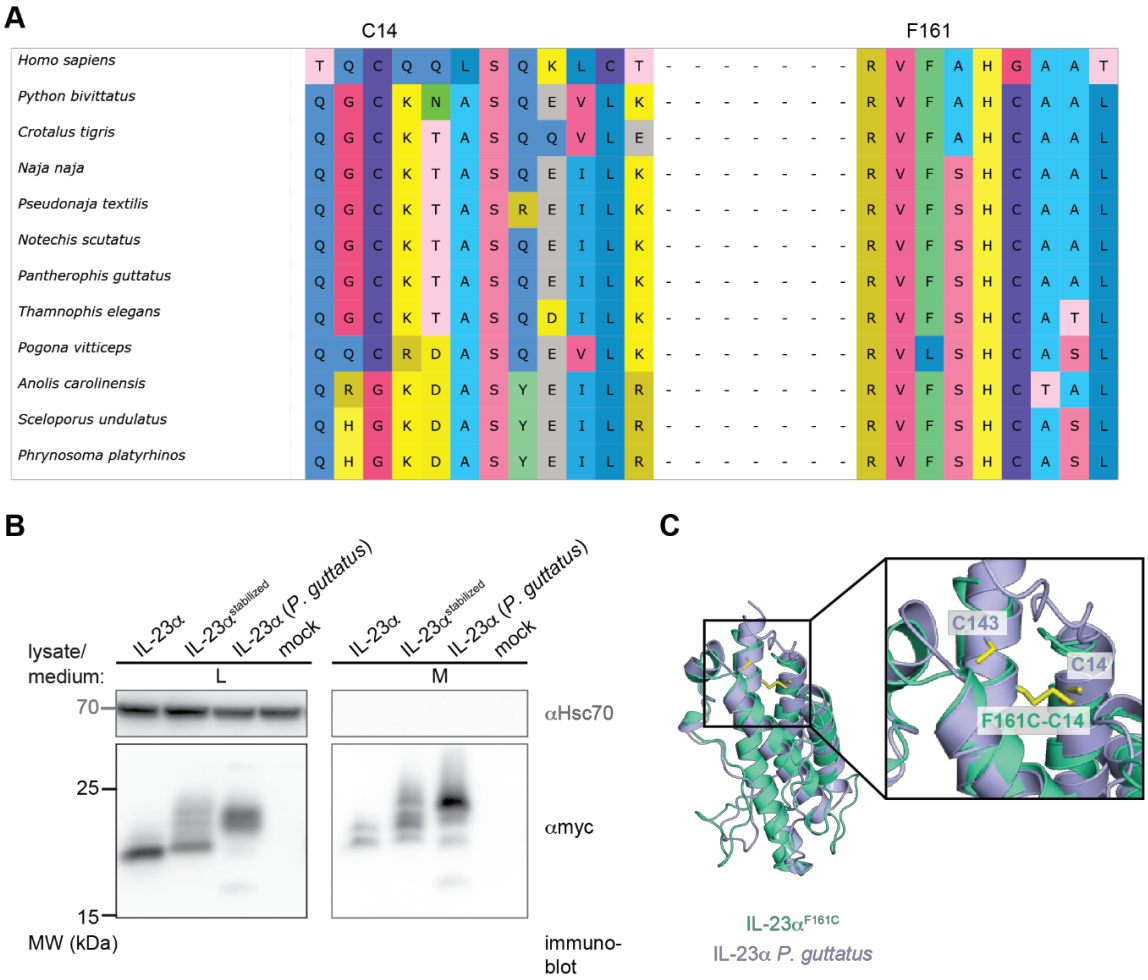


**Supplementary Fig. 6: IL-23α subunits of the Toxicofera clade. A** Multiple sequence alignment of IL-23α of species belonging to the Toxicofera clade with human IL-23α. Sequence regions and amino acid conservation around Cys14 and Phe161 are shown. In engineered IL-23α$^{stabilized}$ Phe161 was mutated to Cys to allow intramolecular disulfide bond formation with Cys14. In the Toxicofera clade, cysteine residues at human positions Cys14 and G164 are highly conserved, whereas Cys22 is missing. **B** Immunoblot of transiently transfected HEK 293T cells show secretion of *P. guttatus* IL-23α (medium, M), similar to human engineered IL-23α$^{stabilized}$. Slight secretion of IL-23α wildtype can be attributed to the myc-tag. Hsc70 serves as loading control. MW, molecular weight. **C** Structural alignment of IL-23α$^{F161C}$ (limon) and AlphaFold model for IL-23α from *P. guttatus*. Residues forming an extra intramolecular disulfide bond (F161C-C14) as well as cysteine residues (C14, C143) in IL-23α from the corn snake, responsible for a putative disulfide bridge, are shown as yellow sticks in an enlarged view (box).